



ISSN 2409-9074

Міністерство освіти і науки України  
Національний університет  
«Полтавська політехніка імені Юрія Кондратюка»

---

Ministry of Education and Science of Ukraine  
National University  
«Yuri Kondratyuk Poltava Polytechnic»

**ЗБІРНИК НАУКОВИХ ПРАЦЬ**  
**ГАЛУЗЕВЕ МАШИНОБУДУВАННЯ,**  
**БУДІВНИЦТВО**  
**Випуск 2 (59)' 2022**

---

**ACADEMIC JOURNAL**  
**INDUSTRIAL MACHINE BUILDING,**  
**CIVIL ENGINEERING**  
**Issue 2 (59)' 2022**



Міністерство освіти і науки України  
Національний університет  
«Полтавська політехніка імені Юрія Кондратюка»

---

Ministry of Education and Science of Ukraine  
National University «Yuri Kondratyuk Poltava Polytechnic»

# **ЗБІРНИК НАУКОВИХ ПРАЦЬ**

ГАЛУЗЕВЕ МАШИНОБУДУВАННЯ,  
БУДІВНИЦТВО

**Випуск 2 (59)' 2022**

---

**ACADEMIC JOURNAL**  
INDUSTRIAL MACHINE BUILDING,  
CIVIL ENGINEERING  
**Issue 2 (59)' 2022**

Полтава – 2022

---

Poltava – 2022



[www.znp.nupp.edu.ua](http://www.znp.nupp.edu.ua)  
<http://journals.nupp.edu.ua/znp>

## **Збірник наукових праць. Галузеве машинобудування, будівництво / Національний університет «Полтавська політехніка імені Юрія Кондратюка»**

Збірник наукових праць видається з 1999 р., періодичність – двічі на рік.

Засновник і видавець – Національний університет «Полтавська політехніка імені Юрія Кондратюка».

Свідцтво про державну реєстрацію КВ 24621-14561ПР від 14.12.2020 р.

Збірник наукових праць уключений до переліку наукових фахових видань (категорія Б), у яких можуть публікуватися результати дисертаційних робіт (Наказ МОН України №1218 від 07.11.2018 року).

Збірник наукових праць рекомендовано до опублікування вченою радою Національного університету «Полтавська політехніка імені Юрія Кондратюка» протокол №20 від 29.11.2022 р.

У збірнику представлені результати наукових і науково-технічних розробок у галузі машинобудування, автомобільного транспорту та механізації будівельних робіт; із проектування, зведення, експлуатації та реконструкції будівельних конструкцій, будівель і споруд; їх основ та фундаментів; будівельної фізики та енергоефективності будівель і споруд; а також у галузях гірництва, нафтогазової інженерії та технологій, екології.

Призначений для наукових й інженерно-технічних працівників, аспірантів і магістрів.

### **Редакційна колегія:**

<b>Пічугін С.Ф.</b>	– головний редактор, д.т.н., професор, Національний університет «Полтавська політехніка імені Юрія Кондратюка» (Україна), <a href="mailto:pichugin.sf@gmail.com">pichugin.sf@gmail.com</a>
<b>Винников Ю.Л.</b>	– заступник головного редактора, д.т.н., професор, Національний університет «Полтавська політехніка імені Юрія Кондратюка» (Україна), <a href="mailto:vyunnykov@ukr.net">vyunnykov@ukr.net</a>
<b>Льченко В.В.</b>	– відповідальний секретар, к.т.н., доцент, Національний університет «Полтавська політехніка імені Юрія Кондратюка» (Україна), <a href="mailto:znrbud@gmail.com">znrbud@gmail.com</a>
<b>Аніскін А.</b>	– к.т.н., доцент, університет Північ (Хорватія)
<b>Болтрік М.</b>	– д.т.н., професор, Білостоцький технологічний університет (Польща)
<b>Вамболь В.В.</b>	– д.т.н., професор, Національний університет «Полтавська політехніка імені Юрія Кондратюка» (Україна)
<b>Вамболь С.В.</b>	– д.т.н., професор, Національний технічний університет «Харківський політехнічний інститут» (Україна)
<b>Вінеке-Тумауї Б.</b>	– д.т.н., професор, Університет прикладних наук м. Банденбург (Німеччина)
<b>Галінська Т.А.</b>	– к.т.н., доцент, Національний університет «Полтавська політехніка імені Юрія Кондратюка» (Україна)
<b>Гасімов А.Ф.</b>	– к.т.н., доцент, Азербайджанський архітектурно-будівельний університет (Азербайджан)
<b>Голік Ю.С.</b>	– к.т.н., професор, Національний університет «Полтавська політехніка імені Юрія Кондратюка» (Україна)
<b>Дмитренко В.І.</b>	– к.т.н., доцент, Національний університет «Полтавська політехніка імені Юрія Кондратюка» (Україна)
<b>Ємельянова І.А.</b>	– д.т.н., професор, Харківський національний університет будівництва та архітектури (Україна)
<b>Жусупбеков А.Ж.</b>	– д.т.н., професор, Євразійський національний університет ім. Л.М. Гумільова (Казахстан)
<b>Зезекало І.Г.</b>	– д.т.н., професор, Національний університет «Полтавська політехніка імені Юрія Кондратюка» (Україна)
<b>Зія Я.</b>	– к.т.н., професор, Краківська гірничо-металургійна академія ім. С. Сталіца (Польща)
<b>Зоценко М.Л.</b>	– д.т.н., професор, Національний університет «Полтавська політехніка імені Юрія Кондратюка» (Україна)
<b>Зурло Франческо</b>	– д.т.н., професор, Міланська політехніка (Італія)
<b>Камал М.А.</b>	– д.т.н., доцент, Мусульманський університет Алігарха (Індія)
<b>Качинський Р.</b>	– д.т.н., професор, Білостоцький технологічний університет (Польща)
<b>Коробко Б.О.</b>	– д.т.н., професор, Національний університет «Полтавська політехніка імені Юрія Кондратюка» (Україна)
<b>Коровяка Є.А.</b>	– к.т.н., доцент, Національний технічний університет «Дніпровська політехніка» (Україна)
<b>Косіор-Казберук М.</b>	– д.т.н., професор, Білостоцький технологічний університет (Польща)
<b>Лукін О.Ю.</b>	– д.г.-м.н., професор, Національний університет «Полтавська політехніка імені Юрія Кондратюка» (Україна)
<b>Назаренко І.І.</b>	– д.т.н., професор, Київський національний університет будівництва та архітектури (Україна)
<b>Павліков А.М.</b>	– д.т.н., професор, Національний університет «Полтавська політехніка імені Юрія Кондратюка» (Україна)
<b>Панг С.</b>	– к.т.н., професор, Китайський університет нафти – Пекін (Китай)
<b>Педченко Л.О.</b>	– к.т.н., доцент, Національний університет «Полтавська політехніка імені Юрія Кондратюка» (Україна)
<b>Позрібний В.В.</b>	– к.т.н., с.н.с., Національний університет «Полтавська політехніка імені Юрія Кондратюка» (Україна)
<b>Савик В.М.</b>	– к.т.н., доцент, Національний університет «Полтавська політехніка імені Юрія Кондратюка» (Україна)
<b>Семко О.В.</b>	– д.т.н., професор, Національний університет «Полтавська політехніка імені Юрія Кондратюка» (Україна)
<b>Степова О.В.</b>	– д.т.н., професор, Національний університет «Полтавська політехніка імені Юрія Кондратюка» (Україна)
<b>Сулевська М.</b>	– д.т.н., професор, Білостоцька політехніка (Польща)
<b>Харченко М.О.</b>	– к.т.н., доцент, Національний університет «Полтавська політехніка імені Юрія Кондратюка» (Україна)
<b>Шаповал В.Г.</b>	– д.т.н., професор, Національний технічний університет «Дніпровська політехніка» (Україна)

Адреса видавця та редакції – Національний університет «Полтавська політехніка імені Юрія Кондратюка»

Науково-дослідницька частина, к. 320Ф, Першотравневий проспект, 24, м. Полтава, 36011.

Тел.: (05322) 29875; e-mail: [v171@pntu.edu.ua](mailto:v171@pntu.edu.ua); [www.pntu.edu.ua](http://www.pntu.edu.ua)

Макет та тиражування виконано у поліграфічному центрі Національного університету «Полтавська політехніка імені Юрія Кондратюка», Першотравневий проспект, 24, м. Полтава, 36011.

Свідцтво про внесення суб'єкта видавничої справи до державного реєстру видавців, виготівників і розповсюджувачів видавничої продукції (ДК № 3130 від 06.03.2008 р.).

Комп'ютерна верстка – В.В. Льченко.

Підписано до друку 30.11.2022 р.

Папір ксерокс. Друк різнограф. Формат 60x80 1/8. Ум. Друк. Арк. – 13,25.

Тираж 300 прим.

**Academic journal. Industrial Machine Building, Civil Engineering /  
National University «Yuri Kondratyuk Poltava Polytechnic»**

Academic journal was founded in 1999, the publication frequency of the journal is twice a year.

Founder and Publisher is National University «Yuri Kondratyuk Poltava Polytechnic».

State Registration Certificate KB 24621-14561IIP dated 14.12.2020.

Academic journal is included into the list of specialized academic publications where graduated thesis results could be presented (Order of Department of Education and Science of Ukraine № 1218 dated 07.11.2018).

Academic journal was recommended for publication by the Academic Board of National University «Yuri Kondratyuk Poltava Polytechnic», transactions №20 of 29.11.2022.

The results of scientific and scientific-technical developments in the sphere of mechanical engineering, automobile transport and mechanization of construction works; designing, erection, operation and reconstruction of structural steels, buildings and structures; its bases and foundations; building physics and energy efficiency of buildings and structures are presented in the collection; as well as in the fields of mining, oil and gas engineering and technology; ecology.

Academic journal is designed for researchers and technologists, postgraduates and senior students.

**Editorial Board:**

<i>Pichugin Sergii</i>	– <i>Editor-in-Chief</i> , DSc, Professor, National University «Yuri Kondratyuk Poltava Polytechnic» (Ukraine), pichugin.sf@gmail.com
<i>Vynnykov Yuriy</i>	– <i>Deputy Editor</i> , DSc, Professor, National University «Yuri Kondratyuk Poltava Polytechnic» (Ukraine), vynnykov@ukr.net
<i>Ilchenko Volodymyr</i>	– <i>Executive Secretary</i> , PhD, Associate Professor, National University «Yuri Kondratyuk Poltava Polytechnic» (Ukraine), znpbud@gmail.com
<i>Aniskin Aleksey</i>	– PhD, Associate Professor, University North (Croatia)
<i>Botlyk Michal</i>	– DSc, Professor, Bialystok Technological University (Poland)
<i>Vambol Viola</i>	– DSc, Professor, National University «Yuri Kondratyuk Poltava Polytechnic» (Ukraine)
<i>Vambol Sergiy</i>	– DSc, Professor, National Technical University «Kharkiv Polytechnic Institute» (Ukraine)
<i>Wieneke-Toutaoui Burghilde</i>	– DSc, Professor, President of Brandenburg University of Applied Sciences (Germany)
<i>Galinska Tatiana</i>	– PhD, Associate Professor, National University «Yuri Kondratyuk Poltava Polytechnic» (Ukraine)
<i>Gasimov Akif</i>	– PhD, Associate Professor, Azerbaijan Architectural and Construction University (Azerbaijan)
<i>Holik Yuriy</i>	– PhD, Professor, National University «Yuri Kondratyuk Poltava Polytechnic» (Ukraine)
<i>Dmytrenko Viktoriia</i>	– PhD, Associate Professor, National University «Yuri Kondratyuk Poltava Polytechnic» (Ukraine)
<i>Emeljanova Inga</i>	– DSc, Professor, Kharkiv National University of Construction and Architecture (Ukraine)
<i>Zhusupbekov Askar</i>	– DSc, Professor, Eurasia National L.N. Gumiliov University (Kazakhstan)
<i>Zezealo, Ivan</i>	– DSc, Professor, National University «Yuri Kondratyuk Poltava Polytechnic» (Ukraine)
<i>Ziaja Jan</i>	– PhD, Professor, AGH University of Science and Technology in Kraków (Poland)
<i>Zotsenko Mykola</i>	– DSc, Professor, National University «Yuri Kondratyuk Poltava Polytechnic» (Ukraine)
<i>Zurlo Francesco</i>	– DSc, Professor, Polytechnic University of Milan (Italia)
<i>Kamal Mohammad Arif</i>	– DSc, Associate Professor, Architecture Section, Aligarh Muslim University (India)
<i>Kaczyński Roman</i>	– DSc, Professor, Bialystok Technological University (Poland)
<i>Korobko Bogdan</i>	– DSc, Professor, National University «Yuri Kondratyuk Poltava Polytechnic» (Ukraine)
<i>Koroviaka Yevhenii</i>	– PhD, Associate Professor, Dnipro University of Technology (Ukraine)
<i>Kosior-Kazberuk Marta</i>	– DSc, Professor, Bialystok Technological University (Poland)
<i>Lukin Alexander</i>	– DSc, Professor, National University «Yuri Kondratyuk Poltava Polytechnic» (Ukraine)
<i>Nazarenko Ivan</i>	– DSc, Professor, Kyiv National Civil Engineering and Architecture University (Ukraine)
<i>Pavlikov Andriy</i>	– DSc, Professor, National University «Yuri Kondratyuk Poltava Polytechnic» (Ukraine)
<i>Pang Xiongqi</i>	– PhD, Professor, China University of Petroleum – Beijing (China)
<i>Pedchenko Larysa</i>	– PhD, Associate Professor, National University «Yuri Kondratyuk Poltava Polytechnic» (Ukraine)
<i>Pohribnyi Volodymyr</i>	– PhD, Associate Professor, National University «Yuri Kondratyuk Poltava Polytechnic» (Ukraine)
<i>Savyk Vasyl</i>	– PhD, Associate Professor, National University «Yuri Kondratyuk Poltava Polytechnic» (Ukraine)
<i>Semko Oleksandr</i>	– DSc, Professor, National University «Yuri Kondratyuk Poltava Polytechnic» (Ukraine)
<i>Stepova Olena</i>	– DSc, Professor, National University «Yuri Kondratyuk Poltava Polytechnic» (Ukraine)
<i>Sulewska Maria</i>	– DSc, Professor, Bialystok University of Technology (Poland)
<i>Kharchenko Maksym</i>	– PhD, Associate Professor, National University «Yuri Kondratyuk Poltava Polytechnic» (Ukraine)
<i>Shapoval Volodymyr</i>	– DSc, Professor, Dnipro University of Technology (Ukraine)

Address of Publisher and Editorial Board – National University «Yuri Kondratyuk Poltava Polytechnic»,  
Research Centre, room 320-F, Pershotravnevyi Avenue, 24, Poltava, 36011, Ukraine.

tel.: (05322) 29875; e-mail: v171@pntu.edu.ua; www.pntu.edu.ua

Layout and printing made in the printing center of National University «Yuri Kondratyuk Poltava Polytechnic»,  
Pershotravnevyi Avenue, 24, Poltava, 36011, Ukraine.

Registration certificate of publishing subject in the State Register of Publishers Manufacturers  
and Distributors of publishing products (DK № 3130 from 06.03.2008).

Desktop Publishing – V. Ilchenko.

Authorize for printing 30.11.2022.

Paper copier. Print rizograf. Format 60x80 1/8. Conventionally printed sheets – 13,25.

Circulation 300 copies.

UDC 666.97.033

## The analytical investigation of the concrete mixture deposition process by the concrete 3d printer extruder

Orysenko Olexandr<sup>1\*</sup>, Nesterenko Mykola<sup>2</sup>, Shokalo Artem<sup>3</sup>

<sup>1</sup> National University «Yuri Kondratyuk Poltava Polytechnic» <https://orcid.org/0000-0003-3103-0096>

<sup>2</sup> National University «Yuri Kondratyuk Poltava Polytechnic» <https://orcid.org/0000-0002-4073-1233>

<sup>3</sup> National University «Yuri Kondratyuk Poltava Polytechnic» <https://orcid.org/0000-0001-6013-9969>

\* Адреса для листування E-mail: [oleksandr.orysenko@gmail.com](mailto:oleksandr.orysenko@gmail.com)

The construction of buildings using 3D printing is becoming increasingly popular. However, this technology, despite its numerous advantages, also has its drawbacks. To minimize the impact of these drawbacks on the quality of construction work, scientifically substantiated approaches can be applied to improve both the technology itself and the machines used in the process. One of the factors that affect the quality of material deposition on the printing surface is the alignment of the extruder's productivity of the construction 3D printer with the speed of its movement above the surface. This can be achieved by considering the physicomaterial properties of the concrete mixture and the method of its delivery to the application area. To describe the mixture's delivery through a narrow channel between the nozzle end of the extruder and the printing surface, the Poiseuille method is proposed, modeling the mixture with the Herschel-Bulkley rheological model. Analytical dependencies have been derived to determine the extruder's productivity and the speed of the mixture extrusion through the nozzle.

**Keywords:** 3D construction, extruder, Herschel-Bulkley model, Poiseuille method, integral average velocity.

## Аналітичне дослідження процесу подачі бетонної суміші екструдером будівельного 3D-принтера

Орисенко О.В.<sup>1\*</sup>, Нестеренко М.М.<sup>2</sup>, Шокало А.В.<sup>3</sup>

<sup>1, 2, 3</sup> Національний університет «Полтавська політехніка імені Юрія Кондратюка»

\*Corresponding author E-mail: [oleksandr.orysenko@gmail.com](mailto:oleksandr.orysenko@gmail.com)

Спорудження об'єктів будівництва способом 3D-друку набуває все більшого поширення. Дана технологія має ряд переваг перед традиційними способами виконання будівельних робіт. Проте, поряд з перевагами 3D-бетонування має також і недоліки, мінімізувати вплив яких на якість виконання будівельних робіт можна застосувавши науково обґрунтовані підходи до вдосконалення як самої технології так і машин, які при цьому використовуються. Одним із факторів, які впливають на якість нанесення матеріалу на поверхню друку є узгодження продуктивності екструдера будівельного 3D-принтера та швидкості його пересування понад поверхню. Цього можна досягти врахувавши реологічні властивості бетонної суміші та спосіб її подачі у зону нанесення. Пропонується суміш для 3D-принтера моделювати реологічною моделлю Гершеля-Балклі, яка дозволяє врахувати зміну дотичних напружень зсуву залежно від в'язкісних властивостей суміші та індексу її течії. Для опису подачі суміші через щілинний канал між торцем сопла екструдера та поверхню друку застосовано методику Пуазейля. Виведено аналітичні залежності для визначення продуктивності екструдера та швидкості витискання суміші через сопло. Передбачається, що швидкість пересування екструдера над поверхню друку повинна дорівнювати середньоінтегральній швидкості витискання суміші через щілинний канал між торцем сопла екструдера та поверхню друку. В подальшому намічено проведення експериментальних досліджень з метою підтвердження запропонованої гіпотези. Для проведення експериментальних досліджень створено лабораторний 3D-принтер, який конструктивно являє собою робот-маніпулятор зі встановленим на ньому екструдером. Пересуванням екструдера по просторовій траєкторії, швидкість обертання лопатей та шнека екструдера здійснюється індивідуальними механізмами, керування якими забезпечується апаратно-програмним забезпеченням на платформі Arduino.

**Ключові слова:** 3D-будівництво, екструдер, модель Гершеля-Балклі, методика Пуазейля, середньоінтегральна швидкість.

## Introduction

In recent times, there has been a rapid development of additive technologies in all sectors of manufacturing, and the construction industry is no exception. The number of structures fabricated using 3D printing has increased significantly in recent years [1-3]. The equipment used for this purpose is construction 3D printers. The main advantages of using construction 3D printers compared to traditional construction technologies are as follows [4]:

- Reduction in construction timelines
- Improved quality of construction work
- Decreased labor costs
- Possibility of implementing modular production
- Reduction in costs associated with construction and tooling
- Increased safety in production and improved working conditions
- Enhanced environmental performance of construction activities through waste reduction
- Ability to construct buildings with diverse architectural designs.

Additionally, several economic factors also support the adoption of 3D printing [5]. However, as researchers point out [4], this technology is not without its drawbacks. The following disadvantages should be considered:

- Relatively high initial investments due to the high cost of 3D printing equipment.
- Frequent breakdowns of 3D printers, especially during continuous usage.
- The need for improvement and development of new construction materials for use in 3D printers.
- Comparatively rough appearance of the constructed structure, requiring finishing works.

Considering the mentioned advantages and disadvantages of using 3D printing in the construction industry, we can conclude that this technology currently requires further improvement, which can be achieved through the application of scientifically grounded technical solutions. Therefore, scientific research in the field of improving and developing 3D printing equipment remains relevant.

## Review of the research sources and publications

A significant number of publications by both domestic and international researchers are dedicated to improving equipment for 3D printing. In works [6, 7], an analysis of existing types of construction 3D printers was conducted, and their shortcomings that require improvement were identified. Promising designs of 3D printers and their components were also proposed, aiming to expand the technological capabilities of the equipment and increase work productivity.

Another direction for improving the quality of construction works using 3D printing is the improvement and development of construction mixtures. The results of a critical review of methods for investigating interlayer regions of 3D-printed concrete are presented in work [8]. Testing methods used to assess the strength of interfacial bonding, the influence of printing parameters, material composition, and other factors on the

strength of interfacial connections are discussed. Relevant modification methods are considered, and ideas for future research are proposed.

The rheological properties of the concrete mixture used in 3D printers are the subject of study in work [9]. Two contrasting strategies that can be applied in the construction of concrete structures using extrusion are discussed: using concrete with high and low workability. The behavior of fresh cement paste and construction mortar under various influences (shear, compression, tension) is investigated for different water-to-cement ratios.

## Definition of unsolved aspects of the problem

The construction of a structure using a construction 3D printer involves layer-by-layer deposition of a concrete mixture onto the printing surface. At the beginning of the construction, this surface may be a specially prepared platform, and subsequently, it becomes the lower layers of the already printed structure.

It is evident that to ensure quality printing with this method of application for each subsequent layer, it is necessary to coordinate the amount of concrete mixture supplied to the printing zone and the speed of movement of the extruder over the surface. If the amount of supplied mixture exceeds the required amount, an excess will be extruded not only behind the extruder in the direction of its movement but also from the sides and in the area ahead, leading to a deterioration in the appearance of the structure, excessive material consumption, and additional resistance to movement. On the other hand, if the feed rate of the mixture is lower than the speed of the extruder's movement, the required layer thickness will not be achieved, resulting in poor print quality.

This problem can be addressed through a theoretically justified coordination of the properties of the mixture used for 3D printing and the parameters and operating principles of the machine that deposits this mixture. However, the scientific literature provides insufficient coverage of these issues.

## Problem statement

Thus, the objective of this research is to develop a scientifically justified methodology that allows for the coordination of the amount of mixture supplied to the printing zone and the speed of movement of the extruder. At the initial stage of the investigation, it is necessary to develop a mathematical model of the process of mixture deposition in the printing zone.

## Basic material and results

To conduct scientific research at the Yuri Kondratyuk Poltava National Technical University, a laboratory 3D printer has been created (Figure 1), which is a robotic manipulator with an installed extruder. The deposition of mixture layers onto the printing surface is carried out by the extruder as it moves above this surface. The robotic manipulator enables the movement of the extruder along a spatial trajectory through individually controlled mechanisms.

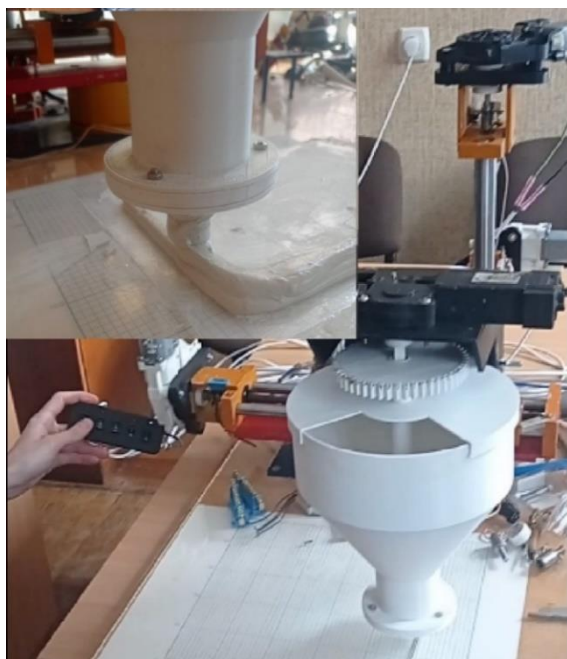


**Figure 1 – 3D Printer in our laboratory**

Structurally, the extruder consists of a container with individual shafts on which blades and an auger are installed (Figure 2). One of the shafts is hollow, allowing the other shaft to pass through it. The blades are used to mix the concrete mixture, preventing it from solidifying and keeping it in a fluid state. The auger is responsible for feeding the concrete mixture to the nozzle, which is located at the bottom of the extruder and has a cylindrical shape. The loading of the mixture is carried out cyclically through a loading opening as it is consumed.

The spatial trajectory of the extruder's movement is defined (Figure 3) by the hardware and software provided on the Arduino platform. This hardware and software also determine the necessary rotational speed of the blades and auger. This allows for various operating modes to be set and enables the deposition of the mixture along the specified trajectory.

The adjustment of the mixture layer thickness  $H$  (Figure 3) using the specified extruder design is achieved by setting the desired height of the nozzle above the printing surface. In this case, the mixture, under the pressure generated by the auger, will be extruded through the narrow channel formed between the nozzle tip and the printing surface. In the case of a cylindrical nozzle, the extruded material will form a ring-shaped cross-section of length  $B$  (Figure 4). Unfolding this ring on a plane, we obtain a narrow channel through which the mixture is supplied in the form of a parallelepiped with width  $B$ , height  $H$ , and length  $L$ . The geometric dimensions of this channel remain constant during the operation of the 3D printer.

Therefore, the amount of mixture delivered to the printing zone will depend on the speed at which it passes through the specified channel.

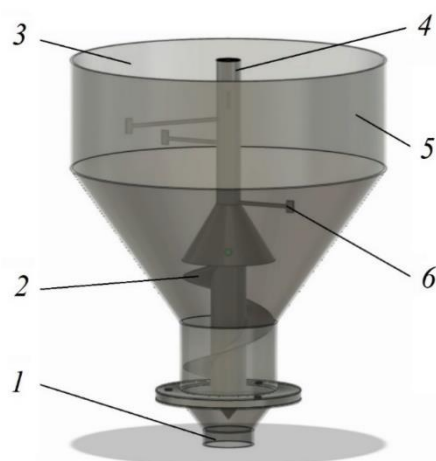


**Figure 2 – The structure of the extruder of the laboratory 3D printer is as follows:**

- 1 – extruder nozzle; 2 – concrete mixture feeding auger;
- 3 – loading window; 4 – shaft for driving the auger and blades; 5 – container for the concrete mixture;
- 6 – blades for mixing the mixture



**Figure 3 – The application of a layer of the concrete mixture onto the printing surface along a specified trajectory**

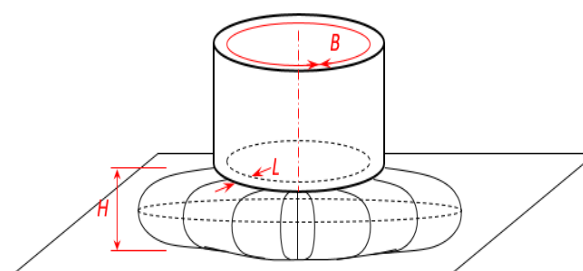


**Figure 4 – The diagram of material flow through a slotted circular channel**

Considering the characteristics of the structure and operation principle of the proposed construction 3D printer extruder, the following requirements can be additionally formulated for the concrete mixture:

- Taking into account the vertical positioning of the extruder and the location of the feeding opening at its



lower part, the mixture should possess certain viscosity properties that prevent it from self-advancing through the feeding opening under the influence of gravity.

- The consistency of the mixture should be such that it exhibits plastic properties and can be extruded through the nozzle opening when the screw is rotating.

- After being deposited onto the printing surface, the plasticity of the mixture should rapidly diminish, and it should not exhibit excessive flow or spreading behaviour.

Based on the existing scientific research on the rheological properties of concrete mixtures, it can be concluded that a mixture with specific strength characteristics in a quiescent state that acquires fluid-like properties when subjected to external loading best satisfies these requirements. Such a mixture is considered a viscoelastic material that exhibits its maximum strength under the influence of external loading.

Typically, the physico-mechanical properties of such materials are described by the Shvedov-Bingham rheological model, which takes the following form:

$$\tau = \tau_0 + \mu_p \cdot \gamma, \quad (1)$$

where  $\tau_0$  – shear yield stress, Pa;

$\mu_p$  – plastic viscosity, Pa·s;

$\gamma$  – velocity gradient, 1/s.

However, this relationship does not account for the change in tangential stresses with varying shear rates, and in this case, inaccurately reflects the behavior of concrete at different rates of applied loading.

A more accurate description of concrete behavior during extrusion is provided by the stepped rheological models, such as the Herschel-Bulkley model [13], which has the following analytical expression:

$$\tau = \tau_s + \mu \cdot \gamma^\varphi, \quad (2)$$

where  $\tau_s$  – shear yield stress, Pa;

$\mu$  – a coefficient proportional to the viscosity at a unit velocity gradient;

$\gamma$  – velocity gradient, 1/s;

$\varphi$  – flow index.

Therefore, the objective of this research is to adapt the mentioned rheological model to describe the material flow process through the slit channel between the nozzle face of the extruder and the printing surface. Since the nozzle of the proposed construction 3D printer has a circular shape, the slit channel will also be circular. The width of the channel will be equal to the circumference length  $B$ , and the length will be the thickness of the nozzle face  $L$ . When the concrete mixture is fed, a layer of thickness  $H$  is formed.

To derive an analytical expression for the material flows through the slit channel, we apply Poiseuille's method [14], which describes the flow rates of a viscoelastic fluid through a cylindrical channel.

Further calculations are carried out using the scheme depicted in Figure 5. The diagram shows the forces acting on an elementary layer of material with a thickness, which is assumed to be undeformed. We assume posi-

tive shear stresses occur on the lower and upper surfaces of the elementary layer. Then the external force creating pressure will have a negative sign, and the equation of force equilibrium will take the form:

$$2 \cdot B \cdot L \cdot \tau = -2 \cdot h \cdot B \cdot q, \quad (3)$$

where  $h$ ,  $B$ ,  $L$  – length, and width of the slit, respectively (in the case of a circular channel, the length of the channel is equal to the circumference);

$q$  – pressure at the inlet of the channel.

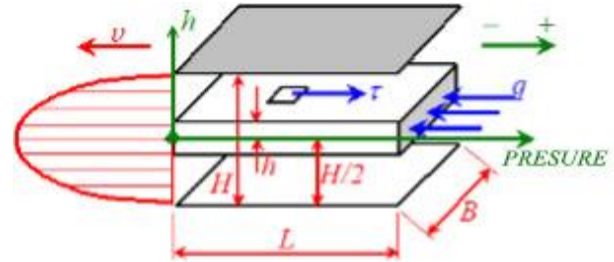


**Figure 5 – Computational scheme of material flow through the slit channel**

From equation (3), we determine the dependence of shear stresses in a material layer with height on the pressure of the material at the inlet of the slit channel:

$$\tau = \frac{q \cdot h}{L}. \quad (4)$$

We transform formula (1) into the following form:

$$-\gamma = \frac{dv}{dh} = \left[ \frac{(\tau - \tau_s)}{\mu} \right]^{\frac{1}{\varphi}} = \left[ \frac{(\tau - \tau_s)}{\mu} \right]^n, \quad (5)$$

where  $n$  – is the reciprocal of the flow index,  $n = 1/\varphi$ .

The minus sign before the velocity gradient symbol indicates that the directions of velocity and shear stresses are opposite. Since the velocity gradient is, formula (5) can be written as:

$$-dv = \left[ \frac{\left( \frac{q \cdot h}{L} - \tau_s \right)}{\mu} \right]^n dh, \quad (6)$$

By integrating both sides of equation (6), we obtain:

$$-v = \frac{\left( \frac{q \cdot h}{L} - \tau_s \right)^{n+1} \cdot L}{(n+1) \cdot q \cdot \mu^n} + C. \quad (7)$$

Assuming that the flow velocity near the wall is zero [14] ( $v = 0$  when  $h = H/2$ ), we find the constant of integration  $C$  as:

$$C = \frac{\left( \frac{q \cdot h}{2 \cdot L} - \tau_s \right)^{n+1} \cdot L}{(n+1) \cdot q \cdot \mu^n}. \quad (8)$$

By substituting the constant of integration into the velocity equation (7), we find the velocity distribution equation along the channel height:

$$v(h) = \left[ \left( \frac{q \cdot H}{2 \cdot L} - \tau_s \right)^{n+1} - \left( \frac{q \cdot h}{L} - \tau_s \right)^{n+1} \right] \times \frac{L}{(n+1) \cdot q \cdot \mu^n} \quad (9)$$

Formula (9) allows us to calculate the velocity of the concrete mixture layers as they advance through the height of the slit channel. Since the velocity of individual layers of the mixture will vary with height, to determine the extruder's movement speed above the printing surface, we need to use the average integral value of velocity, which we find as:

$$v_{ci} = \frac{1}{\Delta H} \int_0^{H/2} \left[ \left( \frac{q \cdot H}{2 \cdot L} - \tau_s \right)^{n+1} - \left( \frac{q \cdot h}{L} - \tau_s \right)^{n+1} \right] \times \frac{L}{(n+1) \cdot q \cdot \mu^n} dh \quad (10)$$

Taking into account that:

$$\Delta H = 0.5H - 0 = 0.5H \quad (11)$$

the expression (10) takes the form:

$$v_{ci} = \frac{2}{H} \int_0^{H/2} \left[ \left( \frac{q \cdot H}{2 \cdot L} - \tau_s \right)^{n+1} - \left( \frac{q \cdot h}{L} - \tau_s \right)^{n+1} \right] \times \frac{L}{(n+1) \cdot q \cdot \mu^n} dh \quad (12)$$

Equation (12) enables the adjustment of the material feed rate through the extruder channel with the movement of the 3D printer extruder, ensuring a uniform cross-section of the applied mixture layer on the printing surface.

To determine the productivity of the extruder  $Q$ ,  $m^3/s$ , we evaluate the definite integral of the obtained function (9) and multiply it by 2, since formula (9) describes only half of the channel height. Additionally, we multiply the resulting equation by - the channel width. For convenience, we express the channel width in terms of the average nozzle diameter, that is:

$$B = \pi \cdot D \quad (13)$$

Then the expression for calculating the extruder's productivity takes the form:

$$Q = \left( \int_0^{H/2} \left[ \left( \frac{q \cdot H}{2 \cdot L} - \tau_s \right)^{n+1} - \left( \frac{q \cdot h}{L} - \tau_s \right)^{n+1} \right] \times \frac{L}{(n+1) \cdot q \cdot \mu^n} dh \right) \cdot 4 \cdot D \quad (14)$$

## Conclusions

The conducted research allows us to state the following:

1. The application of additive technologies is currently a promising direction in the development of the construction industry.

2. The equipment used for 3D printing of building products and structures has several disadvantages, which can be avoided by applying scientifically substantiated technical solutions.

3. Ensuring high-quality 3D printing is possible by coordinating the amount of mixture supplied to the printing zone and the extruder's movement speed along the printing surface.

4. The scientific novelty of the obtained results lies in the derivation of analytical dependencies that relate the technical parameters of the construction 3D printer to the rheological properties of the extrusion material used.

## References

1. Заяць Є., Богданов І., Невгомонний Г., Мерилова І., Речиц О. (2021). Особливості використання технологій 3D-друку в будівництві. *Містобудування та територіальне планування*, (76), 83-93 <https://doi.org/10.32347/2076-815x.2021.76.83-93>
2. Hamidreza Gh.S., Corker J., Fan M. (2018). Additive manufacturing technology and its implementation in construction as an eco-innovative solution. *Automation in Construction*, 93, 1-11 <https://doi.org/10.1016/j.autcon.2018.05.005>
3. Андрийчук О.В., Оласюк П.Я. (2015). Застосування технології 3D-друку в будівництві. *Сучасні технології та методи розрахунків у будівництві*, 3, 11-18 <https://doi.org/10.1016/j.autcon.2018.05.005>
4. Лаухін Д.В., Дадіверіна Л.М., Твердохліб О.М., Матсук І.М. (2020). Аналіз застосування в будівельному виробництві адитивних технологій 3D-друку. *Збірник наукових праць національного гірничого університету*, 61, 163-177 <https://doi.org/10.33271/crpnmu/61.163>
1. Zayats Y., Bohdanov I., Nevhomonnyi H., Merilova I., Rechits O. (2021). Features of Using 3D Printing Technologies in Construction. *Urban Planning and Spatial Planning*, (76), 83-93 <https://doi.org/10.32347/2076-815x.2021.76.83-93>
2. Hamidreza Gh.S., Corker J., Fan M. (2018). Additive manufacturing technology and its implementation in construction as an eco-innovative solution. *Automation in Construction*, 93, 1-11 <https://doi.org/10.1016/j.autcon.2018.05.005>
3. Andriychuk O.V., Olasiuk P.Ya. (2015). Application of 3D Printing Technology in Construction. *Modern Technologies and Calculation Methods in Construction*, 3, 11-18 <https://doi.org/10.1016/j.autcon.2018.05.005>
4. Laukhin D.V., Dadyverina L.M., Tverdokhlib O.M., Matsyuk I.M. (2020). Analysis of the Application of Additive Manufacturing Technologies in Construction Production. *Collection of Scientific Papers of the National Mining University*, 61, 163-177 <https://doi.org/10.33271/crpnmu/61.163>

5. Згалат-Лозинська Л., Згалат-Лозинський О. (2020). Розвиток та впровадження інноваційних технологій 3D-друку у будівництві. *Вчені записки Таврійського національного університету імені В.І. Вернадського. Серія: Економіка і управління*, 31(70), 45-51  
<https://doi.org/10.32838/2523-4803/70-5-7>
6. Шатов С.В., Савицький М.В., Марченко І.О. (2019). Удосконалення обладнання 3D-друку об'єктів. *Вісник Придніпровської державної академії будівництва та архітектури*, 6(259-260), 90-101  
<https://doi.org/10.30838/J.BPSACEA.2312.261119.91.593>
7. Lipson H., Kurman Melba (2013). *Fabricated. The New World of 3D Printing*. Wiley
8. Ding T., Xiao J., Mechtcherine V. (2023). Microstructure and mechanical properties of interlayer regions in extrusion-based 3D printed concrete: A critical review. *Cement and Concrete Composites*, 141  
<https://doi.org/10.1016/j.cemconcomp.2023.105154>
9. Jacquet Y., Perrot A., Picandet V. (2021). Assessment of asymmetrical rheological behavior of cementitious material for 3D printing application. *Cement and Concrete Composites*, 140  
<https://doi.org/10.1016/j.cemconres.2020.106305>
10. Дворкін Л., Житковський В., Степасюк Ю., Марчук В. (2020). Ефективні будівельні розчини для 3D-принтера. *Будівельні матеріали та вироби*, 1-2(101), 16-21  
<https://doi.org/10.48076/2413-9890.2020-101-03>
11. Дворкін Л., Марчук В., Зятюк Ю. (2021). Цементно-шлакові суміші для 3D-принтеру. *Будівельні матеріали та вироби*, 1-2(102), 14-19  
<https://doi.org/10.48076/2413-9890.2021-102-02>
12. Теліцина Н. Є., Скіданова Г. М., Суруп І. В. (2010). Алгоритм підбору СБС на повітряних в'язучих із заданими реологічними показниками. *Східно-Європейський журнал передових технологій*, 2/10(44), 71-74  
<http://journals.uran.ua/eejet/article/view/2785/2591>
13. Крих Г.Б. (2007). Особливості застосування реологічних моделей неньютонівських рідин. *Вісник Національного університету «Львівська політехніка»*, 581, 71-82
14. Колчунов В.І. (2004). *Теоретична та прикладна гідромеханіка*. Київ: НАУ

5. Zgalat-Lozinska L., Zgalat-Lozinskyi O. (2020). Development and Implementation of Innovative 3D Printing Technologies in Construction. *Scientific Notes of V.I. Vernadsky Tavria National University. Series: Economics and Management*, 31(70), 45-51  
<https://doi.org/10.32838/2523-4803/70-5-7>
6. Shatov S.V., Savitsky M.V., Marchenko I.O. (2019). Improvement of Equipment for 3D Printing of Objects. *Bulletin of the Pridneprovsk State Academy of Civil Engineering and Architecture*, 6(259-260), 90-101  
<https://doi.org/10.30838/J.BPSACEA.2312.261119.91.593>
7. Lipson H., Kurman Melba (2013). *Fabricated. The New World of 3D Printing*. Wiley
8. Ding T., Xiao J., Mechtcherine V. (2023). Microstructure and mechanical properties of interlayer regions in extrusion-based 3D printed concrete: A critical review. *Cement and Concrete Composites*, 141  
<https://doi.org/10.1016/j.cemconcomp.2023.105154>
9. Jacquet Y., Perrot A., Picandet V. (2021). Assessment of asymmetrical rheological behavior of cementitious material for 3D printing application. *Cement and Concrete Composites*, 140  
<https://doi.org/10.1016/j.cemconres.2020.106305>
10. Dvorkin L., Zhytkovskiy V., Stepasyuk Y., Marchuk V. (2020). Efficient Construction Mixtures for 3D Printing. *Construction Materials and Products*, 1-2(101), 16-21  
<https://doi.org/10.48076/2413-9890.2020-101-03>
11. Dvorkin L., Marchuk V., Ziatyuk Y. (2021). Cement-Slag Mixtures for 3D Printing. *Construction Materials and Products*, 1-2(102), 14-19  
<https://doi.org/10.48076/2413-9890.2021-102-02>
12. Telitsina N.Ye., Skidanova G.M., Surup I.V. (2010). Algorithm for Selecting Fine-Grained Air-Binding Compositions with Given Rheological Indicators. *Eastern-European Journal of Advanced Technologies*, 2/10(44), 71-74  
<http://journals.uran.ua/eejet/article/view/2785/2591>
13. Krykh H.B. (2007). Features of Applying Rheological Models of Non-Newtonian Fluids. *Bulletin of Lviv Polytechnic National University*, 581, 71-82
14. Kolchunov V.I. (2004). *Теоретична та прикладна гідромеханіка*. Kyiv: NAU

UDC 332.83

## Organizational and technological aspects of applying ecological criteria in innovative low-rise construction

Perehinets Ivan<sup>1</sup>, Nazarenko Ivan<sup>2</sup>, Nesterenko Mykola<sup>3\*</sup>, Nesterenko Tetiana<sup>4</sup>

<sup>1</sup>Kyiv National University of Construction and Architecture <https://orcid.org/0000-0002-1888-3687>

<sup>2</sup>Kyiv National University of Construction and Architecture <https://orcid.org/0000-0003-3812-6509>

<sup>3</sup>National University «Yuri Kondratyuk Poltava Polytechnic» <https://orcid.org/0000-0002-4073-1233>

<sup>4</sup>National University «Yuri Kondratyuk Poltava Polytechnic» <https://orcid.org/0000-0002-2387-8575>

\*Corresponding author E-mail: [nesterenkonikola@gmail.com](mailto:nesterenkonikola@gmail.com)

At the current stage of society's development, more and more attention is paid to the search for constructive solutions to facilitate a healthy lifestyle. The work presents a cluster approach to the formation of the project of an innovative low-rise building under the conditions of ensuring environmental criteria, the principles of green construction by the flow method of raising buildings from ecological materials and quickly assembled modular elements. Such houses have low energy costs and make the most of the circle of quality and comfortable living. The solution of the specified approach and the adoption of relevant decisions were carried out using classical parametric system analysis and structural synthesis.

**Keywords:** flow construction method, energy efficiency, cluster construction, digitalization of the construction industry, low-rise construction

## Організаційно-технологічні аспекти застосування екологічних критеріїв в інноваційному малоповерховому будівництві

Перегінець І.І.<sup>1</sup>, Назаренко І.І.<sup>2</sup>, Нестеренко М.М.<sup>3\*</sup>, Нестеренко Т.М.<sup>4</sup>

<sup>1</sup>Київський національний університет будівництва та архітектури

<sup>2</sup>Київський національний університет будівництва та архітектури

<sup>3</sup>Національний університет «Полтавська політехніка імені Юрія Кондратюка»

<sup>4</sup>Національний університет «Полтавська політехніка імені Юрія Кондратюка»

\*Адреса для листування E-mail: [nesterenkonikola@gmail.com](mailto:nesterenkonikola@gmail.com)

У роботі запропоновано комплексний підхід на основі кластерного аналізу для розробки інноваційних рішень для малоповерхової забудови з акцентом на екологічні критерії та принципи «зеленого будівництва». Проведено аналіз, який підкреслює актуальну потребу у більш енергоефективному та сталому житловому фонді України та показує значну різницю в споживанні енергії між Україною та країнами-членами Європейського Союзу. Виділено неефективність існуючого житлового фонду та необхідність використання енергоефективних технологій протягом усього життєвого циклу будівництва. Доведено, що інтеграція моделей кластерів у будівельний процес дає різноманітні переваги, включаючи скорочення часу виведення інноваційних продуктів на ринок інновацій будівельних процесів, підвищення стабільності логістичних зв'язків, зменшення фінансових ризиків та розширення ринку збуту. Дослідження розглядає ключові аспекти організації будівництва, планування, управління та контролю якості в контексті кластерів. Досліджено метод потокового будівництва, який поєднує послідовний та паралельний методи, мінімізуючи їхні недоліки. Цей підхід ілюструється на прикладі проекту Bucha Techno Garden та показує, як даний метод може призвести до зниження витрат і зміцнення співпраці між учасниками кластера. Крім того, досліджено використання технології Building Information Modeling (BIM) як інструменту для ефективного управління інформацією, моніторингу процесів та оптимізації витрат протягом життєвого циклу будівництва. Цей підхід відповідає загальній тенденції цифровізації у будівельній галузі. Запропоновано підходи, що сприяють створенню житла, яке не лише відповідає сучасним екологічним та енергоефективним стандартам, але й направлені на підвищення комфорту і якості життя для мешканців.

**Ключові слова:** потоковий метод будівництва, енергоефективність, кластерне будівництво, цифровізація будівельної галузі, малоповерхова забудова

## Introduction

The work analyzes the suitability of residential and public buildings, which must be comfortable and safe, which are the initial environmental criteria. As you know, these criteria must be ensured in the design of one or another building, according to the purpose. To a large extent, this refers to the comfort conditions of living in low-rise buildings, since in such buildings the number of apartments and the number of residents are important. This is determined by the criterion that defines functional comfort, as the ability of people to live and communicate with each other in such a limited space. An important aspect of ensuring environmental sustainability is the constructive and planning solutions of architectural objects in such a space [1].

At the current stage of society's development, more and more attention is paid to the search for constructive solutions to ensure a healthy lifestyle. The cluster approach of forming the project of an innovative low-rise building under the conditions of ensuring ecological criteria, the principles of green construction by the flow method of raising buildings from ecological materials and quickly assembled modular elements is substantiated and developed [2, 3].

The main positive aspects of the cluster approach are:

- permanent participation of scientific and research and development sectors in the activities of the cluster;
- shortening the period of bringing innovative product units to the market;
- the formation of more stable logistic connections between enterprises;
- increasing predictability and predictability of cash flows;
- significant reduction of financial and credit risks;
- expansion of the sales market;
- growth of incentives to increase labor productivity;
- determination of the enterprise's share in the final innovative product and the integrated economic effect.

## Research results

The housing fund of Ukraine is in an unsatisfactory state from the point of view of fuel and energy efficiency. According to energy surveys, in residential buildings of mass construction of the past years, heat losses through the walls are 42%, through the windows - 16%, through the roof - 7%, through the basement - 5%, in the process of air exchange - 30%. (Table 1). In fact, the efficiency of thermal energy use in Ukrainian buildings is 3-5 times lower than in Western countries. Thus, according to experts' estimates, the specific consumption of heat and hot water in Ukraine is two times higher than that of EU member states with similar climatic conditions. The average specific energy consumption for heating per year in Ukraine is 264 kWh per square meter, while in EU countries - 130 kWh per square meter [7].

Construction of new community territories should be carried out exclusively using energy-efficient technologies during the life cycle [5].

**Table 1 – Heat losses through the enclosing structures of buildings**

Walls	Windows	Roof	Basement	Air exchange
%	%	%	%	%
42	16	7	5	30

Innovations in the organizational and production process during the construction of urban planning objects are a necessary condition for the transformation of the company's activities, which are accompanied by significant financial and time costs. Clusters make it possible to reduce such costs both at the stage of changing the structure of organizational and production processes and at the cost of current financial, organizational, technological and infrastructural transactions when producing a joint construction product by the flow method of construction. [4]

The organization of construction production based on cluster models provides for the following areas of scientific and production activity:

1. Construction organization - a system of formation or selection of a production enterprise (complex of enterprises) included in a cluster designed to fulfill the assigned task.

2. Planning – development of a system of linking construction and installation works, providing the construction process with material and technical resources.

3. Management – a system of compliance with design and estimate indicators and operational management of changes.

4. Quality control of construction and assembly, engineering and finishing works - a system of quality control of the supply of construction materials, structures and equipment, as well as the performance of the respective types of work.

Construction theory and practice distinguishes three main methods of construction of buildings and structures: sequential, parallel and flow [6].

With the sequential method of construction, each object of urban planning is erected after the completion of all works on the previous object. This method of work performance by crews carrying out various construction processes is accompanied by forced interruptions in work.

It is possible to start and finish construction processes on all objects at the same time. In this case, the construction time of all objects will be equal to the construction time of one object, but significant material and technical resources will be required. This method of conducting construction and assembly works is called a parallel method of construction.

The flow method of construction and assembly works in the development of territories according to the Comprehensive Spatial Development Plans (Fig. 1) combines sequential and parallel methods, preserving the advantages of both methods and eliminating the disadvantages.



Reducing the cost of the final construction product gives competitive advantages to cluster formations. The frequency of mutual contacts between the subjects of the cluster with the flow method of construction is so dense that their interaction goes from a purely production to a social-cooperative aspect, strengthening moral and ethical obligations and joint responsibility for the quality of the final result.

The cluster approach allows small and medium-sized construction firms to consolidate without losing their legal and financial autonomy, promotes the development of the middle class, gives clusters greater flexibility and speed of decision-making, which is not characteristic of larger bureaucratized companies. [2] Multiplication of cluster participants in production and geographical aspects integrally forms the most optimal composition of the material, technical and executive resource base for the construction of a building object as a separate commodity unit with specified operational

parameters, at a fixed price, in a specific UTC of Ukraine, at a specific time [1].

The cluster method of territory development involves the use of BIM technologies, as a new approach to digital information management, which is used in construction and urban planning and involves the collection and complex processing of all architectural, design, technological, economic and other information about the object. Thanks to their application, it is possible to virtually reproduce the object even before its construction begins, to monitor the life cycle processes of the construction object - from design to its construction, operation and dismantling. This approach makes it possible to increase the safety and reliability of buildings and structures, implement operational management of construction processes and control the quality of construction works, significantly reduce the probability of errors in projects, reduce the cost of construction and optimize costs at the operational stage.



**Figure 1 - Bucha Techno Garden project for the development of the territory of Bucha united territorial community, Kyiv region**

An example of the organization of innovative construction production is the cluster form (Fig. 2) of the branch of the Academy of Construction of Ukraine "Intersectoral Scientific and Production Cluster of Innovative Construction".

The important aspects of ensuring environmental sustainability are the constructive and planning solutions of architectural objects in a given space. The following requirements are put forward to the main volume-planning and constructive means of greening buildings:

- application of rational planning and construction solutions (in accordance with specific climatic conditions);
- maximum use of underground space;
- using the protective properties of the terrain;
- construction of "ecohouse" and "intelligent building" houses;
- landscaping of all surfaces of the building (walls, roof) and the surrounding area.

To ensure these conditions, an analysis of the suitability of residential and public buildings was carried out with the use of classical parametric system analysis and structural synthesis. Those buildings must be comfortable and safe, which are the original ecological criteria. As you know, these criteria must be ensured in the design decisions according to the purpose of the building. To a large extent, this refers to the comfort conditions of living in low-rise buildings, since in such buildings the number of apartments and the number of residents are important. This is determined by the criterion that defines functional comfort, as the ability of people to live and communicate with each other in such a limited space. Such a house should have low energy costs, making the most of the circle of quality and comfortable living (Fig. 3) [1].

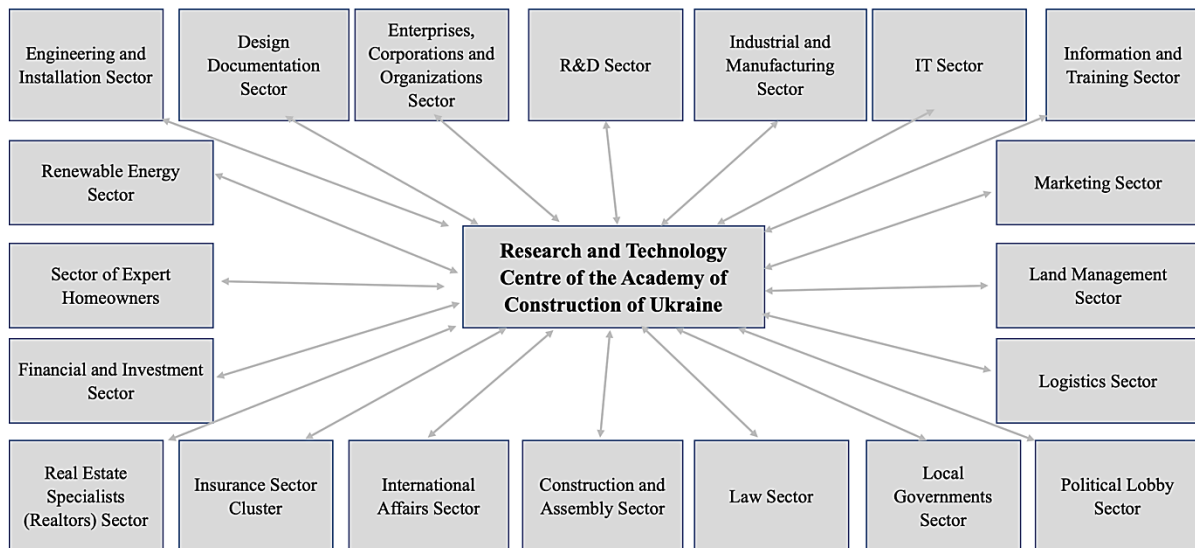


**Figure 2 – Graphic structure of the cluster of the Academy of Construction of Ukraine**

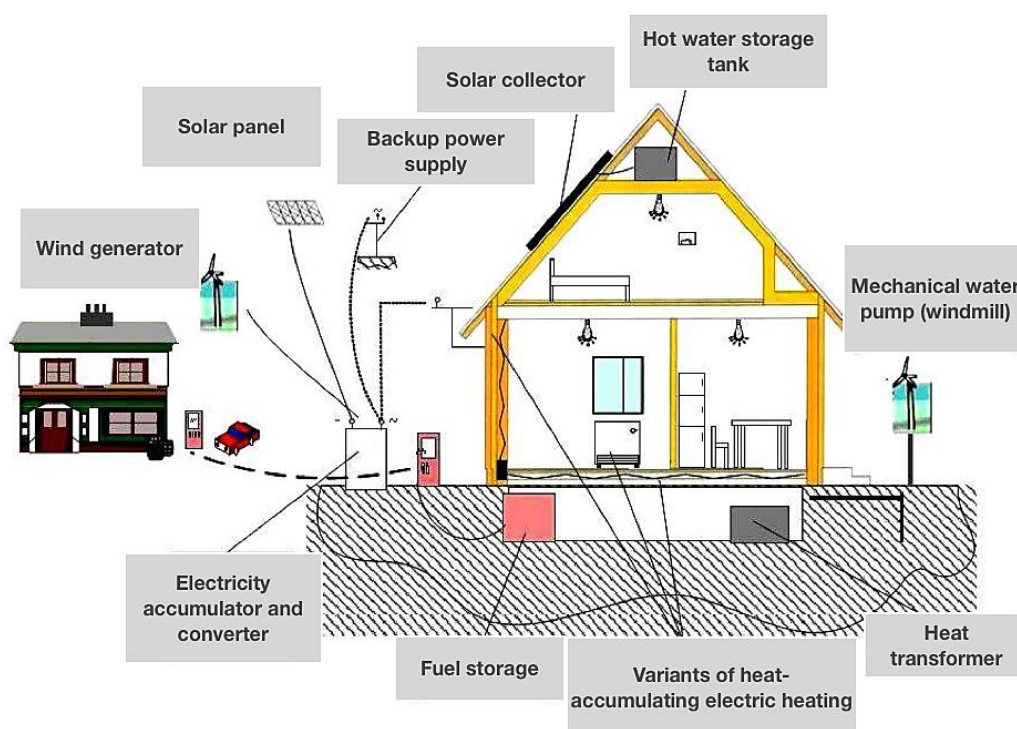


**Figure 3 – Schematic diagram of creating an ecological and energy-efficient house**

Effective and rational means in the field of energy-saving architectural and planning solutions include:

- simplification of the configuration of buildings (reduction of the area of enclosure structures relative to the total area);
- construction of attic floors in existing buildings;
- optimization of architectural forms in accordance with climatic features;
- optimal orientation of buildings to wind and sun.

Simplifying the configuration of buildings is relevant because it allows to reduce heat exchange with the environment due to the reduction of the area of contact surfaces. Hence, priorities shift towards greater values of life, the search for ways and means of survival of

humanity under the conditions of progressive deterioration of the ecological and social situation. In this regard, they are actively revising the traditional attitude to both man and nature, searching for new spiritual foundations for further civilizational development, forming new ideals of human activity and a new understanding of the human perspective. The solution of the mentioned approach and the adoption of appropriate decisions are implemented in the proposed comfortable and energy-saving eight-apartment building with the symbolic name "BIDEN", including the rationally considered aspects of anthropometry and psychology of human behavior in such a space (Fig. 4).





**Figure 4 – General view of an ecological and energy-efficient building with the symbolic name "BIDEN"**

Special attention is paid to the psychological aspect, which is demonstrated in specific constructive solutions. The accepted condition is the well-known statement that the psychological aspect is related to the fact that space is evaluated by a person in terms of distances and orientation: large spaces can "separate" people, and small rooms cause a feeling of discomfort. Figure 5 shows the spatial model of the house of the "Biden" project.



**Figure 5 – Spatial model of the house of the BIDEN project**

In the proposed innovative project, for the first time in a low-rise building, the maximum use of the underground space, which can actually be attributed to the elements of underground urbanism, is realized. The presence of a reinforced concrete shelter under the house against possible artillery, rocket or small arms attacks is essential to preserving people's lives and health. That is why the basement of the "Biden" house is made as a monolithic reinforced concrete structure of the floor and walls with a reinforced monolithic floor of the basement part of the house, which is 80% submerged below the ground level. This makes it possible to save basement structures from shock waves or ruptures. An important parameter of quality shelter is also the presence of an additional exit, so as not to get trapped under the debris of construction structures.

The BIDEN project provides for an exit through an adjacent room located at 90° from the first one. Finishing of the basement is at the residential level: polymer seamless floor coverings; high-quality painting of the walls and ceiling, ceramic heating panels with digital temperature control; LED lighting; the possibility of installing bathrooms. In peacetime, the premises can be used as an office, gym, dressing room, food pantry, etc. Entrance to the shelter/basement from one's own plot of land. All 8 basement rooms of the house are equipped with ventilation systems with recuperation, fire extinguishers, axes and long-lasting battery lights.

Plants are an important means of greening buildings and the architectural environment as a whole. It is generally known about the ability of plants to absorb carbon dioxide and produce oxygen, to protect buildings from wind and noise, that is, to improve the quality of the ecological parameters of the environment. In addition, plants have a positive effect on the psycho-emotional state of people, mitigating the aggressive effect of the urbanized environment. Because of this, a tendency to green all surfaces of the building arose and is actively developing in the world. Buildings and structures organically connected with living nature (with a green roof, walls, etc.) are called biopositive.

During the reconstruction of the existing building and the construction of new biopositive structures, it is advisable to provide archophytomelioration measures: landscaping of basement floors (biopositive constructions of extensions and plinths, creation of phytoscreening wall coverings, etc.); landscaping of all free areas of the territory and above-ground territories above the objects of underground urbanism; vertical landscaping of walls (verandahs, terraces, ampelous coverings, hanging systems); winter gardens inside the buildings [9].

Ecological architecture involves energy saving, the use of ecologically compatible building materials and structures, the use of alternative energy sources and the correct disposal of waste.

## Conclusions

The research presents a cluster-based approach to innovative low-rise building projects with a strong emphasis on environmental sustainability and green construction principles. The study underscores the urgent need for energy-efficient housing solutions in Ukraine, given the significant energy consumption gap with EU member states. The integration of cluster models into construction processes offers numerous advantages, including shorter time-to-market for innovative products and enhanced logistic connections. The flow method of construction, combining sequential and parallel methods, proves to be a viable approach for cost reduction and cooperative synergy within cluster formations.

Additionally, the utilization of Building Information Modeling (BIM) technology emerges as a pivotal tool for efficient project management and cost optimization. This study contributes valuable insights into sustainable building practices, aligning them with the evolving societal needs for healthier, greener, and more energy-efficient living spaces.



## References

1. Pereghinets I.I. (2017). Cluster forms of construction production organization in the conditions of development of socio-economic transformations of modern Ukraine. *Urban planning and territorial planning*, 64, 560-569
2. Malyar S.A. (2022). Formation of the organizational and economic mechanism for the development of the housing stock. *Bulletin of the Khmelnytskyi National University. Economic sciences*, 1, 305-309
3. Zayats V.S. (2019). The development of housing construction as a factor in the formation of housing conditions of the population. *Demography and social economy*, 2(3), 137-151
4. Biloshytska N.I., Biloshytskyi M.V., Tatarchenko Z.S., Medvid I.I. (2019). Analysis of Comfortability of House Territories of Different Building Types In Severodonetsk Town. *Visnik of Volodymyr Dahl East Ukrainian National University*, 8(256), 23-29  
<https://doi.org/10.33216/1998-7927-2019-256-8-23-29>
5. Yurin O., Avramenko Y., Leshchenko M., Rozdabara O. (2020) Research of Possible Methods of Increasing the Duration of the Insolation of Rooms in Residential Buildings. *Lecture Notes in Civil Engineering*, 73, 312-323  
[https://doi.org/10.1007/978-3-030-42939-3\\_32](https://doi.org/10.1007/978-3-030-42939-3_32)
6. ДБН В.2.1-10: 2018 (2018). *Основи і фундаменти будівель та споруд. Основні положення*. Київ: Міністерство регіонального розвитку, будівництва та житлово-комунального господарства України
7. Kariuk A., Mishchenko R., Pents V., Shchepak V. (2019). Energy performance of buildings in European Union countries and Ukraine. *Academic Journal. Industrial Machine Building, Civil Engineering*, 1(52), 185-190  
<https://doi.org/10.26906/znp.2019.52.1695>
8. ДБН В.2.2-15-2015 (2015). *Житлові будинки. Основні положення*. Київ: Мінбуд України
9. Koshlaty O., Kariuk A. & Mischenko R. (2015). The development and prospects analysis of buildings thermal protection standardization in Ukraine. *Intern. Scientific Journal «Theoretical & Applied Science»*, 09(29), 21-23
1. Pereghinets I.I. (2017). Cluster forms of construction production organization in the conditions of development of socio-economic transformations of modern Ukraine. *Urban planning and territorial planning*, 64, 560-569
2. Malyar, S.A. (2022). Formation of the organizational and economic mechanism for the development of the housing stock. *Bulletin of the Khmelnytskyi National University. Economic sciences*, 1, 305-309
3. Zayats V.S. (2019). The development of housing construction as a factor in the formation of housing conditions of the population. *Demography and social economy*, 2(3), 137-151
4. Biloshytska N.I., Biloshytskyi M.V., Tatarchenko Z.S. & Medvid I.I. (2019). Analysis of Comfortability of House Territories of Different Building Types In Severodonetsk Town. *Visnik of Volodymyr Dahl East Ukrainian National University*, 8(256), 23-29  
<https://doi.org/10.33216/1998-7927-2019-256-8-23-29>
5. Yurin O., Avramenko Y., Leshchenko M., Rozdabara O. (2020) Research of Possible Methods of Increasing the Duration of the Insolation of Rooms in Residential Buildings. *Lecture Notes in Civil Engineering*, 73, 312-323  
[https://doi.org/10.1007/978-3-030-42939-3\\_32](https://doi.org/10.1007/978-3-030-42939-3_32)
6. ДБН В.2.1-10: 2018. (2018). *Bases and foundations of buildings and structures. Main principles*. Kyiv: Ministry of Regional Development, Construction, and Housing of Ukraine
7. Kariuk A., Mishchenko R., Pents V., Shchepak V. (2019). Energy performance of buildings in European Union countries and Ukraine. *Academic Journal. Industrial Machine Building, Civil Engineering*, 1(52), 185-190  
<https://doi.org/10.26906/znp.2019.52.1695>
8. ДБН В.2.2-15-2015. (2015). *Residential buildings. Fundamentals principles*. Kyiv: Ministry of Construction of Ukraine
9. Koshlaty O., Kariuk A. & Mischenko R. (2015). The development and prospects analysis of buildings thermal protection standardization in Ukraine. *Intern. Scientific Journal «Theoretical & Applied Science»*, 09(29), 21-23

УДК 621.01:69]-868

## Determination of the vibrating table kinetic energy

Korobko Bogdan<sup>1\*</sup>, Zhyhylii Serhii<sup>2</sup>, Korotych Yuriy<sup>3</sup>

<sup>1</sup> Poltava National Technical Yuri Kondratyuk University <https://orcid.org/0000-0002-9086-3904>

<sup>2</sup> Poltava National Technical Yuri Kondratyuk University <https://orcid.org/0000-0001-5829-9226>

<sup>3</sup> Poltava National Technical Yuri Kondratyuk University <https://orcid.org/0000-0002-1961-5318>

\*Corresponding author E-mail: [korobko@pntu.edu.ua](mailto:korobko@pntu.edu.ua)

The article determines the total kinetic energy of the vibrating table, in which the vibrator is fixed on a lever vertically in the center under the vibrating plate. To find the total kinetic energy, a kinematic diagram of the vibrating table under study was drawn up, and the functional dependence of the vibrating table total kinetic energy on the factors acting on it obtained. A graph of the change in the vibrating table kinetic energy under study was drawn depending on the lever length, on which the vibrator was fixed. The analysis of the resulting dependence indicates an increase in the kinematic energy of the vibrating table with an increase in the lever length. The obtained kinetic energy is necessary for the development of an above-mentioned equipment mathematical model, which will be compiled later using Lagrange equations of the second kind

**Keywords:** vibrating table, lever, vibrator, imbalance, degree of freedom, kinetic energy

## Визначення кінетичної енергії вібраційного столу

Коробко Б. О.<sup>1\*</sup>, Жигилій С. М.<sup>2</sup>, Коротич Ю. Ю.<sup>3</sup>

<sup>1</sup> Національний університет «Полтавська політехніка імені Юрія Кондратюка»

<sup>2</sup> Національний університет «Полтавська політехніка імені Юрія Кондратюка»

<sup>3</sup> Національний університет «Полтавська політехніка імені Юрія Кондратюка»

\*Адреса для листування E-mail: [korobko@pntu.edu.ua](mailto:korobko@pntu.edu.ua)

В статті проводиться визначення загальної кінетичної енергії технологічного комплексу обладнання для виробництва бетонних виробів (вібростолу), у якого вібробудувач закріплюється на важелі вертикально по центру під віброплиною. Дане обладнання використовується для виготовлення малогабаритних бетонних виробів. При виконанні досліджень були використані методи математичної фізики та фізико-математичне моделювання методами прикладної механіки. Для визначення положення і опису вільних рухів матеріальних тіл, з яких складається розглядувана механічна система, була застосована ортогональна вібраційна система відліку з трьох систем координат. Для знаходження загальної кінетичної енергії, що є сумою кінетичних енергій декількох матеріальних тіл - плити, корпусу вібробудувача, дебаланса і смоні з бетонною сумішшю, була складена кінематична схема досліджуваного вібростолу і отримана функціональна залежність загальної кінетичної енергії вібростолу від діючих на нього факторів. Був побудований графік зміни кінетичної енергії досліджуваного вібраційного столу залежно від довжини важеля, на якому закріплювався вібробудувач, із врахуванням номінальних чисельних значень величин параметрів вібростолу. Аналіз одержаної залежності вказує на збільшення кінематичної енергії вібростолу при збільшенні довжини важеля, що підтверджує ефективність важільного закріплення вібробудувача. Це в свою чергу призводить до зменшення енерговитрат під час віброущільнення бетонних виробів за рахунок зменшення потужності використовуваного для ущільнення вібробудувача. Отримана функціональна залежність кінетичної енергії також необхідна для складання в подальшому математичної моделі вищезгаданого обладнання за допомогою рівнянь Лагранжа другого роду

**Ключові слова:** вібростіл, важіль, вібратор, дебаланс, ступінь вільності, кінетична енергія

## Introduction

Vibration is the most common method of compacting concrete composites [1,2]. More than 90% of all construction products made of concrete and reinforced concrete are made using this method of concrete mix compaction [3]. This is explained by the fact that in the process of vibrational action on concrete mixtures, favorable conditions for thixotropic rarefaction and the most compact placement of aggregate particles are created [4,5].

The modern development of construction requires the introduction of the latest technologies and the installation of engineering equipment for various purposes according to the criteria of energy minimization and high efficiency of the technological process. There are a huge variety of vibration machines used in construction, which differ in design and purpose. And, above all, great attention should be paid to the development and implementation of energy-saving technologies and equipment.

A review of various vibration equipment designs shows, that in the manufacture of a wide concrete products range equipment with the required operating parameters used, with the help of which high-quality vibration compaction of the concrete mix is achieved. In order to find out the influence of individual parameters of the developed by us technological set of equipment for the manufacture of concrete products [6] on the movement of its working body and energy consumption, it is necessary to determine the kinetic energy and make a mathematical model of this mechanical system.

## Review of the research sources and publications

Extensive use of vibration technology, numerous theoretical and experimental studies of the dynamics of vibrating machines made it possible to identify the features of their work, to explain and put into practice the peculiar effects that occur during the action of vibration on mechanical systems [7,8,9]. Therefore, a lot of research and development is devoted to this issue [10,11], which reveals such advantages of vibration equipment as high sealing efficiency, simplicity of design, high reliability and relatively low metal consumption and energy intensity. One of the priority directions of construction vibration equipment development is to reduce energy costs in production. Energy saving technologies along with increasing productivity and improving product quality occupy a priority place in modern construction.

In our case, we need to create a vibrating table, which by placing a vibration exciter on the vertical lever under the vibrating plate would save energy in the manufacture of concrete products by reducing the power of the vibrator while maintaining the required parameters of vibration compaction.

## Definition of unsolved aspects of the problem

It is necessary to make a mathematical model of the developed and constructed vibration table according to the kinematic scheme, that has not been used before, having previously determined its kinetic energy.

## Problem statement

The purpose of this work is to obtain the functional dependence of mechanical system total kinetic energy, that simulates a vibrating table with a vibrating exciter placed on a vertical lever under the vibrating plate. This functional dependence of kinetic energy is necessary for the analysis of technological factors, in particular the length of the lever, having an impact on the energy intensity of this mechanical system, as well as for further compilation of a technological equipment set mathematical model for the manufacture of concrete products (vibrating table) using the Lagrange equations of the second order.

To achieve a certain goal, it is necessary to solve the following tasks:

1. Create a kinematic diagram of the vibrating table with a vibration exciter placed on a vertical lever under the vibrating plate.
2. To determine the kinetic energy of individual material bodies composing the vibro-table.
3. Formulate the functional dependence of the total kinetic energy of the vibro-table on the factors affecting it.
4. Build a graphical dependence of the change in the kinetic energy of the vibrating table under study depending on the length of the lever on which the vibration exciter is fixed.

## Basic material and results

To clarify the general trend of vibration table for the manufacture of small-sized concrete products individual parameters influence on the movement of his working body, as well as the mutual influence of the vibrating table individual nodes movement let us consider it as a mechanical system, get this mechanical system a mathematical model, and solve it.

The general view of the technological set of equipment for the concrete products manufacture (vibrating table) is shown in Fig. 1.

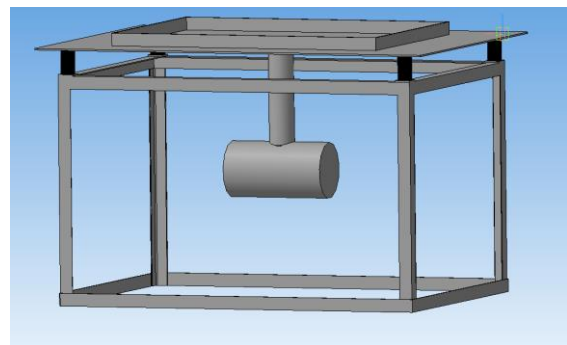


**Figure 1 – General view of the technological set of equipment for the manufacture of concrete products**

Technological set of equipment (subsequently vibrating table) consists (see Fig. 2) from the plate 1 with dimensions  $2a_1 \times 2b_1$  in projections and thickness  $2\delta_1$ , which rests on a fixed supporting surface with the help of four elastic elements with rigidity  $C$  each. To the plate 1 lever 2 is rigidly attached with length  $l_{lever}$ , to the lower end of which is also rigidly attached mechanical

centrifugal imbalanced oscillator exciter (vibrator), de-balancing shaft axis of rotation 4 which, at rest, the vibrating table is parallel to the longer axis of symmetry of the plate 1. On shaft 4 imbalance 5 rigidly fixed, the rotation of which generates, provides and determines the working technological movement of the vibrating table under consideration. On plate 1 symmetrically placed and rigidly fixed technological tank for concrete products molding.

Undoubtedly, the primary source of operation for the vibrating table used in the production of small-sized concrete products is the rotation of the unbalanced shaft 4 with imbalance 5 of exciter, parameters and characteristics of which completely determine the structure, magnitude and effectiveness of the dynamic action on the processed medium [12].

To obtain a mathematical model, let us use the Lagrange equations of the second order [13]

$$\frac{d}{dt} \left( \frac{\partial T}{\partial \dot{q}_i} \right) - \frac{\partial T}{\partial q_i} = Q_i \quad (i = 1, 2, \dots, s), \quad (1)$$

where  $T$  – kinetic energy of a mechanical system.

To find kinetic energy  $T$  let us consider in Figure 3 the kinematic scheme of the vibration table, as a mechanical system consisting of a plate 1, which is the working body of the vibrating table and which we will consider as an absolutely solid body in the form of a homogeneous rectangular parallelepiped with mass  $m_1$ . The external restraints that limit the movement of the slab are elastic elements (springs), with distances between vertical longitudinal axes equal to  $2a$  and  $2b$  (see. Fig. 2). Lever weight 2 ignored. The exciter consists of its body 3, which we take for an absolutely solid homogeneous hollow circular cylinder with a mass  $m_3$ ,

inside which the debalanced shaft 4 has the ability to rotate (the mass of which is also neglected) with an imbalance 5 located on it, with mass  $m$  and eccentricity  $e$ . Central longitudinal axis of the body 3 of exciter determines the rotation axis position of its debalancing shaft 4.

In a first approximation, the container fixed on the slab, together with the concrete mix to be molded, will be considered as a homogeneous solid with mass  $m_6$  in the form of a rectangular parallelepiped dimensions  $2a_6 \times 2b_6 \times 2h_6$ , which is rigidly attached to the plate 1 (see Fig. 2).

Thus, the considered vibration device is modeled by a mechanical system consisting of four material bodies.

During the direct vibration action, which determines the process of manufacturing (molding) concrete products, material bodies 1, 3 and 6 carry out complex spatial movements that can be considered as free. The movement of a free solid can be decomposed in many ways [14] for two movements: a) translational motion together with an arbitrarily selected fixed point of the body, which is called the pole; b) spherical motion around this pole.

To determine the position and description of the free motions of material bodies of the mechanical system under consideration, we apply an orthogonal vibration reference frame [15], which consists of three coordinate systems: fixed  $Oxyz$  and movable  $Cx'y'z'$  and  $Cx_1y_1z_1$ . Start of count  $O$  of system  $Oxyz$  let us associate with the center of plate 1 inertia  $C$  in the position of mechanical system static equilibrium, which is shown in the Figure 2, by aligning the corresponding coordinate axes with the main central axes of plate inertia.

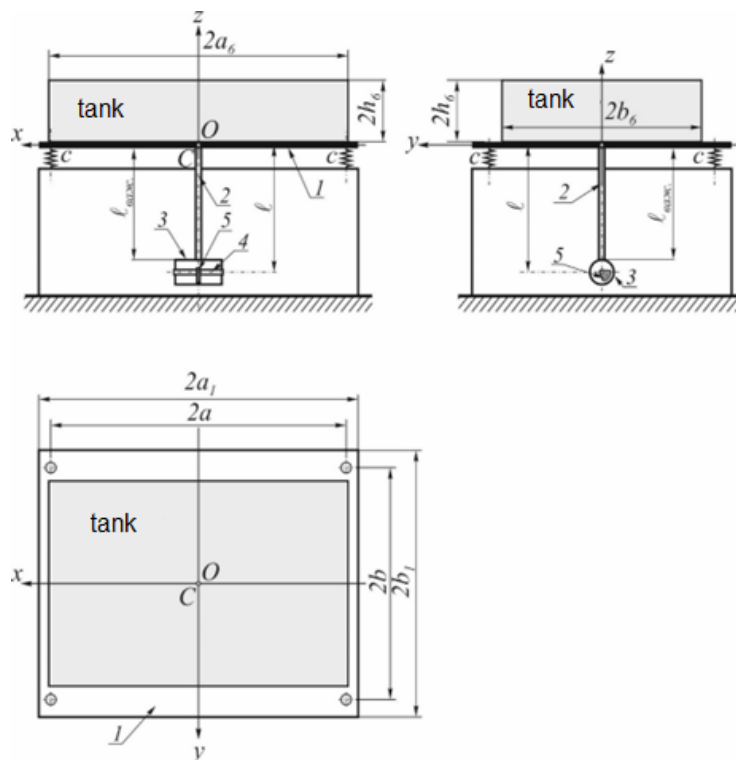
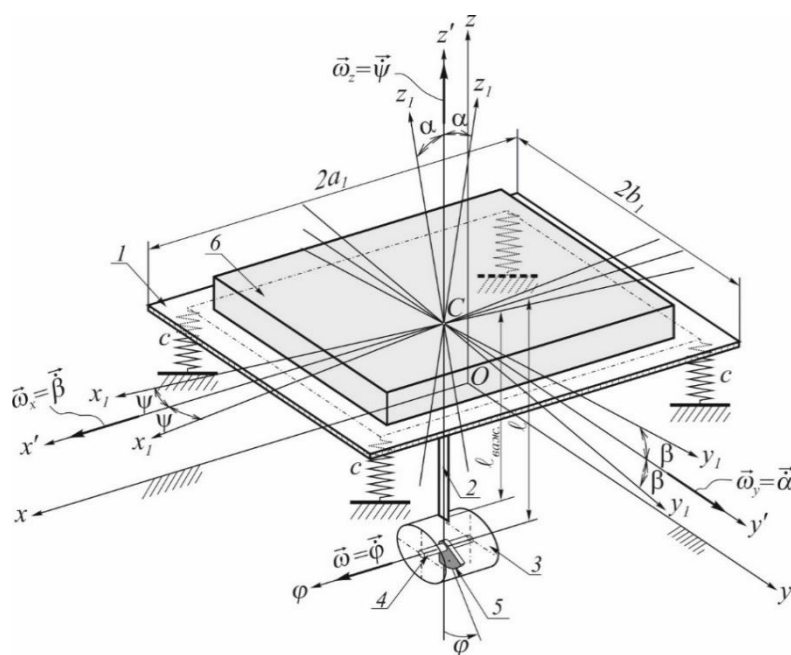


Figure 2 – Vibrating table for the manufacture of concrete products



**Figure 3 – Kinematic scheme of the vibrating table**

The origin of both moving coordinate systems moves with the point  $C$ ; In this case, the system  $Cx'y'z'$  moves progressively, so that its axes remain parallel to the axes of the fixed coordinate system, and the system  $Cx_1y_1z_1$  rigidly bound to the plate 1. In the static equilibrium position of a mechanical system, all three coordinate systems coincide, and when a mechanical system moves, a point  $C$  uniquely characterizes the motion of the center of inertia of a plate relative to a fixed coordinate system  $Cxyz$ .

Euler's angles of rotation of the moving system relative to the fixed one will be replaced by vibrational angles of rotation  $\alpha$ ,  $\beta$  and  $\psi$  (Fig. 4), where:

- $\alpha$  specifies the plate rotation angle 1 (or movable system  $Cx_1y_1z_1$ ) in the frontal coordinate plane  $Cx'z'$  around the axis  $Cy'$  or (which is the same) around a fixed axis  $Oy$  with angular velocity  $\dot{\alpha}$ ;
- $\beta$  – plate 1 rotation angle in the profile plane  $Cy'z'$  around the axis  $Ox$  with angular velocity  $\dot{\beta}$ ;
- $\psi$  – plate 1 rotation angle in the horizontal plane  $Cx'y'$  around the axis  $Oz$  with angular velocity  $\dot{\psi}$ .

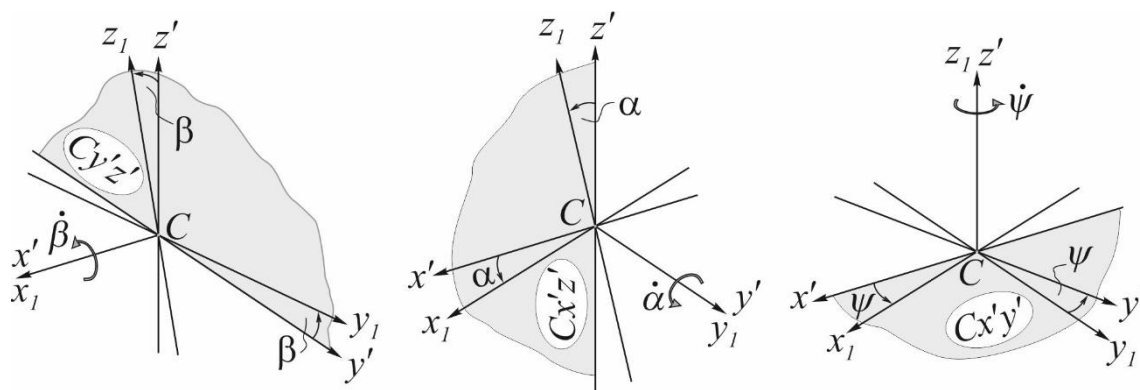


**Figure 4 – Vibration count system**

When moving a mechanical system, vibration angles  $\alpha$ ,  $\beta$  and  $\psi$  acquire only small values, which distinguishes them favorably from Eulerian angles, in which only the nutation angle is small, and the angles of precession and self-rotation may not be small. Vibration angles are of the same order and are given by periodic trigonometric functions; corresponding angular velocities  $\dot{\alpha}$ ,  $\dot{\beta}$  and  $\dot{\psi}$  are same order with angular velocity  $\omega = \dot{\phi}$ .

Such assumptions make it possible to significantly simplify the process of determining kinetic energy and obtain a simpler mathematical model, which describes with a high degree of accuracy the position and movement of any point and individual material body of the table under study.

Since the mechanical system that simulates the vibrating table consists of four material bodies, its kinetic energy



$$T = T_1 + T_3 + T_5 + T_6, \quad (2)$$

where  $T_1, T_3, T_5, T_6$  – accordingly, the kinetic energies of each of the bodies.

To find  $T_1$  let's choose the center of inertia beyond the pole  $C$  of plate 1; then by Koenig's theorem [16]

$$T_1 = \frac{m_1 \cdot v_c^2}{2} + \frac{I_1 \Omega_1 \cdot \omega_1^2 \Omega_1}{2}, \quad (2)$$

Where  $v_c$  – point speed module  $C$ ;

$\omega_1 \Omega_1$  – plate 1 instantaneous angular velocity module around the axis  $\Omega_1$  of instant rotation, which in the considered position of the mechanical system passes through a point  $C$ ;

$I_1 \Omega_1$  – axial moment of plate inertia 1 relative to the instantaneous axis  $\Omega_1$ .

Due to the fact that the origin of the moving reference frame is chosen in the plate 1 inertia center, then [17]

$$T_1 = \frac{m_1}{2} v_c^2 + \frac{1}{2} (I_{1x_1} \omega_{1x}^2 + I_{1y_1} \omega_{1y}^2 + I_{1z_1} \omega_{1z}^2),$$

where  $I_{1x_1}, I_{1y_1}, I_{1z_1}$  – accordingly, the plate 1 inertia moments relative to coordinate axes  $Cx_1, Cy_1$  and  $Cz_1$ ;  $\omega_{1x}, \omega_{1y}, \omega_{1z}$  – projections of instantaneous angular velocity  $\vec{\omega}_{1\Omega_1}$  on the corresponding axes of the fixed system  $Oxyz$ .

Next, we note that  $\omega_{1x} = \dot{\beta}$ ,  $\omega_{1y} = \dot{\alpha}$  and  $\omega_{1z} = \dot{\psi}$ , and with the coordinate method of determining the point motion [18] module  $v_c = \sqrt{v_{cx}^2 + v_{cy}^2 + v_{cz}^2}$ , where  $v_{cx} = \dot{x}_c$ ,  $v_{cy} = \dot{y}_c$  and  $v_{cz} = \dot{z}_c$  – vector projections  $\vec{v}_c$  to the axis  $Oxyz$ . Then

$$v_c^2 = \dot{x}_c^2 + \dot{y}_c^2 + \dot{z}_c^2.$$

Substituting all the above values, we finally get that

$$T_1 = \frac{m_1}{2} (\dot{x}_c^2 + \dot{y}_c^2 + \dot{z}_c^2) + \frac{I_{1x_1}}{2} \dot{\beta}^2 + \frac{I_{1y_1}}{2} \dot{\alpha}^2 + \frac{I_{1z_1}}{2} \dot{\psi}^2, \quad (3)$$

To find  $T_3$  we choose the center of inertia for the pole  $C_3$  of the exciter body 3. Similar to the definition  $T_1$  we get that

$$T_3 = \frac{m_3}{2} v_{C_3}^2 + \frac{1}{2} (I_{3x_3} \omega_{3x}^2 + I_{3y_3} \omega_{3y}^2 + I_{3z_3} \omega_{3z}^2).$$

Since the plate 1, lever 2 and body connected rigidly, then according to the concepts of theoretical mechanics these three different physical bodies are one material body, because of which

$$\omega_{3x} = \omega_{1x} = \dot{\beta},$$

$$\omega_{3y} = \omega_{1y} = \dot{\alpha},$$

$$\omega_{3z} = \omega_{1z} = \dot{\psi}.$$

Absolute speed [19] vector  $\vec{v}_3$  of body mass center 3

$$\vec{v}_{C_3} = \vec{v}_{C_3e} + \vec{v}_{C_3r},$$

where  $\vec{v}_{C_3e}$  and  $\vec{v}_{C_3r}$  – respectively, the vectors of portable and relative velocities of the point  $C_3$ .

Since portable movement is free, then

$$\vec{v}_{C_3e} = \vec{v}_{C_3e1} + \vec{v}_{C_3e2},$$

where  $\vec{v}_{C_3e1}$  – pole velocity;  $\vec{v}_{C_3e2}$  – point velocity  $C_3$  in its spherical motion around the pole.

Since a point is chosen as the pole  $C$ , then

$$\vec{v}_{C_3e1} = \vec{v}_C = \vec{i} \cdot \dot{x}_C + \vec{j} \cdot \dot{y}_C + \vec{k} \cdot \dot{z}_C.$$

To find  $\vec{v}_{C_3e2}$  let's apply vibration angles and depict body 3 inertia center  $C_3$  (see Fig. 5) in three orthogonal projections, where  $\ell = CC_3 = \ell_{\text{в.а.ж.}} + (\delta_1 + R_3)$ ;  $R_3$  – outer body radius 3.

Let's write  $\vec{v}_{C_3e2}$  as the sum of three addends

$$\vec{v}_{C_3e2} = \vec{v}_{3xy} + \vec{v}_{3xz} + \vec{v}_{3yz},$$

where  $\vec{v}_{3xy}, \vec{v}_{3xz}$  and  $\vec{v}_{3yz}$  – vector projections  $\vec{v}_{C_3e2}$  to planes  $xy, yz$  and  $zx$

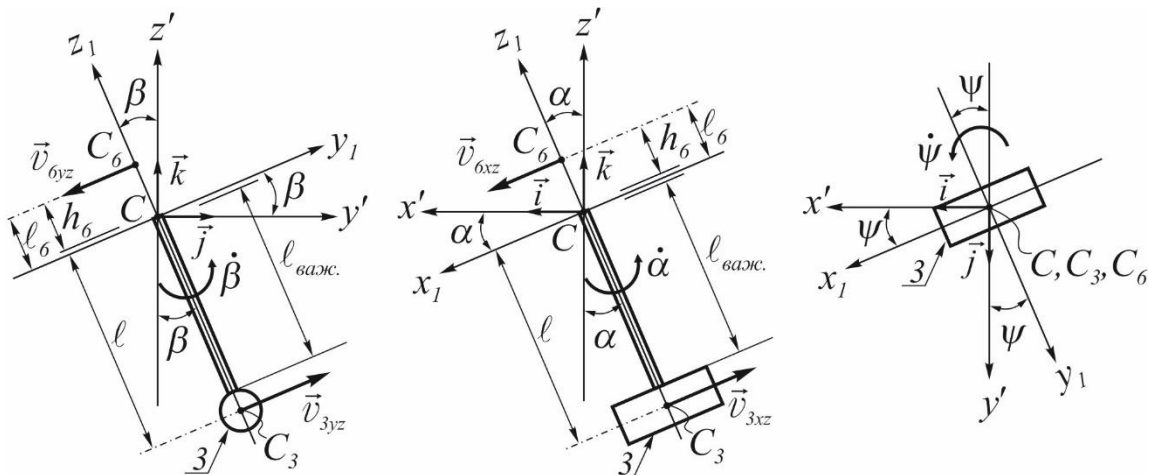


Figure 5 – To determining a portable speed  $\vec{v}_{C_3e2}$  and  $\vec{v}_{C_3e1}$

From Figure 5 it is obvious that the velocity modules  $v_{3yz} = \dot{\beta} \cdot l$ ,  $v_{3xz} = \dot{\alpha} \cdot l$  and  $v_{3xy} = \dot{\psi} \cdot 0 = 0$ , and the corresponding projections on the specified planes:

$$\begin{aligned}\vec{v}_{3yz} &= \vec{j} \cdot v_{3yz} \cdot \cos\beta + \vec{k} \cdot v_{3yz} \cdot \sin\beta = \\ &= \vec{j} \cdot \dot{\beta} \cdot l \cdot \cos\beta + \vec{k} \cdot \dot{\beta} \cdot l \cdot \sin\beta\end{aligned}$$

$$\begin{aligned}\vec{v}_{3xz} &= -\vec{i} \cdot v_{3xz} \cdot \cos\alpha + \vec{k} \cdot v_{3xz} \cdot \sin\alpha = \\ &= -\vec{i} \cdot \dot{\alpha} \cdot l \cdot \cos\alpha + \vec{k} \cdot \dot{\alpha} \cdot l \cdot \sin\alpha\end{aligned}$$

Adding, we get that

$$\begin{aligned}\vec{v}_{C_3e_2} &= -\vec{i} \cdot \dot{\alpha} \cdot l \cdot \cos\alpha + \vec{j} \cdot \dot{\beta} \cdot l \cdot \cos\beta + \\ &+ \vec{k} \cdot (\dot{\alpha} \cdot l \cdot \sin\alpha + \dot{\beta} \cdot l \cdot \sin\beta)\end{aligned}$$

$$\begin{aligned}\vec{v}_{C_3e} &= \vec{i}(\dot{x}_c - \dot{\alpha} \cdot l \cdot \cos\alpha) + \vec{j}(\dot{y}_c + \dot{\beta} \cdot l \cdot \cos\beta) + \\ &+ \vec{k}(\dot{z}_c + \dot{\alpha} \cdot l \cdot \sin\alpha + \dot{\beta} \cdot l \cdot \sin\beta)\end{aligned}$$

Since the plate 1, lever 2 and body 3 connected rigidly, then any movement of the point  $C_3$  relative to the point  $C$  absent, which is why  $\vec{v}_{C_3r} = 0$ , and

$$\begin{aligned}\vec{v}_{C_3} &= \vec{i}(\dot{x}_c - \dot{\alpha} \cdot l \cdot \cos\alpha) + \vec{j}(\dot{y}_c + \dot{\beta} \cdot l \cdot \cos\beta) + \\ &+ \vec{k}(\dot{z}_c + \dot{\alpha} \cdot l \cdot \sin\alpha + \dot{\beta} \cdot l \cdot \sin\beta)\end{aligned}$$

Squaring the resulting expression and substituting the value  $v_{C_3}^2$  into the formula of kinetic energy  $T_3$  for body 3, we get

$$\begin{aligned}T_3 &= 0.5m_3(\dot{x}_c^2 + \dot{y}_c^2 + \dot{z}_c^2) - m_3 \cdot l \cdot \dot{x}_c \cdot \dot{\alpha} \cdot \cos\alpha + \\ &+ m_3 \cdot l \cdot \dot{y}_c \cdot \dot{\beta} \cdot \cos\beta + m_3 \cdot l \cdot \dot{z}_c \cdot \dot{\alpha} \cdot \sin\alpha + \\ &+ m_3 \cdot l \cdot \dot{z}_c \cdot \dot{\beta} \cdot \sin\beta + 0.5m_3 \cdot l^2 \cdot \dot{\alpha}^2 + \\ &+ 0.5I_{3x_3} \cdot \dot{\beta}^2 + 0.5I_{3y_3} \cdot \dot{\alpha}^2 + 0.5I_{3z_3} \cdot \dot{\psi}^2.\end{aligned}\quad (4)$$

Choosing center of Inertia  $C_6$  as pole of material body 6, similar to the definition  $T_3$  we consistently establish that

$$\begin{aligned}T_6 &= 0.5m_6(\dot{x}_c^2 + \dot{y}_c^2 + \dot{z}_c^2) - m_6 \cdot l_6 \cdot \dot{x}_c \cdot \dot{\alpha} \cdot \cos\alpha - \\ &- m_6 \cdot l_6 \cdot \dot{y}_c \cdot \dot{\beta} \cdot \cos\beta + m_6 \cdot l_6 \cdot \dot{z}_c \cdot \dot{\alpha} \cdot \sin\alpha - \\ &- m_6 \cdot l_6 \cdot \dot{z}_c \cdot \dot{\beta} \cdot \sin\beta + 0.5m_6 \cdot l_6^2 \cdot \dot{\alpha}^2 - \\ &- m_6 \cdot l_6 \cdot \dot{z}_c \cdot \dot{\alpha} \cdot \dot{\beta} \cdot \sin\alpha \cdot \sin\beta + 0.5m_6 \cdot l_6^2 \cdot \dot{\beta}^2 + \\ &+ 0.5I_{6x_6} \cdot \dot{\beta}^2 + 0.5I_{6y_6} \cdot \dot{\alpha}^2 + 0.5I_{6z_6} \cdot \dot{\psi}^2.\end{aligned}\quad (5)$$

To determine  $T_5$  let's decompose the complex movement of imbalance 5 on portable with the body 3 and relative movement with respect to the specified body. Portable movement is free. The relative motion of the imbalance is rotation with angular velocity  $\omega = \dot{\phi}$ . By Koenig's theorem

$$T_5 = 0.5m \cdot v_{c_5}^2 + 0.5I_5' \cdot \dot{\phi}^2.$$

where  $I_5'$ —moment of imbalance inertia 5 relative to the axis passing through its center of mass parallel to the axis of rotation of the debalancing shaft 4.

Vector  $\vec{v}_{C_5}$  of absolute velocity of the imbalance center of mass 5

$$\vec{v}_{C_5} = \vec{v}_{C_5e} + \vec{v}_{C_5r},\quad (6)$$

Since portable movement is free, then

$$\vec{v}_{C_5e} = \vec{v}_{C_5e1} + \vec{v}_{C_5e2},\quad (7)$$

where  $\vec{v}_{C_5e1}$ —pole velocity;

$\vec{v}_{C_5e2}$ —center of mass imbalance velocity 5 in its spherical motion around the pole.

To simplify rather complex and cumbersome calculations, we apply a coordinate method for determining motion and its kinematic characteristics.

Since a point is chosen as the pole  $C_3$ , then

$$\begin{aligned}\vec{v}_{C_5e1} &= \vec{v}_{C_3} = \vec{i}(\dot{x}_c - \dot{\alpha} \cdot l \cdot \cos\alpha) + \\ &+ \vec{j}(\dot{y}_c + \dot{\beta} \cdot l \cdot \cos\beta) + \\ &+ \vec{k}(\dot{z}_c + \dot{\alpha} \cdot l \cdot \sin\alpha + \dot{\beta} \cdot l \cdot \sin\beta)\end{aligned}$$

To find  $\vec{v}_{C_5e2}$  we will use vibration angles and for clarity we will depict schematically in the figure 6 the imbalance 5 center of inertia  $C_5$  in three orthogonal projections, where  $e = C_3C_5$ —its eccentricity.

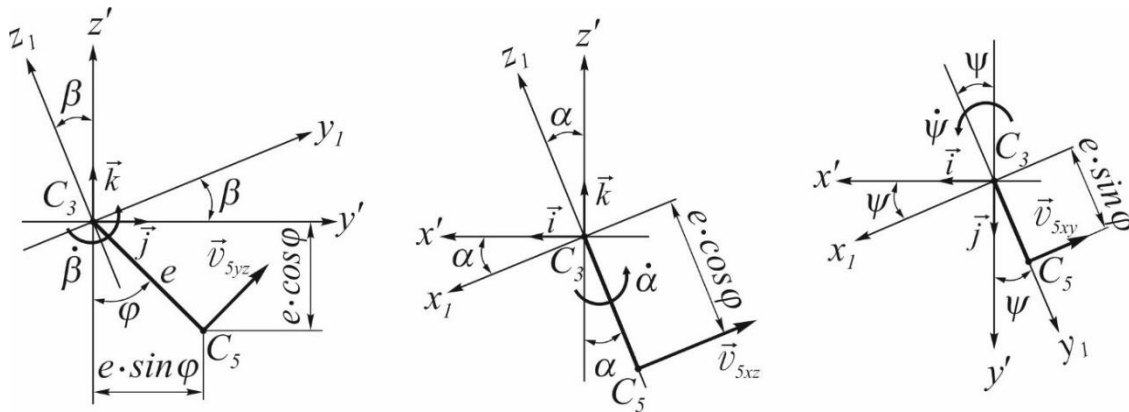


Figure 6 – Decomposition  $\vec{v}_{C_5e2}$  into three components

Let's write now  $\vec{v}_{C_5e2}$  as the sum of three terms:

$$\vec{v}_{C_5e2} = \vec{v}_{5xy} + \vec{v}_{5xz} + \vec{v}_{5yz}, \quad (8)$$

where  $\vec{v}_{5xy}$ ,  $\vec{v}_{5xz}$  and  $\vec{v}_{5yz}$  – velocity vector  $\vec{v}_{C_5e2}$  projections to coordinate planes  $xy$ ,  $yz$  and  $xz$ . From Figure 6 it is obvious that the velocity modules

$$v_{5yz} = \dot{\beta} \cdot e, \quad v_{5xz} = \dot{\alpha} \cdot e \cdot \cos\phi \quad \text{and} \quad v_{5xy} = \dot{\psi} \cdot e \cdot \sin\phi,$$

and the corresponding projections on the specified planes

$$\begin{aligned} \vec{v}_{5yz} &= \vec{j} \cdot v_{5yz} \cdot \cos\phi + \vec{k} \cdot v_{5yz} \cdot \sin\phi = \vec{j} \cdot \dot{\beta} \cdot e \cdot \cos\phi + \vec{k} \cdot \dot{\beta} \cdot e \cdot \sin\phi, \\ \vec{v}_{5xz} &= -\vec{i} \cdot v_{5xz} \cos\alpha + \vec{k} \cdot v_{5xz} \sin\alpha = -\vec{i} \cdot \dot{\alpha} \cdot e \cos\phi \cos\alpha + \vec{k} \cdot \dot{\alpha} \cdot e \cos\phi \sin\alpha, \\ \vec{v}_{5xy} &= -\vec{i} \cdot v_{5xy} \cos\psi - \vec{j} \cdot v_{5xy} \sin\psi = -\vec{i} \cdot \dot{\psi} \cdot e \sin\phi \cos\psi - \vec{j} \cdot \dot{\psi} \cdot e \sin\phi \sin\psi. \end{aligned}$$

Substituting these values in formula (8), and the values of  $\vec{v}_{C_5e1}$  and  $\vec{v}_{C_5e2}$  in formula (7), we have

$$\begin{aligned} \vec{v}_{C_5e} &= \vec{i} \cdot (\dot{x}_C - \dot{\alpha} \cdot \ell \cdot \cos\alpha - \dot{\alpha} \cdot e \cdot \cos\phi \cdot \cos\alpha - \dot{\psi} \cdot e \cdot \sin\phi \cdot \cos\psi) + \\ &+ \vec{j} \cdot [\dot{y}_C + \dot{\beta} \cdot \ell \cdot \cos\beta + \dot{\beta} \cdot e \cdot \cos\phi - \dot{\psi} \cdot e \cdot \sin\phi \cdot \sin\psi] + \\ &+ \vec{k} \cdot [\dot{z}_C + \dot{\alpha} \cdot \ell \cdot \sin\alpha + \dot{\alpha} \cdot e \cdot \cos\phi \cdot \sin\alpha + \dot{\beta} \cdot \ell \cdot \sin\beta + \dot{\beta} \cdot e \cdot \sin\phi]. \end{aligned}$$

Since the relative motion of the imbalance is rotational, then (see Fig. 7) the module  $v_{C_5r} = C_3 C_5 \cdot \omega = e \cdot \dot{\phi}$ , and a vector

$$\vec{v}_{C_5r} = \vec{j} \cdot v_{C_5r} \cdot \cos\phi + \vec{k} \cdot v_{C_5r} \cdot \sin\phi = \vec{j} \cdot \dot{\phi} \cdot e \cdot \cos\phi + \vec{k} \cdot \dot{\phi} \cdot e \cdot \sin\phi.$$

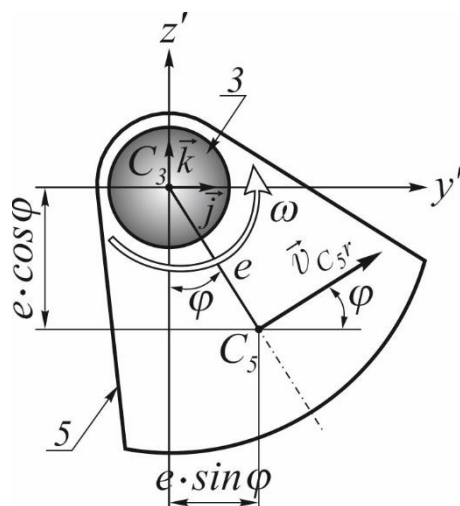


**Fig. 7. To determine the relative speed  $\vec{v}_{C_5r}$  of an imbalance**

After substitution  $\vec{v}_{C_5e}$  and  $\vec{v}_{C_5r}$  into formula (6), squaring and substituting the value  $v_{C_5e}^2$  into the formula of kinetic energy  $T_5$ , we get

$$\begin{aligned} T_5 &= \frac{m}{2} \cdot (\dot{x}_C^2 + \dot{y}_C^2 + \dot{z}_C^2) - \\ &- m \cdot \ell \cdot \dot{x}_C \cdot \dot{\alpha} \cdot \cos\alpha - m \cdot e \cdot \dot{x}_C \cdot \dot{\alpha} \cdot \cos\alpha \cdot \cos\phi - m \cdot e \cdot \dot{x}_C \cdot \dot{\psi} \cdot \cos\psi \cdot \sin\phi + \\ &+ m \cdot \ell \cdot \dot{y}_C \cdot \dot{\beta} \cdot \cos\beta + m \cdot e \cdot \dot{y}_C \cdot \dot{\beta} \cdot \cos\phi - \\ &- m \cdot e \cdot \dot{y}_C \cdot \dot{\psi} \cdot \sin\psi \cdot \sin\phi + m \cdot e \cdot \dot{y}_C \cdot \dot{\phi} \cdot \cos\phi + \\ &+ m \cdot \ell \cdot \dot{z}_C \cdot \dot{\alpha} \cdot \sin\alpha + m \cdot \ell \cdot \dot{z}_C \cdot \dot{\beta} \cdot \sin\beta + \\ &+ m \cdot e \cdot \dot{z}_C \cdot \dot{\alpha} \cdot \sin\alpha \cdot \cos\phi + m \cdot e \cdot \dot{z}_C \cdot \dot{\beta} \cdot \sin\phi + m \cdot e \cdot \dot{z}_C \cdot \dot{\phi} \cdot \sin\phi - \\ &- \frac{m}{2} \cdot \ell^2 \cdot \dot{\alpha}^2 \cdot \cos 2\alpha + m \cdot \ell \cdot e \cdot \dot{\alpha}^2 \cdot \cos\phi - \frac{m}{2} \cdot e^2 \cdot \dot{\alpha}^2 \cdot \cos^2\phi \cdot \cos 2\alpha + \\ &+ \frac{m}{2} \cdot \ell^2 \cdot \dot{\beta}^2 + m \cdot \ell \cdot e \cdot \dot{\beta}^2 \cdot \cos(\beta - \phi) + \frac{m}{2} \cdot e^2 \cdot \dot{\beta}^2 - \frac{m}{2} \cdot e^2 \cdot \dot{\psi}^2 \cdot \sin^2\phi + \\ &+ m \cdot \ell^2 \cdot \dot{\alpha} \cdot \dot{\beta} \cdot \sin\alpha \cdot \sin\beta + m \cdot \ell \cdot e \cdot \dot{\alpha} \cdot \dot{\beta} \cdot \sin\alpha \cdot \sin\beta \cdot \cos\phi + \\ &+ m \cdot \ell \cdot e \cdot \dot{\alpha} \cdot \dot{\beta} \cdot \sin\alpha \cdot \sin\phi + m \cdot \ell \cdot e \cdot \dot{\alpha} \cdot \dot{\psi} \cdot \cos\alpha \cdot \cos\psi \cdot \sin\phi + \\ &+ m \cdot \ell \cdot e \cdot \dot{\alpha} \cdot \dot{\phi} \cdot \sin\alpha \cdot \sin\phi + \frac{m}{2} \cdot e^2 \cdot \dot{\alpha} \cdot \dot{\beta} \cdot \sin\alpha \cdot \sin 2\phi + \\ &+ \frac{m}{2} \cdot e^2 \cdot \dot{\alpha} \cdot \dot{\psi} \cdot \cos\alpha \cdot \cos\psi \cdot \sin 2\phi + \frac{m}{2} \cdot e^2 \cdot \dot{\alpha} \cdot \dot{\phi} \cdot \sin\alpha \cdot \sin 2\phi - \\ &- m \cdot \ell \cdot e \cdot \dot{\beta} \cdot \dot{\psi} \cdot \cos\beta \cdot \sin\psi \cdot \sin\phi + m \cdot \ell \cdot e \cdot \dot{\beta} \cdot \dot{\phi} \cdot \cos(\beta - \phi) - \end{aligned}$$



$$-\frac{m}{2} \cdot e^2 \cdot \dot{\beta} \cdot \dot{\psi} \cdot \sin \psi \cdot \sin 2\phi + m \cdot e^2 \cdot \dot{\beta} \cdot \dot{\phi} - \frac{m}{2} \cdot e^2 \cdot \dot{\psi} \cdot \dot{\phi} \cdot \sin \psi \cdot \sin 2\phi + \frac{I_5 \cdot \dot{\phi}^2}{2}. \quad (9)$$

Substituting values (3), (4), (5) and (9) to the formula (2), and having performed legitimate transformations, we get that the kinetic energy of the vibrating table

$$\begin{aligned} T = & \frac{M}{2} \cdot \dot{x}_C^2 + \frac{M}{2} \cdot \dot{y}_C^2 + \frac{M}{2} \cdot \dot{z}_C^2 - \\ & - [(m_3 + m) \cdot \ell + m_6 \cdot \ell_6] \cdot \dot{x}_C \cdot \dot{\alpha} \cdot \cos \alpha - m \cdot e \cdot \dot{x}_C \cdot \dot{\alpha} \cdot \cos \alpha \cdot \cos \phi - \\ & - m \cdot e \cdot \dot{x}_C \cdot \dot{\psi} \cdot \cos \psi \cdot \sin \phi + [(m_3 + m) \cdot \ell - m_6 \cdot \ell_6] \cdot \dot{y}_C \cdot \dot{\beta} \cdot \cos \beta + \\ & + m \cdot e \cdot \dot{y}_C \cdot \dot{\beta} \cdot \cos \beta - m \cdot e \cdot \dot{y}_C \cdot \dot{\psi} \cdot \sin \psi \cdot \sin \phi + \\ & + m \cdot e \cdot \dot{y}_C \cdot \dot{\phi} \cdot \cos \phi + [(m_3 + m) \cdot \ell + m_6 \cdot \ell_6] \cdot \dot{z}_C \cdot \dot{\alpha} \cdot \sin \alpha + \\ & + m \cdot e \cdot \dot{z}_C \cdot \dot{\alpha} \cdot \sin \alpha \cdot \cos \phi + [(m_3 + m) \cdot \ell - m_6 \cdot \ell_6] \cdot \dot{z}_C \cdot \dot{\beta} \cdot \sin \beta + \\ & + m \cdot e \cdot \dot{z}_C \cdot \dot{\beta} \cdot \sin \beta + m \cdot e \cdot \dot{z}_C \cdot \dot{\phi} \cdot \sin \phi + \frac{m_3 \cdot \ell^2 + m_6 \cdot \ell_6^2}{2} \cdot \dot{\alpha}^2 - \\ & - \frac{m \cdot \ell^2}{2} \cdot \dot{\alpha}^2 \cdot \cos 2\alpha + m \cdot \ell \cdot e \cdot \dot{\alpha}^2 \cdot \cos \phi - \frac{m \cdot e^2}{2} \cdot \dot{\alpha}^2 \cdot \cos^2 \phi \cdot \cos 2\alpha + \\ & + \frac{(m_3 + m) \cdot \ell^2 + m_6 \cdot \ell_6^2 + m \cdot e^2}{2} \cdot \dot{\beta}^2 + m \cdot \ell \cdot e \cdot \dot{\beta}^2 \cdot \cos(\beta - \phi) - \\ & - \frac{m \cdot e^2}{2} \cdot \dot{\psi}^2 \cdot \sin^2 \phi + [(m_3 + m) \cdot \ell^2 - m_6 \cdot \ell_6^2] \cdot \dot{\alpha} \cdot \dot{\beta} \cdot \sin \alpha \cdot \sin \beta + \\ & + m \cdot \ell \cdot e \cdot \dot{\alpha} \cdot \dot{\beta} \cdot \sin \alpha \cdot \sin \beta \cdot \cos \phi + \\ & + m \cdot \ell \cdot e \cdot \dot{\alpha} \cdot \dot{\beta} \cdot \sin \alpha \cdot \sin \phi + m \cdot \ell \cdot e \cdot \dot{\alpha} \cdot \dot{\psi} \cdot \cos \alpha \cdot \cos \psi \cdot \sin \phi + \\ & + m \cdot \ell \cdot e \cdot \dot{\alpha} \cdot \dot{\phi} \cdot \sin \alpha \cdot \sin \phi + \frac{m \cdot e^2}{2} \cdot \dot{\alpha} \cdot \dot{\beta} \cdot \sin \alpha \cdot \sin 2\phi + \\ & + \frac{m \cdot e^2}{2} \cdot \dot{\alpha} \cdot \dot{\psi} \cdot \cos \alpha \cdot \cos \psi \cdot \sin 2\phi + \frac{m \cdot e^2}{2} \cdot \dot{\alpha} \cdot \dot{\phi} \cdot \sin \alpha \cdot \sin 2\phi - \\ & - m \cdot \ell \cdot e \cdot \dot{\beta} \cdot \dot{\psi} \cdot \cos \beta \cdot \sin \psi \cdot \sin \phi + m \cdot \ell \cdot e \cdot \dot{\beta} \cdot \dot{\phi} \cdot \cos(\beta - \phi) - \\ & - \frac{m \cdot e^2}{2} \cdot \dot{\psi} \cdot \dot{\phi} \cdot \sin \psi \cdot \sin 2\phi + \frac{I_y}{2} \cdot \dot{\alpha}^2 + \frac{I_x}{2} \cdot \dot{\beta}^2 + \frac{I_z}{2} \cdot \dot{\psi}^2 + \frac{I_5}{2} \cdot \dot{\phi}^2. \quad (10) \end{aligned}$$

where  $M = m_1 + m_3 + m_6 + m$  – the total weight of the vibrating table;

$I_x = I_{1x_1} + I_{3x_3} + I_{6x_6}$ ,  $I_y = I_{1y_1} + I_{3y_3} + I_{6y_6}$  and  $I_z = I_{1z_1} + I_{3z_3} + I_{6z_6}$  – reduced moving part inertia moments of the table relative to the corresponding axes.

As an example of the application of equation (10), we construct a graph of the change in kinetic energy  $T$  of vibrating table under study, which it is able to reproduce depending on the length of the lever  $\ell_{\text{взж.}}$ , to which the vibration alarm is fixed in the center under the vibrating plate. For construction, the mathematical program "Mathcad Prime" was used and taking into account the nominal numerical values of the greatness of the parameters of the vibrating table, which are included in the equation (10) (See. Table. 1).

**Table 1 – Nominal parameters of the vibrating table.**

№	Parameter name	Denomination	Unit of measure	Size
1.	Mass of vibrating plate	$m_1$	kg	170
2.	Mass of the excitor	$m_3$	kg	10
3.	Mass of imbalance	$m$	kg	2
4.	Mass of load with form	$m_6$	kg	50
5.	Imbalance eccentricity	$e$	m	0,03

A vibration excitor ИВ-99БУ2 was used (power  $N=0,5$  Kw, frequency 50 Hz, rotational speed  $n = 3000$  rpm, acting force  $P = 2,5$  KN), which was fixed to the vibrating plate in size  $2a \times 2b = 1,6 \text{ m} \times 1,3 \text{ m}$ , thru the lever. Lever length  $\ell_{\text{взж.}}$  was accepted equal accordingly 0; 100; 200; 300 mm based on constructive images.

The plot is shown in Fig. 8. The dependence curve increases, which confirms the effectiveness of the lever fastening of the vibrating device to the vibrating table.

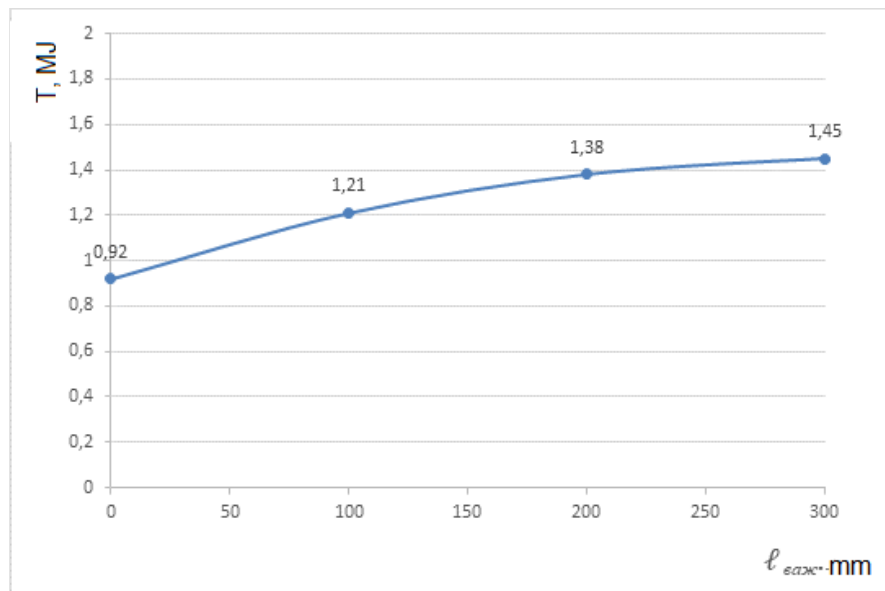


**Fig 8. Graph of the change in the kinetic energy of the vibrating table  $T$ , which it is able to introduce when compacting concrete products, depending on the length of the lever  $l_{\text{важ.}}$**

### Conclusions

To obtain a mathematical model of the developed design of the vibrating table, we proposed to use the Lagrange equation of the second kind. This method is the most common method used in solving problems regarding the motion of mechanical systems.

The considered vibrating table was modeled by a mechanical system, which consists of several material bodies - plate, vibration exciter body, imbalance and tank with concrete mix. To determine the position and description of the mechanical system above-mentioned material bodies free motions under consideration, an orthogonal vibration reference system from three coordinate systems was used.

The total kinetic energy of the vibrating table was determined, which is the sum of the kinetic energy of the four material bodies that make up it.

This functional dependence of the total kinetic energy will later be used to compile a mathematical model of

the vibration table in the Lagrange equations of the second kind, with the help of which it will be possible to analyze the influence of its constituent parameters – geometric and kinematic – on the process of compacting the concrete mix to reduce energy consumption during vibration compaction of products.

As an example of the application of functional dependence, a graph of changes in the kinetic energy of the investigated vibration table depending on the length of the lever was constructed, on which the vibration excitor was fixed. Analysis of the obtained dependence indicates an increase in the kinematic energy of the vibrating table with increasing lever length. The lever made it possible to create conditions for successful power transfer from the vibration excitor to the table without unforeseen losses.

### References

1. Назаренко І.І. Вібраційні машини і процеси будівельної індустрії: навчальний посібник / І.І. Назаренко. – К.: КНУБА, 2007. – 230 с
2. Дудар І. Н. Теоретичні основи технології виробів із пресованих бетонів : моногр. / І. Н. Дудар. – Вінниця : УНІВЕРСУМ-Вінниця, 2006. – 89 с. – ISBN 966-641-163-6.
3. Гусев Б. В. Вібраційна технологія бетону / Б. В. Гусев, В. Г. Зазимко. – К.: Будівельник, 1991. – 230 с
4. Ручинський, М.М. Огляд і аналіз існуючих режимів ущільнення бетонних сумішей/ М.М. Ручинський, А.Г. Свідерський, О.С. Д'яченко// МНТК «Прогресивна техніка, технологія та інженерна освіта». – Київ, 2019.
5. Назаренко І. І. Фізичні основи механіки будівельних матеріалів / І. І. Назаренко, М. М. Ручинський. – Львів:
1. Nazarenko I.I. Vibrational Machines and Processes in the Construction Industry: A textbook / I.I. Nazarenko. – Kyiv: KNUBA, 2007. – 230 p.
2. Dudar I.N. Theoretical Foundations of Technology for Products Made of Pressed Concretes: Monograph / I.N. Dudar. – Vinnytsia: UNIVERSUM-Vinnytsia, 2006. – 89 p. – ISBN 966-641-163-6.
3. Gusev B.V., Zazymko V.G. Vibrational Technology of Concrete / B.V. Gusev, V.G. Zazymko. – Kyiv: Budivelnik, 1991. – 230 p.
4. Ruchynskiy, M.M., Sviderskyi, A.G., D'yachenko, O.S. Review and Analysis of Existing Compaction Modes for Concrete Mixtures. MNTK 'Progressive Technics, Technology, and Engineering Education'. – Kyiv, 2019.
5. Nazarenko I.I., Ruchynskiy M.M. Physical Principles of Mechanics of Building Materials. – Lviv: Afisha, 2002.

- Афіша, 2002. – 128 с.
6. Пат. 146691 Україна. МПК B28B 1/08 (2006.01). Виброствіль з важливим закріпленням вібробудувача / Коробко Б.О., Коротич Ю.Ю., Васильєв Є.А.; власник Національний університет "Полтавська політехніка імені Юрія Кондратюка". – № у 2020 06563; заявл. 12.10.2020; опубл. 10.03.2021, Бюл. № 10.
7. Дворкін Л. Й. Проектування складів бетону із заданими властивостями / Дворкін Л. Й. Дворкін О. Л., Гарніцький Ю. В. – Рівне : Вид-во РДТУ, 2000. – 215 с.
8. Nesterenko M.P. Study of vibrations of plate of oscillation cassette setting as active working organ / M.P. Nesterenko, P.O. Molchanov // Conference reports materials «Problems of energ and nature use 2013» (Poltava National Technical Yuri Kondratyuk University, University of Tuzla, China University of Petroleum). – Budapest, 2014. – P. 146 – 151.
9. Конструкційні матеріали нового покоління та технології їх впровадження у будівництво / [Р. Ф. Рунова, В. І. Братчун, В. І. Гоц та ін.] – К. : УВПК ЕксОб, 2008. – 360 с.
10. Нестеренко М.П. Класифікація та оцінка споживчих якостей сучасних вібраційних машин для формування залізобетонних виробів / М.П. Нестеренко // Збірник наукових праць (галузевого машинобудування, будівництва). – Полтава: ПолтНТУ, 2007. – Вип. 20. – С. 20 – 25.
11. Загребя, В. П. Технологія роздільного віброімпульсного формування каменобетонних виробів : монографія / В. П. Загребя, І. Н. Дудар, А. О. Коваленко. — Вінниця : ВНТУ, 2012. — 92 с.
12. Zhyhylyi S.M. Mathematical model of the dynamic action of the controlled vibration exciter on the processed medium of mixer with toroidal working container / S.M. Zhyhylyi, M.O. Kharchenko, J.O. Katella // International Journal of Engineering & Technology Vol. 7, No. 3.2, 2018. – Pp. 478 – 485  
DOI: [10.14419/ijet.v7i3.2.14576](https://doi.org/10.14419/ijet.v7i3.2.14576)
13. Morin D. Introduction to Classical Mechanics: With Problems and Solutions / David Morin. – Cambridge University Press; 1st edition, 2008. – 734 p.
14. Павловський М.А. Теоретична механіка: підручник / М.А. Павловський. – К.: Техніка, 2002. – 512 с.
15. Сердюк Л.І. Основи теорії, розрахунків і конструювання керованих вібраційних машин з дебалансними вібробудувачами: Дис...д-ра техн. наук: 05.02.02 і 01.02.06. Харків. політехн. ін-т. – Харків, 1991. – 301 с.
16. Seely F. Analytical mechanics for engineers / Fred B. Seely, Newton E. Ensign. – Chapman & Hall, Limited, New York, London; 3d ed., rewritten [View all formats and editions](#), 1941. – 488 p.
17. Beer F. Vector mechanics for engineers: statics and dynamics, tenth edition / Ferdinand P. Beer, E. Russell Johnston, Jr., David F. Mazurek, Phillip J. Cornwell – New York: McGraw-Hill Companies, Inc., 2013. – 1360 p.
18. Жигилій С.М. Кінематика точки: курс лекцій з дисципліни «Теоретична механіка» для студентів технічних спеціальностей усіх форм навчання / С.М. Жигилій. – Полтава : ПолтНТУ, 2017. – 194 с.
19. Ruina A. Introduction to Statics and Dynamics / Andy Ruina, Rudra Pratap. – Oxford University Press (Preprint), 2011. – 1029 p.
- 128 p.
6. Pat. 146691 Ukraine. IPC B28B 1/08 (2006.01). Vibration table with lever-mounted vibrator / Korobko B.O., Korotych Yu.Yu., Vasilyev Ye.A.; owner National University 'Poltava Polytechnic named after Yuri Kondratyuk'. – No. u 2020 06563; filed 12.10.2020; published 10.03.2021, Bull. No. 10.
7. Dvorkin L.Y. Designing Concrete Mixtures with Specified Properties / Dvorkin L.Y., Dvorkin O.L., Harnitskyi Yu.V. – Rivne: Publishing House of RSTU, 2000. – 215 p.
8. Nesterenko M.P. Study of vibrations of plate of oscillation cassette setting as active working organ / M.P. Nesterenko, P.O. Molchanov // Conference reports materials «Problems of energ and nature use 2013» (Poltava National Technical Yuri Kondratyuk University, University of Tuzla, China University of Petroleum). – Budapest, 2014. – P. 146 – 151.
9. Advanced Construction Materials and Technologies for Implementation in Construction / [R. F. Runova, V. I. Bratchun, V. I. Hots, et al.] – Kyiv: UVPK ExOb, 2008. – 360 p.
10. Nesterenko M.P. Classification and Assessment of Consumer Qualities of Modern Vibrating Machines for Forming Reinforced Concrete Products / M.P. Nesterenko // Collection of Scientific Papers (Branch Mechanical Engineering, Construction). – Poltava: PoltNTU, 2007. – Issue 20. – Pp. 20 – 25.
11. Zagreba, V.P. Technology of Separate Vibro-impulse Formation of Stone Concrete Products: Monograph / V.P. Zagreba, I.N. Dudar, A.O. Kovalenko. — Vinnytsia: VNTU, 2012. — 92 p.
12. Zhyhylyi S.M. Mathematical model of the dynamic action of the controlled vibration exciter on the processed medium of mixer with toroidal working container / S.M. Zhyhylyi, M.O. Kharchenko, J.O. Katella // International Journal of Engineering & Technology Vol. 7, No. 3.2, 2018. – Pp. 478 – 485  
DOI: [10.14419/ijet.v7i3.2.14576](https://doi.org/10.14419/ijet.v7i3.2.14576)
13. Morin D. Introduction to Classical Mechanics: With Problems and Solutions / David Morin. – Cambridge University Press; 1st edition, 2008. – 734 p.
14. Pavlovskiy M.A. Theoretical Mechanics: Textbook / M.A. Pavlovskiy. – Kyiv: Tekhnika, 2002. – 512 p.
15. Serdjuk L.I. Fundamentals of Theory, Calculation, and Design of Controlled Vibrating Machines with Unbalanced Vibration Exciters: Dissertation for the Degree of Doctor of Technical Sciences: Specializations 05.02.02 and 01.02.06. Kharkiv Polytechnic Institute – Kharkiv, 1991. – 301 p.
16. Seely F. Analytical mechanics for engineers / Fred B. Seely, Newton E. Ensign. – Chapman & Hall, Limited, New York, London; 3d ed., rewritten [View all formats and editions](#), 1941. – 488 p.
17. Beer F. Vector mechanics for engineers: statics and dynamics, tenth edition / Ferdinand P. Beer, E. Russell Johnston, Jr., David F. Mazurek, Phillip J. Cornwell – New York: McGraw-Hill Companies, Inc., 2013. – 1360 p.
18. Zhyhiliy S.M. Point Kinematics: Lecture Course on Theoretical Mechanics for Students of Technical Specialties of All Forms of Education / S.M. Zhyhiliy. – Poltava: PoltNTU, 2017. – 194 p.
19. Ruina A. Introduction to Statics and Dynamics / Andy Ruina, Rudra Pratap. – Oxford University Press (Preprint), 2011. – 1029 p.

UDC 666.97.033.16

## Reasoning of the expediency of using vibration supports with variable parameters

Sheka Oleksandr<sup>1\*</sup>, Yakovenko Andrii<sup>2</sup>, Vedmid Vasyi<sup>3</sup>

<sup>1</sup>National University «Yuri Kondratyuk Poltava Polytechnic» <https://orcid.org/0009-0005-1328-1416>

<sup>2</sup>National University «Yuri Kondratyuk Poltava Polytechnic» <https://orcid.org/0000-0003-0818-6332>

<sup>3</sup>National University «Yuri Kondratyuk Poltava Polytechnic» <https://orcid.org/0000-0003-1514-1212>

\*Corresponding author E-mail: [asheka51@ukr.net](mailto:asheka51@ukr.net)

The problem of reducing the negative impact of vibration on staff and equipment and their compliance with sanitary standards is always relevant for construction vibrating machines with vibration exciters of various types and modes. So, in practice, vibration isolation of vibroactive elements of vibrating machines and technological equipment is applied using systems with quasi-zero stiffness. This article highlights the results of experimental studies of changes in the elastic qualities of vibration support parameters at different pressure levels and changes in the length of the free part of the elastic element. Therefore, the construction of a vibration support with a limiter of the free part of the elastic element was developed. The stiffness of the support changes as a result of changing the free part of the support with metal limiters. The results of the search experiment showed that the deformation of the rubber element is carried out according to a law close to the linear one. Therefore, a mathematical model in the form of regression was built to conduct the main experiment and process the obtained data. The obtained regression equation makes it possible to establish the dependence of the shrinkage of the support when the pressure on it changes and the height of the free part of the elastic element.

**Keywords:** vibration amplitude, vibration support, vibration isolation, vibration platform, vibration exciter

## Обґрунтування доцільності застосування вібраційних опор зі змінними параметрами

Шека О.П.<sup>1\*</sup>, Яковенко А.М.<sup>2</sup>, Ведмідь В.В.<sup>3</sup>

<sup>1, 2, 3</sup> Національний університет «Полтавська політехніка імені Юрія Кондратюка»

\*Адреса для листування E-mail: [asheka51@ukr.net](mailto:asheka51@ukr.net)

При створенні вібраційних машин з віброзбудниками різних типів і способів дії завжди актуальною є проблема зменшення негативного впливу вібрації на персонал та обладнання та їх відповідність санітарним нормам. Для її розв'язання на практиці застосовують віброізоляцію віброактивних елементів вібраційних машин і технологічного обладнання з використанням систем із квазінульовою жорсткістю. Зокрема, у віброплощадках із класичною двомасовою системою віброізоляція машини від фундаменту або робочого органу та рами здійснюється шляхом зміни жорсткості параметрів їх вібраційних опор. В статті висвітлюється результати експериментальних досліджень зміни пружних властивостей параметрів вібраційної опори при різних значеннях навантаження та зміни довжини вільної частини пружного елемента. Відповідно була розроблена конструкція віброопори з обмежувачем вільної частини пружного елемента. При нерівномірному розподілі навантаження на вібраційну машину запропонована конструкція опори дозволяє підібрати параметри жорсткості для її рівномірної роботи шляхом обмеження висоти робочої частини опори. Жорсткість опори змінюється внаслідок зміни вільної частини опори металевими обмежувачами. З метою отримання достовірної математичної моделі експериментальні дослідження ґрунтуються на методах математичного планування експерименту та математичної статистики. Результати пошукового експерименту показали, що деформація гумового елемента здійснюється за законом, близьким до лінійного. Тому для проведення основного експерименту та обробки одержаних даних побудовано математичну модель у вигляді регресії. Розраховані значення коефіцієнтів регресії перевірено за критерієм Стюдента. Отримане рівняння регресії дозволяє встановити залежність усадки опори при зміні навантаження на неї та висоти вільної частини пружного елемента. За отриманими даними можна припустити, що змінюючи жорсткість пружної вібраційної опори, можна змінювати в потрібних межах амплітуду вимушених коливань рухомої частини віброплощадки відповідно, забезпечувати потрібну якість ущільнення бетонної суміші.

**Ключові слова:** амплітуда віброколивань, вібраційна опора, віброізоляція, вібраційна площадка, віброзбуджувач

## Introduction

The development of the construction industry in our country and abroad is impossible without the creation of high-performance energy-saving machines and equipment. The technical operation of machines for the production and compaction of building materials (sieves, vibrating plates, conveyors, vibrating stands, etc.) causes vibrations, which inevitably increases the intensity and widens the spectrum of their vibration field's negative effects. Vibration in machines contributes to the growth of dynamic pressure in structural elements, joints and connections, causes the formation and increasing the number of cracks, decreases the load-bearing capacity of structural parts, and has a negative impact on the health of staff [1]. Problems of vibration isolation of dynamic objects arise in almost all branches of modern technology. The use of vibration isolation for vibroactive elements of machines allows to reduce the negative impact of vibration on technological equipment and technical staff.

In construction engineering, vibration isolation systems installed between the source of vibration and the protective object are widely used to protect against the dynamic effects of vibrating objects [1,2]. It is better to use passive vibration isolation systems to protect from the harmful effects of vibration in practice, as simple and economic version.

The main characteristics of passive vibration isolation systems are the frequency of their own oscillations and load-bearing capacity (reaction to static pressure) [3]. The lower the frequency of natural oscillations of the vibration isolator, the wider the range of frequencies of the disturbing force in which the action of the vibration isolator is effective can be. However, in linear vibration systems, ensuring the load-bearing capacity of the vibration isolator is usually accompanied by an increase in its overall dimensions.

Non-linear systems with quasi-zero stiffness are also used for the construction of anti-vibration systems with a low natural frequency of oscillation [4]. These systems are distinguished by the fact that in the working range they have a gentle section of the force characteristic and, therefore, have a comparatively low stiffness, while maintaining a high load-bearing capacity in the equilibrium position. This allows such systems to be used as a vibration isolation for objects of large mass, effective at low vibration frequencies [5], although their construction may cause certain technological difficulties.

An urgent task that requires a solution is the usage of systems with quasi-zero stiffness is to ensure vibration isolation of structural elements of technological equipment with vibration processes and unbalanced moving joints [4,6].

## Review of Research Resources and Publications

A significant number of scientific developments are devoted to the study of the influence of the parameters of elastic vibration supports on the characteristics of vibrations of moving parts of vibrating machines [7]. In particular, one study emphasizes that one of the important characteristics that determine the amplitude of

vibrations of the concrete mixture is the stiffness of the elastic support. Also, in the scientific thesis it is stated that the stiffness of the elastic vibration supports is one of the key parameters for determining the amplitude of vibration movements of the points of the movable frame of the vibrating platform [8].

Oscillations in different configurations can be achieved by adjusting the stiffness of the support in the horizontal and vertical directions and accordingly choosing the trajectory that best meets the process conditions [9].

## Definition of unsolved aspects of the problem

The characteristics of vibration supports are selected in accordance with the mass, size and frequency parameters of the equipment being isolated, as well as in accordance with the conditions of its fixation [10]. In most cases a classic two-mass system is implemented for building vibrating construction machines, since it makes it possible to isolate the machine from the foundation or from the working body and frame. Depending on the mass of the sealing medium or the mode of operation of the vibrating machine, there is a need to change the parameters of the vibration supports by changing their stiffness. This can be achieved by replacing elastic elements with others with other stiffness parameters. However, this effect can also be achieved by changing the length of the free part of the elastic support element. Therefore, there is a need to study the change in the elastic properties of the support depending on the length of its free part.

This article examines the question of changing the stiffness of the support by installing auxiliary variable bushings of different heights without replacing the support itself. At a constant value of the mass of the sealing medium, reducing the length of the free part of the elastic element of the support, as is known, leads to an increase in its stiffness, and vice versa. As a result, their rigidity changes for the same design of the supports.

## Problem statement

The purpose of this article is to highlight the results of the study of changes in the elastic properties of the parameters of the vibration support at different pressure values and changes in the length of the free part of its elastic element.

## Basic material and results

The elastic supports of vibrating platforms simultaneously perform several functions. The most important of them are the perception of the force of gravity from those parts of the vibrating platform that are in oscillating motion and their isolation from the foundation.

It is known that the quality of concrete mixture compaction depends on the vibration parameters of the moving part of the vibrating platform [11,12]. The main parameters that affect this are the amplitude and frequency of oscillations of the moving part of the vibrating platform. Also, the moving part of the vibrating platform is in a state of forced oscillations, the frequency of which is set by the vibration exciter, and the amplitude depends on the mass of the moving part with

the mixture and the stiffness of the elastic parts of the vibration supports [13]

In addition, a change in the stiffness of vibration supports affects the amplitude of oscillations of the moving part of the vibrating machine [14], which follows from equation (1):

$$A = \frac{f_0}{\sqrt{(\omega_0^2 - \omega^2)^2 + 4\beta^2\omega^2}}, \quad (1)$$

where  $A$  – displacement amplitude of the working body;

$f_0 = F_0 / m$ ;

$\omega$  – natural cyclic frequency of forced oscillations of the working body;

$\beta = b / 2m$ ;

$b$  – coefficient of dissipative viscous resistance;

$$\omega_0^2 = \frac{k}{m}, \quad (2)$$

where  $k$  – stiffness coefficient of the elastic support;

$m$  – mass of vibrating parts of the vibrating platform.

From equations (1) and (2) it follows that with an increase in the cyclic frequency  $\omega_0$  of the free oscillations of the system under the action of an elastic force, which is caused by an increase in the stiffness  $k$  of the elastic support at a constant mass  $m$  of its vibrating parts, the amplitude  $A$  of the forced vibrations of the moving part of the vibrating machine will be decreasing.

In addition, according to these equations, the amplitude of forced oscillations of the working body depends indirectly on the mass of the vibrating part of the vibrating platform, if its other parameters do not change.

In production conditions, there are often cases when products of different nomenclature are formed on the same vibrating platform [10, 11]. This means that the masses of molding products fluctuate within certain limits, which also negatively affects the quality of sealing.

Taking into account this circumstance, we come to the conclusion that elastic supports, which have design possibilities for operational changes of their parameters, in particular for changing stiffness, allow to select the necessary amplitudes of vibrations of the moving part of the vibrating machine during the formation of concrete products of various nomenclature, which ensures the proper quality of compaction for the according concrete mixtures.

We proposed the construction of an elastic support (Fig. 1), consisting of a rubber cylindrical hollow central part, lower and upper sleeves and variable metal limiters of the working height of the support. As elastic elements of vibration dampers, we suggest using rubber cord sleeves [15].

Limitations of the working height of the support are proportional to the amplitudes of oscillations of the working body or the moving frame of the vibrating platform.

With uneven distribution of the load, the proposed design of the elastic support allows, by limiting the working height of the support, to select such parameters of its stiffness that ensure uniform operation of the vibrating platform.

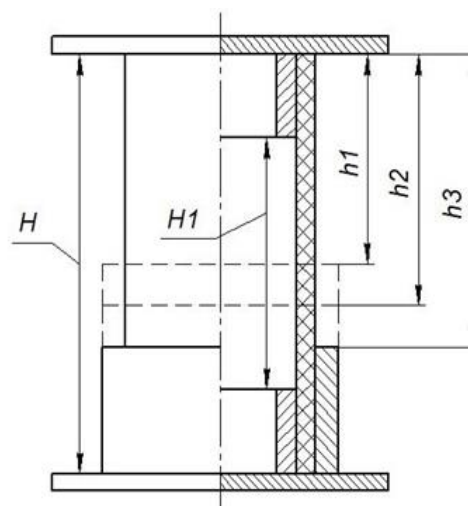


**Figure 1 – Diagram of a vibration support with limiters of the free part of the elastic support element**

$H$  – support height;  $H_1$  – working height of the support;

$h_1$  – limiter height 1, high 50 mm;

$h_2$  – limiter height 2, high 40 mm;

$h_3$  – limiter height 3, high 30 mm.

In order to study the elastic qualities of the support of the proposed structure, experimental measurements of support shrinkage were carried out within the ranges of changes in the initial factors - the load on the vibration support and the height limitation of the free part of its elastic element (Fig. 2), and the statistical processing and analysis of the obtained experimental data was carried out.

The methods of mathematical planning and mathematical statistics were applied during the experimental studies in order to obtain a reliable mathematical model of the elastic support [16].

Measurements of support shrinkage were carried out in the ranges of change of the initial factors described above, the numerical values of which are shown in table 1.

The results of the search experiment showed that the deformations of the elastic element of the support satisfy the conditions of dependence close to linear. Therefore, a two-factor linear experimental design was adopted for the main experiment.

**Table 1 – Ranges of change of initial factors**

Code	Code value	Factor values	
		$X_1$ (load)	$X_2$ (free part of elastic support)
The main level	0	85	75
Variation interval	$\Delta X_i$	45	25
Upper level	+	130	100
Lower level	-	40	50





**Figure 2 – Measurement of the load on the vibration damper with a limiter**

The experimental planning matrix and obtained measurement results are shown in table 2.

**Table 2 - Implementation of the experimental plan**

№	Experiment plan		Interaction	Y <sub>1</sub>	Y <sub>2</sub>	Y <sub>3</sub>	Y <sub>cp</sub>
	X <sub>1</sub>	X <sub>2</sub>	X <sub>1</sub> X <sub>2</sub>				
1	+	+	+	7,9	8	7,85	7,92
2	-	+	-	2,6	2,7	2,5	2,6
3	+	-	-	5,9	5,4	5,6	5,63
4	-	-	+	1,9	1,7	1,9	1,83

The implementation of this experiment and the processing of the obtained data allow obtaining a mathematical model of elastic support in the form of a regression equation (3):

$$y = b_0 + b_1 X_1 + b_2 X_2 + b_3 X_1 X_2, \quad (3)$$

where y – support shrinkage;

b<sub>0</sub>, b<sub>1</sub>, b<sub>2</sub>, b<sub>3</sub> – regression equation coefficients.

As a result of the calculations, the numerical values of the regression coefficients were obtained:

$$b_0 = 4,5;$$

$$b_1 = 2,28;$$

$$b_2 = 0,76;$$

$$b_3 = 0,38.$$

The calculated values of the regression coefficients were tested for significance according to the Student's test and found that all of them are significant.

So, the required regression equation has such form (3):

$$y = 4.5 + 2.28 X_1 + 0.76 X_2 + 0.38 X_1 X_2, \quad (4)$$

The resulting equation establishes the dependence of support shrinkage on changes in the external pressure on it and the height of the free part of the elastic support element.

This equation was tested for adequacy by the Fisher test. It was established that the difference between the corresponding values of the experimental data and those calculated according to the regression equation does not exceed the permissible limits and the regression equation reflects the real process of the vibration support with sufficient accuracy.

The value of the elastic support shrinkage during the experiment is given in table 3.

Corresponding graphs were constructed according to the obtained dependence. Thus, the graph of the dependence of the shrinkage of the elastic support on the pressure during the absence of a limiter is shown in (Fig. 3).

In order to determine the statistical relationship between the shrinkage of the elastic support and the pressure applied to it, the correlation coefficient (5) was calculated for each of the options for limiting the free part of the support, which are presented in table 4.

$$r_{xy} = \frac{\sum_{i=1}^m (x_i - \bar{x}) \cdot (y_i - \bar{y})}{\sqrt{\sum_{i=1}^m (x_i - \bar{x})^2 \sum_{i=1}^m (y_i - \bar{y})^2}} = \frac{cov(x, y)}{\sqrt{s_x^2 s_y^2}}, \quad (5)$$

The calculation was carried out using the Microsoft Office Excel spreadsheet.

Thus, for the free part with a height of 100 mm, 75 mm, and 50 mm, accordingly, the correlation coefficients exceed r = 0.99, which indicates the existence of a statistically significant relationship between the variables under investigation.

**Table 3 - Results of measurements**

№	Pressure F, H	Shrinkage S, mm								
		Free part, L=100 mm (Without restrictions)			Free part, L=75 mm			Free part, L=50 mm		
1	40	2,1	2,7	2,8	1,9	2,1	2,1	1,5	1,6	1,7
2	80	4,7	5,5	5,5	3,9	4,1	3,9	3,5	3,6	3,5
3	120	7,1	7,6	7,8	6,6	6,6	6,3	5,2	5,2	5,2
4	130	8,31	8,7	8,4	7,0	7,0	6,7	5,8	5,7	5,7

**Table 4 – Correlation coefficients**

Free part	Correlation coefficient
L=100 mm (without limiter)	0,997
L=75 mm	0,999
L=50 mm	0,999

The coefficient of variation (6) for is also calculated, which allows you to compare the level of variation between different limit variants that have different values.

$$K_{\sigma} = \frac{S_i^2}{\bar{S}} \cdot 100, \quad (6)$$

$$S_i^2 = \frac{\sum_{j=1}^m (y_{ji} - \bar{y}_i)^2}{m-1}, \quad (7)$$

where  $y_{ji}$  – value of the optimization parameter in the  $j$ -th parallel experiment;

$\bar{y}$  – the arithmetic average value of the optimization parameter from  $m$  repeated experiments in each  $i$ -th experiment;

$m$  – number of parallel experiments.

The calculated values of the coefficient of variation are presented in table 5, which do not exceed 10%. So, we can talk about sufficiently high reproducibility of measurement results during experiments.

**Table 5 – Coefficients of variation**

Free part	Coefficient of variation
L=100 mm (without limiter)	3,74%
L=75 mm	0,47%
L=50 mm	0,48%

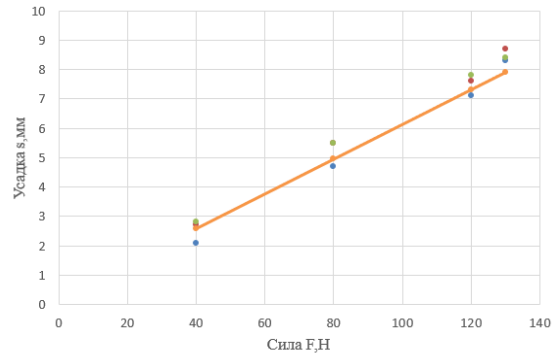


**Figure 3 – Graph of the dependence of the shrinkage of the elastic support under the pressure with the absence of a limiter.**

A mathematical model of support with two factors in natural values was also obtained.

If in the above obtained regression equation (4) to accept:

$$\begin{aligned} X_1 &= \frac{F_i - F_{cp}}{\Delta F} = \frac{F_i - 85}{45}; \\ X_2 &= \frac{S_i - S_{cp}}{\Delta S} = \frac{S_i - 75}{25}; \end{aligned} \quad (8)$$

then we obtain the functional dependence of the shrinkage  $h_i$  of the elastic support under the external pressure  $F_i$  on the elastic support and on the height  $S_i$  of the limiter of the free part of the elastic element of the support:

$$h_i = -1,32 + 0,04 F_i + 0,02 S_i + 0,00012 F_i \cdot S_i \quad (9)$$

Graphs of the dependence of the shrinkage of the vibration support under the external pressure on the support at different values of the limiter are shown in (Fig. 4, 5).



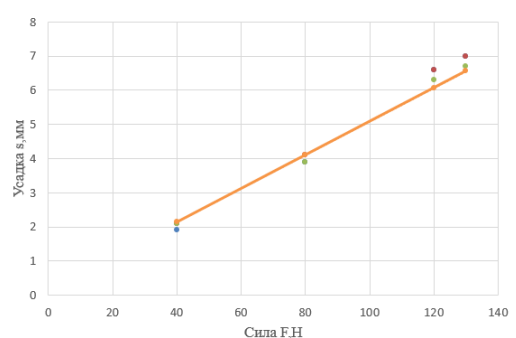


**Figure 4 – Graph of the dependence of the shrinkage of the elastic support under the pressure with a free part of 75 mm.**

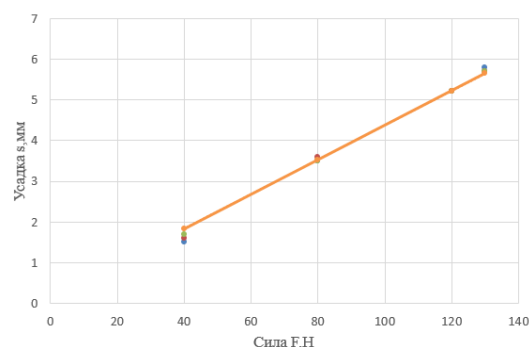


**Figure 5 – Graph of the dependence of the shrinkage of the elastic support under the pressure with a free part of 50 mm**

Using the regression equation, it is possible to determine the shrinkage of the support at arbitrary values of the external pressure and the height of the free part of the elastic element within the above-mentioned ranges of changes in the numerical values of these initial factors: force values - from 40 N to 130 N; the height of the free part is from 50 mm to 100 mm.

### Conclusions

1 It is described the method of changing the stiffness of an elastic support by changing the linear size of the free part of its elastic element with limiters of different heights.

2 Experimental dependences were obtained to determine the shrinkage of the support while the external pressure on it changes and the height of the free part of its elastic element changes.

3 Practical value of the research is presented in designed vibration resistance with variable stiffness parameters. By changing the stiffness of the elastic vibration support, it is possible to change within the required limits the amplitude of the forced vibrations of the moving part of the vibrating platform or its moving frame and, accordingly, ensure the required quality of compaction of the concrete mixture.

### References

1. Podobed, I. M., Bykovsky, A. I., & Kobasov, V. M. (2014). Перспективні засоби захисту працівників від шкідливої дії вібрації та шуму на рейковому транспорті. *Проблеми охорони праці в Україні*, (28), 39-46.
2. Wang, S., Xin, W., Ning, Y., Li, B., & Hu, Y. (2020). Design, Experiment, and Improvement of a Quasi-Zero-Stiffness Vibration Isolation System. *Applied Sciences*, 10(7), 2273. <https://doi.org/10.3390/app10072273>
3. Клітної, В. В. (2015). Аналіз використання активних віброзахисних систем з керованою квазінульовою жорсткістю. *Енергосбереження. Енергетика. Енергоаудит*, (2), 66-71. [http://nbuv.gov.ua/UJRN/ecee\\_2015\\_2\\_10](http://nbuv.gov.ua/UJRN/ecee_2015_2_10)
4. Ma, Z., Zhou, R., & Yang, Q. (2022). Recent advances in quasi-zero stiffness vibration isolation systems: An overview and future possibilities. *Machines*, 10(9), 813. <https://doi.org/10.3390/machines10090813>
5. Kowal, J., Pluta, J., Konieczny, J., & Kot, A. (2008). Energy recovering in active vibration isolation system – results of experimental research. *Journal of Vibration and Control*, 14(7), 1075–1088. <https://doi.org/10.1177/10775463080888980>
6. Massarsch, K. R., & Fellenius, B. H. (2019). Evaluation of vibratory compaction by in situ tests. *Journal of Geotechnical and Geoenvironmental Engineering*, 145(12). [https://doi.org/10.1061/\(asce\)gt.1943-5606.0002166](https://doi.org/10.1061/(asce)gt.1943-5606.0002166)
7. Федоряк, Н.В., Лях, М.М. & Михайлів, В.В. 2020. Аналіз чинників, що впливають на траєкторію руху ситополотна вібратора. *Prospecting and Development of Oil and Gas Fields*. 3(76), 61–70. [https://doi.org/10.31471/1993-9973-2020-3\(76\)-61-70](https://doi.org/10.31471/1993-9973-2020-3(76)-61-70)
8. Nesterenko, M. P., Sklyarenko, T. O., & Malinsky, S. (2014). Promising means of protecting workers from the harmful effects of vibration and noise on rail transport. *Problems of labor protection in Ukraine*, (28), 39-46.
9. Wang, S., Xin, W., Ning, Y., Li, B., & Hu, Y. (2020). Design, Experiment, and Improvement of a Quasi-Zero-Stiffness Vibration Isolation System. *Applied Sciences*, 10(7), 2273. <https://doi.org/10.3390/app10072273>
10. Klitnoi, V. V. (2015). Analysis of the use of active anti-vibration systems with controlled quasi-zero stiffness. *Energy saving. Power engineering. Energy audit*, (2), 66-71. [http://nbuv.gov.ua/UJRN/ecee\\_2015\\_2\\_10](http://nbuv.gov.ua/UJRN/ecee_2015_2_10)
11. Ma, Z., Zhou, R., & Yang, Q. (2022). Recent advances in quasi-zero stiffness vibration isolation systems: An overview and future possibilities. *Machines*, 10(9), 813. <https://doi.org/10.3390/machines10090813>
12. Kowal, J., Pluta, J., Konieczny, J., & Kot, A. (2008). Energy recovering in active vibration isolation system – results of experimental research. *Journal of Vibration and Control*, 14(7), 1075–1088. <https://doi.org/10.1177/10775463080888980>
13. Massarsch, K. R., & Fellenius, B. H. (2019). Evaluation of vibratory compaction by in situ tests. *Journal of Geotechnical and Geoenvironmental Engineering*, 145(12). [https://doi.org/10.1061/\(asce\)gt.1943-5606.0002166](https://doi.org/10.1061/(asce)gt.1943-5606.0002166)
14. Fedoliak, N. V., Liakh, M. M., & Mykhayliv, V. V. (2020). The analysis of factors influencing the trajectory of the vibrating screen. *Prospecting and Development of Oil and Gas Fields*, 3(76), 61–70. [https://doi.org/10.31471/1993-9973-2020-3\(76\)-61-70](https://doi.org/10.31471/1993-9973-2020-3(76)-61-70)
15. Nesterenko, M. P., Sklyarenko, T. O., & Malinsky, S. (2014). Promising means of protecting workers from the harmful effects of vibration and noise on rail transport. *Problems of labor protection in Ukraine*, (28), 39-46.

8. Нестеренко, М. П., Скляренко, Т. О., & Малинський, С. М. (2009). Дослідження руху віброплощадки із циліндричними та конічними опорами. *Збірник наукових праць галузеве машинобудування, будівництво*, 23(2), 56–62. <http://reposit.pntu.edu.ua/handle/PoltNTU/8328>
9. Лях, М. М., Федоряк, Н. В., & Вакалюк, В. М. (2015). Дослідження впливу коливальних рухів сітки на ефективність роботи вібросити. *Prospecting and Development of Oil and Gas Fields*, (4(57)), 36–42. [http://nbuv.gov.ua/UJRN/rngr\\_2015\\_4\\_6](http://nbuv.gov.ua/UJRN/rngr_2015_4_6)
10. Назаренко, І. І. (2007). *Вібраційні машини і процеси будівельної індустрії*. Київ: КНУБА.
11. Назаренко, І. І., & Туманська, О. В. (2004). *Машини і устаткування підприємств будівельних матеріалів: Конструкції та основи експлуатації*. Київ: Вища школа.
12. Juradin, S., Baloević, G., & Harapin, A. (2014). Impact of vibrations on the final characteristics of normal and self-compacting concrete. *Materials Research*, 17(1), 178–185. <https://doi.org/10.1590/S1516-14392013005000201>
13. Сівко В.Й., Кузьмінець М.П. (2012). Оцінка впливу робочого середовища на режими коливань вібраційних машин. *Теорія і практика будівництва*, 10, 3–5
14. Нестеренко, М. П., Воскобійник, О. П., Павленко, А. М. (2017). Розроблення пружних опор вібраційних площадок для формування залізобетонних виробів. *ACADEMIC JOURNAL Industrial Machine Building, Civil Engineering*, 1(43), 238–243. <http://journals.nupp.edu.ua/znp/article/view/129>
15. Гурин, В. А., Востріков, В. П., & Кузьмич, Л. В. (2019). *Основи промислових технологій і матеріалознавства*. Рівне: НУВГП.
16. Нечасв, В. П., Берідзе, Т. М., & Кононенко, В. В. (2005). *Теорія планування експерименту*. Київ: Кондор.
- M. (2009). Study of the movement of a vibrating platform with cylindrical and conical supports. *Collection of scientific works branch engineering, construction*, 23(2), 56–62. <http://reposit.pntu.edu.ua/handle/PoltNTU/8328>
9. Lyakh, M. M., Fedolyak, N. V., & Vakalyuk, V. M. (2015). Study of the effect of vibrating net movements on the efficiency of the vibrating screen. *Prospecting and Development of Oil and Gas Fields*, (4(57)), 36–42. [http://nbuv.gov.ua/UJRN/rngr\\_2015\\_4\\_6](http://nbuv.gov.ua/UJRN/rngr_2015_4_6)
10. Nazarenko I.I. (2007). *Vibration machines and the processes of the construction industry*. Kyiv: KNUCA
11. Nazarenko, I. I., & Tumanska, O. V. (2004). *Machines and equipment of building materials enterprises: Designs and basics of operation*. Kyiv: Higher School.
12. Juradin, S., Baloević, G., & Harapin, A. (2014). Impact of vibrations on the final characteristics of normal and self-compacting concrete. *Materials Research*, 17(1), 178–185. <https://doi.org/10.1590/S1516-14392013005000201>
- 13 Sivko V.Y., Kuzminets M.P. (2012). Estimation of influence of the working environment on vibration modes of vibrating machines. *The Theory and practice of construction*, 10, 3–5.
14. Nesterenko, M. P., Voskobiynyk, O. P., Pavlenko, A. M. (2017). Development of elastic supports of vibrating platforms for the formation of reinforced concrete products. *ACADEMIC JOURNAL Industrial Machine Building, Civil Engineering*, 1(43), 238–243. <http://journals.nupp.edu.ua/znp/article/view/129>
15. Guryn, V. A., Vostrikov, V. P., & Kuzmych, L. V. (2019). *Basics of industrial technologies and materials science*. Rivne: NUWEE.
16. Nechaev, V. P., Beridze, T. M., & Kononenko, V. V. (2005). *Theory of experiment planning*. Kyiv: Condor.

UDC 629.331

## Spatial interaction analytical links study of category M1 road trains

Orysenko Oleksandr<sup>1\*</sup>, Skoryk Maksym<sup>2</sup>, Kryvorot Anatolii<sup>3</sup>, Virchenko Viktor<sup>4</sup>

<sup>1</sup> National University «Yuri Kondratyuk Poltava Polytechnic» <https://orcid.org/0000-0003-3103-0096>

<sup>2</sup> National University «Yuri Kondratyuk Poltava Polytechnic» <https://orcid.org/0000-0001-9001-4913>

<sup>3</sup> National University «Yuri Kondratyuk Poltava Polytechnic» <https://orcid.org/0000-0001-5919-7352>

<sup>4</sup> National University «Yuri Kondratyuk Poltava Polytechnic» <https://orcid.org/0000-0001-7681-5124>

\*Corresponding author E-mail: [oleksandr.orysenko@gmail.com](mailto:oleksandr.orysenko@gmail.com)

During the movement of a road train, the towing device takes on the load from one link of the road train and transmits it to another. In the study of the processes of links interaction in real traffic conditions, a spatial system of forces acts on each road train link and there is a need to bring them to the calculated plane. It is proposed to consider each link in a separate spatial coordinate system, which is fixed with this link, and then, using the developed transition tables, to bring these forces to the coordinate system, which is fixed with another link

**Keywords:** road train, traction and coupling device, trailer, rotation matrices, fixed and moving coordinate systems.

## Аналітичне дослідження просторової взаємодії ланок автопоїзда категорії М1

Орисенко О.В.<sup>1\*</sup>, Скорик М.О.<sup>2</sup>, Криворот А.І.<sup>3</sup>, Вірченко В.В.<sup>7</sup>

<sup>1, 2, 3, 4</sup> Національний університет «Полтавська політехніка імені Юрія Кондратюка»

\* Адреса для листування E-mail: [oleksandr.orysenko@gmail.com](mailto:oleksandr.orysenko@gmail.com)

Під час руху автомобільного поїзда взаємодія між його окремими ланками відбувається через тягово-зчіпний пристрій. Саме цей вузол сприймає на себе навантаження від однієї ланки автопоїзда та передає його до іншої. Тому вірно визначення величини та напрямку сил, які виникають в тягово-зчіпному пристрої є актуальною задачею, яка дозволяє вирішити ряд питань пов'язаних з дослідженням експлуатаційних властивостей автопоїзда, таких як: динаміка руху, гальмівні властивості, паливна економічність, стійкість, безпека руху, зручність керування та ряд інших. Також це є важливим і при проектуванні його окремих деталей і вузлів, таких, наприклад, як тягово-зчіпний пристрій. Зазвичай, при дослідженні динамічної взаємодії ланок автопоїзда та кінематики його руху обмежуються плоскими розрахунковими схемами, які дозволяють розглядати протікання цих процесів лише в одній площині. Проте, в реальних умовах руху на кожну ланку автопоїзда діє просторова система сил і виникає потреба у їх приведенні до розрахункової площини. У протилежному випадку облік складових, що впливають на взаємодію ланок буде неповним, а отже і неточним. Для більш повного врахування силової взаємодії між ланками автопоїзда пропонується розглядати кожну ланку у окремій просторовій системі координат, яка нерухомо пов'язана з цією ланкою, а потім за допомогою розроблених таблиць переходу приводити ці сили до системи координат, яка нерухомо пов'язана з іншою ланкою. Застосовуючи такий підхід, на прикладі розрахунку динамічних навантажень у тягово-зчіпному пристрої автопоїзда категорії М1 у випадку відхилення напрямку його руху від горизонтального прямолінійного показано, що динамічний вплив причепа на автомобіль-тягач виявлятиметься не лише у повздовжньому напрямку, а й у складових по інших осям просторової системи координат, що дозволяє прогнозувати вплив причепа на характер руху автопоїзда в цілому.

**Ключові слова:** автопоїзд, тягово-зчіпний пристрій, причіп, матриці поворотів, нерухома та рухома системи координат.

## Introduction

The study of the road train links interaction today remains an urgent task. This is due to the fact that this interaction determines the nature of the movement of the train as a whole and affects such indicators as: motion dynamics, braking properties, fuel efficiency, resistance, traffic safety, ease of operation and a number of others [1]. It is also necessary to take into account the load on the power plant, the transmission of the tractor car and the towing device, which determines their wear, reliable and trouble-free operation during the established service life.

Given that this interaction occurs through a towing device, it can be argued that knowledge of the magnitude and direction of the forces applied by one of the links of the road train to the towing device makes it possible to predict how the other link and the road train as a whole will react to this influence.

Therefore, the correct determination of the magnitude and direction of the forces brought to the towing device is an urgent issue, since it allows solving a number of problems related to the design and operation of road trains.

## Review of the research sources and publications

The interaction of the links of the road train during movement is devoted to a number of works by domestic and foreign scientists. The issues of determining the stability indicators of road trains of category M1 are devoted to the work [2-4], the development of the trains mathematical model movement is devoted to the work [5, 7], and simulation of his work is considered in [6, 8, 9]. The study of braking processes is devoted to the work [10].

The study of the loads influence of the towing device on the category M1 road train movement stability during transient driving modes is given in the work [11].

In work [12] systems of differential equations are given, which take into account the law of change in the force arising in the towing device in the case of using the usual and dynamic drawbar of the road train trailed link. It is also shown that the cause of longitudinal dynamic loads in the towing device is the oscillations of the trailer in the longitudinal vertical plane.

This interaction of the links of the road train is explained by the fact that any spatial system of forces that affect a separate link of a road train can be led to one equilibrium, which is then decomposed into projections along the axes of the spatial coordinate system [13]. Since the power interaction between the links of the road train is carried out through a towing device, it becomes necessary to bring the equilibrium projections of the forces spatial system to this particular device and decomposition on the projections along the axes of the spatial coordinate system associated with this device.

In the preparation of differential equations given in [12], the following assumptions are made:

- the traction car and trailer are absolutely solid bodies that do not change their size in the process of movement;
- the link that has elastic and dissipative properties in this system is only a towing device;

- gaps in the towing device are neglected, given their small size;
- the traction car and trailer move in a straight line;
- the traction car moves on a flat horizontal surface, and oscillations in the longitudinal vertical plane are performed only by the trailer.

## Definition of unsolved aspects of the problem

The analysis of scientific papers devoted to the study of the interaction of links of a road train shows that to compile differential equations of motion or establish kinematic dependencies, the authors use design schemes that lie in the same plane – horizontal or vertical. However, under real conditions, each of the links is affected by a spatial system of forces in which a number of components do not belong to the calculated plane, but affect the train movement nature.

Consideration of such components is possible provided that there is a mathematical model that allows you to bring spatial forces to the axes of coordinate systems that are associated with each individual link of the train.

## Problem statement

The purpose of this publication is to highlight the results of a trailer influence analytical study on a traction car, taking into account the spatial interactions of these links on the M1 category road train example.

## Basic material and results

In work [14] a table of transition between coordinate systems is given, one of which is fixed with a traction car and the other with a trailer.

The compilation of such a table is carried out on the basis of the assumption that the traction car and the trailer interact with each other through a traction coupling device, which has the shape of a sphere and in which there are no gaps. Under such conditions, the translational movements of the traction car and trailer relative to each other can be neglected and assume that the mutual change in the position of these links is carried out only in the form of deviations of one link relative to another at certain angles in the planes of the spatial coordinate system. It is also assumed that while driving, the tractor car is always on a flat horizontal surface, and when overcoming road irregularities, only the trailer changes its position.

The use of this approach allows you to carry out operations with forces that affect one of the links of the road train in its own coordinate system, and then, if necessary, bring these forces to the coordinate system of the other link.

When choosing the location of fixed and moving coordinate systems, the requirements of SAE were taken into account when describing the dynamic processes of the car (Figure 1). In this case, a right-handed orthogonal coordinate system is used, with a beginning in the center of mass of the vehicle. It is assumed that this coordinate system is motionlessly connected to the vehicle and moves with it. According to the SAE convention, the axes of the coordinate system have the following directions:

–  $O_X$  – located in the plane of the longitudinal axis of symmetry of the car and directed in the direction of its movement forward;

–  $O_Y$  – lies in the horizontal plane and is directed sideways to the right side of the vehicle;

–  $O_Z$  – directed downward in relation to the vehicle.

Rotations around these axes have the following names:

–  $p$  – rotate around an axis  $X$  (roll);

–  $q$  – rotate around an axis  $Y$  (pitch);

–  $r$  – rotate around an axis  $Z$  (yawing).

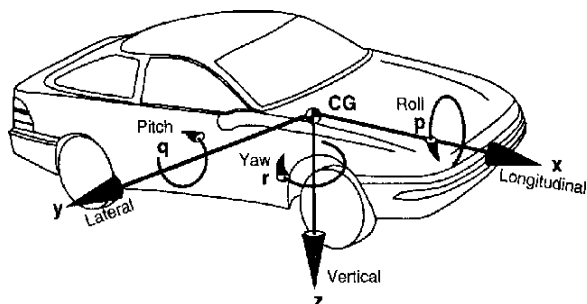


**Figure 1 – Vehicle axle system according to SAE**

In our case, the location of the coordinate systems is as follows. We associate the beginning of the  $O_{XYZ}$  coordinate system with the center of the hinge of the towing device, which is rigidly connected to the traction car and does not change its position relative to it while driving (Figure 2). The position of the coordinate axes of this system is as follows: the  $O_X$  axis is horizontal and is located along the longitudinal axis of symmetry of the car and is directed in the direction opposite to the movement; the  $O_Y$  axis is also in the horizontal plane and directed to the left side of the car;  $O_Z$  axis pointing vertically upwards.

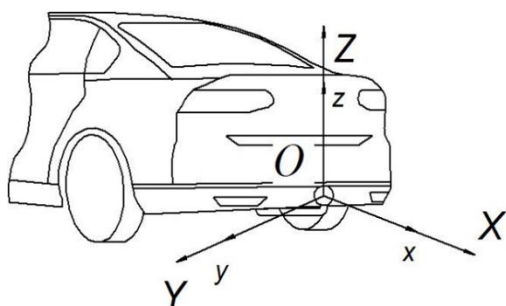


**Figure 2 – Coordinate systems of the car and trailer in the initial period of time**

The rotation from the  $O_X$  axis to the  $O_Z$  axis is clockwise (left-handed coordinate system).

Another  $Oxyz$  coordinate system also originates in the center of the hinge of the towing device, the direction of its axes in the initial period of time coincides with the direction of the axes of the  $Oxyz$  coordinate system, but it is rigidly connected to the trailer and does not change its position relative to it while driving. Thus, we have two coordinate systems, fixed  $Oxyz$  and movable  $Oxyz$  (in relation to the tractor car), which originate in the center of the hinge of the towing device and coincide in the initial period of time (Figure 2).

When driving, overcoming the irregularities of the supporting surface, the trailer will change its position relative to the car. The axes of the  $Oxyz$  coordinate system will deviate from their original position, and therefore from the axes of the  $Oxyz$  coordinate system.

In this case, the change in the position of the links relative to each other is conveniently represented as a spherical motion.

As is known [13], with spherical motion, the position of the body in space can be set using three coordinates, which represent the angles of rotation of the moving coordinate system relative to the fixed axes. Usually, a moving coordinate system is associated with the body under study, and a fixed one with the surface of the earth, or a body that is mistaken for stationary. The axes of both coordinate systems originate at the same point and coincide at the initial point in time.

In work [14] it is shown that each of the rotations around the axes of a fixed coordinate system corresponds to a matrix that determines the position of the axes of the moving coordinate system relative to the stationary one. By introducing the following notation of rotation angles around the axes of a fixed coordinate system,  $\alpha$  – rotation angle around axis  $O_X$ ,  $\beta$  – rotation angle around axis  $O_Y$ ,  $\gamma$  – rotation angle around axis  $O_Z$ , we obtain the rotation matrices given in the table 1.

In cases where the position of a moving body relative to a fixed one is described using several turns, the resulting matrix is used, which is obtained by multiplying the matrices of individual turns.

In [14], the resulting matrix for the sequence of rotations around the axes is given  $O_X$ ,  $O_Y$ ,  $O_Z$  (Figure 3) respectively at angles  $\alpha$ ,  $\beta$ ,  $\gamma$ .

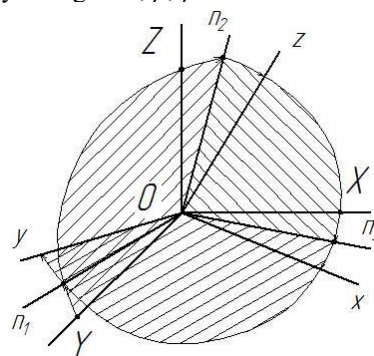


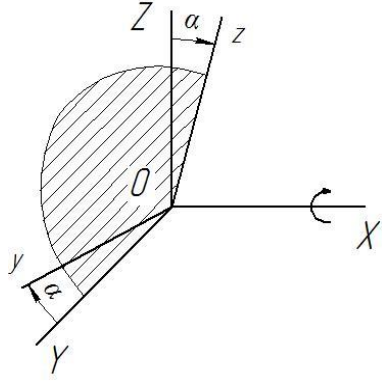
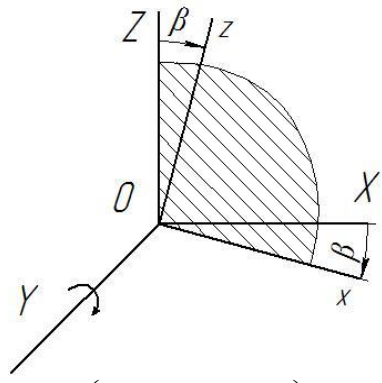
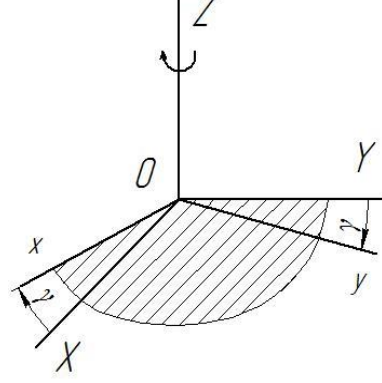
**Figure 3 – The position of the moving coordinate system relative to stationary with sequential execution of three turns around the axes  $O_X$ ,  $O_Y$ ,  $O_Z$**

This matrix will have the form

$$\begin{pmatrix} \cos \gamma & -\sin \gamma & 0 \\ \sin \gamma & \cos \gamma & 0 \\ 0 & 0 & 1 \end{pmatrix} \times \begin{pmatrix} \cos \beta & 0 & \sin \beta \\ 0 & 1 & 0 \\ -\sin \beta & 0 & \cos \beta \end{pmatrix} \times \begin{pmatrix} 1 & 0 & 0 \\ 0 & \cos \alpha & -\sin \alpha \\ 0 & \sin \alpha & \cos \alpha \end{pmatrix} = \begin{pmatrix} \cos \beta \cdot \cos \gamma & \sin \alpha \cdot \sin \beta \cdot \cos \gamma - \cos \alpha \cdot \sin \beta \cdot \cos \gamma + \\ & -\cos \alpha \cdot \sin \gamma & +\sin \alpha \cdot \sin \gamma \\ \cos \beta \cdot \sin \gamma & \sin \alpha \cdot \sin \beta \cdot \sin \gamma + \cos \alpha \cdot \sin \beta \cdot \sin \gamma - \\ & +\cos \alpha \cdot \cos \gamma & -\sin \alpha \cdot \cos \gamma \\ -\sin \beta & \sin \alpha \cdot \cos \beta & \cos \alpha \cdot \cos \beta \end{pmatrix}$$



**Table 1 – Matrices of rotation  
around axes  $Ox$ ,  $Oy$ ,  $Oz$**

<b>Rotate around an axis <math>Ox</math></b>	
	$\begin{pmatrix} 1 & 0 & 0 \\ 0 & \cos \alpha & -\sin \alpha \\ 0 & \sin \alpha & \cos \alpha \end{pmatrix}$
<b>Rotate around an axis <math>Oy</math></b>	
	$\begin{pmatrix} \cos \beta & 0 & \sin \beta \\ 0 & 1 & 0 \\ -\sin \beta & 0 & \cos \beta \end{pmatrix}$
<b>Rotate around an axis <math>Oz</math></b>	
	$\begin{pmatrix} \cos \gamma & -\sin \gamma & 0 \\ \sin \gamma & \cos \gamma & 0 \\ 0 & 0 & 1 \end{pmatrix}$

Transposing the matrix, we obtain a table of transition between moving and fixed coordinate systems (Table 2).

**Table 2 – Transition table between moving and fixed coordinate systems**

Оси систем координат	$Ox$	$Oy$	$Oz$
$Ox$	$\cos \beta \cdot \cos \gamma$	$\cos \beta \cdot \sin \gamma$	$-\sin \beta$
$Oy$	$\sin \alpha \cdot \sin \beta \cdot \cos \gamma - \cos \alpha \cdot \sin \gamma$	$\sin \alpha \cdot \sin \beta \cdot \sin \gamma + \cos \alpha \cdot \cos \gamma$	$\sin \alpha \cdot \cos \beta$
$Oz$	$\cos \alpha \cdot \sin \beta \cdot \cos \gamma + \sin \alpha \cdot \sin \gamma$	$\cos \alpha \cdot \sin \beta \cdot \sin \gamma - \sin \alpha \cdot \cos \gamma$	$\cos \alpha \cdot \cos \beta$

The use of such a transition table allows you to bring the spatial system of forces that affect the link of the trailer to the associated coordinate system. In the future, using the above table, you can bring the indicated forces to the coordinate system of another link.

Since the product of the matrices is not commutative, it is obvious that the transition tables between coordinate systems will differ depending on the sequence of rotations adopted. If we take into account that the rotation around each of the axes of a fixed coordinate system is carried out only once, then as shown in [14] there are six possible variants of transition tables. The question arises what will be the difference in the values of the projections of forces on the axis of a fixed coordinate system with different possible variants of the sequence of rotations and, accordingly, when using different transition tables?

For this purpose, a computational study was conducted. The force, the value of which was conventionally taken as 100 units and the direction of action of which in the moving coordinate system  $Oxyz$  coincides with the axis  $Oh$ , is reduced to a fixed system  $Oxyz$  using the transition tables given in the work [14]. The angles of rotation were also conventionally assumed to be the same and with a magnitude of 0.2 radians. The calculations carried out show that the choice of the matrix does not affect the final result. The discrepancy in the results lies within the accuracy of the calculations.

For an analytical study of the interaction of road train links, we consider the case of the dynamic influence of a trailer on a tractor car during transient modes of movement of a transport train, taking into account the possible deviation of the road from the rectilinear direction and the presence of bows in the transverse and longitudinal directions.

We use the equation of dynamic interaction of the links of the train, which is given in [12]. We neglect the forces of dissipative resistance, since the task is to determine the maximum possible loads.

$$P_d = \frac{T \cdot m_2 + F \cdot m_1}{(m_1 + m_2)} \cdot (1 - \cos kt), \quad (1)$$

where  $T$  – traction force of the traction car;

$F$  – trailer resistance force when towing;

$m_1, m_2$  – weight of traction car and trailer, respectively;

$k$  – trailer natural frequency;

$t$  – time.

We use the transition table between moving and fixed coordinate systems in the sequence of turns  $Ox$ ,  $Oy$ ,  $Oz$  (Table 2).

Then the component of the dynamic impact falling on the  $Ox$  axis of the coordinate system associated with the tractor car is defined as

$$P_{dx} = \frac{T \cdot m_2 + F \cdot m_1}{(m_1 + m_2)} \cdot (1 - \cos kt) \cdot \cos \gamma \cdot \cos \beta, \quad (2)$$

where  $\gamma, \beta$  – angles of rotation of the axes of the moving coordinate system relative to the fixed axes, respectively; OZ, OY.

Component of dynamic influence per axis OY

$$P_{dy} = \frac{T \cdot m_2 + F \cdot m_1}{(m_1 + m_2)} \cdot (1 - \cos kt) \cdot \sin \gamma \cdot \cos \beta. \quad (3)$$

Component of dynamic influence per axis OZ

$$P_{dz} = \frac{T \cdot m_2 + F \cdot m_1}{(m_1 + m_2)} \cdot (1 - \cos kt) \cdot \sin \beta. \quad (4)$$

After analyzing equations 2 – 4, we come to the conclusion that the component of the dynamic load, which in the coordinate system of the trailer had a direction only along the OX axis, will affect the tractor car also along the OY and OZ axes, which makes it possible to take into account the vertical and transverse horizontal dynamic components acting on the towing device.

So, for example, for a road train of category M1, which includes a passenger car and a passenger trailer with the technical characteristics given in Table 3, we have the results shown in the graph (Figure 4). The calculation of load values for possible sequences of turns was obtained in the application Mathcad 15.

**Table 3** – Brief technical characteristics of the traction car and trailer

No	Name	Value
Car		
1	Gross weight, $m_1$ kg	1595
2	Design traction force on the drive wheels T, N	7050
Trailer		
1	Gross weight $m_2$ , kg	700
2	Design resistance to movement F, N	686,7
Towing device		
1	Natural frequency of the system, k	543,38

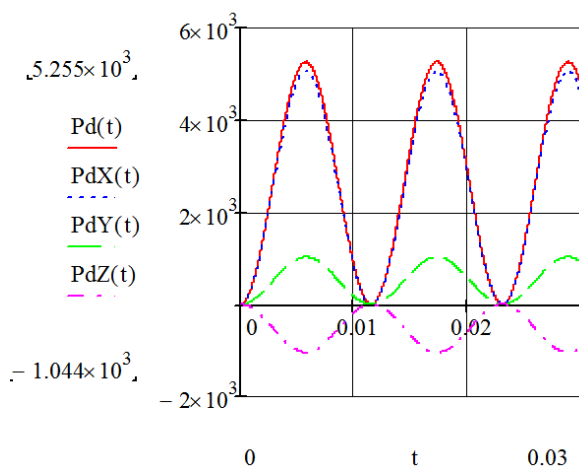


**Figure 4** – Graph of the spatial load of the towing device during the sequence of turns OX, OY, OZ

In order to determine the maximum and minimum values of loads on the towing device for a given sequence of turns, we will check the function for extremes.

To do this, we find the first-time derivative of the function, equate it to zero, solve the equation and substitute the found roots into the function equation.

We find the first-time derivative of function (1) at constant values of quantities  $T = 7050$ ;  $F = 686,7$ ;  $m_1 = 1595$ ;  $m_2 = 700$ ;  $k = 543,38$ ;  $\alpha = 0,2$ ;  $\beta = 0,2$ ;  $\gamma = 0,2$ .

$$\frac{dP_d}{dt} = k \cdot \sin kt \cdot \frac{T \cdot m_2 + F \cdot m_1}{m_1 + m_2}. \quad (5)$$

We equate (5) to zero

$$k \cdot \sin kt \cdot \frac{T \cdot m_2 + F \cdot m_1}{m_1 + m_2} = 0. \quad (6)$$

Obviously, this function will be zero provided  $\sin kt = 0$ , what is possible with

$$kt = \pi \cdot n, \quad (7)$$

where  $n \in \mathbb{Z}$  –  $\mathbb{Z}$  the set of natural numbers, i.e.  $\mathbb{Z} = 1, 2, 3, \dots$

With  $n = 1$ , time  $t$ , s

$$t = \pi \frac{n}{k}. \quad (8)$$

$$t = \pi \frac{1}{543,38} = 5,782 \cdot 10^{-3}. \quad (9)$$

Then  $P_d, N$ ,

$$P_d = \frac{7050 \cdot 700 + 686,7 \cdot 1595}{(1595 + 700)} \times (1 - \cos(543,38 \cdot 5,782 \cdot 10^{-3})) = 5,255 \cdot 10^3 \quad (10)$$

With  $n = 2$  time will be  $t = 0,012$ .

Then the value of  $P_d, N$ ,

$$P_d = \frac{7050 \cdot 700 + 686,7 \cdot 1595}{(1595 + 700)} \times (1 - \cos(543,38 \cdot 0,012)) = 0 \quad (11)$$

Subsequently, with increasing values of  $n$ , the value of  $P_d$  will be repeated based on the frequency of the function  $\cos$ .

Find the maximum values of dynamic load projections  $P_d$  on the axis of the fixed coordinate system OXYZ, taking into account the spatial impact.

The projection onto the OX axis will have expression (2). Then the first time derivative

$$\frac{dP_{dx}}{dt} = k \cdot \sin kt \cdot \cos \gamma \cdot \cos \beta \cdot \frac{T \cdot m_2 + F \cdot m_1}{m_1 + m_2}. \quad (12)$$

Equating to zero (12) and solving the equation, we obtain the value  $t = 5,782 \cdot 10^{-3}$  with  $n = 1$  and  $t = 0,012$  with  $n = 2$ .

With these  $t$  values, the value of the projection on the OX axis will be  $P_{dx} = 5,084 \cdot 10^3$  N and  $P_{dx} = 0$ .

We carry out similar calculations to determine the values of the projections of the dynamic load  $P_d$  on the axis of a fixed coordinate system OY and OZ. For the same values of angles of rotation, we have maximum projection values  $P_{dy} = 1,023 \cdot 10^3$  N,  $P_{dz} = -1,044 \cdot 10^3$  N with  $n = 1$  and  $P_{dy} = P_{dz} = 0$  with  $n = 2$ .

We find the percentage ratio of individual projections and dynamic load, which is obtained without taking

into account the rotation of the coordinate system according to the formula

$$\frac{P_a}{P_{ai}} \cdot 100\% . \quad (13)$$

For projection onto an axis OX, %

$$\frac{P_{ax}}{P_a} = \frac{5,084 \cdot 10^3}{5,255 \cdot 10^3} \cdot 100\% = 96,7 . \quad (14)$$

For projection onto an axis OY, %

$$\frac{P_{ay}}{P_a} = \frac{1,023 \cdot 10^3}{5,255 \cdot 10^3} \cdot 100\% = 19,5 . \quad (15)$$

For projection onto an axis OZ, %

$$\frac{P_{az}}{P_a} = \frac{1,044 \cdot 10^3}{5,255 \cdot 10^3} \cdot 100\% = 19,9 . \quad (16)$$

## Conclusions

Based on the calculations of the maximum values of projections of dynamic loads in the towing device on the axis of the fixed coordinate system with the sequence of turns OX, OY, OZ and graphical dependencies are constructed (**Figure 1**) we come to the following conclusions:

– in case of deviation of the direction of movement of the road train from the horizontal rectilinear dynamic effect of the trailer on the tractor car will be manifested not only in the longitudinal component along the OX

axis, but also along other axes of the spatial coordinate system;

– as a percentage, the magnitude of the projections of dynamic impact at the angles of deviation of the moving coordinate system relative to a fixed one by an angle of 0.2 rad is: along the OX axis – 96.7%, which is the largest value among the projections; OY axis – 19.5%; on the OZ axis – 19.9% in the negative direction;

– The dynamic component that occurs during transient modes of movement of a road train under these conditions, in addition to loading in the longitudinal direction, causes a force effect on the tractor car also in the lateral direction, which under certain conditions can lead to skidding of the car;

– The vertical component of the dynamic impact has a negative direction, that is, it is directed downwards and will contribute to pressing the wheels of the rear axle of the car to the supporting surface, which, in addition to the positive effect for movement due to an increase in the coefficient of adhesion of the wheels to the road, has negative consequences, expressed in raising the front of the car and, as a result, deterioration in handling and adhesion of the drive wheels to the supporting surface for front-wheel drive cars.

## References

1. Подригало М.А., Шелудченко В.В. (2015). *Нове в теорії експлуатаційних властивостей автомобілів та тракторів*, Суми: Сумський національний аграрний університет
2. Сахно В.П., Кузнецов Р.М., Стельмашук В.В., Козачук Л.С. (2014). До визначення показників стійкості автопоїзда категорії М1 у перехідних режимах руху. *Сучасні технології в машинобудуванні та транспорті*, 2, 123-128  
[http://nbuv.gov.ua/UJRN/ctmbt\\_2014\\_2\\_20](http://nbuv.gov.ua/UJRN/ctmbt_2014_2_20)
3. Козачук Л.С. (2014). До визначення стійкості руху автопоїзда категорії М1. *Вісник ЖДТУ. Серія «Технічні науки»*, 2(69), 121-128  
[http://nbuv.gov.ua/UJRN/Vzhdtu\\_2014\\_2\\_23](http://nbuv.gov.ua/UJRN/Vzhdtu_2014_2_23)
4. Стельмашук В.В., Пазін Р.В. (2016). До питання комплектації автопоїзда з причепом категорії О2. *Вісник машинобудування та транспорту*, 2, 97-105
5. Сахно В.П., Шарай С.М., Мурованій І.С., Човча І.В. (2021). До розробки математичної моделі автопоїзда з причепом категорії О1 у поперечній площині. *Сучасні технології в машинобудуванні та транспорті*, 2(17), 151-160
6. Fratila D., Darling J. (1996). Simulation of Coupled Car and Caravan Handling Behavior. *Vehicle System Dynamics*, 26:6, 397-429  
<http://worldcat.org/issn/00423114>
7. Zhang N., Yin G., Mi T., Li X., Chen N. (2017). Analysis of Dynamic Stability of Car-trailer Combinations with Nonlinear Damper Properties. *Procedia IUTAM*, 22, 251-258  
<https://doi.org/10.1016/j.piutam.2017.08.033>
8. Mohajer N., Abdi H., Nelson K., Nahavandi S. (2015). Vehicle motion simulators, a key step towards road vehicle dynamics improvement. *Vehicle System Dynamics*, 53:8, 1204-1226  
<https://doi.org/10.1080/00423114.2015.1039551>
1. Podrigalo M.A., Sheludchenko V.V. (2015). *New in the theory of operational properties of cars and tractors*. Sumy: Sumy National Agrarian University
2. Sakhno V.P., Kuznetsov R.M., Stelmashchuk V.V., Kozachuk L.S. (2014). To determine the stability indices of a M1 category train in transitional modes of movement. *Modern technologies in machine building and transport*, 2, 123-128  
[http://nbuv.gov.ua/UJRN/ctmbt\\_2014\\_2\\_20](http://nbuv.gov.ua/UJRN/ctmbt_2014_2_20)
3. Kozachuk L.S. (2014). To determine the stability of the road train category M1. *Bulletin of ZhSTU. «Technical Sciences»*, 2(69), 121-128  
[http://nbuv.gov.ua/UJRN/Vzhdtu\\_2014\\_2\\_23](http://nbuv.gov.ua/UJRN/Vzhdtu_2014_2_23)
4. Stelmashchuk V.V., Pazin R.V. (2016). On the question of completing a road train with a trailer of category O2. *Bulletin of Mechanical Engineering and Transport*, 2, 97-105
5. Sakhno V.P., Sharay S.M., Murovany I.S., Chovcha I.V. (2021). To the development of a mathematical model of a road train with a trailer of category O1 in the transverse plane. *Modern technologies in machine building and transport*, 2(17), 151-160
6. Fratila D., Darling J. (1996). Simulation of Coupled Car and Caravan Handling Behavior. *Vehicle System Dynamics*, 26:6, 397-429  
<http://worldcat.org/issn/00423114>
7. Zhang N., Yin G., Mi T., Li X., Chen N. (2017). Analysis of Dynamic Stability of Car-trailer Combinations with Nonlinear Damper Properties. *Procedia IUTAM*, 22, 251-258  
<https://doi.org/10.1016/j.piutam.2017.08.033>
8. Mohajer N., Abdi H., Nelson K., Nahavandi S. (2015). Vehicle motion simulators, a key step towards road vehicle dynamics improvement. *Vehicle System Dynamics*, 53:8, 1204-1226  
<https://doi.org/10.1080/00423114.2015.1039551>



9. Gomez-Bravo F., Cuesta F., Ollero A. (2005). Autonomous tractor-trailer back-up manoeuvring based on changing trailer orientation. *IFAC Proceedings Volumes*, 38(1), 301-306

[https://www.researchgate.net/publication/289879510\\_Autonomous\\_tractor-trailer\\_back-up\\_manoeuvring\\_based\\_on\\_changing\\_trailer\\_orientation](https://www.researchgate.net/publication/289879510_Autonomous_tractor-trailer_back-up_manoeuvring_based_on_changing_trailer_orientation)

10. Zhang N., Wu J., Li T., Zhao Z. Yin G. (2021). Influence of braking on dynamic stability of car-trailer combinations. *Proceedings of the Institution of Mechanical Engineers, Part D: Journal of Automobile Engineering*, 235(2-3), 455-464

<https://doi.org/10.1177/0954407020959895>

11. Сахно В.П., Кузнецов Р.М., Стельмашук В.В., Козачук Л.С. (2015). Вплив навантаження на тягово-зчипний пристрій на стійкість руху автопоїзда категорії М1 у перехідних режимах руху. *Сучасні технології в машинобудуванні та транспорті*, 1(3), 148-157

<https://doi.org/10.36910/automash.v1i3>

12. Orysenko O.V., Skoryk M.O., Kryvorot A.I., Shapoval M.V. (2018). The Dynamic Processes Mathematical Modeling in the Traction Coupling Device From Cars to the Trailers. *International Journal of Engineering & Technology*, 7(4.8), 473-477

<https://doi.org/10.14419/ijet.v7i4.8.27291>

13. Павловський М.А. (2002). *Теоретична механіка*. Київ: Техніка

14. Orysenko O., Skoryk M., Kryvorot A., Rassoha I. (2021). Determination of spatial interaction of the individual road train links. *Academic Journal. Industrial Machine Building, Civil Engineering*, 2(57), 98-104

<https://doi.org/10.26906/znp.2021.57.2591>

9. Gomez-Bravo F., Cuesta F., Ollero A. (2005). Autonomous tractor-trailer back-up manoeuvring based on changing trailer orientation. *IFAC Proceedings Volumes*, 38(1), 301-306

[https://www.researchgate.net/publication/289879510\\_Autonomous\\_tractor-trailer\\_back-up\\_manoeuvring\\_based\\_on\\_changing\\_trailer\\_orientation](https://www.researchgate.net/publication/289879510_Autonomous_tractor-trailer_back-up_manoeuvring_based_on_changing_trailer_orientation)

10. Zhang N., Wu J., Li T., Zhao Z. Yin G. (2021). Influence of braking on dynamic stability of car-trailer combinations. *Proceedings of the Institution of Mechanical Engineers, Part D: Journal of Automobile Engineering*, 235(2-3), 455-464

<https://doi.org/10.1177/0954407020959895>

11. Sakhno V.P., Kuznetsov R.M., Stelmashchuk V.V., Kozachuk L.S. (2015). Influence of loading on the traction coupling device on stability of movement of a road train of category M1 in transient modes of movement. *Modern technologies in mechanical engineering and transport*, 1(3), 148-157

<https://doi.org/10.36910/automash.v1i3>

12. Orysenko O.V., Skoryk M.O., Kryvorot A.I., Shapoval M.V. (2018). The Dynamic Processes Mathematical Modeling in the Traction Coupling Device From Cars to the Trailers. *International Journal of Engineering & Technology*, 7(4.8), 473-477

<https://doi.org/10.14419/ijet.v7i4.8.27291>

13. Pavlovsky M.A. (2002). *Theoretical mechanics*. Kyiv: Tekhnika

14. Orysenko O., Skoryk M., Kryvorot A., Rassoha I. (2021). Determination of spatial interaction of the individual road train links. *Academic Journal. Industrial Machine Building, Civil Engineering*, 2(57), 98-104

<https://doi.org/10.26906/znp.2021.57.2591>

UDC 621.437

## Development prospects of the rotary combustion engine as a car power unit

Zubenko Bohdan<sup>1\*</sup>, Vasyliov Oleksiy<sup>2</sup>, Rohozin Ivan<sup>3</sup>, Skoryk Maksym<sup>4</sup>

<sup>1</sup> National University «Yuri Kondratyuk Poltava Polytechnic» <https://orcid.org/0009-0002-1541-2369>

<sup>2</sup> National University «Yuri Kondratyuk Poltava Polytechnic» <https://orcid.org/0000-0002-9914-5482>

<sup>3</sup> National University «Yuri Kondratyuk Poltava Polytechnic» <https://orcid.org/0000-0002-9052-4806>

<sup>4</sup> National University «Yuri Kondratyuk Poltava Polytechnic» <https://orcid.org/0000-0001-9001-4913>

\*Corresponding author E-mail: [bogdanzubenko77@gmail.com](mailto:bogdanzubenko77@gmail.com)

The article briefly describes the main advantages and disadvantages of a rotary combustion engine as a car power unit and considers the option of improving the engine performance specifications due to the use of hydrogen as a fuel. Analyzing the researches, it was established the possibility of hydrogen rotary combustion engines safe work and improvement of the fuel mixture combustion indicators. Hydrogen rotary engines have been found to have low emissions. A scheme for integrating the hydrogen injection system into the design of a rotary internal engine is proposed. The operation of the apex seal between the rotor and the engine block was studied by modeling. It is reasonable to assume that rotary engines equipped to run on hydrogen fuel in the future can potentially be used as car power units, but today their design still needs further technological improvement.

**Keywords:** combustion, emission, fuel injection, hydrogen, rotary engine.

## Перспективи розвитку роторного двигуна як рушія автомобіля

Зубенко Б.С.<sup>1\*</sup>, Васильов О.С.<sup>2</sup>, Рогозін І.А.<sup>3</sup>, Скорик М.О.<sup>4</sup>

<sup>1, 2, 3, 4</sup> Національний університет «Полтавська політехніка імені Юрія Кондратюка»

\*Адреса для листування E-mail: [bogdanzubenko77@gmail.com](mailto:bogdanzubenko77@gmail.com)

У статті коротко описані основні переваги та недоліки роторного ДВЗ як рушія автомобіля та розглянуто варіант поліпшення характеристик двигуна за рахунок використання водню як палива. Аналізуючи багаторічні дослідження щодо застосування водневого палива для живлення роторного двигуна, встановлено можливість безаварійної роботи даних водневих ДВЗ за рахунок особливостей їх конструкції. Також з'ясовано, що заміна робочого палива фактично нівелює недоліки пов'язані з поганим згоранням бензино-повітряної суміші та викидами її недогорілих частин у атмосферу. Наведено опис основних характеристик водню (межі займистості, швидкість поширення полум'я, температура самозаймання та ін.) та його переваги в порівнянні з бензиновим паливом при застосуванні в роторному ДВЗ. Встановлено, що водневі роторні двигуни мають низький рівень викидів у порівнянні з бензиновими версіями, також для них доцільно застосувати системи рециркуляції вихлопних газів (EGR) для додаткового зниження рівня шкідливих речовин та одночасно з тим збільшення теплової ефективності. Запропоновано схему можливої інтеграції водневої системи живлення в конструкцію роторного ДВЗ, що складається з форсунок безпосереднього впорскування та форсунок зовнішнього впорскування, та коротко описано її роботу. Розглянуто вирішення проблеми слабкого крутного моменту роторного двигуна в діапазоні низьких обертів. Наведено дані 2022 року стосовно виробництва та застосування в автомобільному транспорті водневих роторних двигунів. Досліджено шляхом моделювання роботу верхівкового ущільнення між ротором і поверхнею корпусу двигуна з метою визначення обсягів витоків робочих газів та доведено, що вони не будуть чинити критичний вплив на ефективність двигуна. Обґрунтовано, що обладнані для роботи на водневому паливі роторні двигуни в майбутньому, потенційно, можуть використовуватися як рушії транспортних засобів, проте на сьогоднішній день дана силова установка не досягла свого найкращого рівня розвитку, її конструкція все ще потребує подальшого технологічного вдосконалення.

**Ключові слова:** згорання, викиди, система живлення двигуна, водень, роторний двигун.

## Introduction

In the last years the use of hydrogen as an alternative to fossil fuels for powering traditional internal combustion engines is one of the promising directions for the further road transport development. After all, the main advantages of hydrogen fuel are high combustion efficiency, high thermal efficiency and extended ignition bounds, and its combustion produces sufficiently clean energy. It is also important that there is a possibility of generating this fuel from renewable energy sources.

In addition, hydrogen internal combustion engines (HICE) require less investment to set up serial production compared to hydrogen fuel cells (HFC) due to the complexity of the manufacturing technology and the high cost of their components, which contain precious metals.

However, nowadays the wide implementation of piston engines equipped to work on hydrogen fuel in automobile transport is hindered by problems related to the risk of abnormal fuel combustion. But unlike piston internal combustion engines, the rotary engine can be converted to operate on hydrogen fuel without the risk of emergency modes. And it can be thanks to its design features. In addition, it will make it possible to get rid of some shortcomings those arise when using gasoline fuel.

## Review of research sources and publications

The first studies on the possibility of using hydrogen as a fuel for a rotary engine began in the mid-70s of the last century. In the early 1980s, German companies Audi and FEV conducted research on the suitability of hydrogen for rotary engines. It was determined that with a light modification of the rotary engine, it is possible to use hydrogen as a fuel. At the same time, the specific power of a rotary engine can remain as high as that has a conventional gasoline piston engine [1].

Mazda Motor Corporation as a automotive manufacturer has been researching the technology of using hydrogen fuel in rotary combustion engines for many years. In 1992, the company experimentally proved that a rotary hydrogen engine with preliminary mixture formation reaches a power of up to 63% of similar indicators when working on gasoline, while a piston hydrogen engine with preliminary mixture formation reaches only 50%. Also, in the case of a rotary engine, the injection cycle can be easily implemented with an output power at the level of 75% of the gasoline engine characteristics [2].

In 2011, scientists from the Kyushu University Engineering Faculty (Japan) together with Mazda engineers focused on optimizing the combustion process of hydrogen fuel in a rotary engine by increasing the combustion speed, increasing turbulence and changing the place of combustion. The effectiveness of the turbulence formation in the lower part of the combustion chamber, which was created with the help of a protrusion located in the depression of the rotor side wall, was proven, as it increased the flame propagation speed [3].

Among the latest scientific works on the use of hydrogen in engines, it is possible to highlight the study of the abnormal combustion problem for this fuel in a

rotary engine and in a piston engine with reciprocating piston movement (2022) [4].

Comparing a hydrogen rotary engine and a hydrogen piston engine, the researchers found that the first one can provide more power per chamber unit volume while maintaining roughly the same efficiency. It was also established that thanks to the physical and chemical properties of hydrogen, it is possible to significantly reduce the emissions and improve the thermal efficiency of the engine [5].

## Definition of unsolved aspects of the problem

To fully realize the potential of the rotary mechanism for the car engine, it is necessary to eliminate the main shortcomings of its design. In the future, this will provide him with the opportunity to become one of the promising power units in road transport.

## Problem statement

The goal of our research is to analyze the possibility of eliminating some shortcomings of the rotary engine and improving its operational characteristics due to the use of hydrogen as fuel. Assess the current situation with the production and use of hydrogen rotary engines.

## Basic material and results

We will take the design of a Wankel rotary engine as a basis for the research. It is an internal combustion engine and produces power similar to a conventional piston engine. The engine block parts form an insulated space around the rotor and function similar to the cylinders in a reciprocating piston engine. So the rotor rotates and simultaneously performs the work that the piston, connecting rod and valves do together. A cross-sectional view of the engine rotor mechanism is presented in fig. 1.

The rotor does not just rotate, but rolls with its internal toothed crown around the fixed gear, thus forming three combustion chambers in which cycles of injection, compression, ignition and emission take place sequentially.

All the functions of the valve train in this engine are performed by the intake and exhaust ports in the engine block side walls and the rotor itself, which opens and closes them in rotating movement.

Let's consider the advantages and shortcomings of the design of gasoline rotary engines compared to piston internal combustion engines.

### *Advantages:*

1. Compactness and higher power-to-weight ratio than a similar piston engine.
2. Ensuring the smoothness of the torque change thanks to a short interval between working strokes.
3. More time for gas exchange (intake and exhaust) – provides more torque at high revs.
4. Low vibration and noise.
5. Less weight of the engine.
6. Extended range of rotation frequency.
7. Serial production of engines has lower cost.
8. The engine is well suited for working on hydrogen.

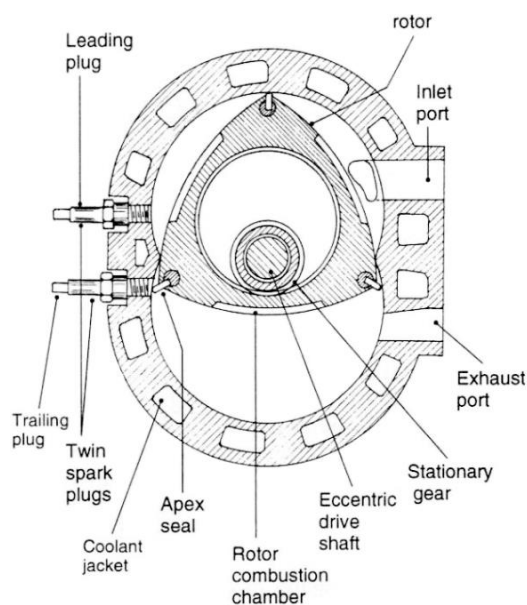


**Figure 1 – Cross-sectional view scheme of the engine rotor mechanism**

*Shortcomings:*

1. The problem of working gases leaks between the rotor apex seals and the engine block.
2. The need to control the level and condition of the lubricant in the engine (under operating conditions, part of the lubricant is burned together with the fuel).
3. The problem of uneven thermal load on the engine body parts within the working chamber of the rotor.
4. Low torque in the low revs range.
5. Slow combustion of the working mixture.
6. Low fuel economy.
7. High emissions.

As can be seen from the above shortcomings, the classic gasoline rotary engine, despite its compactness and universal design, is difficult to compete with gasoline piston internal combustion engines in terms of fuel efficiency, while complying with today's strict environmental standards. Thus, in 2012, due to non-compliance with the Euro 5 environmental standard, serial production of the Mazda RX-8 car, which was equipped with the most advanced version of the gasoline rotary engine at the time, was completed [6].

However, since the design of the rotary engine is well adapted to work on different fuels, over the years of researches and experimentations, it has been found possible to eliminate the shortcomings associated with poor combustion of the gasoline-air mixture and emissions. This was realized by converting the engine to burn hydrogen.

Hydrogen, as a fuel, has unique properties that ensure stable combustion processes, even for highly diluted mixtures. As a result, the combustion rate of the hydrogen-air working mixture increases and the overall engine fuel efficiency improves [7].

Also, the hydrogen diffusivity not only ensures high-quality mixture formation, but also in the leak event, hydrogen quickly disperses in the air, preventing the occurrence of dangerous situations. A comparison of

the hydrogen and gasoline fuel properties is shown in Table 1 [8].

**Table 1 – Basic properties of hydrogen and gasoline fuel**

Properties		Gasoline	Hydrogen
Molar mass, [kg/kmol]		114	2.016
Theoretical ratio of air to fuel, [kg/kg]		14.5	34.32
Density at 0°C and 760 mmHg, [kg/m <sup>3</sup> ]		0.735-0.760	0.0899
Ignition bounds in air at 20°C and 760 mmHg	% mas.	1.48-2.3	4.1-75.6
	air ratio, $\lambda$	1.1-0.709	10.12-0.136
Flame propagation speed in air ( $\lambda=1$ ) at 20°C and 760 mmHg, [m/s]		0.12	2.37
Octane rating		90-98	>130
Min. ignition energy in air, [mJ]		0.2-0.3	0.018
Auto-ignition temperature, [K]		753-823	848-853
Lower heating value (gas at 0°C and 760mmHg);	Stoichiometric fuel-air mixture, [kJ/m <sup>3</sup> ]	3661	3178
	[kJ/kg]	42690	119600

Below is a description of the main characteristics hydrogen and their advantages in comparison with gasoline fuel when used in a rotary combustion engine.

*Extended ignition bounds.* Hydrogen has an extended ignition bounds in air, which allows the use of enriched or depleted mixtures. This property in combination with high turbulence in the combustion chamber expands the rotary engine using possibilities. Thus, lean fuel-air mixture operation results in better fuel economy due to more complete fuel combustion and lower NO<sub>x</sub> emissions due to lower combustion temperatures.

*Shorter extinguishing distance.* Extinguishing distance is the distance between the cylinder wall or block wall in the case of a rotary engine and the point where the flame is extinguished. Hydrogen fuel has an extinguishing distance of 0.6 mm, while gasoline has an extinguishing distance of 2 mm.

*High flame propagation speed.* The hydrogen engine has an almost ideal thermodynamic cycle due to the high flame propagation speed when stoichiometric conditions are ensured. Thanks to the rapid combustion of hydrogen, the engine can operate at high revs, which leads to an increase in power, but at the same time, its economy decreases.

*Minimum ignition energy.* It is defined as the minimum energy required to initiate fuel combustion. A hydrogen-air mixture requires a smaller energy by ignition source compared to a gasoline-air mixture. The minimum ignition energy of a hydrogen-air mixture is 0.02 mJ, while a gasoline-air mixture requires 0.24 mJ.

*High auto-ignition temperature.* The minimum temperature at which the fuel ignites without the use of an external ignition source is determined by the auto-ignition temperature. For hydrogen, it is higher than for other fuels, and is about 585 °C. Because of this, it is difficult to initiate the combustion of hydrogen only due to an increase in temperature, so an external ignition source is necessary. Due to the high auto-ignition temperature, a higher compression ratio can be used for a hydrogen-powered engine compared to a gasoline engine.

Regarding the emissions situation, the hydrogen rotary engine produces very low emissions compared to gasoline rotary engines [7]. And residual toxic substances in the exhaust gases, such as hydrocarbons (HC), carbon monoxide (CO) and nitrogen oxides (NO<sub>x</sub>) are cleaned when passing through a catalytic converter.

Since in order to lubricate the rotor seals inside the combustion chamber, it is necessary to constantly add oil to the working mixture in small proportions. So a CO-neutral solution would be the use of bio-oils or synthetic materials.

To overcome the problem of uneven thermal load on the engine block parts within the working chamber, the use of an exhaust gas recirculation system (EGR) is proposed in its working cycle. The thermal and dilution effects of the EGR system reduce the temperature of the rotor and block working surfaces inside the engine, thereby reducing the amount of nitrogen oxides (NO<sub>x</sub>) produced by the combustion of hydrogen. The EGR system is also an effective factor in increasing thermal efficiency and output power while simultaneously reducing the emissions of harmful substances [9-11].

Separately, it can be noted that unlike piston engines, a rotary combustion engine has separate low-temperature intake zones and high-temperature combustion chambers, and it also have no exhaust valves, which are a potential hot zone too. Accordingly, in a rotary engine running on hydrogen, there is no risk of pre-ignition in the part of the operating cycle when hydrogen is injected. This makes engines more resistant to interruptions in operation [4].

Also, the physical separation of the intake and combustion zones allows for direct hydrogen injection, as a safe temperature is provided for the rubber seals of the hydrogen injectors. Thus, injectors can be installed in the engine block next to the intake chambers for direct injection [12].

Below in fig. 2, a scheme of the possible hydrogen power system integration into the design of the rotary combustion engine is proposed.

This scheme (fig. 2) shows that direct hydrogen injectors are mounted in the upper part of the engine block (one for each rotor) and inject fuel directly into the working chamber.

This design assumes that air from the intake manifold is sucked through a port in the engine block side into the working chamber, where it mixes with atomized gaseous hydrogen. And an additional external injection system is installed on the intake manifold body in order to ensure a higher quality working mixture at high revs.

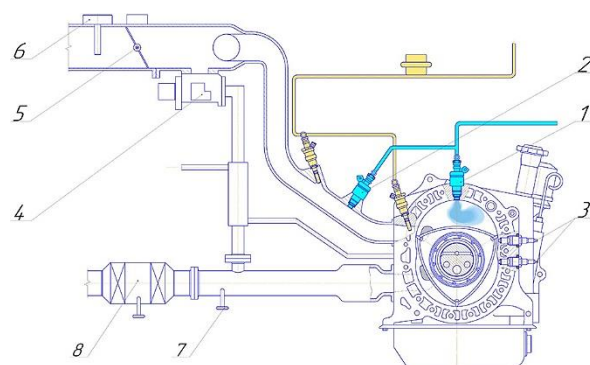


**Figure 2 – The main elements of the fuel injection system and the exhaust system of a rotary engine equipped to work on hydrogen:**

- 1 – hydrogen injector (direct injection);
- 2 – hydrogen injector (external injection); 3 – spark plugs;
- 4 – EGR system valve; 5 – electric throttle;
- 6 – mass air flow sensor; 7 – lambda sensor;
- 8 – catalytic converter

To overcome the problem of low torque in the low revs range, it is recommended to install one or more auxiliary electric motors. The electric motor will increase the torque, which is low for initial acceleration, until the engine revs up.

Such a solution was tested by Mazda engineers on one of the experimental cars with rotary engine [13].

The hydrogen rotary engines advantages of the serial production lower cost and the high efficiency of their use can be made even more significant by conducting research in this direction.

For example, Mazda company experimented with various hydrogen injection systems for rotary engines. And at the beginning of the 2000s, several batches of experimental RX-8 Hydrogen RE cars (Fig. 3) were produced on the basis of the RX-8 sports car, which were successfully operated by Japanese government departments [14, 15].

The automotive manufacturer also demonstrated other vehicle prototypes with hydrogen rotary engines, but nowadays their production, at least in small series, has not been realized.

In addition to Mazda, the German company Wankel Supertec, which specializes in the production of multi-fuel rotary engines for aviation and ground vehicles, is engaged in the development of a hydrogen rotary engine as a motor for cars [16]. Since 2019, the enterprise has established production several models of hydrogen rotary power plants in small quantity. The future hydrogen hybrid drive concept by Wankel Supertec is presented in fig. 4. Among its main components is a rotary combustion engine.



**Figure 3 – Experimental RX-8 Hydrogen RE car**



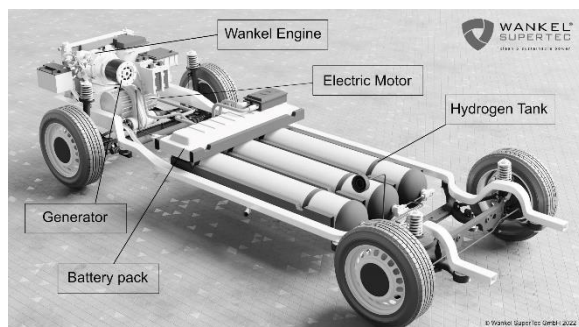


**Figure 4 – The future hydrogen hybrid drive concept by Wankel Supertec**

As of the end of 2022, the company was working on a project of a light truck equipped with a hydrogen rotary engine. Over time, it is planned to present it on the market under its own brand [17].

The analysis of shortcomings in the rotary engine operation showed that one of the main affecting factors its efficiency is the problem of working gases leaks between the rotor apex seals and the engine block. Accordingly, gas leaks between the working chambers directly depend on the contact area between the apex seal on the triangular rotor and the engine block surface.

And since the engine performance as a whole depends on the sealing efficiency, it is important to study their influence on the volumetric efficiency in the engine. Therefore, it was decided to conduct a study of the internal gas flow characteristics using Computational Fluid Dynamics (CFD) instruments for the Mazda RX-8 Hydrogen RE engine.

To carry out the research using CFD, a rotary engine CAD model was previously designed. To simplify construction, the top seals are integral with the rotor, and the intake and exhaust ports are located on the engine block.

Modeling was performed using the SolidWorks. In this study, a gas flow simulation was built based on the conservation of mass and momentum using the finite volume method.

The initial data and boundary conditions for the gas flow are as follows. For the convenience of modeling, air was taken as internal working gas with a density of  $1.29 \text{ kg/m}^3$  and a viscosity of  $1.8\text{E-}05 \text{ kg/m}\cdot\text{s}$ . The inlet pressure is equal to twice the atmospheric pressure of 202.6 kPa; the output pressure is equal to atmospheric amount 101.3 kPa; the rotational frequency of the engine eccentric shaft is 2000 rpm.

Also, for the correct simulation of the gas flow, it is assumed that the gas flow is built on the basis of a turbulent model; the flow of gases is uneven, turbulent and under pressure; the influence of accompanying heat exchange and radiation is not taken into account; the flow is initially stationary, two-dimensional.

As it is known, a rotary engine during operation is affected by unbalanced gas pressure and centrifugal forces of rotation, changing the contact conditions with the apex seal, causing its vertical displacements. As a

result, there is a small gap between the end seal and the engine block surface, which can lead to leakage problems. Based on this, for the convenience of building the model, we assume that the set gap is 0.15 mm. After conducting a computer simulation, consider the situation with gas leaks between the working chambers of a rotary engine (fig. 5). Assuming the presence of a defined gap between the engine block surface and the rotor apex seal, the leakage condition is represented by the trajectory lines of the gas flows. It demonstrates that the flow occurs from a zone with high pressure to a zone with low pressure.

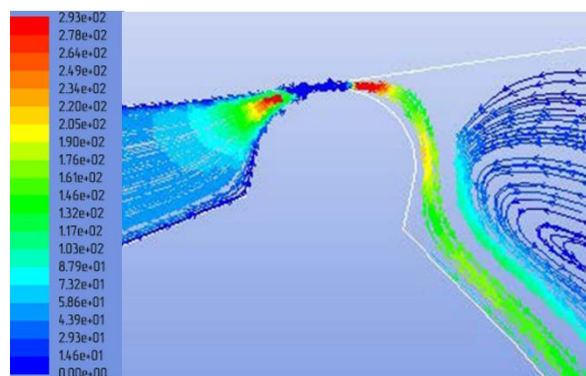


**Figure 5 – Leaks simulation in apex seal**

Trajectory lines are colored according to the speed value diagram (m/s) that is situated on the left side of fig. 5.

As it can be seen from the simulation, the leakage zone is concentrated in the gap, and the flow speed reaches up to 290 m/s in this gap. Under the specified research conditions, a volume of the gas mixture that will not exceed  $4.35\text{E-}05 \text{ m}^3$  will pass through the apex seal gap in one revolution of the engine rotor. And this corresponds to the engine volume efficiency of 96.7%. So we can conclude that such an indicator is not critical and will ensure the rotary engine efficiency, will allow it to be competitive on the market.

### Conclusions

Many years of research and testing by various organizations from around the world testify to the promising design of the rotary engine for operation on hydrogen fuel (hydrogen rotary engine – HRE).

Due to the high turbulence of internal flows and a long operating cycle, the homogeneity of the hydrogen and air mixture is ensured, which causes high efficiency of hydrogen combustion. The short extinguishing distance and high hydrogen ignition speed ensure complete fuel combustion without residues in the exhaust, as happens when using gasoline fuel. And, therefore, a correctly adjusted rotary engine running on hydrogen can even surpass a gasoline piston engine in terms of specific power.

The compact dimensions and low noise level provide the possibility of using these engines in hybrid vehicles as a mileage extender.

Accordingly, hydrogen rotary combustion engines, potentially, in the future, can be used to drive environmentally friendly vehicles. However, nowadays this engine has not yet reached its best level of development and needs further improvement and refinements to optimize fuel economy, durability and reduce the cost of production. There are also other shortcomings of the design that have not been fully resolved, among which is the problem of working gases leaks between the rotor apex seals and the engine block, which requires separate thorough studies with the help of CFD and other

innovative computer modeling methods, the introduction of new materials types into use.

Also important for the effective use of hydrogen engines is the general state of infrastructure development for the production, transportation and distribution of hydrogen as fuel for cars. After all, without solving these issues, it is impossible to achieve proper competitive cars with a rotary engine on hydrogen fuel.

## References

1. Stutzenberger H., Boestfleisch V., Pischinger F. (1983). The suitability of rotary engines for hydrogen operation. *Mtz mot zeitschrift*, 44, 1-25
2. Morimoto K., Teramoto T., Takamori Y. (1992). Combustion Characteristics in Hydrogen Fueled Rotary Engine. *SAE Technical Paper*, 920302, 1-9
3. Jaber N., Mukai M., Kagawa R., Nakakura H., Moriue O., Murase E. (2012). Amelioration of Combustion of Hydrogen Rotary Engine. *International Journal of Automotive Engineering*, 3, 81-88
4. Meng H., Ji C.; Wang D., Xin G., Chang K., Yang J., Wang S. (2022). Research on the load control of hydrogen-fueled Wankel rotary engine. *Int. J. Hydrogen Energy*, 47, 16665–16675  
<https://doi.org/10.1016/j.ijhydene.2022.03.118>
5. Gao J., Tian G., Ma C., Balasubramanian D., Xing S., Jenner P. (2020). Numerical investigations of combustion and emissions characteristics of a novel small scale opposed rotary piston engine fuelled with hydrogen at wide open throttle and stoichiometric conditions. *Energy Convers. Manag.*, 221, 113-178  
<https://doi.org/10.1016/j.enconman.2020.113178>
6. Mazda stops RX-8 production. *Autoblog.com*: веб-сайт. URL: <https://www.autoblog.com/2011/08/22/mazda-stops-rx-8-production/> (дата звернення: 22.04.2023)
7. Meng H., Ji C., Yang J., Wang S., Chang K., Xin G. (2021). Experimental study of the effects of excess air ratio on combustion and emission characteristics of the hydrogen-fueled rotary engine. *Int. J. Hydrogen Energy*, 46, 32261–32272  
<https://doi.org/10.1016/j.ijhydene.2021.06.208>
8. Negurescu N., Pana C., Cernat A. (2012). Aspects of using hydrogen in SI engine. *U.P.B. Sci. Bull. Series D*, Vol. 74, Iss. 1. 1-10
9. Gong C., Si X., Liu F. (2021). Combustion and emissions behaviors of a stoichiometric GDI engine with simulated EGR (CO<sub>2</sub>) at low load and different spark timings. *Fuel*, 295, 120-614  
<https://doi.org/10.1016/j.fuel.2021.120614>
10. Verhelst S., Maesschalck P., Rombaut N., Sierens R. (2009). Increasing the power output of hydrogen internal combustion engines by means of supercharging and exhaust gas recirculation. *Int. J. Hydrogen Energy*, 34, 4406–4412  
<https://doi.org/10.1016/j.ijhydene.2009.03.037>
11. Fontana G., Galloni E. (2010). Experimental analysis of a spark-ignition engine using exhaust gas recycle at WOT operation. *Appl. Energy*, 87, 2187–2193  
<https://doi.org/10.1016/j.apenergy.2009.11.022>
12. Yip H.L., Srna A., Yuen A.C.Y., Kook S. (2019) A Review of Hydrogen Direct Injection for Internal Combustion Engines: Towards Carbon-Free Combustion *Appl. Sci.* 2019, 9(22), 42-48
13. Tokyo Motor Show: Mazda Premacy Hydrogen RE
1. Stutzenberger H., Boestfleisch V., Pischinger F. (1983). The suitability of rotary engines for hydrogen operation. *Mtz mot zeitschrift*, 44, 1-25
2. Morimoto K., Teramoto T., Takamori Y. (1992). Combustion Characteristics in Hydrogen Fueled Rotary Engine. *SAE Technical Paper*, 920302, 1-9
3. Jaber N., Mukai M., Kagawa R., Nakakura H., Moriue O., Murase E. (2012). Amelioration of Combustion of Hydrogen Rotary Engine. *International Journal of Automotive Engineering*, 3, 81-88
4. Meng H., Ji C.; Wang D., Xin G., Chang K., Yang J., Wang S. (2022). Research on the load control of hydrogen-fueled Wankel rotary engine. *Int. J. Hydrogen Energy*, 47, 16665–16675  
<https://doi.org/10.1016/j.ijhydene.2022.03.118>
5. Gao J., Tian G., Ma C., Balasubramanian D., Xing S., Jenner P. (2020). Numerical investigations of combustion and emissions characteristics of a novel small scale opposed rotary piston engine fuelled with hydrogen at wide open throttle and stoichiometric conditions. *Energy Convers. Manag.*, 221, 113-178  
<https://doi.org/10.1016/j.enconman.2020.113178>
6. Mazda stops RX-8 production. *Autoblog.com*: веб-сайт. URL: <https://www.autoblog.com/2011/08/22/mazda-stops-rx-8-production/> (дата звернення: 22.04.2023)
7. Meng H., Ji C., Yang J., Wang S., Chang K., Xin G. (2021). Experimental study of the effects of excess air ratio on combustion and emission characteristics of the hydrogen-fueled rotary engine. *Int. J. Hydrogen Energy*, 46, 32261–32272  
<https://doi.org/10.1016/j.ijhydene.2021.06.208>
8. Negurescu N., Pana C., Cernat A. (2012). Aspects of using hydrogen in SI engine. *U.P.B. Sci. Bull. Series D*, Vol. 74, Iss. 1. 1-10
9. Gong C., Si X., Liu F. (2021). Combustion and emissions behaviors of a stoichiometric GDI engine with simulated EGR (CO<sub>2</sub>) at low load and different spark timings. *Fuel*, 295, 120-614  
<https://doi.org/10.1016/j.fuel.2021.120614>
10. Verhelst S., Maesschalck P., Rombaut N., Sierens R. (2009). Increasing the power output of hydrogen internal combustion engines by means of supercharging and exhaust gas recirculation. *Int. J. Hydrogen Energy*, 34, 4406–4412  
<https://doi.org/10.1016/j.ijhydene.2009.03.037>
11. Fontana G., Galloni E. (2010). Experimental analysis of a spark-ignition engine using exhaust gas recycle at WOT operation. *Appl. Energy*, 87, 2187–2193  
<https://doi.org/10.1016/j.apenergy.2009.11.022>
12. Yip H.L., Srna A., Yuen A.C.Y., Kook S. (2019) A Review of Hydrogen Direct Injection for Internal Combustion Engines: Towards Carbon-Free Combustion *Appl. Sci.* 2019, 9(22), 42-48
13. Tokyo Motor Show: Mazda Premacy Hydrogen RE

hybrid. *Autoblog.com*: веб-сайт. URL: <https://www.autoblog.com/2007/10/24/tokyo-motor-show-mazda-premacy-hydrogen-re-hybrid/> (дата звернення: 22.04.2023)

14. Mazda Hydrogen Rotary Now Street Legal. *newsroom.mazda.com*: веб-сайт. URL: <https://newsroom.mazda.com/en/publicity/release/2004/200410/1027e.html> (дата звернення: 22.04.2023)

15. Mazda Delivers Two Rotary Hydrogen Vehicles to Hiroshima Government Authorities. *newsroom.mazda.com*: веб-сайт. URL: <https://newsroom.mazda.com/en/publicity/release/2006/200604/060421.html> (дата звернення: 22.04.2023)

16. Wankel supertec. *wankelsupertec.de*: веб-сайт. URL: <https://www.wankelsupertec.de/en/> (дата звернення: 22.04.2023)

17. Wankel Super Tec – Success Story: Die Energie der Zukunft soll emissionsfrei und nachhaltig sein. *www.fundernation.eu*: веб-сайт. URL: <https://www.fundernation.eu/blog/wankel-super-tec-success-story-die-energie-der-zukunft-soll-emissionsfrei-und-nachhaltig-sein/> (дата звернення: 22.04.2023)

18. Abdalla A.M., Hossain S., Nisfindy O.B., Azad A.T., Dawood M., Azad A.K. (2018). Hydrogen production, storage, transportation and key challenges with applications: A review. *Energy Convers. Manag.*, 165, 602–627

19. Srinivasan C., Subramanian R. (2014). Hydrogen as a spark ignition engine fuel: technical review. *Int J Mech Mechatron Eng*; 14, 7-111

<https://doi.org/10.2298/HEMIND0206256K>

20. Salvi B.L., Subramanian K.A. (2016). Experimental investigation on effects of compression ratio and exhaust gas recirculation on backfire, performance and emission characteristics in a hydrogen fueled spark ignition engine. *Int J Hydrogen Energy*; 41, 5842-5855

<https://doi.org/10.1016/j.ijhydene.2016.02.026>

hybrid. *Autoblog.com*: веб-сайт. URL: <https://www.autoblog.com/2007/10/24/tokyo-motor-show-mazda-premacy-hydrogen-re-hybrid/> (date of application: 22.04.2023)

14. Mazda Hydrogen Rotary Now Street Legal. *newsroom.mazda.com*: веб-сайт. URL: <https://newsroom.mazda.com/en/publicity/release/2004/200410/1027e.html> (date of application: 22.04.2023)

15. Mazda Delivers Two Rotary Hydrogen Vehicles to Hiroshima Government Authorities. *newsroom.mazda.com*: веб-сайт. URL: <https://newsroom.mazda.com/en/publicity/release/2006/200604/060421.html> (date of application: 22.04.2023)

16. Wankel supertec. *wankelsupertec.de*: веб-сайт. URL: <https://www.wankelsupertec.de/en/> (date of application: 22.04.2023)

17. Wankel Super Tec – Success Story: Die Energie der Zukunft soll emissionsfrei und nachhaltig sein. *www.fundernation.eu*: веб-сайт. URL: <https://www.fundernation.eu/blog/wankel-super-tec-success-story-die-energie-der-zukunft-soll-emissionsfrei-und-nachhaltig-sein/> (дата звернення: 22.04.2023)

18. Abdalla A.M., Hossain S., Nisfindy O.B., Azad A.T., Dawood M., Azad A.K. (2018). Hydrogen production, storage, transportation and key challenges with applications: A review. *Energy Convers. Manag.*, 165, 602–627

19. Srinivasan C., Subramanian R. (2014). Hydrogen as a spark ignition engine fuel: technical review. *Int J Mech Mechatron Eng*; 14, 7-111

<https://doi.org/10.2298/HEMIND0206256K>

20. Salvi B.L., Subramanian K.A. (2016). Experimental investigation on effects of compression ratio and exhaust gas recirculation on backfire, performance and emission characteristics in a hydrogen fueled spark ignition engine. *Int J Hydrogen Energy*; 41, 5842-5855

<https://doi.org/10.1016/j.ijhydene.2016.02.026>

UDC 624.016:624.042.65

## Experimental studies of prestressed steel-concrete wall girders

Semko Oleksandr<sup>1</sup>, Hasenko Anton<sup>2\*</sup>, Drobotia Oleksandr<sup>3</sup>, Marchenko Dmytro<sup>4</sup>

<sup>1</sup> National University «Yuri Kondratyuk Poltava Polytechnic» <https://orcid.org/0000-0002-2455-752X>

<sup>2</sup> National University «Yuri Kondratyuk Poltava Polytechnic» <https://orcid.org/0000-0003-1045-8077>

<sup>3</sup> National University «Yuri Kondratyuk Poltava Polytechnic» <https://orcid.org/0000-0002-0288-081X>

<sup>4</sup> National University «Yuri Kondratyuk Poltava Polytechnic» <https://orcid.org/0000-0001-5773-4484>

\*Corresponding author E-mail: [gasentk@gmail.com](mailto:gasentk@gmail.com)

To reduce the cost of steel for the installation of load-bearing elements of the wall enclosure made of sandwich panels, it is suggested to use prestressed steel-concrete girders with reduced stiffness of the steel part of the cross-section in one plane instead of girders from the pipe. Thus, the span cross-section will be a U-shaped steel profile filled with concrete. Experimental tests were carried out on eight samples of 3000 mm long girders made of bent channel № 10, size 100x50 mm, with a wall thickness of 3 mm, filled with C20/25 class concrete. The prestressing of the cross-section steel part was carried out by pre-bending the cross-section steel part with jacks and fixing it in this position by filling the inner cavity with concrete. As a result of the implementation of these measures during experimental studies, an increase in bearing capacity up to 31% and stiffness up to 57% was confirmed in the case of preliminary bending of the channel and filling with concrete 1.6 times higher than the height of its shelves. The use of such beams makes it possible to reduce steel consumption by 39%.

**Keywords:** prestressing, steel-concrete, wall girder, experimental studies.

## Експериментальні дослідження попередньо напружених сталобетонних стінових прогонів

Семко О.В.<sup>1</sup>, Гасенко А.В.<sup>2\*</sup>, Дроботя О.В.<sup>3</sup>, Марченко Д.П.<sup>4</sup>

<sup>1, 2, 3, 4</sup> Національний університет «Полтавська політехніка імені Юрія Кондратюка»

\*Адреса для листування E-mail: [gasentk@gmail.com](mailto:gasentk@gmail.com)

Стінові прогони являються горизонтальними конструктивними балковими елементами стінового огороження будівлі. Під час використання легких сендвіч-панелей у якості стінового огороження, несучі стінові прогони виконують сталевими. З метою зменшення витрат сталі для влаштування таких прогонів, авторами пропонується використовувати сталобетонні прогони, попередньо напружені у площині зменшеної жорсткості сталеві частини перерізу. Сталобетонні прогони пропонується виготовляти із гнутих швелерів із заповненням коритоподібного сталевих профілю бетоном. Сумісну роботу двох матеріалів слід забезпечувати встановленням системи анкерних стержнів. Суть попереднього напруження полягає в наступному. Спочатку сталевий коритоподібний профіль вигинається домкратом проти експлуатаційного прогину і в такому положенні заповнюється бетоном. Після набору бетоном проектної міцності, домкрат витягується. Утворений таким чином сталобетонний прогін за рахунок сумісної роботи сталі та бетону залишається вигнутим проти експлуатаційного прогину. Під час експлуатаційного навантаження на прогони, спочатку необхідно вибрати їх попередній вигин, повернувши прогони в початковий прямолінійний стан, а лише потім буде виникати прогин від прямолінійної початкової осі балки. Саме цим пояснюється підвищення міцності та жорсткості досліджуваних попередньо напружених сталобетонних прогонів. Для підтвердження наведених викладок було проведено експериментальні випробування восьми зразків прогонів довжиною 3000 мм, виконаних із гнутого швелера №10 розміром 100x50 мм з товщиною стінки 3 мм, заповнених бетоном класу C20/25. Між собою зразки відрізнялися наявністю попереднього напруження сталеві частини перерізу, розміром перерізу бетонного осердя та схемою навантаження. У результаті проведених експериментальних досліджень підтверджено підвищення несучої здатності та жорсткості сталобетонних балок, що складає: 1) у випадку заповнення бетоном внутрішньої порожнини швелера 19% і 27% відповідно; 2) у випадку попереднього вигину сталеві частини перерізу 24% і 29% відповідно; 3) у випадку збільшення в 1,6 рази висоти перерізу бетонного осердя попередньо напруженого зразка 31% і 57% відповідно.

**Ключові слова:** попереднє напруження, сталобетон, стіновий прогін, експериментальні дослідження.



## Introduction

Wall girders are horizontal structural beam elements of the building wall enclosure. The external load on the wall girders is the vertical load from the wall enclosure weight and the horizontal wind load. Thus, wall girders work for bending in two planes. The load from the weight of the wall enclosure, made of light sandwich panels, is approximately equal to the wind impact load on Ukrainian territory. Therefore, in this case, the wall girders are designed with equal strength in two planes.

A light, modern wall enclosure is made of hinged sandwich panels, consisting of two sheets of profiled wall flooring and effective rigid mineral wool insulation between them. Steel girders with a cross-section in the form of a pipe usually serve as the load-bearing elements of such a wall enclosure [1].

## Review of the research sources and publications

Different methods of rational forces adjustment in steel structures are known, which are implemented both at the design stage and at the stage of manufacture and installation. The essence of these methods is described in detail in the work of M.V. Gogol [2].

One of the active methods of increasing the steel structures bearing capacity is the *method of their preliminary deformation*. For the most part, this method regulates the stress in individual rod elements. Preliminary elements deformation is arranged opposite to operational bending. This method consists in the fact that a prestressed deformed rod is formed using several elements connected into one in a pre-bent state (see fig. 1). Welding of curved elements requires significant additional costs of labor and energy, which is a disadvantage of this method [3].

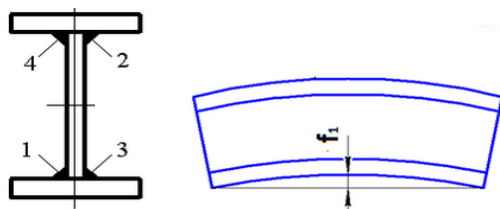


**Figure 1 – Scheme of preliminary stresses creation by the rod layers deformation followed by their welding [3]:**

1, 2, 3, 4 – the order of welding seams

Another method of prestressing is the *arrangement of local bonded tendons* on the beam structures' steel parts in the zone of the maximum bending moment action. Izbash M.Yu. [4] proved the effectiveness of bonded tendons installing both on the lower girdle of the beams with a single-span scheme of their operation, and on the upper girdle above the supports with a non-split scheme (see fig. 2). A positive feature of such a constructive solution of prestressing is that, due to the small value of the angle  $\alpha$ , the pulling force  $F_{sp}$  is almost an order of magnitude less than the reinforcement tension force  $H_{sp}$  created by it [5].

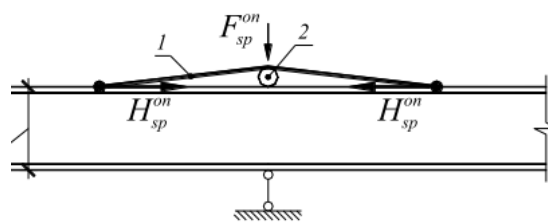


**Figure 2 – Installation of tension rod for prestressing locally on intermediate supports of continuous steel beam [5]:**

1 – tension rod; 2 – fixing cylinder

Preliminary stresses in the elements of bent continuous and spatial steel-reinforced concrete structures can be created both due to a well-chosen design, including nodes, and the development of manufacturing technology or preliminary reinforcing assembly during installation [6; 7], as well as by placing additional prestressed reinforcing bars (bonded tendons) in the stretched cross-sectional area [8; 9].

Scientific studies of reinforced concrete beams prestressing by placing additional prestressed reinforcing bars were conducted under the leadership of L. Storozhenko. In [10] V. Pents with Yu. Kushnir conducted a study of I-beams with side cavities filled with concrete with installed external or internal prestressed bonded tendons (see fig. 3).

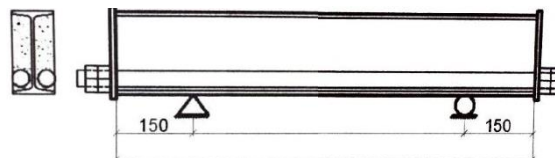


**Figure 3 – Scheme of additional prestressed internal reinforcement of steel-concrete beams [10]**

Similar types of beams were also studied by foreign researchers. In particular, C. Wang, Y. Shen, R. Yang, and Z. Wen (China) [11] conducted a study of prestressed steel-reinforced concrete beams shown in Figure 4. Prestressed steel-reinforced concrete beams have an inverted arch deflection before loading, which is advantageous for service loading. Compared to a conventional steel-reinforced concrete beam, the prestressed one has greater rigidity, which increases the resistance to cracking in tension concrete, but at the same time reduces the overall plasticity of the beam.

A positive result of prestressing by installing additional stressed reinforcing rods is an increase in the bearing capacity and rigidity of steel-reinforced concrete structures. At the same time, the general disadvantage of this method is the additional cost of materials and the installation of additional stressed rods.



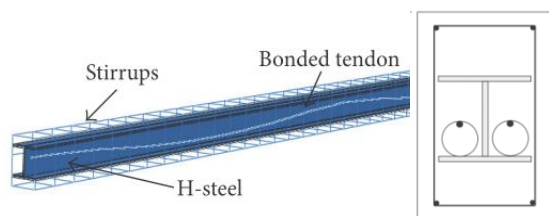


**Figure 4 – Prestressed steel-reinforced concrete beams [11]**

A separate type of steel-reinforced concrete structure self-tension is a special technology for their manufacture, the result of which is a change in the calculation scheme of their operation [12]. In particular, Figure 5 shows prefabricated monolithic steel-reinforced concrete crossbars stressed due to the staged production (concreting). This idea is patented by D. Bibik, V. Semko, and O. Voskbiynyk [13]. The production of prefabricated monolithic crossbars is carried out in several stages - the prefabricated part of the structure is manufactured at the factory, and the monolithic part is in the process of installation. Thus, the calculation scheme of the crossbar operation changes at the stages of its installation. In the first stage, the crossbar is a single-span beam freely supported on two supports. At this stage, the crossbar cross-section is a trough-shaped steel profile filled with concrete. At the second stage of production, prefabricated ribbed reinforced concrete floor slabs are mounted on the lower steel shelf of a trough-like profile, and the crossbar is welded to the embedded parts of the columns. At the same time, the crossbar calculation scheme is changed to a rigidly clamped one-span one. Then, a concrete monolithic upper shelf is arranged, which combines the crossbar with the floor slabs installed on it for joint work on the operational load.

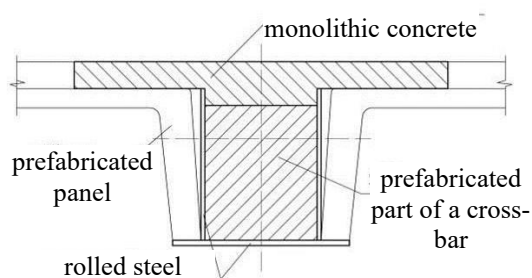


**Figure 5 – Cross-sectional with showing concreting stages [13]**

Experimental studies of steel-reinforced concrete prefabricated monolithic crossbars confirmed the theoretical prerequisites regarding the effect of changing the cross-section during manufacture on the development of deflections and internal forces [14].

#### **Definition of unsolved aspects of the problem**

Thus, an effective method of prestressing the steel part of steel-reinforced concrete structures is their preliminary deformation by bends that are opposite to operational ones. Such bends are arranged either with

jacks [3] or by arranging additional pre-stressed rods [4-5; 9-11]. At the same time, the steel part pre-bent state is fixed either by welding its component parts during manufacture [3], or by changing the conditions for fixing this steel beam part with columns [12-14], or by actually arranging stressed additional rods [4-5; 9-11]. Concreting of the steel part of steel-reinforced concrete structures cross-section in order to fix its pre-bent state was not considered.

#### **Problem statement**

The purpose of the work is to study experimentally the possibility of fixing the pre-bent state by filling with concrete the inner cavity of the steel U-shaped section of the steel-concrete rod, which can be used as a wall girder. The subject of the study is the stress-strain state and bearing capacity of a reinforced concrete rod pre-stressed in this way.

#### **Basic material and results**

*General principles of creating rational preliminary stresses in the layers of reinforced concrete girders.* The essence of the proposed measures set for the rational efforts redistribution is as follows. At the *first stage* of prestressed reinforced concrete girders production, mechanical jacks are used to create the initial bending of the beams' steel part, which is opposite to the operational one (see fig. 6). That is, at this stage, the deformations of the steel beam normal section are created opposite to the operational ones: the beam lower fibers will be compressed, and the upper fibers will be stretched (see fig. 7, a). At the *second stage* of production, the inner cavity of the rod U-shaped steel part is filled with concrete. During concreting and during the period when the concrete reaches the design strength, the jacks remain under the steel beams. That is, the stress-strain state of the steel beams does not change compared to the first stage, and the deformations of the normal section in the concrete are zero (see fig. 7, b). To ensure further compatible operation of the cross-section steel and concrete parts, anchoring means are welded to the inner side of the cross-section steel part in advance. For the useful load (*third stage*), the combined steel-concrete section will work together. In the concrete part, the deformations will develop from the undeformed (zero) state, while in the steel part, the deformations of the normal section will be superimposed on the already existing operational deformations obtained at the first stage of the combined structure (see Fig. 7, c). That is, during the operating load increase, the beam steel part first returns to its original undeformed state and only then it will deform according to the generally accepted scheme: the beam's lower fibers will stretch, and the upper fibers will compress. This explains the increase in the load-bearing capacity of reinforced concrete structures prestressed in this way. It should be noted that by selecting the beams' steel part pre-bending optimal parameters and the rational ratio of the steel and concrete parts' stiffness, it is possible to achieve a significant increase not only in the steel-concrete rod stiffness but also in its bearing capacity.

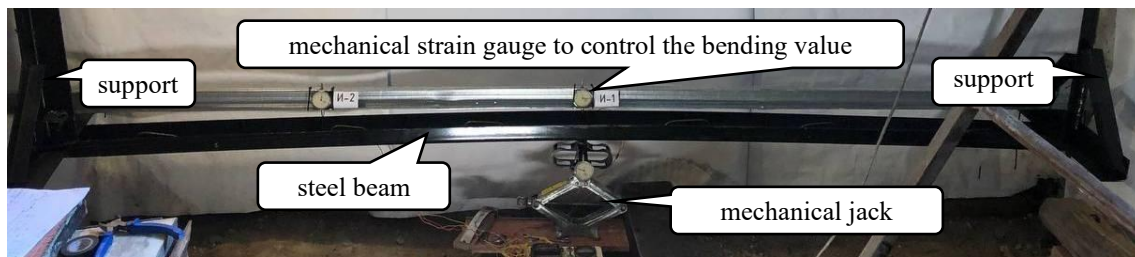


**Figure 6 – General view of the arrangement of the previous opposite to operational bending of the cross-section steel part**

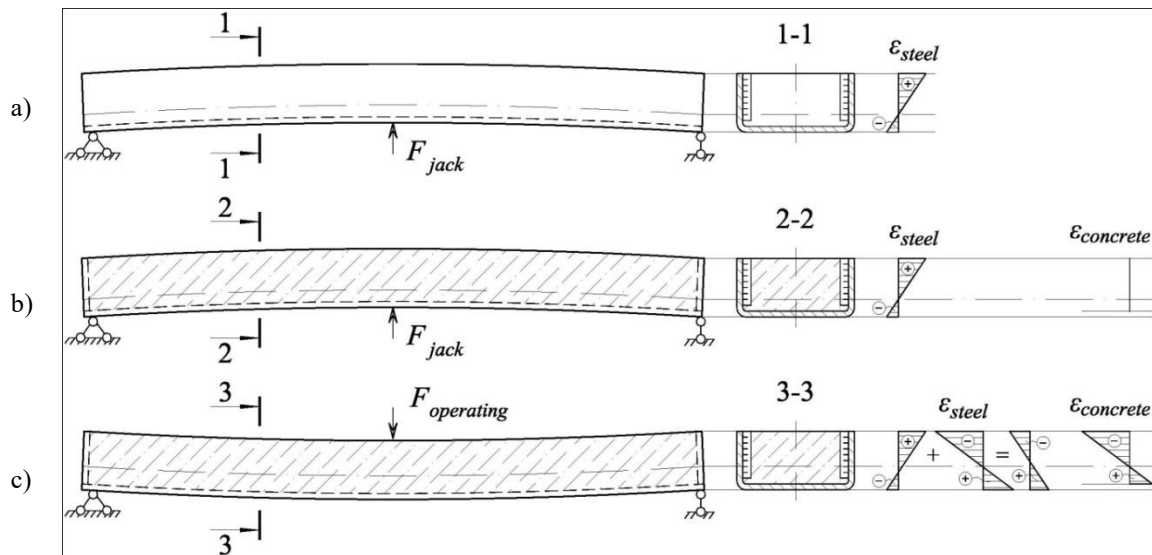


**Figure 7 – Stages of a prestressed reinforced concrete rod work:**

- a) the previous opposite to operational bending of the section steel part; b) filling with concrete the inner cavity of the U-shaped steel part of the rod when the jack is installed; c) the operational stage

*Construction of experimentally studied prestressed reinforced concrete girders.* Samples of prestressed steel-concrete girders were made from steel bent channel № 10, 3000 mm long, with an external cross-sectional dimension of 50×100 mm and a wall thickness of 3 mm, with an internal U-shaped cavity filled with concrete. Experimental prestressed samples differed in the size of the concrete core cross-section and the operational load scheme (see fig. 8). Samples PSC1.1 and PSC1.2 were filled with concrete to the level with the channel shelves edge; the total height of their cross-section was equal to 50 mm, the reinforcement ratio was 11.4% (see section 1-1 in fig. 9). Samples PSC2.1 and PSC2.2 were filled with concrete 30 mm above the level of the channel shelves edge; the total height of their cross-section was equal to 80 mm, the reinforcement ratio was 7.3% (see section 1-1\* in fig. 9). To determine the cross-section steel part prestressing effectiveness, samples SC1.1 and SC1.2 were made with concrete filling to the level of the channel shelves. The beam steel part prestressing was created by jacking it by bending it opposite to its previous operational bending by the amount of 1/300 of the span, which was 10 mm (see fig. 6). To determine the effectiveness of filling the channel inner cavity with concrete, empty steel samples S1.1 and S1.2 were manufactured and tested. Samples S1.1, SC1.1, PSC1.1, and PSC2.1 were loaded by one force in the middle of the span, and samples

S1.2, SC1.2, PSC1.2, and PSC2.2 were loaded by two equal forces equidistant from the supports.

The concrete to fill the internal cavity and the U-shaped steel part of the reinforced concrete beams were combined into a joint operation by means of vertical reinforcing bars of class A240C, 6 mm in diameter and 40 mm long, which were welded to the inside of the channel side shelves at a variable step, shown in figure 9. Since these anchoring means were welded along their entire height to the channel shelves, their own bending during loading is impossible. In addition, in order to prevent the two layers from shifting relative to each other, plates with a thickness of 4 mm were welded on the ends of the beams. Therefore, the investigated beams can be considered as two-layer composite structures with a rigid combination of two layers (steel and concrete).

To ensure the joint operation of the two materials in the plastic stage of their operation, S-shaped anchor rods of class A240C with a diameter of 6 mm are additionally welded from the inner side to the horizontally located wall of the channel, the shape and welding step of which is shown in figure 10. These additional anchoring means were to be included in the work after the loss of the channel shelves local stability and their detachment from the concrete core.

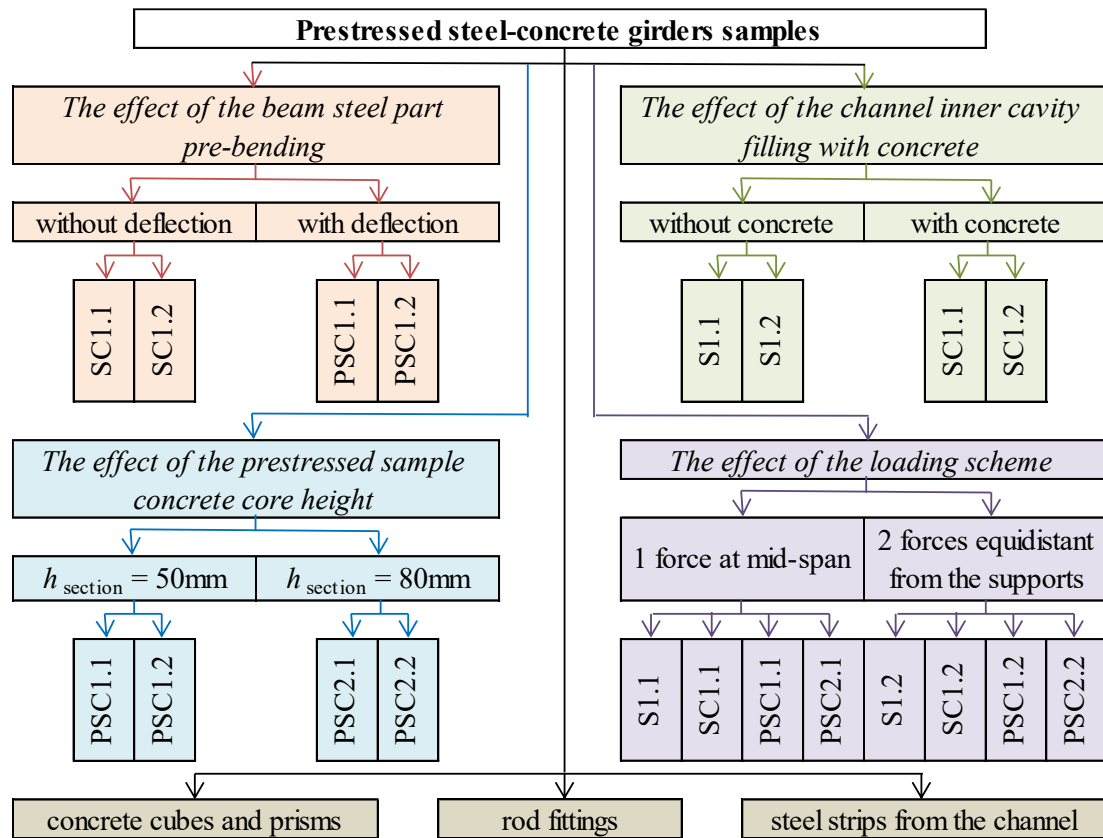


Figure 8 – Scheme of experimental research planning

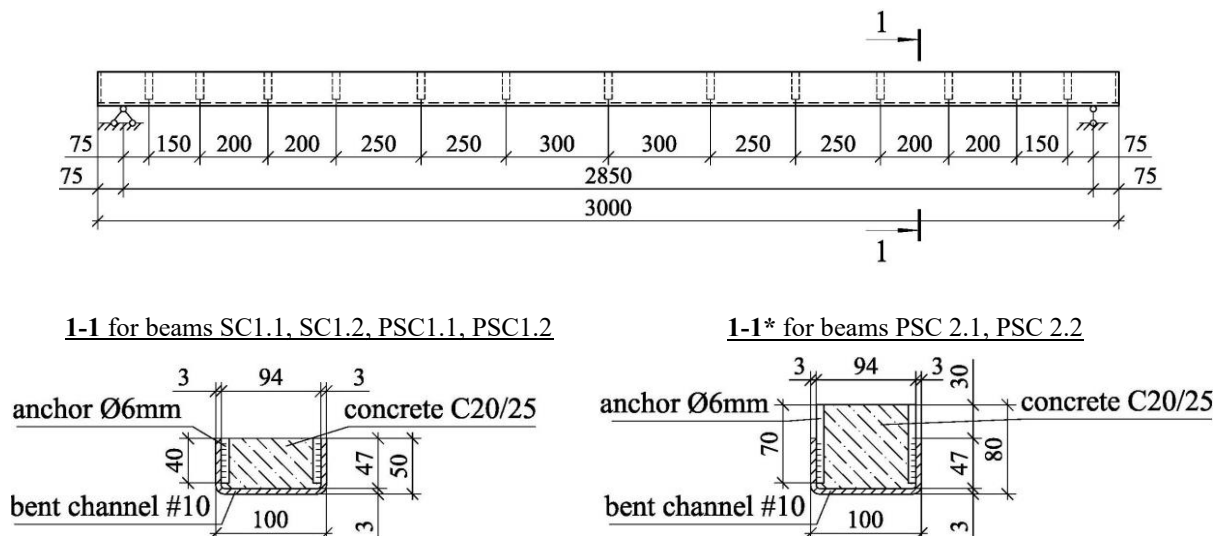


Figure 9 – Geometrical parameters of experimental single-span reinforced concrete girders

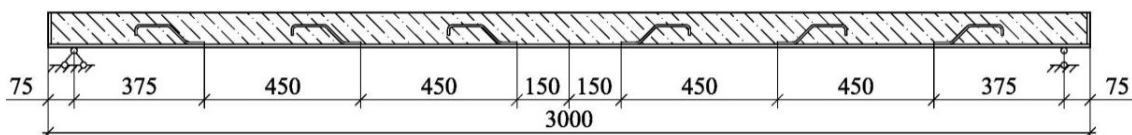


Figure 10 – Scheme of additional anchors placement along the length of the tested samples

The physical and mechanical characteristics of the materials used for the manufacture of samples of prestressed steel-concrete girders (sheet and round steel and concrete) are shown in tables 1 and 2, respectively.

**Table 1 – Physical and mechanical characteristics of rolled steel**

Rolled steel type	Середня міцність, МПа		Normative resistance, MPa:				Coef. var., %		Absolute elongation	Steel strength class	Normative resistance, MPa		Modulus of elasticity $E_s$ , $\cdot 10^5$ МПа
			of sample		average						$R_y$	$R_u$	
	$\sigma_y$	$\sigma_u$	$R_{yn}$	$R_{un}$	$R_{yn}$	$R_{un}$	$V_{yn}$	$V_{un}$	$\varepsilon_{s,u}$ , %				
Channel #10 (sheet steel)	279	393	266	374	253,5	367,5	4,2	2,8	28,4	C245	240	360	2,1
	252	374	240	356									
	267	380	254	362									
	267	397	254	378									
Anchor Ø6 mm (rod steel)	278	383	265	365	262,2	371,7	3,2	1,6	24,2	A240C	240	370	2,1
	266	395	253	376									
	282	393	269	374									

**Table 2 – Physical and mechanical characteristics of concrete cubes and prisms**

Code of samples	Mean value of concrete compressive strength, MPa		Coefficient of variation of concrete strength in a batch $V_c$ , %	Normative compressive strength of concrete, MPa:				Coef. var., %	Concrete class	Design value of concrete:	
				of sample		average				compressive strength	modulus of elasticity
	$f_{cm,cube}$	$f_{cm,prism}$		$f_{ck,cube}$	$f_{ck,prism}$	$f_{ck,cube}$	$f_{ck,prism}$	$V_c$ , %		$f_{cd}$ , MPa	$E_{cd}$ , GPa
SC1	30,4	22,5	12,0	24,4	18,1	26,6	19,7	12,2	C20/25	14,5	23,0
PSC1	29,4	21,8	9,1	25,0	18,5						
PSC2	35,5	26,3	8,9	30,3	22,4						

*Methodology of conducting experimental studies of prestressed reinforced concrete girders.* After the concrete had reached the design strength, the jack was removed, with the help of which the preliminary bending of the beam steel part was created. The setting for reinforced concrete samples testing looked the same as for the preliminary bending of their steel part. Therefore, steel concrete samples were tested with a cavity filled

with concrete to the bottom with a  $\Omega$ -like arrangement of steel channel. Figure 11 shows the general appearance of reinforced concrete samples during tests with the indication of the load application node with one or two forces.

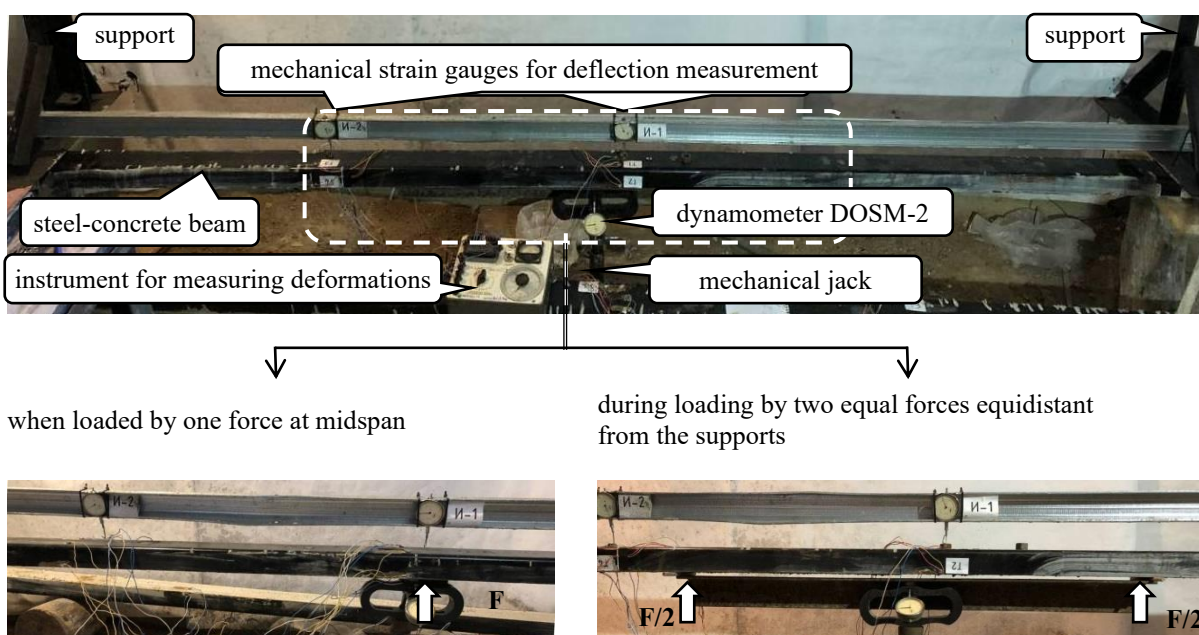


**Figure 11 – General view of reinforced concrete samples during testing**



The strains of steel and concrete were measured in the area of maximum bending moment (in the middle of the span) and at a distance of 0.25 of the span length from the supports using strain gauges with a base of 20 mm (see fig. 12). To control the deformations in the most compressed and stretched fibers of the sample, a 20 mm base Hugenberger mechanical strain gauge with a division value of 0.005 mm was installed, which ensured the accuracy of relative deformation measurements  $25 \times 10^{-5}$ . Clock-type indicators were used to measure deflections in the middle of the span and at a distance of 0.25 of the span length from the supports.

*Results of experimental studies of prestressed reinforced concrete girders.* Figure 13 shows the changes in the distribution of strains of the normal cross-section, located in the middle of the span, of the steel part of the tested samples loaded by one force in the middle of the span. The relative deformations of the stretched part of the cross-section were determined as the arithmetic average between the readings of the electro-tensile resistors T1 and T6, and of the compressed part of the cross-section – as the arithmetic average between the readings of the electro-tensile resistors T2 and T7 (see fig. 12).

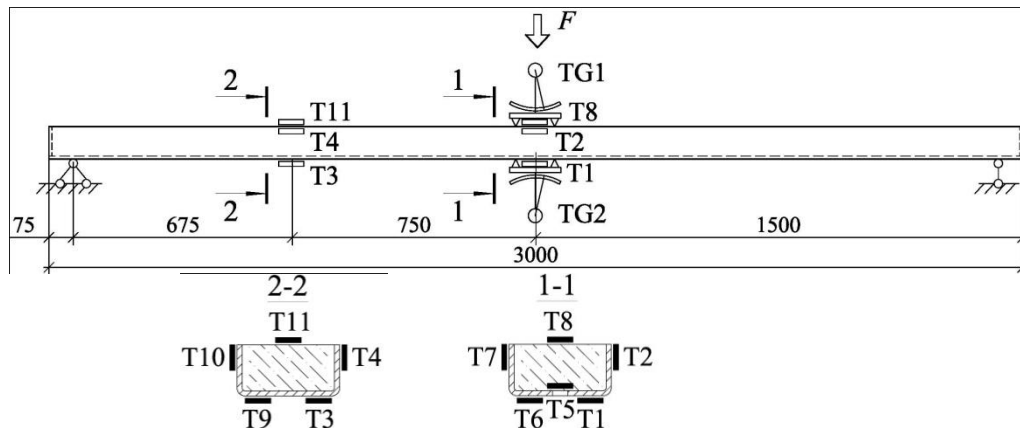


Figure 12 – Scheme of measuring devices location on the studied samples

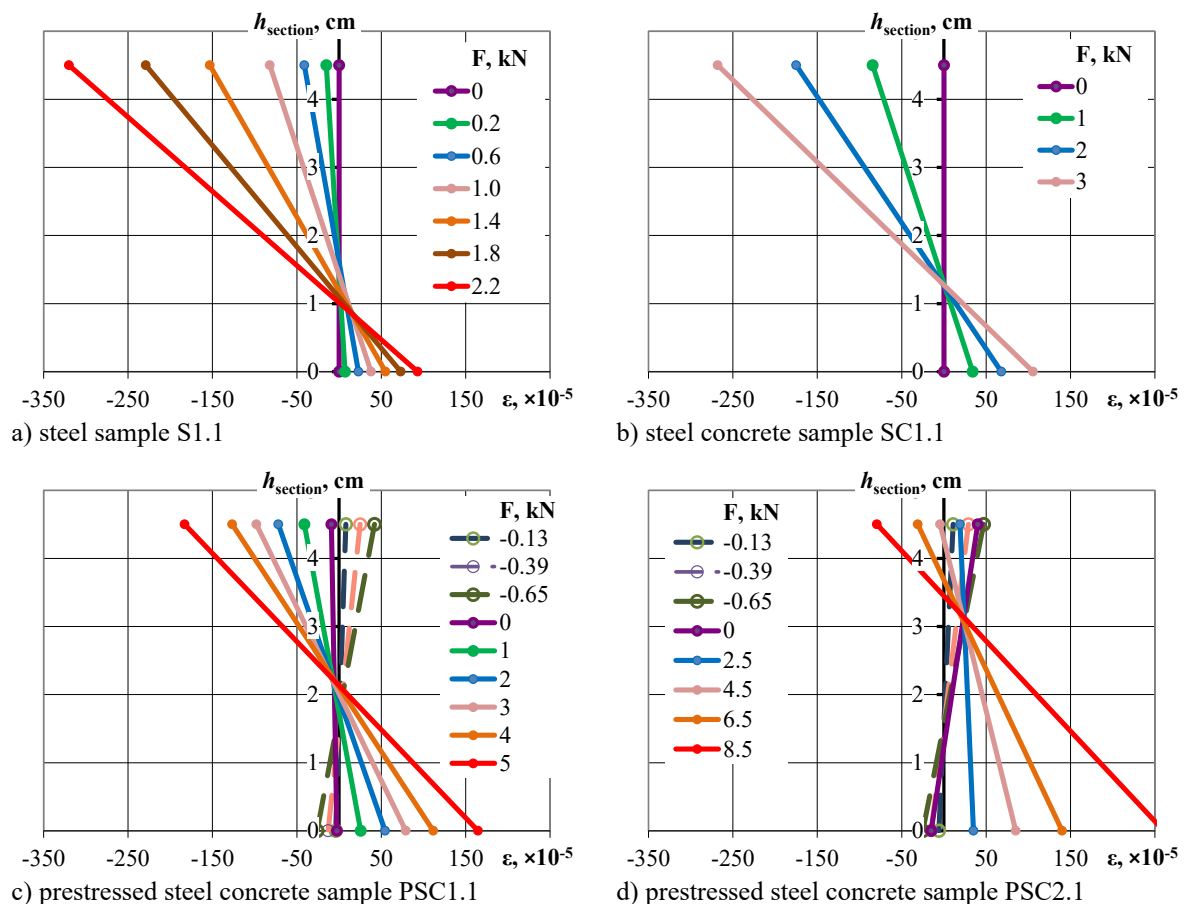


Figure 13 – Changes in the distributions of strains of the steel part normal cross-section located in the middle of the span of samples loaded by one force in the middle of the span



On the distributions of strains of normal cross-sections of the studied samples, the movement of the zero line along the height of the cross-section can be clearly traced. For the empty steel sample S1.1 (see fig. 13, a), the zero line is at the height of the central axis of the used bent channel. For the steel-concrete sample without prestressing SC1.1 (see fig. 13, b), the zero line is located slightly higher. This is explained by the presence of concrete in the cavity, which raises the cross-section central axis. For prestressed steel concrete samples PSC1.1 and PSC2.1 (see fig. 13, c-d), the zero line is higher, the higher the cross-section height of the concrete core. This increase in the position of the zero line is explained, firstly, by the inclusion of concrete in the

work and, secondly, by the presence of previous deformations of steel normal section, which are "subtracted" from the deformations during operational loads. To determine the efficiency of the proposed prestressing of the cross-section steel before its concreting, a comparison of the development of the normal cross-section relative deformations and the deflections of all samples was made. For samples loaded with a single force at mid-span, these comparisons are shown in figure 14. For specimens loaded with two equal forces equidistant from the supports, these comparisons are shown in figure 15.

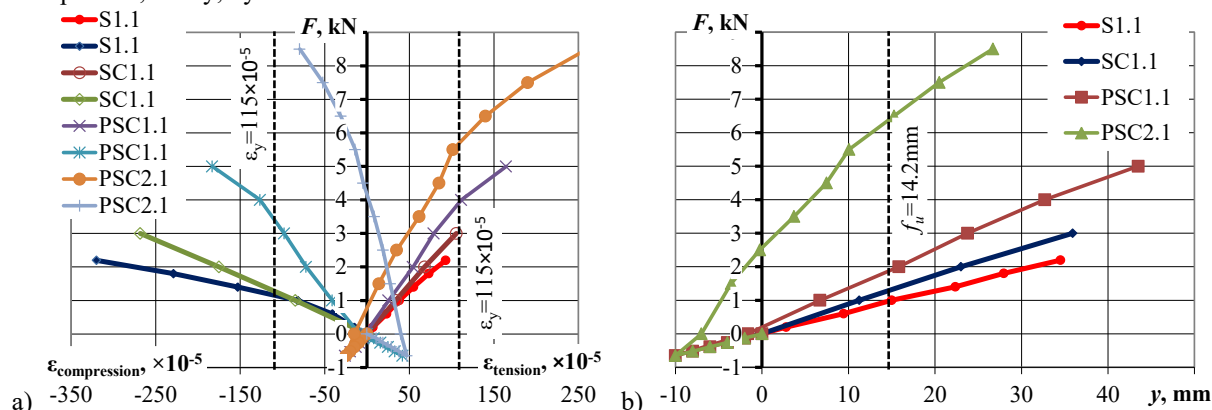


Figure 14 – Comparison of the development of the steel part normal section strains (a) and the deflections (b) of the samples loaded by one force in the middle of the span

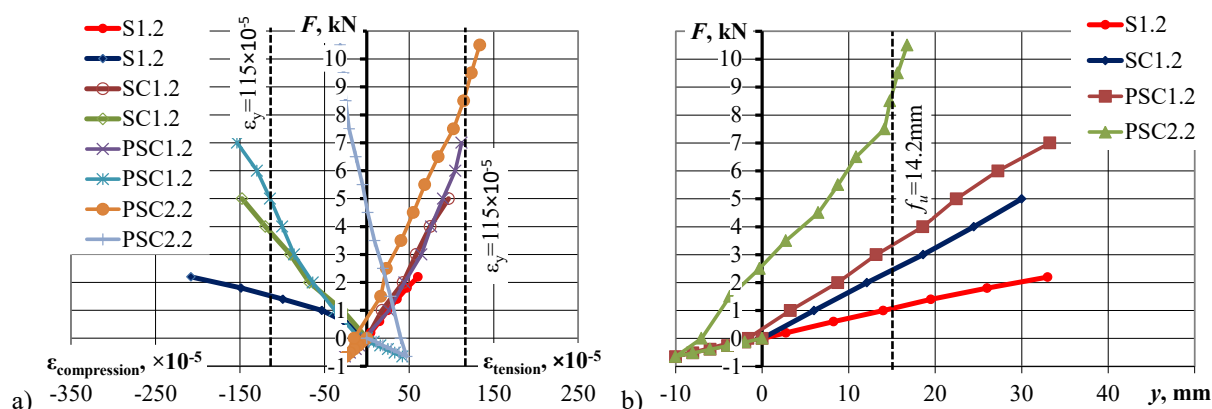


Figure 15 – Comparison of the development of the steel part normal section strains (a) and the deflections (b) of the samples loaded by two equal forces equidistant from the supports

## Conclusions

As a result of experimental studies of prestressed steel-concrete wall girders' stress-strain state and bearing capacity, the following was established:

- by filling the steel U-shaped section inner cavity with concrete, it is possible to fix its pre-bent state. After the concrete gains strength and the jack is released, the preliminary bending decreases by 81% and 31% for samples filled with concrete at the level and 30 mm above of the channel edges suitably;
- preliminary bending of the section steel part increases the load-bearing capacity by 24% and the steel-concrete beam rigidity by 29%;

- filling the channel inner cavity with concrete increases the load-bearing capacity by 19% and the reinforced concrete beam rigidity by 27%;
- a 1.6-fold increase in the cross-sectional height of the concrete core of the prestressed sample increases the load-bearing capacity by 31% and the stiffness of the reinforced concrete beam by 57%.

Thus, the experimentally investigated prestressed reinforced concrete girders consisting of bent channel #10 with a wall thickness of 3 mm filled with concrete have the same load-bearing capacity with a higher stiffness of up to 27%, as a steel beam made of pipe 80×3mm, which reducing steel consumption by 39%.

## References

1. George K.G. (2017). Preliminary Structural Design of Wall-Frame Systems for Optimum Torsional Response. *International Journal of Concrete Structures and Materials*, 11, 45-58
2. Гоголь М.В. (2018). *Регулювання напружень у сталевих комбінованих конструкціях*. Київ: Сталь.
3. Гоголь М.В. (2017). Вплив деформованого стану балки жорсткості на розподіл зусиль в системі. *International Scientific Journal*, 11(33), 45-47  
<https://doi.org/10.25313/2520-2057-1-11-2771>
4. Ізбаш М.Ю. (2011). Пряме проектування підсилення експлуатованих нерозрізних багатопролітних сталезалізобетонних балок. *Комунальне господарство міст. Серія: Технічні науки та архітектура*, 100, 425-434
5. Ізбаш М.Ю. (2008). Зниження витрат напружуваної арматури в локально обтиснутих сталезалізобетонних згинаних конструкціях. *Комунальне господарство міст. Серія: Технічні науки та архітектура*, 81, 15-23
6. Гасенко А.В. (2022). Огляд методів створення попередніх самонапружень у згинаних просторових сталезалізобетонних конструкціях. *Ресурсоекономічні матеріали, конструкції, будівлі та споруди*, 41, 110-118  
<https://doi.org/10.31713/budres.v0i41.12>
7. Vatulina G., Berestianskaya S., Opanasenko E., Berestianskaya A. (2017). Substantiation of concrete core rational parameters for bending composite structures. *MATEC Web of Conf.: DYN-WIND '2017*, 107, 00044  
<https://doi.org/10.1051/mateconf/201710700044>
8. Hasenko A.V. (2021). Previous self-stresses creation methods review in bent steel reinforced concrete structures with solid cross section. *Academic journal. Industrial Machine Building, Civil Engineering*, 2(57), 82-89  
<https://doi.org/10.26906/znp.2021.57.XXXX>
9. Al-Kaimakchi A., Rambo-Roddenberry M. (2021) Structural behavior of concrete girders prestressed and reinforced with stainless steel materials. *Structures*, 35(11)  
<https://doi.org/10.1016/j.istruc.2021.08.134>
10. Кушнір Ю.О., Пенц В.Ф. (2013). Підбір оптимального армування нормального прямокутного перерізу попередньо-напружених сталезалізобетонних балок на основі деформаційної моделі. *Будівельні конструкції. Науково-технічні проблеми сучасного залізобетону*, 78-2, 78-84
11. Wang C., Shen Y., Yang R., Wen Z. (2017). Ductility and Ultimate Capacity of Prestressed Steel Reinforced Concrete Beams. *Hindawi Mathematical Problems in Engineering*, 6, 1467940  
<https://doi.org/10.1155/2017/1467940>
12. Hasenko A.V. (2021). Deformability of bends continuous three-span preliminary self-stressed steel concrete slabs. *Academic journal. Industrial Machine Building, Civil Engineering*, 1(56), 135-141  
<https://doi.org/10.26906/znp.2021.56.2518>
13. Бібік Д.В., Семко В.О., Воскобійник О.П. (2011). Патент України 61921. *Сталезалізобетонний ригель покриття таврового перерізу*. Київ: Український інститут промислової власності
14. Семко О.В., Бібік Д.В., Воскобійник О.П., Семко В.О. (2011). Експериментальні дослідження сталезалізобетонного ригеля прольотом 13,5 м. *Ресурсоекономічні матеріали, конструкції, будівлі та споруди*, 21, 323-330
1. George K.G. (2017). Preliminary Structural Design of Wall-Frame Systems for Optimum Torsional Response. *International Journal of Concrete Structures and Materials*, 11, 45-58
2. Gogol M.V. (2018). *Adjustment of stresses in steel combined structures*. Kyiv: Stal
3. Gogol M.V. (2017). The influence of the deformed state of the stiffening beam on the distribution of forces in the system. *International Scientific Journal*, 11(33), 45-47  
<https://doi.org/10.25313/2520-2057-1-11-2771>
4. Izbash M.Yu. (2011). Direct design of operated uncut multi-span steel-reinforced concrete beams reinforcement. *Communal management of cities. Series: Technical sciences and architecture*, 100, 425-434.
5. Izbash M.Yu. (2008). Reducing costs of prestressed reinforcement in locally pressed steel-reinforced concrete bent structures. *Communal management of cities. Series: Technical sciences and architecture*, 81, 15-23
6. Hasenko A.V. (2022). Methods review of previous self-stresses creation in bended spatial steel reinforced concrete structures. *Resource-saving materials, constructions, buildings and structures*, 41, 110-118  
<https://doi.org/10.31713/budres.v0i41.12>
7. Vatulina G., Berestianskaya S., Opanasenko E., Berestianskaya A. (2017). Substantiation of concrete core rational parameters for bending composite structures. *MATEC Web of Conf.: DYN-WIND '2017*, 107, 00044  
<https://doi.org/10.1051/mateconf/201710700044>
8. Hasenko A.V. (2021). Previous self-stresses creation methods review in bent steel reinforced concrete structures with solid cross section. *Academic journal. Industrial Machine Building, Civil Engineering*, 2(57), 82-89  
<https://doi.org/10.26906/znp.2021.57.XXXX>
9. Al-Kaimakchi A., Rambo-Roddenberry M. (2021) Structural behavior of concrete girders prestressed and reinforced with stainless steel materials. *Structures*, 35(11)  
<https://doi.org/10.1016/j.istruc.2021.08.134>
10. Kushnir, Yu.O. & Pents, V.F. (2013). Selection of optimal reinforcement of pre-stressed steel-reinforced concrete beams normal rectangular section based on a deformation model. *Building constructions. Scientific and technical problems of modern reinforced concrete*, 78-2, 78-84
11. Wang C., Shen Y., Yang R., Wen Z. (2017). Ductility and Ultimate Capacity of Prestressed Steel Reinforced Concrete Beams. *Hindawi Mathematical Problems in Engineering*, 6, 1467940  
<https://doi.org/10.1155/2017/1467940>
12. Hasenko A.V. (2021). Deformability of bends continuous three-span preliminary self-stressed steel concrete slabs. *Academic journal. Industrial Machine Building, Civil Engineering*, 1(56), 135-141  
<https://doi.org/10.26906/znp.2021.56.2518>
13. Bibyk D.V., Semko V.O., Voskobinik O.P. (2011). Patent Ukraine 61921. *Steel-reinforced-concrete cross-section cover beam*. Kyiv: Ukrainian Institute of Intellectual Property
14. Semko O.V., Bibyk D.V., Voskobinik O.P., Semko V.O. (2011). Experimental studies of a steel-reinforced concrete beam with a span of 13.5 m. *Resource-economic materials, constructions, buildings and structures*, 21, 323-330

UDC 697.347

## Economic dependence of the consumer on the feasibility to regulate the heat supply system

Taradai Oleksandr<sup>1</sup>, Bugai Volodymyr<sup>2</sup>, Gvozdetzkyi Oleksandr<sup>3\*</sup>, Diachenko Serhii<sup>4</sup>

<sup>1</sup> Kharkiv National University of Civil Engineering and Architecture <https://orcid.org/0000-0002-4239-9895>

<sup>2</sup> Kharkiv National University of Civil Engineering and Architecture <https://orcid.org/0000-0001-5166-7110>

<sup>3</sup> Kharkiv National University of Civil Engineering and Architecture <https://orcid.org/0000-0001-5590-4689>

<sup>4</sup> Kharkiv National University of Civil Engineering and Architecture <https://orcid.org/0000-0003-0187-0684>

\*Corresponding author E-mail: [npp-tghv@ukr.net](mailto:npp-tghv@ukr.net)

The paper explores the issue of cost-effectiveness of the transition from existing one-pipe, unregulated heating systems to two-pipe regulated apartment systems, with the possibility of installing thermostatic controls on each heater as well as heat meters in each apartment. Four residential buildings with the same specific heat load, which have central regulation, group regulation, local regulation and combined regulation, were selected. The actual heat consumption has been analysed and conclusions drawn as to the possible savings with combined control. One of the main conclusions is that renovation of existing in-house heating systems is an objective necessity

**Keywords:** heat supply system, heating system, control valves, heat meter

## Економічна залежність споживача від можливостей регулювання системи теплопостачання

Тарадай О.М.<sup>1</sup>, Бугай В.С.<sup>2</sup>, Гвоздецький О.В.<sup>3\*</sup>, Дяченко С.В.<sup>4</sup>

<sup>1, 2, 3, 4</sup> Харківський національний університет будівництва та архітектури

\*Адреса для листування E-mail: [npp-tghv@ukr.net](mailto:npp-tghv@ukr.net)

Розглянуте питання економічної ефективності переходу існуючих однотрубних, нерегульованих систем опалення на двотрубні поквартирні, регульовані, з можливістю встановлення терморегуляторів на кожному опалювальному приладі, а також теплोलічильників у кожній квартирі. Для проведення аналізу було обрано чотири житлові будинки, з однаковим питомим тепловим навантаженням, які мають центральне регулювання, групове, місцеве та комбіноване регулювання. Проведено аналіз реального теплоспоживання, згідно до показів теплових лічильників, цих будинків за 2021-2022 опалювальний період. При центральному регулюванні фактична питома спожита тепла енергія склала: 0,106 ГКал/год·м<sup>2</sup>; при груповому регулюванні фактична питома спожита тепла енергія склала: 0,094 ГКал/год·м<sup>2</sup>; при місцевому регулюванні фактична питома спожита тепла енергія склала: 0,085 ГКал/год·м<sup>2</sup>; при комбінованому регулюванні фактична питома спожита тепла енергія склала: 0,054 ГКал/год·м<sup>2</sup>. Якщо розглядається трьохкімнатна квартира площею 67 м<sup>2</sup>, то економія теплоспоживання при комбінованому регулюванні, в порівнянні з централізованим становить 5364 грн. за опалювальний період, тобто 49%. До основних висновків статті можна віднести: лише наявність реальної технічної можливості регулювання виробітку, транспортування та, головне, споживання тепла дає дійсне зниження витрат палива на джерелах та відповідно зменшення грошових витрат споживачів на опалення; Існуюча більшість внутрішньобудинкових систем опалення житлових та цивільних будівель України не мають індивідуального регулювання споживання тепла кожною квартирою та приміщенням; Реконструкція існуючих внутрішньобудинкових систем опалення є об'єктивною необхідністю, без якої реальний вплив абонента на своє теплоспоживання неможливий. Така модернізація диктується і всіма нормативними термінами капітальних ремонтів, систем опалення, які у більшості випадків перевищені більш ніж вдвічі.

**Ключові слова:** система теплопостачання, система опалення, регулююча арматура, теплोलічильник

## Introduction

Saving energy resources is a crucial objective for any country. Currently in Ukraine energy saving is the key to energy security, and is therefore more important than ever.

The issue of heat energy saving is very multifaceted and consists not only in the well-known directions: insulation of buildings; modernization of heat source equipment; replacement of existing heat network pipelines with pre-insulated pipes; replacement of obsolete mixing units (elevator units) with mixing units with mixing pumps and automation.

Undoubtedly, the implementation of all these measures improves the heat supply systems and brings significant economic effect in the form of reduced fuel consumption for the heat source and reduced heat consumption costs.

However, the consumer himself, i.e. the person to whom the comfort conditions for work and relaxation are created, can in no way affect the consumption of heat in his apartment, office, etc.

## Review of the research sources and publications

The existing stock of twentieth-century residential and civic buildings is equipped with vertical single-pipe unregulated heating systems (Figure 1).

Analysis shows that in the majority of all buildings in Ukraine we have unregulated in-house heating systems, which should be regarded as a "single heater" for the entire building. Regulation of such a "single heater" is actually impossible.

In [1-4] issues related to the inability to regulate existing single-pipe heating systems have been addressed.

Reconstruction of existing single-pipe heating systems to two-pipe or single-pipe regulated systems can be found in the articles [5-9].

Reconstruction of single-pipe, unregulated heating systems into two-pipe, horizontal, regulated heating systems is carried out to allow each individual consumer can to affect the heat consumption of their premises. In this case, you can regulate with the thermostat on the heater. And an installed heat meter would allow the consumer to clearly see how much heat he consumed, how to regulate it, and how much he has to pay for it.

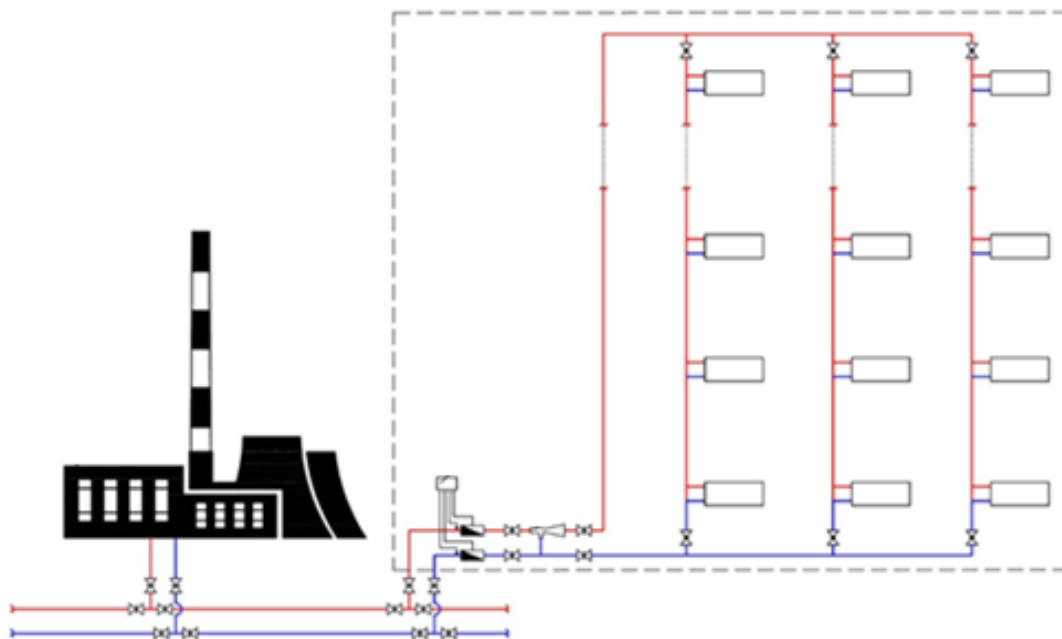


**Figure 1 – One-pipe heating system for twentieth-century buildings**

The electricity, water and gas supply systems in Ukraine, as well as throughout the civilised world, are built on such principles. For a long time now, these systems have allowed the consumer to independently meter, calculate and regulate his or her own consumption.

And only the regulation of heat consumption, the most expensive utility service, remains inaccessible to the consumer, the consumer simply has no real technical feasibility to do so.

Even having a whole-building heat meter does not solve the issue of heat savings by each individual consumer. This requires a heat meter in every apartment, office, hospital treatment block, etc.

## Definition of unsolved aspects of the problem

All previously published papers have considered the technical feasibility of reconstructing existing heating systems, but have not analyzed the actual heat consumption of consumers under different types of regulation.

## Problem statement

In this article we consider the issue of saving by each consumer and, as a consequence, the entire heating system as a whole, based on the actual technical capabilities of the existing heating systems of multi-storey buildings.

Most of Kharkiv's buildings and their heating systems date back to the 20th century. They were all built according to different designs and standards, with different materials, and in completely non-comparable social conditions. Why is this housing development not in line with European norms? Let historians and sociologists talk about it. We, as specialists in our field, must proceed from the actual situation and, based on it, give our recommendations, draw conclusions and make decisions.

### Basic material and results

The purpose of any heat supply system is to cover the load of the heating system, to ensure a comfortable thermal environment at all times of the day and throughout the entire heating season. Only if this task is carried out one hundred percent can the system be said to be running stably, meeting all the required technical and economic parameters. To perform the task of heat supply the system must have the appropriate technical equipment (pumps, valves, sensors, etc.) in all its components: heat energy source, heat networks, equipment for heating substations, in-house piping and heating apparatus. Without such technical equipment along the entire chain: heat generation, transportation and consumption from the heat source to the heater, effective regulation is impossible. The lack of real regulation of any of the elements in this chain leads to overconsumption and consumer discomfort.

According to [10-11], there are the following main generally accepted types of regulation of heat supply systems:

- *central regulation*: carried out at the heat source (boiler-house or combined heat and power plant, CHPP), according to the predominant type of load characteristic of the entire heat consumption area from the given source;

- *group regulation*: carried out at the district heating substations according to the predominant load type of a certain group of subscriptions (residential quarter or neighbourhood, plant site)

The group heating substations are usually constructed for the centralized preparation of hot water for an entire group of buildings.

After using the heat transfer fluid from the heat source at the district heating substation, regulation is carried out according to the predominant heating load:

- *local regulation*: carried out at the individual heating substations of each building according to the average temperature for all rooms in the building

- *individual regulation*: carried out directly on each heating device of each room by the consumer himself, according to his wishes

The types of regulation mentioned above and laid down in [10] correspond to the regulatory principles long accepted and strictly observed in European countries.

In Ukraine, these principles began to be strictly observed only in the 21st century in all newly designed and built facilities, including in-house heating systems of residential and civil buildings.

All heat sources in Ukraine, regardless of their design, capacity and location, practically perform only qualitative regulation of heat supply to the consumer. They are regulated automatically or manually by adhering to a "design temperature schedule".

In all modern individual heating substations there is also a technical capability to perform qualitative-quantitative regulation of heat consumption of the entire object as a whole by setting a certain "average temperature" for this object.

Naturally, with this averaging of temperature, each placement, whether it is a room in a residential building, a ward or operating theatre in a hospital, group rooms and bedrooms in a kindergarten, classrooms in a school, receive an "average" amount of heat, not the amount they need at a given moment.

Only modern two-pipe in-house horizontal heating systems in residential and public buildings by design (Figure 2) allow the user to regulate the amount of heat transfer fluid to each heater by means of a thermostat on each heater.

Thus, the design of modern heating systems in residential and public buildings ensures individual heat consumption in each room. The presence of individual meters in each apartment of a residential building and a building-wide meter at the house inlet provides one hundred percent economy of the whole heat supply system, as each consumer is interested in taking the minimum amount of heat for his comfort, and the system as a whole generates the required amount of heat with minimum consumption of fuel and energy resources.

Today, however, no more than fifteen percent of heat consumers have modern two-pipe horizontal in-house heating systems with thermostat on each heater and heat meter in each apartment.

The remaining more than eighty-five percent of buildings that consume heat were built in the second half of the 20th century, during the period of mass housing construction, and are equipped with unregulated vertical single-pipe systems without thermostat on each heater.

As more than half a century of experience with these heating systems has shown, their design makes it virtually impossible for the consumer to perform any heat regulation.

Moreover, their actual condition precludes even the possibility of one particular heater or riser being switched off completely without significantly affecting the entire heating system.

The result of this ratio of unregulated to regulated in-house heating systems is that heat sources cannot be regulated in any way other than a qualitative regulation based on the "average temperature of the whole district of heat supply".

In buildings constructed in the second half of the 20th century and equipped with vertical single-pipe heating systems, only qualitative regulation is possible also because any change in the amount of heat transfer fluid in the riser pipes with heating devices leads to an arbitrary vertical deregulation of the entire system.



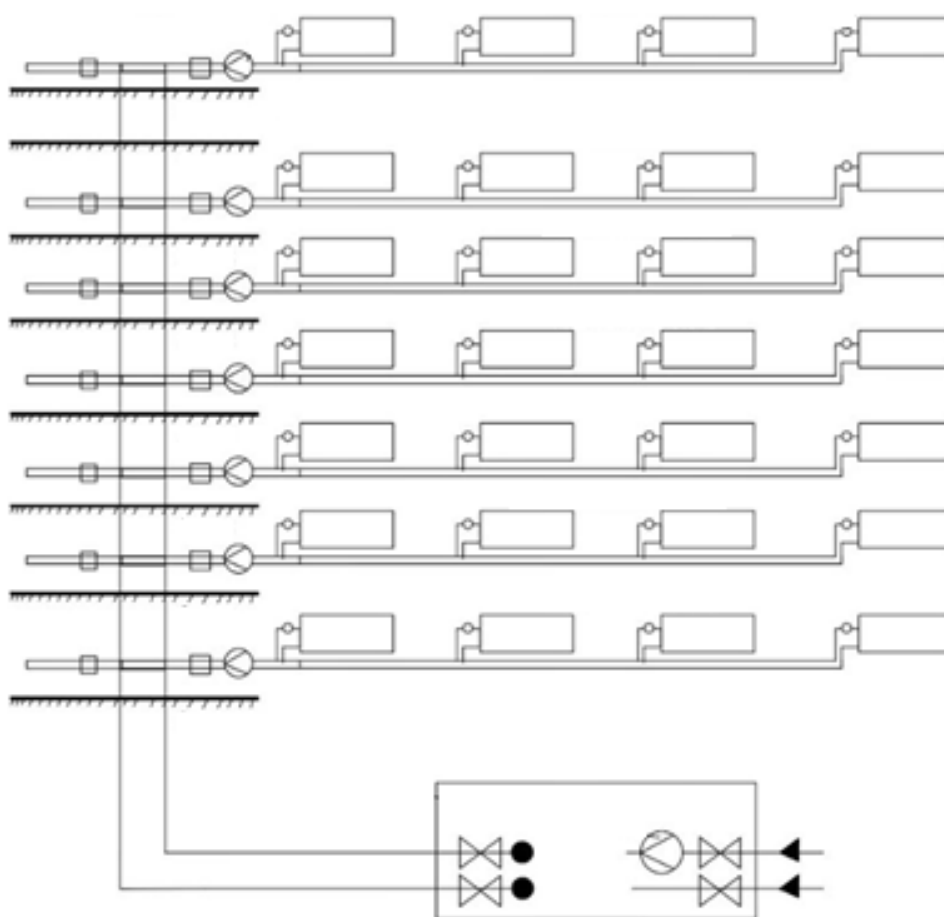


**Figure 2 – Two-pipe horizontal apartment heating system**

Therefore, even in the utterly new individual heating substations, which are now being installed in old buildings, we still only have the possibility of qualitative regulation.

In other words, equipping old buildings with new individual heating substations, we do not solve the problem of comfort of each consumer (tenant) because we only correct the "average temperature of the entire district or neighborhood" to the "average temperature of this building".

Only in modern houses built in the 21st century, which are equipped with horizontal apartment heating systems with meters and thermostats on each heater, does the consumer (tenant) really make the quantitative and qualitative regulation himself to create the comfort conditions he needs, regardless of the needs of other consumers. In doing so, each consumer creates a comfortable environment only for himself, at his own discretion, without preventing other consumers from doing the same.

Technical calculations, confirmed by the actual practice of heat supply companies, show that due to the technical impossibility of regulating heat consumption by each subscriber in each room of his flat, hospital ward or classroom, more than twenty percent of all fuel intended for heat generation in Ukraine is wasted, and each subscriber (a three-room flat with an average area of 70 m<sup>2</sup>) overpays thirty percent each month.

The results of the analysis of the current state of the heat supply from the point of view of heat consumption regulation are given below. All figures are based on actual data from heat supply companies in the Kharkiv region. This article shows the results of a study carried out on houses with both old single-pipe vertical heating systems and old houses with retrofitted new horizontal apartment heating systems with temperature controllers on each appliance.

We have studied the heat consumption of several residential buildings, with the following characteristics:

- regulation of heat supply only at the source, i.e. combined heat and power plant (CHPP) or boiler-house;
- group regulation at the district heating substation;
- local regulation at the individual heating substation;
- combined local regulation at the individual heating substation and individual regulation for each resident.

All residential buildings in question are equipped with heat meters.

The heat consumption analysis is compiled for the 2021-2022 heating season. Due to the fact that all buildings have different heating areas and different maximum heat loads, it was decided to make comparisons based on specific loads, which theoretically all approximately the same (Figure 3).

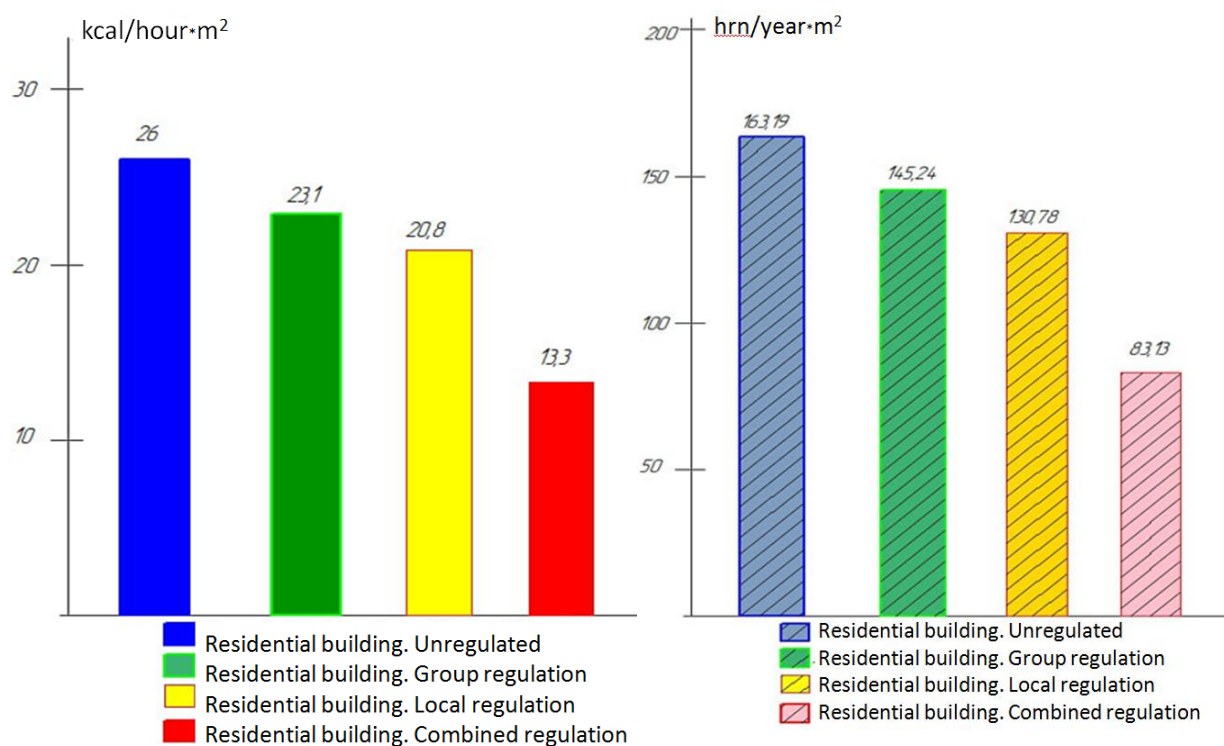


**Figure 3- Plots comparing the actual specific heat loads averaged over the year (amount of heat consumed) and the specific cost of heat consumed over the heating period by residential buildings**

The data for each type of building surveyed are shown below.

1. Residential building equipped with a heat meter, but no regulation. The actual specific heat load averaged over the year (amount of heat consumed) is 26 kcal/year·m². The heating period of 2021-2022 is 4084 hours. The specific heat consumption for the heating period is 0.106 Gcal/year·m². At the cost of 1 GCal in the amount of 1539 UAH 50 kopecks, the unit cost per year is 163.19 UAH/year·m².

2. Residential building equipped with a heat meter, regulation is group. The actual specific heat load averaged over the year (amount of heat consumed) is 23.1 kcal/year·m². The heating period of 2021-2022 is 4084 hours. The specific heat consumption for the heating period is 0.094 Gcal/year·m². At the cost of 1 GCal in the amount of 1539 UAH 50 kopecks, the unit cost per year is 145.24 UAH/year·m².

3. Residential building equipped with heat meter, regulation is local. The actual specific heat load averaged over the year (amount of heat consumed) is 20.8 kcal/year·m². The heating period of 2021-2022 is 4084 hours. The specific heat consumption for the heating period is 0.085 Gcal/year·m². At the cost of 1 GCal in the amount of 1539 UAH 50 kopecks, the unit cost per year is 130.78 UAH/year·m².

4. Residential building equipped with a heat meter, regulation is combined - local and individual. The actual specific heat load averaged over the year (amount of heat consumed) is 13.3 kcal/year·m². The heating period of 2021-2022 is 4084 hours. The specific heat consumption for the heating period is 0.054 Gcal/year·m².

At the cost of 1 Gcal in the amount of 1539 UAH 50 kopecks, the unit cost per year is 83.13 UAH/year·m².

The following are the results of the study on cash savings on heating costs for a three-room apartment of 67 m² in the case of real means of regulation.

In the first case, with regulation at the boiler house only, the cost to be paid by the consumer for the heating period is 10933.73 UAH.

In the second case, with the group regulation, the cost to be paid by the consumer for the heating period is 9731.08 UAH. The saving compared to the first case is 1202.65 UAH or eleven percent.

In the third case, with the local regulation, the cost to be paid by the consumer for the heating period is 8762.26 UAH. The saving compared to the first case is 2171.47 UAH or twenty percent.

In the fourth case, with the local and individual regulation, the cost to be paid by the consumer for the heating period is 5569.71 UAH. The saving compared to the first case is 5,364.02 UAH, or forty-nine percent.

If we consider a residential nine-storey building of three entrances with an area of 7220 m², the savings per year due to combined regulation compared to no regulation is 578033.20 UAH.

To summarize the issue of cash savings to consumers, it should be clearly understood that the heating organization has the same proportional fuel savings.

## Conclusions

1. Only the presence of a real technical possibility to regulate the generation, transportation and, most importantly, consumption of heat provides a real reduction of fuel consumption at sources, and the corresponding reduction of cash costs of consumers for heating.

2. The vast majority of in-house heating systems in residential and civil buildings in Ukraine do not have individual control of heat consumption by each apartment and room.

3. The originally flawed technical design and the actual condition of the in-house heating systems of the vast majority of multi-storey buildings in Ukraine, contradict modern requirements and do not allow for cost-effective heat consumption.

4. Reconstruction of existing in-house heating systems is an objective necessity, without which the subscriber cannot really influence his or her heat consumption. Such modernization is also dictated by all the regulatory terms of major repairs of heating systems, which in most cases are exceeded by more than two times.

## References

1. Долінський А.А., Басок Б.І., Базєєв Є.Т. (2012). Регіональні програми модернізації комунальної теплоенергетики – інноваційна основа технологічного оновлення теплозабезпечення населених пунктів України. Частина 2. *Промислова теплотехніка*, 34(4), 44-51
2. Росковшенко Ю.К., Штиленко В.П. (2013). Індивідуальне автоматичне регулювання та облік теплової енергії в системах водяного опалення. *Енергоефективність в будівництві та архітектурі*, 4, 238-243
3. ДБН В.2.5-67:2013. (2013). *Опалення, вентиляція та кондиціонування*. Київ: Міністерство регіонального розвитку, будівництва та житлово-комунального господарства України
4. Любарєць О.П., Зайцев О.М., Любарєць В.О. (2010). *Проектування водяних систем опалення*. Відень-Київ-Сімферополь
5. Тарадай А.М., Покровський Л.Л., Редько А.Ф., Яременко М.А. (2010). Централизованное поквартирное отопление с регулированием и коммерческим учетом отпуска тепла. *Вентиляція, освітлення та теплогазопостачання*, 14, 36-42
6. Чайка Ю.І., Гвоздецький В.О., Красненко Т.І. (2015). Економічне обґрунтування модернізації існуючих однокотлових систем опалення. *Науковий вісник будівництва*, 2(80), 257-260
7. Тарадай О.М., Бугай В.С., Шахненко Е.Д., Фомич С.В. (2018). Модернізація системи опалення багатоквартирного житлового будинку в м. Чугуєві Харківської області. *Науковий вісник будівництва*, 2(92), 259-264
8. Taraday O., Sigal O., Bugai V. Pavliuk N., Shakhnenko Y. (2019). Reconstruction of heating systems of existing residential buildings by means of equipping apartment heating systems with heat meters. *Scientific Bulletin of Civil Engineering*, 3(97), 70-74
9. Тарадай А.М. (ред.). (2017). *Рекомендации по устройству квартирных систем отопления с теплосчетчиками в существующих многоэтажных жилых зданиях*. Харьков, ХНУБА
10. ДБН В.2.5-39:2008. (2008). *Інженерне обладнання будинків і споруд. Зовнішні мережі та споруди. Теплові мережі*. Київ: Міністерство регіонального розвитку, будівництва та житлово-комунального господарства України
11. Єнін П.М., Швачко Н.А. (2007). *Теплопостачання (частина I «Теплові мережі і споруди»)*. Київ: Кондор
1. Dolinskyi A.A., Basok B.I., Bazieiev Ye.T. (2012). The regional programs of communal power engineering modernization are an innovative base of the technological modernization of the heating settlements systems supply of Ukraine. Part 2. *Industrial Heat Engineering*, 34(4), 44-51
2. Roskovshenko Yu.K., Shtylenko V.P. (2013). Individual automatic regulation and metering of heat energy in water heating systems. *Energy-Efficiency in Civil Engineering and Architecture*, 4, 238-243
3. DBN B.2.5-67:2013. (2013). *Heating, Ventilation and Air Conditioning*. Kyiv: Ministry of Regional Development, Construction and Housing of Ukraine
4. Liubarets O.P., Zaitsev O.M., Liubarets V.O. (2010). *Designing water heating systems*. Viden-Kyiv-Simferopol
5. Taradai A.M., Pokrovskiy L.L., Redko A.F., Yaremenko M.A. (2010). Centralised apartment heating with regulation and commercial metering of heat supply. *Ventilation, Illumination and Heat-Gas Supply*, 14, 36-42
6. Chaika Yu.I., Hvozdetzkyi V.O., Krasnenko T.I. (2015). Economic justification for the modernization of existing single-pipe heating systems. *Scientific Bulletin of Civil Engineering*, 2(80), 257-260
7. Taradai O.M., Buhai V.S., Shakhnenko E.D., Fomych S.V. (2018). Modernization of the heating system of a multistory residential house in Chuhuiv of Kharkiv Region. *Scientific Bulletin of Civil Engineering*, 2(92), 259-264
8. Taraday O., Sigal O., Bugai V. Pavliuk N., Shakhnenko Y. (2019). Reconstruction of heating systems of existing residential buildings by means of equipping apartment heating systems with heat meters. *Scientific Bulletin of Civil Engineering*, 3(97), 70-74
9. Taradai A. M. (ed.). (2017). *Recommendations for apartment heating systems with heat meters in existing multi-story residential buildings*. Kharkiv, KhNUBA
10. DBN V. 2.5-39:2008. (2008). *Engineering equipment of buildings and structures. External networks and structures. Heating networks*. Kyiv: Ministry of Regional Development, Construction and Housing of Ukraine
11. Yenin P.M., Shvachko N.A. (2007). *Heat supply (part I "Heating networks and facilities")*. Kyiv: Kondor

UDC 624.042

## Comparison of design methods for steel silos

Pichugin Sergii<sup>1</sup>, Oksenenko Kateryna<sup>2\*</sup>

<sup>1</sup> National University «Yuri Kondratyuk Poltava Polytechnic» <https://orcid.org/0000-0001-8505-2130>

<sup>1</sup> National University «Yuri Kondratyuk Poltava Polytechnic» <https://orcid.org/0000-0002-5171-3583>

\*Corresponding author E-mail: [shvadchenkokate@gmail.com](mailto:shvadchenkokate@gmail.com)

The article describes the types of silos depending on the wall design. A review of the standard documents that are in force on the territory of Ukraine and regulate the determination of loads and forces in silos is carried out. The differences between the calculations of horizontal and vertical pressures on the walls of silos according to DBN B2.2-8-98 Enterprises, buildings and structures for grain storage and processing and DSTU-N B EN 1991-4:2012 Eurocode 1: Actions on structures – Part 4: Silos and tanks were analyzed. The design formulas for defining pressures according to two standards are given. The spreads of statistical properties of particulate solids are analyzed. The normative horizontal pressure and vertical frictional pressures for a flexible silo were calculated according to two standards. Graphs of horizontal and vertical pressures of particulate solids material on the walls of a flexible silo are presented. According to the calculations, it is concluded that the spreads of statistical properties of particulate solids has a significant impact on the magnitude of loads on the vertical walls of silos. It is noted that the value of the wall friction coefficient has a significant impact on the calculation of horizontal pressure

**Keywords:** silo, horizontal pressure, vertical pressure, friction forces, particulate solids

## Порівняння методик розрахунку конструкцій сталевих силосів

Пічугін С.Ф.<sup>1</sup>, Оксененко К.О.<sup>1\*</sup>

<sup>1,2</sup> Національний університет «Полтавська політехніка імені Юрія Кондратюка»

\*Адреса для листування E-mail: [shvadchenkokate@gmail.com](mailto:shvadchenkokate@gmail.com)

У статті розглянуто типи силосних ємностей, в залежності від конструкції стінки. Проведений огляд нормативних документів, які діють на території України, що регламентують питання визначення навантажень та зусиль в силосних ємностях. Проаналізовано відмінності між розрахунками горизонтальних та вертикальних тисків на стіни силосів за ДБН В2.2-8-98 Підприємства, будівлі та споруди по зберіганню та переробці зерна та ДСТУ-Н Б EN 1991-4:2012 Єврокод 1. Дії на конструкції. Ч. 4. Бункери і резервуари. Наведені розрахункові формули, для визначення тисків за двома стандартами. Проведено порівняння значень питомої ваги  $\gamma$ , кута природнього укосу  $\phi$ , кута внутрішнього тертя  $\phi$  та коефіцієнта бокового тиску  $K$  різних сільськогосподарських культур за двома стандартами. Визначені нижні та верхні характеристичні значення таких сипких матеріалів: пшениця, кукурудза, ячмінь та соя. Проаналізовані розкиди статистичних характеристик сипкого матеріалу. Проведені розрахунки нормативних горизонтального тиску та вертикального від сил тертя тисків для гнучкого силосу за двома нормами. Наведені графіки значень горизонтального та вертикального тисків сипкого матеріалу на стіни гнучкого. На основі розрахунків зроблено висновок, що розкид статистичних характеристик сипких матеріалів, має значний вплив на величину навантажень на вертикальні стіни силосних ємностей. Відзначено що, значення коефіцієнту тертя об стіни має значний вплив на розрахунок горизонтального тиску

**Ключові слова:** силос, горизонтальний тиск, вертикальний тиск, сили тертя, сипкий матеріал

## Introduction

Metal capacitive structures for storing various types of particulate solids are among the most common types of building structures. Silo dimensions, shape, foundation support methods, and layout are determined in accordance with the requirements of the technological process, loading and unloading conditions, and technical and economic factors. Silos are produced in round, square, rectangular, hexagonal and polygonal shapes. Round silos are preferred because they are easy to manufacture. With this shape, the walls are mainly subject to tensile forces. Therefore, their thickness can be small. Depending on the wall construction, metal silos are of the following types: welded silos, panel silos, and spiral-fold silos [1].

The body of a welded silo (Fig. 1a) consists of metal sheets that are welded together. The advantages of such silos are tightness and durability. Welded silos are designed to store particulate solids with the smallest particle size, such as cement, coke, slag, and others. The disadvantages of these structures are high material consumption and a large number of welds.

The body of the panel silo (Fig. 1b) is made of corrugated or smooth panels connected to each other with bolts. The advantages of panel silos are the ability to perceive a large radial load from the material, the absence of welds, high strength. The disadvantages of this version of silos are a large number of bolted connections. This type of silo construction is the most common in Ukraine and abroad for storing grain crops.

One of the most progressive types of thin-walled spatial structures are highly industrial and economic metal silos of the spiral-fold type (Fig. 1c). The construction of the silo was developed in 1968 by the German scientist Xaver Lipp [2], who used special equipment for processing sheet metal and applied it to the construction of spiral-wound silos. The first such silo was built in Germany in 1969. The spiral-fold silo has a cylindrical body, which is a system of spiral connection of steel strips. The formation of the body of the spiral-fold silo is based on the continuous building up of the wall structure from below, with the simultaneous bending of the steel strip along the arc of a circle and the connection of the bent longitudinal edges of the strip by double rolling into a closed-type fold lock. The advantages of these silos are: high degree of automation and speed of installation; minimizing the human factor in the installation good sealing, water resistance; it is possible to store waste water, oil, petroleum products, cement and other materials; when using stainless steel it is possible to store food; alcohol, wine, flour, malt, molasses, sunflower oil, etc;

The disadvantages spiral-fold silos are: for installation, the silo assembly equipment must be transported to the construction site, which increases the cost of production.



a)



b)



c)

**Figure 1 - Types of metal silos:**  
a – welded silo; b – panel silo;  
c – spiral-fold silo



## Review of the research sources and publications

A number of domestic and foreign scientists were involved in the analysis of structures, calculation methods and experimental studies of cylindrical shells of metal silos for strength and stability [1-7]. The behavior and physical characteristics of bulk material in silos were studied and described in detail by Kachurenko V. [3]. Bannikov D. presented his theoretical concept of the interaction of particulate solids with elements of capacitive building structures in his monograph [4]. Selamovic I. and Balevicius R. analyzed in detail the influence of rolling friction on the distribution of wall pressure and speed inside the flowing material [5]. Schultz D. discusses the general characteristics of particulate solids, starting from the flow properties of solid particles to the flow behavior of powders and particulate materials in bins and silos [6]. Coelho L. and Calil C. in their work [7] presented software for calculating the pressure in cylindrical silos, taking into account all the requirements of the European standard EN 1991-4 2006 [8]. Bibik M. and Moroz P. compared Ukrainian and European standards in their work [9] and made calculations according to both standards, depending on the flexibility of silos.

## Definition of unresolved aspects of the problem

The main normative document in Ukraine that regulates the design of steel silos, classification of their structures, determination of loads and forces in the elements is DBN B2.2-8-98 Enterprises, buildings and structures for storage and processing of grain [8], which was issued to replace SNiP 2.10.05-85 Enterprises, buildings and structures for storage and processing of grain [9]. Another normative document in Ukraine is DSTU-N B EN 1991-4:2012 Eurocode 1: Actions on structures – Part 4: Silos and tanks. [10], which defines the effects on silo structures. Since these two documents are valid on the territory of Ukraine and are in slightly different positions, the question of their comparison arises.

## Problem statement

The purpose of this article is to review the normative documents which regulate the determination of loads and forces in silos and compare them.

## Basic material and results

*Normative documents of Ukraine.* The main normative document in Ukraine that regulates the design of metal structures, including thin-walled shells, is DBN B.2.6-198:2014 Steel Structures [11]. This document contains general recommendations for assessing the strength and stability of torsional shells. Other normative documents in Ukraine are DBN B2.2-8-98 [8], which regulates the design of silos, classification of their structures, determination of loads and forces in elements, and DSTU-N B EN 1991-4:2012 [10], which defines only the effects on structures. These two documents regulate the principles for the calculation of loads from particulate solids that occur inside the silos.

*DBN B2.2-8-98.* According to these norms, the main loads and influences on the silo are: horizontal and vertical (due to friction) loads from the pressure of particulate solids, taking into account the central unloading of the silo; own weight of the structure; load from snow on the surface; influence of temperature; load from thermal suspensions; load from wind pressure (for an unfilled silo).

Normative horizontal pressure  $P_h^n$ , vertical pressure from frictional forces  $P_f^n$  and vertical pressure on the bottom of the silo  $P_v^n$  from the action of particulate solids are determined by the formulas:

$$P_h^n = \frac{\gamma \rho}{f} (1 - e^{-\lambda f z / \rho}), \quad (1)$$

$$P_f^n = f P_h^n, \quad (2)$$

$$P_v^n = \frac{a_4}{\lambda} P_h^n, \quad (3)$$

where  $\rho$  is the hydraulic radius of the cross-section of the silo, m, which is determined by the formula  $\rho = A/U$ ;

$A$ ,  $U$  are area and perimeter of the silo cross-section, respectively,  $m^2$  and  $m$ ;

$\lambda$  is the lateral pressure ratio of particulate solids,  $\lambda$  is characterized by the ratio of the average values of horizontal and vertical pressure according to p. 4.6 [8]

and is determined by the formula:  $\lambda = \operatorname{tg}^2 \left( 45^\circ - \frac{\varphi}{2} \right)$ ;

$e$  is the base of the natural logarithm;

$\gamma$  is bulk unit weight,  $\text{kgf/m}^3$ , taken according to tab. A.1 [8];

$\varphi$  is the angle of internal friction, degrees, taken according to tab. A.1 [17];

$f$  is coefficient of wall friction, taken according to tab. A.1 [8].

Also, for the walls of steel round sheet silos not reinforced with ribs, the annular horizontal pressure is taken into account  $P_{h1}^n$ , which is determined by the

formula:  $P_{h1}^n = a_1 P_h^n$ ,

where  $a_1$  is the coefficient of local pressure increase, which is taken in accordance with the requirements of 4.11. [8] depending on the  $h/d$  ratio;

$h$  is height of silo from the hopper apex to the equivalent surface, m.

The sum of the limit calculated values of uniformly distributed horizontal pressures with the limit calculated values of annular horizontal pressures is determined by the formula:

$$\Sigma P_i = \gamma_{fm} (P_h^n + P_{h1}^n), \quad (4)$$

where  $\gamma_{fm}$  is load reliability factor.

*DSTU-N B EN 1991-4:2012.* This normative document assumes that the value of loads during the movement of particulate solids in a silo structure depends on the flexibility of the structure, the class of impacts, the category of the wall surface, and the amount of eccentricity after loading and during

discharge. In this regard, various procedures are given for determining the horizontal pressure  $p_{hf}$ , wall frictional traction  $p_{wf}$  and vertical pressure  $p_{vf}$  which are applied to the silo body after loading and

symmetrical pressures during discharge  $p_{he}$  and  $p_{we}$ . Symmetrical loads after filling and during storage for slender silos are determined by the formulas given in Table 1.

**Table 1 – Formulas for determining the loads on the vertical walls of slender silos**

Loads on the vertical walls of slender silos	Loads after loading	Loads during discharge
Horizontal pressure	$p_{hf}(z) = p_{ho} Y_J(z)$	$p_{he} = C_h p_{pf}$
Wall frictional traction	$p_{wf}(z) = \mu p_{ho} Y_J(z)$	$p_{we} = C_w p_{wf}$
Substitute uniform pressure increase for patch loads	$p_{hf.u} = p_{hf} (1 + 0,5 C_{pf})$ $p_{wf.u} = p_{wf} (1 + C_{pf})$	$p_{he.u} = p_{he} (1 + 0,5 C_{pe})$ $p_{we.u} = p_{we} (1 + C_{pe})$
Notes: $p_{ho} = \gamma K z_o$ , $z_o = \frac{1}{K\mu} \frac{A}{U}$ , $Y_J(z) = 1 - e^{-z/z_o}$		

Definitions in Table 1:

$\gamma$  is the characteristic value of the unit weight;

$\mu$  is the characteristic value of the wall friction coefficient for solid sliding on the vertical wall;

$K$  is the characteristic value of the lateral pressure ratio;

$z$  is the depth below the equivalent surface of the solid;

$A$  is the plan cross-sectional area of the silo;

$U$  is the internal perimeter of the plan cross-section of the silo;

$C_h$  horizontal pressure discharge factor (load magnifying factor);

$C_w$  wall frictional traction discharge factor (load magnifying factor);

$C_{pf}$  filling patch load factor (load magnifying factor);

$C_{pe}$  discharge patch load factor (load magnifying factor)

The characteristic values of the particulate solids are taken in accordance with E.1 [10].

It should be noted that when determining the maximum load  $p_{hf}$ ,  $p_{wf}$ ,  $p_{vf}$  for a cylinder, different extreme values of the properties of particulate solids are used (Table 2).

Table 3 shows the values of particulate solids  $\gamma$ ,  $\phi_r$ ,  $\phi_i$ ,  $K$  which are taken into account in the calculations of horizontal and vertical loads, depending on the design standards.

As it can be seen from Tab. 3, the differences in the values of the weight  $\gamma$  are insignificant. At the same time, the angle of repose  $\phi_r$ , angle of internal friction  $\phi_i$  and the lateral pressure ratio  $K$  have significant deviations. In Table 4 values of the wall friction coefficient are given.

**Table 2 – Values of properties to be used for different wall loading assessments**

For the vertical wall or cylinder	Characteristic value to be adopted		
	Wall friction coefficient $\mu$	Lateral pressure ratio $K$	Weight $\gamma$
Maximum normal pressure on vertical wall	Lower	Upper	Upper
Maximum frictional traction on vertical wall	Upper	Upper	Upper
Maximum vertical load on hopper or silo bottom	Lower	Lower	Upper

**Table 3 – Value of weight  $\gamma$ , angle of repose  $\phi_r$ , angle of internal friction  $\phi_i$  and lateral pressure ratio  $K$  of agricultural crops**

Normative document	The type of particulate solids	Weight $\gamma$ , kN/m <sup>3</sup>	Angle of repose $\phi_r$	Angle of internal friction $\phi_i$	Lateral pressure ratio $K$
DBN	All grains and legumes	8	25	25	0.406
DSTU	Wheat	7.5* – 9**	34	27* – 34**	0.49* – 0.6**
	Corn	7* – 8**	35	27* – 35**	0.46* – 0.6**
	Barley	7* – 8**	31	24* – 32**	0.53* – 0.65**
	Soy	7* – 8**	29	22* – 29**	0.57* – 0.7**
Notes: * lower characteristic value; ** upper characteristic value of weight $\gamma$ taken according to tab. E.1 DSTU; * lower characteristic value; ** the upper characteristic value of the angle of internal friction $\phi_i$ and lateral pressure ratio $K$ , calculated by formulas (4.1) and (4.2), (4.5) and (4.6) DSTU					

**Table 4 - The value of the wall friction coefficient  $\mu$**

Normative document	The type of particulate solids	Wall surface definitions	Wall friction coefficient $\mu$
DBN	All grains and legumes	metal walls	0.4
		concrete walls	0.4
DSTU	Wheat	Wall category D1	0.21* – 0.28**
		Wall category D2	0.33* – 0.44**
	Corn	Wall category D1	0.18* – 0.27**
		Wall category D2	0.29* – 0.45**
	Barley	Wall category D1	0.21* – 0.28**
		Wall category D2	0.28* – 0.38**
	Soy	Wall category D1	0.21* – 0.28**
		Wall category D2	0.33* – 0.44**

**Notes:** \* lower characteristic value; \*\* upper characteristic value, calculated according to formulas (4.3) and (4.4) DSTU  
The wall surface categories are given in tab. 4.1 DSTU:  
wall type D1 - classified as "Slippery" - polished stainless steel;  
wall type D2 - classified as "Smooth" - smooth mild carbon steel (welded, bolted construction);

The wall friction coefficient  $\mu$  shows a large discrepancy in the values depending on the regulatory documents.

It is worth noting that the calculation of horizontal and vertical pressures on silo walls according to DBN has the following differences from DSTU: flow forms during discharge are not taken into account, silo structures are not divided by flexibility, and therefore the calculation of horizontal and vertical pressures for all types of structures is performed by one formula. The statistical variation of particulate solids properties is also not taken into account, namely the characteristic value of weight  $\gamma = 8 \text{ kN/m}^3$  is assumed for all grain crops, the angle of repose  $\varphi_r$  and angle of internal friction  $\phi_i$  are assumed to be the same  $\varphi = 25^\circ$ . It is also worth noting that in the DBN, the wall friction coefficient for both metal and concrete silos corresponds to the value of  $\mu = 0.4$ .

In order to compare these building codes, the horizontal pressure  $p_{hf}$  and wall frictional traction  $p_{wf}$  that act on the walls of the silo were determined according to both standards. The following data were used for the calculation. Geometric parameters of the silo: diameter 6 m, height 15 m. A silo of this size is classified as slender according to DSTU, and therefore the calculation of horizontal pressure and wall frictional traction according to both standards is performed by using the same formula. To assess the effect of the particulate solids properties on the loads that it causes in the silo structure, were made the calculations for different types of particulate solids, namely wheat, barley, corn, and soybeans. The results of comparing horizontal pressure and wall frictional traction are shown in Fig. 2.

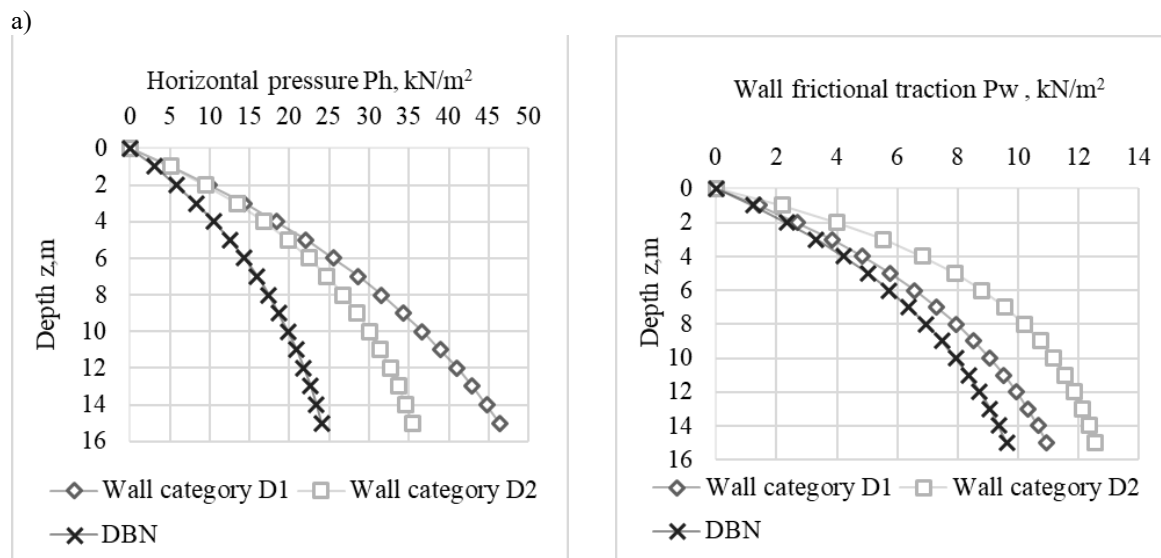
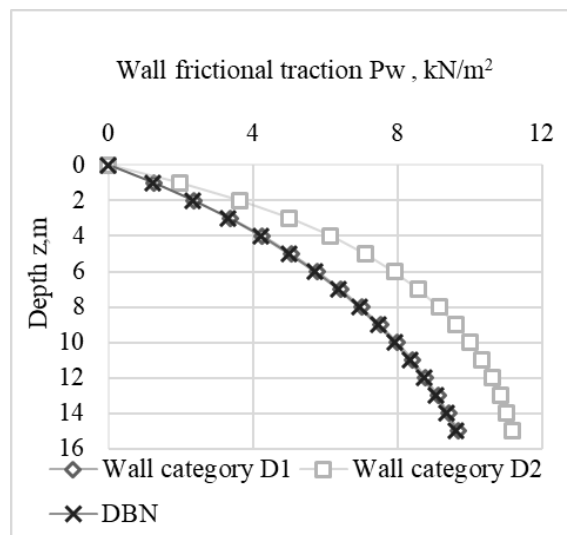
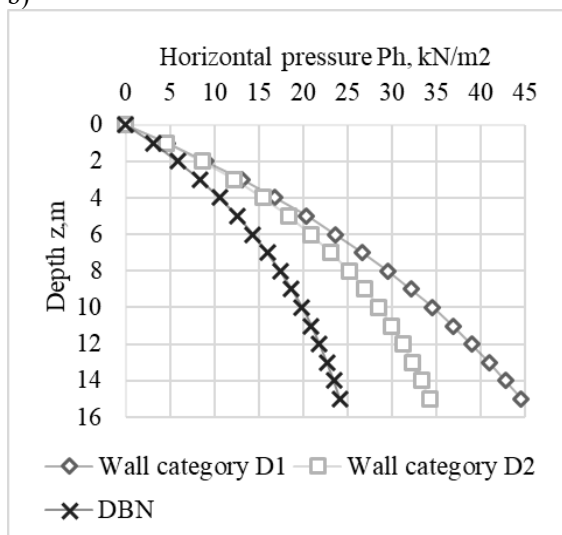
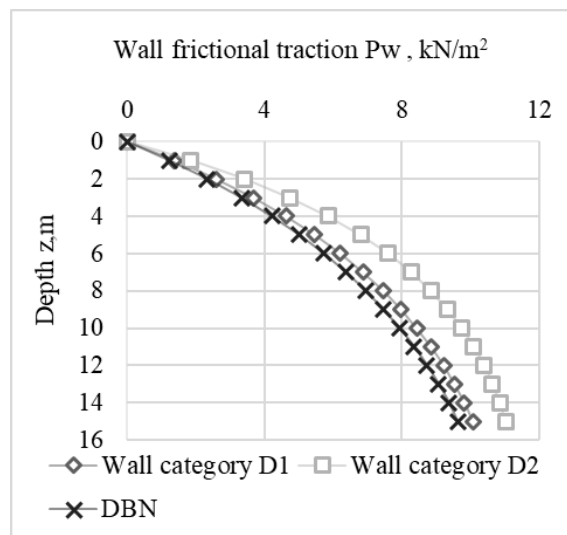
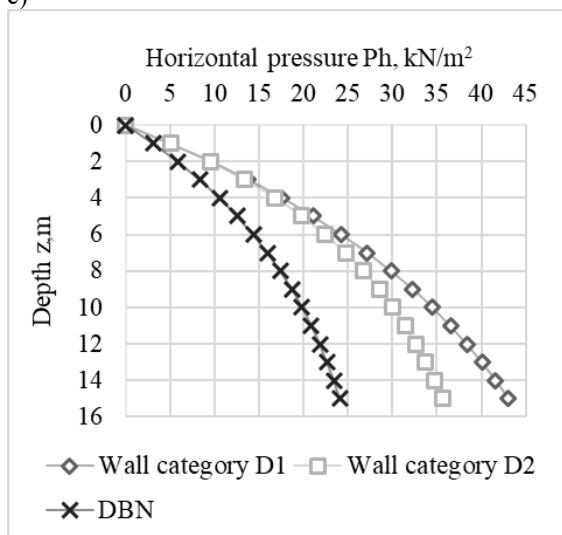


**Figure 2 –The value of horizontal pressure and wall frictional traction of the particulate solids on the walls of a slender silo:**  
a) wheat (Note: the type of wall is given in Table 4)

b)



c)



d)

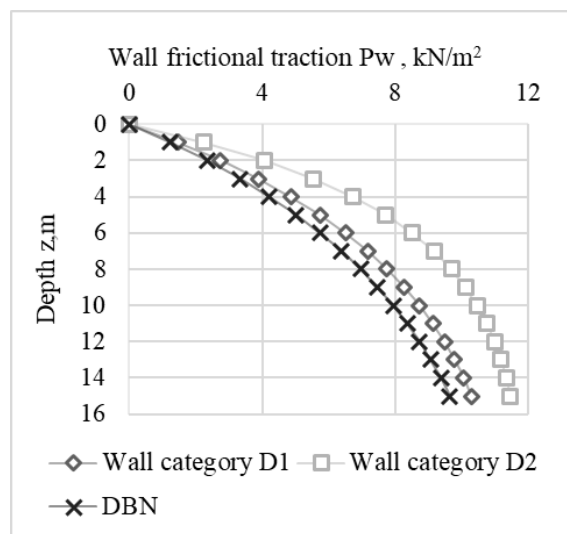
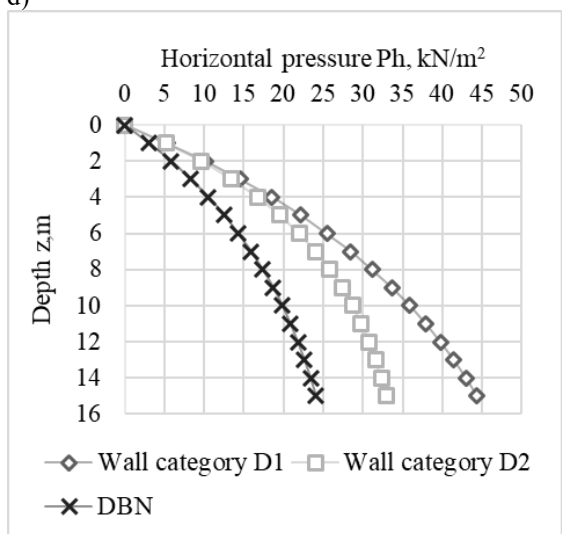


**Figure 2\* –The value of horizontal pressure and wall frictional traction of the particulate solids on the walls of a slender silo:**

b) corn; c) barley; d) soybeans (Note: the type of wall is given in Table 4)

Figure 2 shows an increase in pressure with increasing of silo depth. The values of the horizontal pressures on the silo wall according to DSTU, which took into account the spread of particulate solids, are 27-48% higher than the calculations according to DBN; the wall frictional traction are 1-23% higher. It is worth noting that the maximum difference in horizontal pressure values between the two standards reaches a maximum deviation of 48% for a D1 wall category, which is characterized as very smooth according to DSTU. While the difference in wall frictional traction between the two standards reaches a maximum deviation of 23% for a D2 wall category, which is characterized as smooth according to DSTU. Consequently, the value of the wall friction coefficient has a significant impact on the horizontal pressure calculation. Having analyzed the obtained graphs, it can be concluded that the spreads of statistical properties of particulate solids has a significant impact on the magnitude of loads on the vertical walls of silos.

## Conclusions

The article reviews the normative documents that are in force on the territory of Ukraine, which regulate the determination of loads and forces in silos. During the comparison, it was noted that horizontal and vertical pressures on silo walls according to DBN has the following differences from DSTU: flow forms during discharge are not taken into account, silo structures are not divided by flexibility, and therefore the calculation of horizontal and vertical pressures for all types of structures is performed by one formula. The statistical variation of particulate solids properties is also not taken into account. When comparing the pressures that act on the walls of a slender silo according to both standards, it was noted that the value of the wall friction coefficient has a significant impact on the calculation of horizontal pressure.

## References

1. Pichugin S., Oksenenko K. (2019). Comparative analysis of design solutions of metal silos. *Academic journal. Industrial Machine Building, Civil Engineering*, 2(53), 54-60  
<https://doi.org/10.26906/znp.2019.53.1890>
2. Haver Lipp. Взято з <https://xaver-lipp.com/>
3. Качуренко В.В., Банников Д.О. (2016). *Конструктивні рішення сталевих ємностей для сипких матеріалів*. Дніпропетровськ: Нова ідеологія.
4. Банников Д.О. (2009). *Сипучий матеріал в ємнісній конструкції*. Дніпропетровськ: Нова ідеологія
5. Sielamowicz I., Balevicius R. (2013). *Experimental and computational analysis of granular material flow in model*. Warsaw: Institute of Fundamental Technological Research Polish Academy of Experimental Sciences
6. Schulze D. (2009). *Powders and Bulk Solids. Behavior, Characterization, Storage and Flow*. Springer
7. Coelho L.C., Calil C.(Jr) (2017). Software to Calculate Pressures in Cylindrical Metal Silos. *Journal of Advances in Information Technology*, 8(1), 47-51
8. EN 1991-4:2011 (2011). Eurocode 1 - *Actions on structures - Part 4: Silos and tanks*
9. Бібік М.В., Мороз П.С. (2014). Визначення горизонтального навантаження на вертикальні стіни ємнісних конструкцій за різними нормами. *Збірник наукових праць: Галузеве машинобудування, будівництво*, 1(40), 166-174
10. ДБН В.2.2-8-98 (1998). *Підприємства, будівлі та споруди по зберіганню та переробці зерна*. Київ: Держбуд України
11. СНиП 2.10.05-85 (1985). *Підприємства, будівлі та споруди для зберігання і переробки зерна*. М.: ЦТП Держбуду.
12. DSTU-NB EN 1991-4:2012. Єврокод 1. (2012). *Дії на конструкції. Ч. 4. Бункери і резервуари*. Київ: Мінбуд України
13. ДБН В.2.6-198:2014 (2014). *Сталеві конструкції. Норми проектування*. Київ, Мінрегіон України
1. Pichugin S., Oksenenko K. (2019). Comparative analysis of design solutions of metal silos. *Academic journal. Industrial Machine Building, Civil Engineering*, 2(53), 54-60  
<https://doi.org/10.26906/znp.2019.53.1890>
2. Haver Lipp. Retrieved from <https://xaver-lipp.com/>
3. Kachurenko V.V., Bannikov D.O. (2016). *Constructive solutions of steel tanks for bulk materials*. Dnepropetrovsk: New ideology
4. Bannikov D.O. (2009). *Bulk material in capacitive construction*. Dnepropetrovsk: Nova Ideology
5. Sielamowicz I., Balevicius R. (2013). *Experimental and computational analysis of granular material flow in model*. Warsaw: Institute of Fundamental Technological Research Polish Academy of Experimental Sciences
6. Schulze D. (2009). *Powders and Bulk Solids. Behavior, Characterization, Storage and Flow*. Springer
7. Coelho L.C., Calil C.(Jr) (2017). Software to Calculate Pressures in Cylindrical Metal Silos. *Journal of Advances in Information Technology*, 8(1), 47-51
8. EN 1991-4:2011 (2011). Eurocode 1 - *Actions on structures - Part 4: Silos and tanks*
9. Bibyk M.V., Moroz P.S. (2014). Determination of the horizontal load on the vertical walls of capacity structures according to various standards. *Academic journal. Industrial Machine Building, Civil Engineering*, 1(40), 166-174
10. DBN B.2.2-8-98 (1998). *Enterprises, buildings and structures for storage and processing of grain*. Kyiv: State Construction Committee of Ukraine
11. SNiP 2.10.05-85 (1985). *Enterprises, buildings and structures for storage and processing of grain*. M.: CИTP Gosstroy
12. DSTU-NB EN 1991-4:2012. Eurocode 1. (2012). *Actions on structures. Part 4. Bunkers and tanks*. Kyiv: Ministry of Construction of Ukraine
13. DBN B.2.6-198: 2014 (2014). *Steel structures. Design standards*. Kyiv, Ministry of Regional Development of Ukraine



UDC 624.012.4:691.328.4:620.17

## Strength of fiber concrete (concrete) under local compression according to the theory of plasticity and experimental studies

Kuznietsova Iryna<sup>1\*</sup>, Dovzhenko Oksana<sup>2</sup>, Pohribnyi Volodymyr<sup>3</sup>, Pents Volodymyr<sup>4</sup>

<sup>1</sup> National University «Yuri Kondratyuk Poltava Polytechnic» <https://orcid.org/0000-0002-5859-4636>

<sup>2</sup> National University «Yuri Kondratyuk Poltava Polytechnic» <https://orcid.org/0000-0002-2266-2588>

<sup>3</sup> National University «Yuri Kondratyuk Poltava Polytechnic» <https://orcid.org/0000-0001-7531-2912>

<sup>4</sup> National University «Yuri Kondratyuk Poltava Polytechnic» <https://orcid.org/0000-0001-9580-1457>

\*Corresponding author E-mail: [oldfiedeik@gmail.com](mailto:oldfiedeik@gmail.com)

Local compression of concrete is often implemented in supporting joints of reinforced concrete structures. As a strength calculation method for this case, a variational method in the theory of plasticity is proposed, which is based on the consideration of the failure stage and takes into account the full set of determining factors of strength: the dimensions of the sample, the shape and dimensions of the loading platform, its location, the ratio of the dimensions of the loading device and the element, type and class of concrete (by taking into account both strength characteristics). In experimental studies, the kinematic schemes of failure adopted in the calculation and the influence of determining factors were confirmed. A comparative analysis of the strength calculated by the proposed method with the experimental one for 78 samples showed that they are sufficiently close.

**Keywords:** local compression; strength; variational method; theory of plasticity; fiber concrete

## Міцність фібробетону (бетону) при місцевому стисненні за даними теорії пластичності й експериментальних досліджень

Кузнєцова І.Г.<sup>1\*</sup>, Довженко О.О.<sup>2</sup>, Погрібний В.В.<sup>3</sup>, Пенц В.Ф.<sup>4</sup>

<sup>1, 2, 3, 4</sup> Національний університет «Полтавська політехніка імені Юрія Кондратюка»

\*Адреса для листування E-mail: [oldfiedeik@gmail.com](mailto:oldfiedeik@gmail.com)

Прикладом місцевого стиснення бетону слугує вузол обпирання залізобетонних колон багатоповерхових будинків на бетонні елементи, які входять до складу цокольної або підвальної їх частин. Для підвищення точності розрахунку при змінанні запропонований варіаційний метод у теорії пластичності бетону, розроблений у Національному університеті «Полтавська політехніка імені Юрія Кондратюка». Випробувані стандартні куби із бетону (фібробетону на базальтовій фібрі) при односторонньому місцевому стисненні, в котрих ділянка навантаження змінювалася від квадрату до смуги. Характер руйнування дослідних зразків підтвердив кінематично можливі схеми руйнування, прийняті в теоретичних розрахунках залежно від форми площадки завантаження (квадрат, прямокутник, смуга). Визначено вплив на міцність співвідношення ширини ділянки завантаження до ширини і висоти дослідного зразка. Введення базальтової фібри в склад бетону не змінює характер руйнування, але збільшує міцнісні характеристики бетону при стиску і розтягу, та як результат міцність при місцевому стисненні. Для забезпечення достовірності запропонованої методики розрахунку виконано порівняння теоретичної міцності, підрахованої за варіаційним методом у теорії пластичності, з експериментальною для 78 дослідних зразків, у тому числі й авторських. За широкого інтервалу варіювання параметрів експериментальних зразків теоретична міцність добре сходиться із дослідною: середнє значення відношення її теоретичного значення до дослідного складає  $m=1,02$  з коефіцієнтом варіації  $v=13,16\%$ . Отримані результати дозволяють рекомендувати варіаційний метод у теорії пластичності бетону у якості теоретичної основи для розрахунку бетонних елементів при місцевому стисненні, як такий що базується на розгляді стадії руйнування та враховує вплив повної сукупності визначальних факторів міцності.

**Ключові слова:** місцеве стиснення; варіаційний метод; міцність; теорія пластичності; фібробетон

## Introduction

In the practice of construction, there are quite often cases of transfer of large concentrated loads to concrete wall or foundation elements. As an example (Fig. 1), it is possible to cite the supporting of reinforced concrete columns of multi-story buildings or supports of hanging walls on concrete members of different heights, thicknesses and dimensions in plan, which are part of the basement, basement or other structural parts of buildings (structures). At the same time, there is a local compression of concrete in structural members.

One of the reserves for increasing the operational reliability of such concrete (fiber concrete) members is the improvement of their calculation methods. At the moment, it is necessary to shift from empirical dependences in the calculation of crushing, characteristic of current standards, to other methods that are close to the results of experimental studies, taking into account the stress-strain state of the elements and characteristic kinematics.



Figure 1 – A case of local compression

## Review of the research sources and publications

At the National University “Yury Kondratyuk Poltava Polytechnic” a variational method in the theory of plasticity of concrete is proposed as a theoretical basis for calculating the strength of concrete (fiber concrete) members under local compression [1]. The general sequence of tasks is as follows: the failure character is modeled for the case under consideration (a cinematically possible failure scheme is created: with the help of unknown geometric parameters, the outline of the failure surface is outlined and the directions of movement (velocities) of individual discs separated by the failure surface are set); as a rule, geometric parameters are the angles of inclination of the failure areas to the vertical; at the same time, they operate with relative values of velocities; there are velocity jumps on the sections of the failure surface and their area; the functional of the method is recorded, the corresponding mathematical transformations are performed; the functional is examined for a stationary state, in the process of

which a formula is derived for calculating the ultimate load in the function from unknown parameters; this function is studied for the extremum (unconditional during translational motion of rigid disks on the kinematic scheme or conditional in another case: equilibrium equations are used as additional conditions); the ultimate load value is determined.

The variational method in the theory of plasticity [2] solved the problem of the strength of concrete (fiber concrete) members with one-sided central crushing, while taking into account the ratio of the length of the loading platform to the height (cross-sectional dimensions) of the member, the scheme and method of load transfer, the type of concrete (both characteristics of its strength); impact of basalt fiber.

Analysis of experimental studies of the bearing capacity of fiber concrete members under local compression [3 – 8] indicates their insufficient number. As a rule, the variable parameters were the volumetric percentage of fiber reinforcement (only steel), the ratio of the load area to the cross-sectional dimensions of the sample; both cubes and prisms were used as test samples.

## Definition of unsolved aspects of the problem

Basalt fiber was not used in crushing experiments. According to experimental studies [7], the optimal dimensions of basalt fiber are – length 12 mm, diameter 20  $\mu\text{m}$ , percentage content – 0.2%. At the same time, the tensile and compressive strength increases significantly compared to unreinforced concrete [9].

## Problem statement

The purpose of the work is to compare the strength of concrete (fiber concrete) members under local compression, calculated according to the proposed method, with experimental data, including those obtained by the authors.

## Basic material and results

The method of manufacturing and testing experimental samples is given in [10]. According to the test results of standard cubes and prisms, which were made together with the test samples, the average value of the cubic strength of heavy concrete without the use of plasticizer is  $f_{cm,cube} = 28.7 \text{ MPa}$ , with the use of plasticizer  $f_{cm,cube} = 33.1 \text{ MPa}$ , fiber concrete  $f_{cm,cube} = 39.8 \text{ MPa}$  (20% increase). The average value of the prism strength and the tensile strength, respectively, are  $f_{cm,prizm} = 22.7 \text{ MPa}$ ,  $f_{ctm} = 1.6 \text{ MPa}$ ;  $f_{cm,prizm} = 27.2 \text{ MPa}$ ,  $f_{ctm} = 1.8 \text{ MPa}$ ;  $f_{cm,prizm} = 35.1 \text{ MPa}$  (29% increase),  $f_{ctm} = 2.3 \text{ MPa}$  (28% increase). There is a steady tendency to increase the value of the strength characteristics both when adding a plasticizer and when it is combined with basalt fiber, while both the prismatic strength and the tensile strength increased by almost the same amount.

Table 1 presents the results of experimental studies. The addition of basalt fiber increases the resistance of concrete to local compression.

**Table 1 – Results of experimental studies**

№ of sample	Sample key	№ of batch	Load, t	Strength, $f_{loc}$ , MPa	$f_{loc}/f_{c,prizm}$
1	F1KC50	1	14.2	56.8	1.62
2	F1KC100	1	36.86	73.71	2.1
3	F1KC150	1	32.9	43.86	1.25
4	B2KC50	2	21.22	84.86	3.12
5	B2KC100	2	25.2	50.4	1.85
6	B2KC150	2	25.9	34.5	1.27
7	B3KC50	3	17.2	68.8	3.03
9	B3KC100	3	29.85	59.7	2.63
10	B3KC150	3	23.84	31.79	1.40

In Table 1, the following marking of test samples is adopted: B – heavy concrete or F – fiber concrete (the first letter in the marking); 1 (with the addition of the addition of only a plasticizer), 3 (basic composition) – series number; KC – type of experimental sample (standard cubes were tested for local compression (fig. 2); 50, 100, 150 (fig. 3) – the stamp width  $b_{loc}$  when the load is applied locally, mm (the stamp length  $l_{loc}$  for all samples is the same and is equal to 50 mm).



**Figure 2 – Sample testing for local compression in the press ПГ-125**

In the process of experimental research, failure character of cubes during central one-sided compression was revealed, which was taken as a basis for theoretical calculations under the conditions of a space stress state: the sample is divided into three parts: a pyramid with a square (fig. 4) or rectangular (fig. 5) base, which is equal to the load platform, two halves of a cube, separated by a splitting plane and a shear surface, which move away from each other in the horizontal plane.

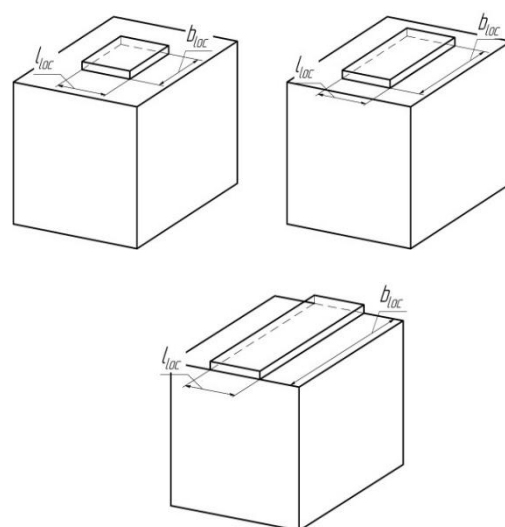


**Figure 3 – Loading scheme of cubes with size 150×150×150 mm through stamps with size  $l_{loc} \times b_{loc} = 50 \times 50$  mm,  $50 \times 100$  mm,  $50 \times 150$  mm**

The obtained results confirm the data of the study of strength to local compression of concrete obtained by other authors [11-15].

In order the features of the structures in the ultimate state. to ensure the reliability of the proposed calculation method, it is important to create a cinematically possible scheme for the members failure, which should take into account.

There is also an asymmetric failure character under symmetrical loading (fig. 6), which is explained by the concentration of stresses near the corners of the stamp and the heterogeneous structure of the concrete. The proposed calculation method allows you to take into account such case of failure by making changes to the cinematically possible scheme.

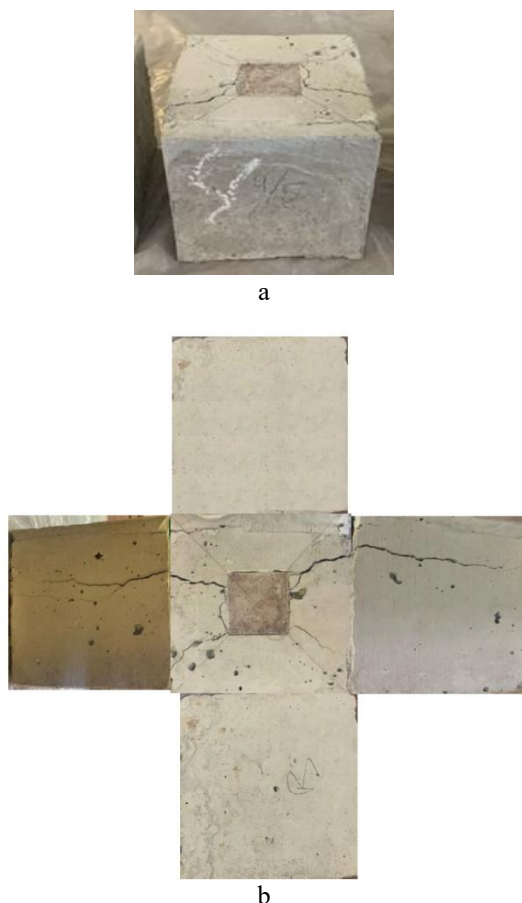


**Figure 4 – Failure character (a) and surface view (b) of the destroyed sample B3KC50**

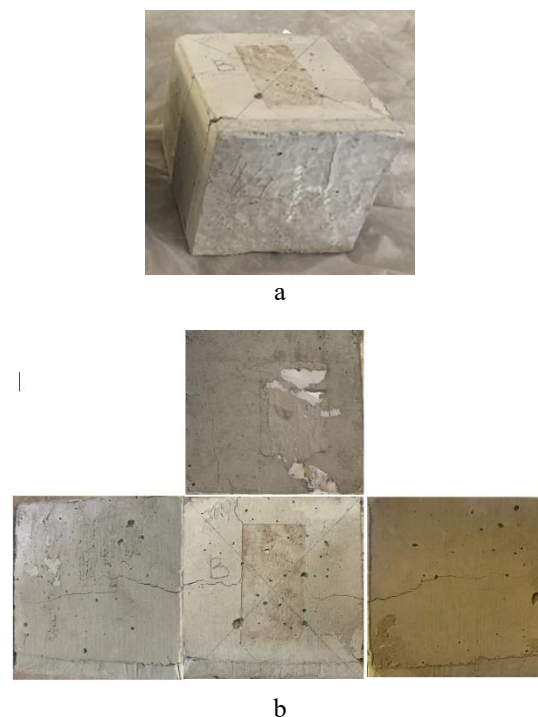


**Figure 5 – Failure character (a) and surface view (b) of the destroyed sample B3KC100**

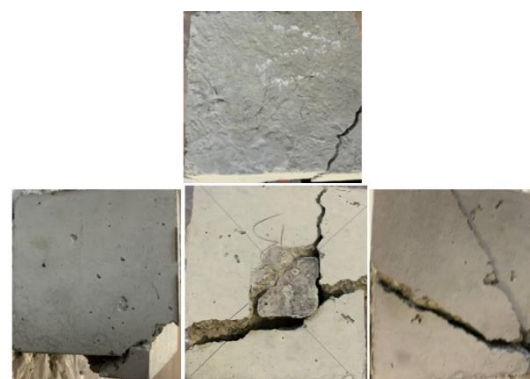


**Figure 6 – Surface view of the destroyed sample F1KC50**

The use of fiber does not fundamentally change the failure character of samples, but it becomes more plastic, stretched over time.

Changing the width of the loading platform (from a square to a strip stamp) affects the magnitude of local compressive stresses: within the limits of the experiment, the stress decreases up to 2 times (table 1).

The addition of basalt fiber increases the strength characteristics, reduces the probability of brittle failure and the presence of microcracks in concrete, and ultimately the resistance of concrete to local compression.

To confirm the validity of the proposed calculation method [1], a comparative analysis of the theoretical strength with the experimental strength was performed for 78 test samples tested by Gladyshev B.M., Piradov A.B., Dovzhenko O.O. and Mytrofanov V.P.,

Ince R. and Arici E., Au T. and Baird D.L., Keras V., Augonis M., Adamukaitis N., Vaitekūnaitė E. and authors [10] with parameters that differed significantly: the dimensions of the cube varied from 50 mm to 300 mm; ratio  $h/l_{loc}$  (ratio of the height of the cube to the length of the loading platform) was from 1 to 6.67; value of concrete tensile strength  $f_{ct}$  was from 0.4 MPa to 4.8 MPa; value of concrete strength under compression  $f_c$  was from 3.87 MPa to 48 MPa; samples were concrete and fiber concrete: steel fiber content was from 25 kg/m<sup>3</sup> to 40 kg/m<sup>3</sup>, basalt fiber was 18 kg/m<sup>3</sup>. It should be noted that all test samples were loaded with a square stamp, a rectangular stamp was used only in the author's experiments.

The results of the comparison are presented in tables 2, 3, 4 and in fig. 7.

**Table 2 – Comparison of the theoretical strength calculated according to the variational method with the experimental one for concrete cubes**

№	$l \times b \times h$ , cm	$l_{loc}$ , cm	$\alpha = h / l_{loc}$	$\chi = f_{ct} / f_c$	$\frac{f_{c,loc}^{test}}{f_c}$	$\frac{f_{c,loc}^{calc}}{f_c}$	$\frac{f_{c,loc}^{calc}}{f_{c,loc}^{test}}$
1	2	3	4	5	6	7	8
Samples of Gladyshev B.M. [11]							
1	20×20×20	5	4	0.103	4.85	5.07	1.04
2	20×20×20	5	4	0.109	4.24	5.12	1.21
3	20×20×20	5	4	0.099	4.81	4.99	1.04
4	20×20×20	5	4	0.099	4.96	4.99	1.01
5	20×20×20	5	4	0.103	3.47	3.85	1.11
6	15×15×15	5	3	0.079	3.06	3.60	1.17
7	25×25×25	10	2.5	0.119	2.88	3.53	1.22
Piradov A.B. [12]							
1	30×30×30	5	5	0.05	5.34	5.48	1.03
2	20×20×20	3	3	0.103	8.99	8.73	0.97
3	20×20×20	3	3	0.099	8.05	8.55	1.06
4	20×20×20	3	3	0.057	6.75	6.47	0.96
5	15×15×15	3	3	0.079	5.28	5.62	1.07
6	20×20×20	3	3	0.094	8.05	8.32	1.03
7	20×20×20	3	3	0.099	8.60	8.55	0.99
Dovzhenko O.O., Mytrofanov V.P. [13]							
1	20×20×20	5	4	0.08	4.11	4.55	1.11
2	15×15×15	5	3	0.08	3.07	3.59	1.17
3	15×15×15	5	3	0.08	2.73	3.59	1.31
Ince R., Arici E. [14]							
1	5×5×5	2	2.5	0.13	4.72	3.61	0.76
2	10×10×10	4	2.5	0.13	3.45	3.61	1.05
3	20×20×20	8	2.5	0.13	2.9	3.61	1.24
4	5×5×5	2	2.5	0.09	4.23	3.32	0.78
5	10×10×10	4	2.5	0.09	3.64	3.32	0.91
6	20×20×20	8	2.5	0.09	2.7	3.32	1.23
7	5×5×5	4	2.5	0.09	3.99	3.32	0.83
8	10×10×10	8	2.5	0.09	3.25	3.32	1.02
9	20×20×20	4	2.5	0.09	3.57	3.29	0.92
10	5×5×5	2	2.5	0.07	4.39	3.14	0.72
11	10×10×10	4	2.5	0.07	3.46	3.14	0.91
12	20×20×20	8	2.5	0.07	2.45	3.14	1.28
13	10×10×10	2.5	4	0.09	6.36	4.90	0.77
14	20×20×20	5	4	0.09	4.83	4.90	1.01
Au T. and Baird D. L. [15]							
1	10×10×10	10	1	0.09	2.06	2.46	1.19
2	10×10×10	8	1.25	0.09	2.77	2.66	0.96



**Table 3 – Comparison of the theoretical strength calculated according to the variation method with the experimental strength according to the authors' data for concrete samples**

№	$l \times b \times h$ , cm	$l_{loc}$ , cm	$\alpha = h / l_{loc}$	$\chi = f_{ct} / f_c$	$\frac{f_{c,loc}^{test}}{f_c}$	$\frac{f_{c,loc}^{calc}}{f_c}$	$\frac{f_{c,loc}^{calc}}{f_{c,loc}^{test}}$
1	2	3	4	5	6	7	8
1	15×15×15	5	3	0.07	3.62	3.48	0.96
2	15×15×15	10 (5)	3	0.07	2.29	2.47	1.08
3	15×15×15	15 (5)	3	0.07	1.95	2.25	1.15
4	15×15×15	5	3	0.06	3.55	3.42	0.96
5	15×15×15	10 (5)	3	0.06	2.26	2.46	1.08
6	15×15×15	15 (5)	3	0.06	1.93	2.25	1.16
7	15×15×15	5	3	0.06	3.54	3.41	0.96
8	15×15×15	15 (5)	3	0.06	1.93	2.25	1.16

**Table 4 – Comparison of theoretical strength with experimental strength for fiber concrete samples**

№	$l \times b \times h$ , cm	$l_{loc}$ , cm	Content of metal fibers, kg/m <sup>3</sup>	$\alpha = h / l_{loc}$	$\chi = f_{ct} / f_c$	$\frac{f_{c,loc}^{test}}{f_c}$	$\frac{f_{c,loc}^{calc}}{f_c}$	$\frac{f_{c,loc}^{calc}}{f_{c,loc}^{test}}$
1	2	3	4	5	6	7	8	9
Samples of Keras V., Augonis M., Adamukaitis N., Vaitekūnaitė E. [7]								
1	15×15×15	3	25	5	0.17	6.06	6.58	1.08
2	15×15×15	3	25	5	0.17	6.06	5.41	0.89
3	15×15×15	3	25	5	0.17	6.06	6.72	1.10
4	15×15×15	3	25	5	0.17	6.06	5.59	0.92
5	15×15×15	3	25	5	0.17	6.06	6.58	1.08
6	15×15×15	3	30	5	0.15	5.75	5.03	0.87
7	15×15×15	3	30	5	0.15	5.75	5.21	0.90
8	15×15×15	3	30	5	0.15	5.75	5.35	0.93
9	15×15×15	3	30	5	0.15	5.75	4.34	0.75
10	15×15×15	3	30	5	0.15	5.75	5.97	1.04
11	15×15×15	3	35	5	0.19	6.36	7.15	1.12
12	15×15×15	3	35	5	0.19	6.36	6.62	1.04
13	15×15×15	3	35	5	0.19	6.36	6.62	1.04
14	15×15×15	3	35	5	0.19	6.36	7.77	1.22
15	15×15×15	3	35	5	0.19	6.36	7.06	1.11
16	15×15×15	3	40	5	0.15	5.75	6.14	1.06
17	15×15×15	3	40	5	0.15	5.75	5.56	0.96
18	15×15×15	3	40	5	0.15	5.75	5.02	0.87
19	15×15×15	3	40	5	0.15	5.75	4.79	0.83
20	15×15×15	3	40	5	0.15	5.75	5.63	0.98
21	15×15×15	5.3	25	2.83	0.05	3.12	3.33	1.06
22	15×15×15	5.3	25	2.83	0.05	3.12	2.37	0.76
23	15×15×15	5.3	25	2.83	0.05	3.12	2.90	0.93
24	15×15×15	5.3	25	2.83	0.05	3.12	2.97	0.95

Continuation of Table 4

1	2	3	4	5	6	7	8	9
25	15×15×15	5.3	30	2.83	0.05	3.12	3.15	1.01
26	15×15×15	5.3	30	2.83	0.05	3.12	3.29	1.05
27	15×15×15	5.3	30	2.83	0.05	3.12	3.11	0.99
28	15×15×15	5.3	30	2.83	0.05	3.12	3.22	1.03
29	15×15×15	5.3	35	2.83	0.11	3.27	4.17	1.06
30	15×15×15	5.3	35	2.83	0.11	3.27	4.31	1.1
31	15×15×15	5.3	35	2.83	0.11	3.27	4.40	1.12
32	15×15×15	5.3	35	2.83	0.11	3.27	4.13	1.05
33	15×15×15	5.3	40	2.83	0.05	3.12	3.27	1.05
34	15×15×15	5.3	40	2.83	0.05	3.12	3.03	0.97
35	15×15×15	5.3	40	2.83	0.05	3.12	3.07	0.98
36	15×15×15	5.3	40	2.83	0.05	3.12	3.14	1.00

According to the data of tables 2-4 and fig. 7, it can be claimed that the results obtained by the proposed method are fairly close to the experimental data: the average arithmetic value of the ratio of theoretical strength to experimental strength is  $m=1.02$  with a coefficient of variation  $\nu=13.16\%$ .

Similarly, a comparative analysis of the theoretical strength calculated according to the standards [17 - 22]

and some author's methods showed much worse statistical indicators: the best convergence is given by the standard method of DSTU [18]  $m=0.78$ ,  $\nu=22.52\%$ , the worst one – by the method of ACI and NZ standards [21, 22],  $m=0.28$ ,  $\nu=30.01\%$ , among the authors' methods the best indicators were of the proposed method by V.G. Kvasha [23]:  $m=0.81$ ,  $\nu=52.32\%$ , the worst indicators – S.K. Niyogi [24]  $m=0.43$ ,  $\nu=16.71\%$ .

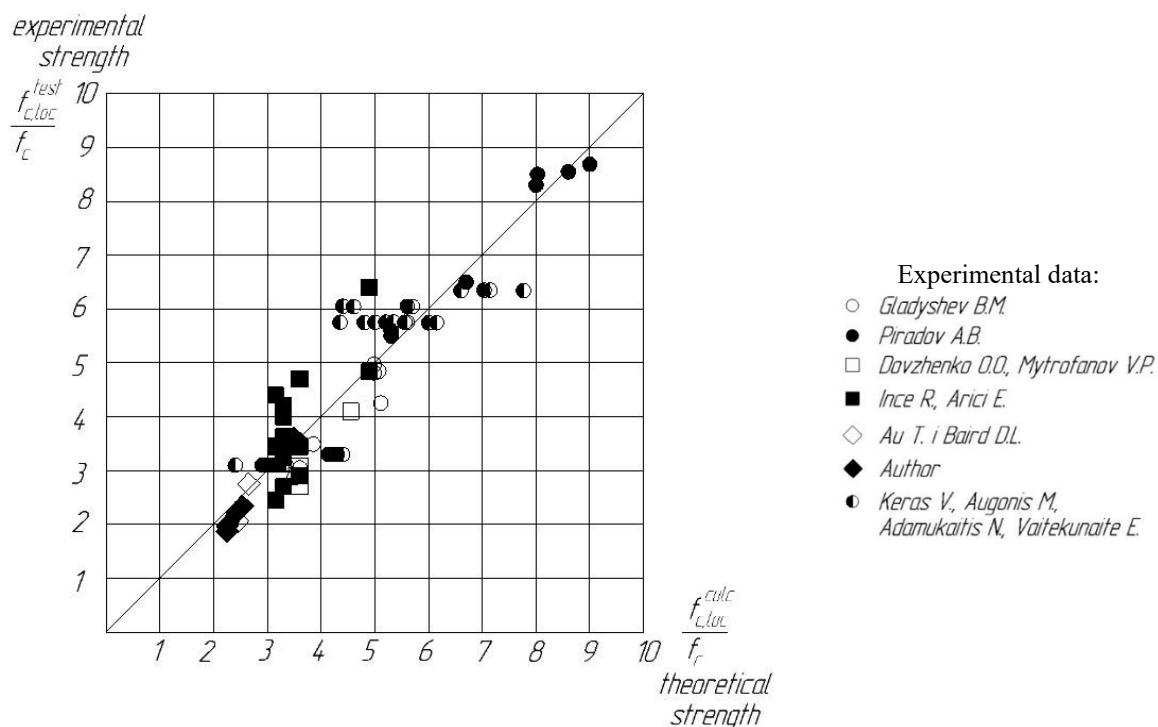


Figure 7 – Comparison of the theoretical strength obtained by the variational method with the experimental one

## Conclusions

The failure character of cubes under one-sided central local compression, which is taken as a basis for theoretical calculations under the conditions of a space stress state, has been confirmed. The use of basalt fiber (length 12 mm, diameter 20  $\mu\text{m}$ , percentage content - 0.2%) does not fundamentally change the failure character of the samples, but it occurs more plastically.

Changing the width of the loading platform (from a square to a strip stamp) affects the magnitude of local compression stresses: within the limits of the experiment, they decrease up to 2 times. The addition of basalt fiber increases the strength characteristics of concrete (by approximately 25% the in compression and tension), reduces the probability of brittle failure and the presence of microcracks in concrete, and ultimately increases the resistance of concrete to local compression.

The statistical indicators of the comparison of the theoretical strength, calculated according to the proposed method, with the experimental one (arithmetic mean value of the theoretical strength to the experimental one  $m = 1.02$  with the coefficient of variation  $\nu = 13.16\%$ ) indicate their sufficient proximity and allow recommending the variational method in the theory of concrete plasticity as a method for calculating the strength of concrete (fiber concrete) under local compression.

## References

1. Kuznietsova I., Dovzhenko O., Pohribnyi V., Usenko I. (2020). Influence of the sizes and the loading platform form on the strength of concrete elements at local compression. *Proceedings of the 2020 Session of the 13th fib International PhD Symposium in Civil Engineering*, 2020, 63-69
2. Кузнєцова І., Довженко О., Погрибний В. (2021). Міцність бетону за місцевого стиснення з урахуванням відношення висоти елемента до розміру ділянки навантаження. *Український журнал будівництва та архітектури*, 5(005), 61-67  
<https://doi.org/10.30838/J.Bpsacea.2312.261021.61.802>
3. Chen W.F., Carson J.L. (1974). Bearing capacity of fiber reinforced concrete. *ACI Special Publication*, SP-44, 209-220
4. Kameswara Rao C.V.S. (1974). Bearing strength of steel fibre reinforced concrete. *Building Science*, 9(4), 263-268
5. Al-Ta'an S.A. (2005). Bearing capacity of steel fibrous concrete. *Al-Rafidain Engineering*, 14(1), 1-11
6. Breitenbücher R. (2014). Experimental and numerical study on the load-bearing behavior of steel fiber reinforced concrete for precast tunnel lining segments under concentrated loads. *Proceedings of Joint ACI-fib International Workshop: Fibre Reinforced Concrete: from Design to Structural Applications*, 431-443
7. Keras V., Augonis M., Adamukaitis N., Vaitekūnaitė E. (2015). Research of local compression concrete reinforced by steel fibres. *Journal of Sustainable Architecture and Civil Engineering*, 2(No. 11, 72-78.  
<https://doi.org/10.5755/j01.sace.11.2.12568>
8. Song F. (2017). Steel fiber reinforced concrete under concentrated load. Dissertation for the degree Doctor of Engineering (Dr.-Ing.). *Ruhr University, Bochum*
9. Новіцький А.Г. (2010). Аспекти застосування базальтового волокна для армування бетонів. *Науково-технічний збірник «Будівельні матеріали, виробництво та санітарна техніка»*, Київ, Вип. 36, 22-26.
10. Кузнєцова І. (2022). Міцність фібробетонних елементів при місцевому стисненні. *Findings of modern engineering research and developments: Scientific monograph*. Riga, Latvia: «Baltija Publishing», 214-232  
<https://doi.org/10.30525/978-9934-26-207-4-8>
11. Гладішев Б.М. (1987). Механічна взаємодія елементів структури та міцність бетону. *Вища школа*.
12. Пірадов А.Б. (1973). Конструктивні властивості легкого бетону та залізобетону. Будвидав.
1. Kuznietsova I., Dovzhenko O., Pohribnyi V., Usenko I. (2020). Influence of the sizes and the loading platform form on the strength of concrete elements at local compression. *Proceedings of the 2020 Session of the 13th fib International PhD Symposium in Civil Engineering*, 2020, 63-69
2. Kuznietsova I., Dovzhenko O., Pohribnyi V. (2021). Strength of concrete under local compression taking into account the relationship of the element height to the size of the loading area. *Ukrainian Journal of Civil Engineering and Architecture*, 5(005), 61-67  
<https://doi.org/10.30838/J.Bpsacea.2312.261021.61.802>
3. Chen W.F., Carson J.L. (1974). Bearing capacity of fiber reinforced concrete. *ACI Special Publication*, SP-44, 209-220
4. Kameswara Rao C.V.S. (1974). Bearing strength of steel fibre reinforced concrete. *Building Science*, 9(4), 263-268
5. Al-Ta'an S.A. (2005). Bearing capacity of steel fibrous concrete. *Al-Rafidain Engineering*, 14(1), 1-11
6. Breitenbücher R. (2014). Experimental and numerical study on the load-bearing behavior of steel fiber reinforced concrete for precast tunnel lining segments under concentrated loads. *Proceedings of Joint ACI-fib International Workshop: Fibre Reinforced Concrete: from Design to Structural Applications*, 431-443
7. Keras V., Augonis M., Adamukaitis N., Vaitekūnaitė E. (2015). Research of local compression concrete reinforced by steel fibres. *Journal of Sustainable Architecture and Civil Engineering*, 2(No. 11, 72-78.  
<https://doi.org/10.5755/j01.sace.11.2.12568>
8. Song F. (2017). Steel fiber reinforced concrete under concentrated load. Dissertation for the degree Doctor of Engineering (Dr.-Ing.). *Ruhr University, Bochum*
9. Novitsky A.G. (2010). Aspects of the use of basalt fiber for concrete reinforcement. *Scientific and technical collection "Construction materials, products and sanitary equipment" Kyiv*, Vol. 36, 22-26
10. Kuznietsova I. (2022). Strength of fiber concrete elements under local compression. *Findings of modern engineering research and developments: Scientific monograph*. Riga, Latvia: «Baltija Publishing», 214-232  
<https://doi.org/10.30525/978-9934-26-207-4-8>
11. Gladyshev B.M. (1987). Mechanical interaction of structural elements and concrete strength. *High school*
12. Piradov A.B. (1973). *Structural properties of lightweight concrete and reinforced concrete*. Stroyizdat

13. Довженко О.А. (1993). Міцність бетонних і залізобетонних елементів при місцевому прикладанні стискувального навантаження: дис. канд. техн. наук: спец. 05.23.01. *Полтава: ПДТУ*.
14. Ince R. (2004). Size effect in bearing strength of concrete cubes. *Construction and Building Materials*, 18, 603-609  
<https://doi.org/10.1016/j.conbuildmat.2004.04.002>
15. Au T. (1960). Bearing capacity of concrete blocks. *Journal of the America Concrete Institute*, 56, 869-880
16. Cao H. (2017). Experimental investigation on the static and impact behaviors of basalt fiber-reinforced concrete. *The Open Civil Engineering Journal*, 11(1), 64-71  
<https://doi.org/10.2174/1874149501711010014>
17. СНиП 2.03.01–84. (1989). *Бетонні та залізобетонні конструкції*. ЦТП Держбуду СРСР.
18. ДСТУ Б 2.6-156:2010 (2011). *Бетонні та залізобетонні конструкції з важкого бетону. Правила проектування*. Київ: Мінрегіонбуд України, Державне підприємство «Укрархбудінформ»
19. NS 3473:1994. (1994). *Concrete structures. Design and detailing rules*
20. DIN 4219-2: 1979. *Leichtbeton und Stahlleichtbeton mit geschlossenem Gefüge; Bemessung und Ausführung*
21. ACI 318-02. (2002). *Building Code Requirements for Structural Concrete and Commentary (318-02R)*. American Concrete Institute, Farmington Hills, Mich
22. NZ 3101.1:2004. (2004). *Concrete Structures Standard: (draft)*
23. Кваша В.Г. (1966). Розрахунок міцності залізобетонних елементів при місцевому стисканні. *Питання сучасного будівництва: Вісник Львівського політехнічного інституту*, 11, 5–14
24. Niyogi S.K. (1975). Concrete bearing strength-support, nix, size effect. *Proc. of Amer. Soc. of Civil Eng. Journ. of the Structural Division*, 100, 1685-1702
13. Dovzhenko O. (1993). Strength of concrete and reinforced concrete elements under local application of a compressive load: dissertation of candidate of technical sciences: spec. 05.23.01. *Poltava: PSTU*
14. Ince R. (2004). Size effect in bearing strength of concrete cubes. *Construction and Building Materials*, 18, 603-609  
<https://doi.org/10.1016/j.conbuildmat.2004.04.002>
15. Au T. (1960). Bearing capacity of concrete blocks. *Journal of the America Concrete Institute*, 56, 869-880
16. Cao H. (2017). Experimental investigation on the static and impact behaviors of basalt fiber-reinforced concrete. *The Open Civil Engineering Journal*, 11(1), 64-71  
<https://doi.org/10.2174/1874149501711010014>
17. SNiP 2.03.01–84. (1989). *Concrete and reinforced concrete structures*. CИTP Gosstroy of the USSR
18. DSTU B 2.6-156:2010 (2011). *Concrete and reinforced concrete structures made of heavy concrete. Design rules*. Kyiv, Ministry of Regional Construction of Ukraine, State enterprise "Ukrakhbudinform"
19. NS 3473:1994. (1994). *Concrete structures. Design and detailing rules*
20. DIN 4219-2: 1979. *Leichtbeton und Stahlleichtbeton mit geschlossenem Gefüge; Bemessung und Ausführung*
21. ACI 318-02. (2002). *Building Code Requirements for Structural Concrete and Commentary (318-02R)*. American Concrete Institute, Farmington Hills, Mich
22. NZ 3101.1:2004. (2004). *Concrete Structures Standard: (draft)*
23. Kvasha V.G. (1966). Calculation of the strength of reinforced concrete elements under local compression. *Issues of modern construction: Bulletin of the Lviv Polytechnic Institute*, 11, 5-14
24. Niyogi S.K. (1975). Concrete bearing strength-support, nix, size effect. *Proc. of Amer. Soc. of Civil Eng. Journ. of the Structural Division*, 100, 1685-1702

UDC 624.154:624.138.2

## The practice of strengthening the base of a slab foundation of a multi-story building with soil-cement elements

Krysan Vladimir<sup>1</sup>, Krysan Vitali<sup>2</sup>, Hasenko Anton<sup>3\*</sup>

<sup>1</sup> «Geoprotect» LLC, Dnipro <https://orcid.org/0000-0001-7497-4615>

<sup>2</sup> «Geobud» LLC, Dnipro <https://orcid.org/0000-0002-9683-7838>

<sup>3</sup> National University «Yuri Kondratyuk Poltava polytechnic» <https://orcid.org/0000-0003-1045-8077>

\*Corresponding author E-mail: [gasentk@gmail.com](mailto:gasentk@gmail.com)

The characteristic geotechnical conditions of modern high-rise construction are considered. The engineering and geological conditions of the site were analyzed. In particular, it was noted that loose soils lie up to a depth of 2.2 m, and below 13.0...13.5 – eolian-deluvial deposits (sandy and silty loams with a deformation modulus of 5...7 MPa). The territory is flooded. An effective constructive-technological solution was tested using the drilling-mixing method of placing soil-cement elements to strengthen the base made of highly compressible clay soils under the slab foundation of a multi-story residential building with a parking lot under the conditions of the existing building. The results of tests of soil cement samples, which were selected during the execution of works, for uniaxial compression are presented.

**Keywords:** engineering and geological element, eolian-deluvial deposits, ground base, vertical soil-cement element, slab foundation, testing of cement soil for uniaxial compression, soil deformation modulus, settlement

## Практика підсилення ґрунтоцементними елементами основи плитного фундаменту багатоповерхового будинку

Крисан В.І.<sup>1</sup>, Крисан В.В.<sup>2</sup>, Гасенко А.В.<sup>3\*</sup>

<sup>1</sup> ТОВ «Геопротект», м. Дніпро

<sup>2</sup> ТОВ «Геобуд», м. Дніпро

<sup>3</sup> Національний університет «Полтавська політехніка імені Юрія Кондратюка»

\*Адреса для листування E-mail: [gasentk@gmail.com](mailto:gasentk@gmail.com)

Розглянуто характерні геотехнічні умови сучасного багатоповерхового будівництва, як-то: наявність у межах масиву ґрунтів з особливими властивостями (слабкі, просадочні, техногенні й ін.); вплив негативних інженерно-геологічних процесів, наприклад підтоплення; суттєва неоднорідність масиву як за його площею, так і глибиною; щільна забудова; значний тиск на основу, що викликає необхідність застосування плитних фундаментів; необхідність улаштування паркінгів у підвальних приміщеннях. Відзначено, що армовані ґрунтоцементними елементами основи розраховують шляхом приведення деформаційних характеристик до необхідних середньозважених величин, а подальші розрахунки виконують вже з урахуванням визначених параметрів як для природних основ. Проаналізовано інженерно-геологічні умови ділянки. Зокрема, відзначено, що до глибини 2,2 м залягають насипні ґрунти, а нижче до 13,0-13,5 – еолово-делювіальні відклади (супіски та суглинки пілуваті з модулем деформації 5-7 МПа). Територію підтоплено. Апробовано ефективне конструктивно-технологічне рішення з використанням бурозмішувального способу влаштування ґрунтоцементних елементів діаметром 600 мм і з шагом 1,35-1,45 м для підсилення основи, складеної сильностисливими глинистими ґрунтами, під плитний фундамент товщиною 600 мм багатоповерхового житлового будинку з паркінгом за умов існуючої забудови. Подано результати випробувань зразків ґрунтоцементу, що були відібрані при виконанні робіт, на одновісьовий стиск. Модуль деформації матеріалу ґрунтоцементних елементів визначали за нормативною методикою. Встановлено, що отримані характеристики армованого ґрунтоцементного масиву забезпечують достатній рівень надійності функціонування будинку. Зафіксовано, що фактичні абсолютні осідання основи плитного фундаменту багатоповерхового житлового будинку та його крен не перевищили їх граничні значення для відповідного типу будівель і споруд.

**Ключові слова:** інженерно-геологічний елемент, еолово-делювіальні відклади, ґрунтова основа, вертикальний ґрунтоцементний елемент, плитний фундамент, випробування ґрунтоцементу на одновісьовий стиск, модуль деформації ґрунту, осідання



## Introduction

From the global experience of modern multi-story urban construction, it is possible to distinguish the following hard but at the same time sufficiently characteristic geotechnical conditions [1-5]:

- the presence within the massif of soils with special properties, for example, weak, subsidence, able to swell, man-made deposits, etc.;
- the influence of negative engineering and geological processes, such as flooding of the territory, suffusion, karst, landslides, etc.;
- significant heterogeneity of the soil massif both in terms of its area and depth;
- significant pressure on the ground base, which often necessitates the use of slab foundations;
- dense construction, including old, surrounding areas, the presence of underground communications and various engineering structures;
- the need to arrange parking lots in the basements of buildings, etc.

Under such conditions during designing, the problem of substantiation of structural and technological solutions of foundations and foundations of buildings is always relevant.

## Review of the research sources and publications

A large number of scientific works are dedicated to solving this problem, but discussions about the most practical and rational way to solve it continue [3-5].

In particular, under the geotechnical conditions listed above, jet grouting and drilling mixing technologies for the installation of soil-cement piles and soil-cement elements (SCE) have proven to be sufficiently effective (especially for reducing the settlements of the foundations of buildings and structures) and at the same time reliable for the creation of pile or reinforced foundations of foundation slabs [6-13].

The materials for creating such piles and elements are the soil of a specific construction site, cement, water, etc. If necessary, a steel reinforcing frame is immersed in a mobile soil-cement mixture, and the same mixture ensures the stability of the walls of the well even in floating. After hardening of the soil-cement mixture, a soil-cement element or pile of the design embedment depth and diameter is formed.

It is also appropriate to note that according to the results of laboratory and field studies of many geotechnicians [6-12], it was established, in particular, that:

- when the cement content increases from 5% to 50%, the mechanical parameters of the soil cement increase linearly, so the strength of the soil cement can be adjusted by the cement content;
- soils with a lower content of clay particles have higher mechanical properties, sands with a small content of clay particles are more suitable for stronger soil cement;
- reinforcement with a steel frame increases the bearing capacity of soil-cement elements and piles by material to a value that exceeds their bearing capacity by the soil.

According to the building standards of design [1], artificial soil bases reinforced with SCE are calculated by

reducing the deformation characteristics to the required weighted average values, and further calculations are performed already considering the specified parameters as for natural bases.

However, the methods of calculating soil bases reinforced with SCE using the spatial version of the finite element method (FEM) using an elastic-plastic model and simulation modeling of the influence of soil heterogeneity parameters and reinforcement elements on the stress-strain state (SSS) of the system "reinforced SCE base – slab" have also been well tested. foundation" [9, 11, 13].

## Definition of unsolved aspects of the problem

So, today geotechnicians have created a number of technologies for arranging soil-cement piles and foundations. All of them have both positive and negative sides, and therefore the important question for practice regarding the areas of rational use of each group of structural and technological solutions with the use of soil-cement methods of arranging piles and artificial foundations in relation to certain complex geotechnical conditions has not yet been resolved.

## Problem statement

Therefore, the goal of this work is to test the structural and technological solution using the drilling-mixing method of arranging soil-cement elements to strengthen the soil base made of highly compressible clay soils under the slab foundation of a multi-story residential building with parking under the conditions of existing surrounding buildings.

## Basic material and results

In one of the micro-districts of the city of Dnipro, the construction of a multi-storey residential building with parking in its basement was planned.

In terms of geostructure, the built-up area is located within the Middle Dnieper Block of the Ukrainian Crystalline Shield. The surface of the crystalline foundation is wavy, uneven, and the depth of occurrence is uneven on a relatively short length of the profile.

The new building is located in the area of old buildings, where there are abandoned underground communications, basements, etc. From the planning surface, the construction site is complicated by the presence of a layer of construction debris with a thickness of up to 2.2 m.

The engineering and geological section of this construction site is shown in Fig. 1.

The physical and mechanical characteristics of the soils of this plot are summarized in Table 1.

Therefore, according to the set of factors specified in regulatory documents, the site belongs to the middle category of the complexity of engineering and geological conditions.

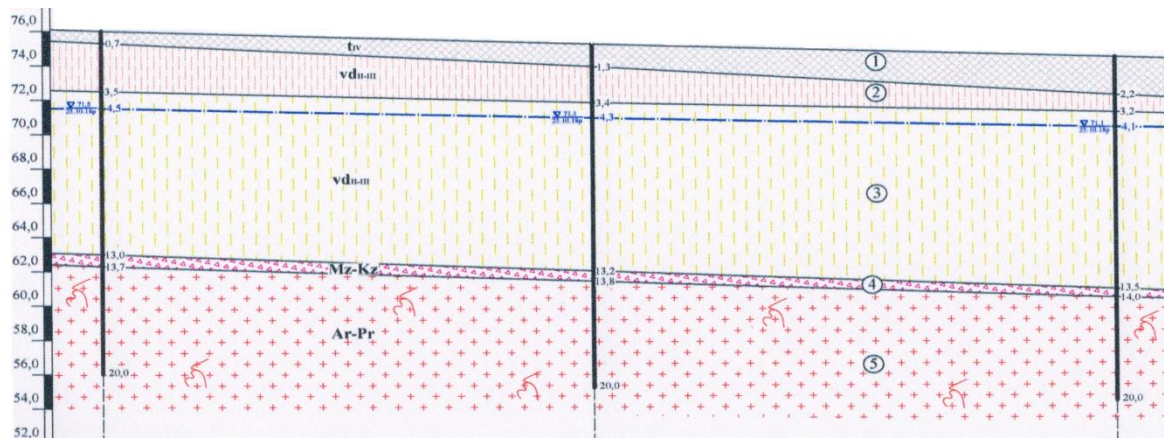


**Figure 1 – Engineering and geological section at the construction site:**

layer 1 – modern man-made deposits (bulky soils, which include a soil-vegetable layer, sand, construction debris, household waste products);  
 layer 2 – loess, dusty, hard sand; layer 3 – loam, light dusty, soft plastic;  
 layer 4 – eluvial deposits, represented by the fragmental zone of the weathering crust of crystalline rocks with sand-clay materials;  
 layer 5 - slightly weathered granites

**Table 1 – Normative and calculated values of indicators of physical and mechanical properties of the soils of the site**

Names and conventional designations of indicators of soil properties		Units of measurement	Layer number		
			2	3	4
Water content, $W$		%	16,7	26,6	12,2
Liquid limit, $W_L$		%	26	29	-
Plastic limit, $W_p$		%	19	20	-
Plasticity index, $I_p$		%	7	9	-
Total unit weight, $\rho$		T/m <sup>3</sup>	1,61	1,82	2,13
Soil elements unit weight, $\rho_s$		T/m <sup>3</sup>	2,67	2,68	2,66
Dry unit weight, $\rho_d$		T/m <sup>3</sup>	1,38	1,44	1,90
Wet unit weight, $\rho_w$		T/m <sup>3</sup>	1,83	-	-
Porosity, $n$		%	48,3	46,3	28,6
Void ratio, $e$		-	0,934	0,862	0,400
Liquidity index, $I_L$		-	< 0	0,73	-
Degree of saturation, $S_r$		-	0,48	0,83	0,81
Granulometric composition	> 10,0 mm	%	-	-	17,7
	10,0-5,0 mm	%	-	-	14,8
	5,0-2,0 mm	%	-	-	15,6
	2,0-1,0 mm	%	-	-	14,1
	1, 0-0,5 mm	%	-	-	10,4
	0,5-0,25 mm	%	-	-	10,3
	0,25-0,1 mm	%	-	-	8,4
	0,1-0,05 mm	%	23,1	21,6	5,6
	0,05-0,01 mm	%	35,9	35,1	2,3
	0,01-0,005 mm	%	34,2	35,2	0,8
	< 0,005 m	%	6,8	8,1	-
Angle of internal friction, $\varphi$ (in a natural state / in a locked state)		degree	21 / 16	18	34
Specific cohesion, $c$ (in a natural state / in a locked state)		kPa	10 / 6	13	45
Deformation modulus, $E$ (in a natural state / in a locked state)		MPa	8 / 5	7	45
Specific gravity of soil, $\gamma_I$ (in a natural state / in a locked state)		kN/m <sup>3</sup>	14,6 / 16,6	16,5	19,3
Angle of internal friction, $\varphi_I$ (in a natural state / in a locked state)		degree	19 / 14	16	32
Specific cohesion, $c_I$ (in a natural state / in a locked state)		kPa	7 / 3	10	42
Specific gravity of soil, $\gamma_{II}$ (in a natural state / in a locked state)		kN/m <sup>3</sup>	15,5 / 17,6	17,5	20,5
Angle of internal friction, $\varphi_{II}$ (in a natural state / in a locked state)		degree	20 / 15	17	33
Specific cohesion, $c_{II}$ (in a natural state / in a locked state)		kPa	8 / 4	11	43

The geological and lithological section from the surface of this site of construction works is represented by the following engineering and geological layers:

- modern man-made deposits – bulk soils, which include a soil-vegetable layer, sand, construction debris, household waste products, etc., with a layer thickness from 0.7 to 2.2 m (layer 1).

From a depth of 0.7–2.2 m, modern man-made sediments are underlain by Middle-Upper Quaternary eolian deluvial sediments, represented by:

- sandy loess, gray, dusty, hard, layer thickness 1.0...2.8 m (layer 2);

- dark brown loam, slightly dusty, soft-plastic, layer thickness 9.5...10.3 m (layer 3);

- from a depth of 13.0 to 13.5 m, there are Mesozoic-Cenozoic eluvial deposits, represented by a fragmental zone of the weathering crust of crystalline rocks with sand-clay materials, with a layer thickness of 0.5...0.7 m (layer 4);

- below the depth of 13.7...14.0 m there are Archean-Proterozoic sediments, represented by slightly weathered granites (layer 5).

In terms of hydrogeology, the site is located within the Ukrainian basin of fractured crystalline waters. The groundwater level was recorded at a depth of 4.1...4.5 m from the site surface. Their replenishment is due to rain and melt water and inflow of water mains. The discharge of the water horizon takes place in the channel of the Dnipro River. Thus, in fact, the territory of this site has already been flooded.

The diagram of the basement of the building in which parking is planned is presented in Fig. 2.

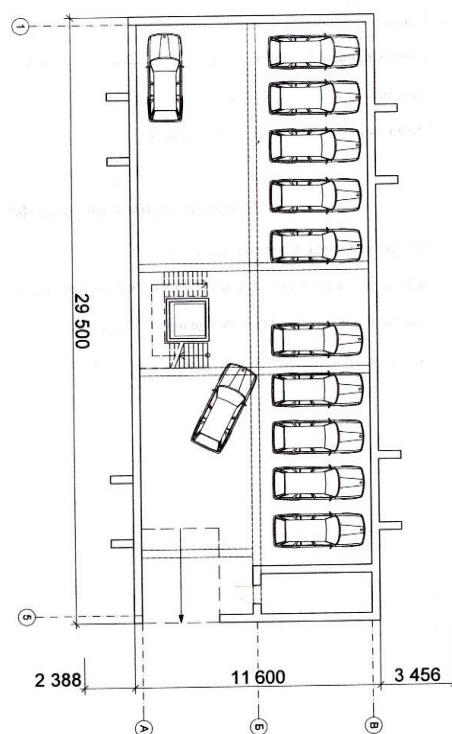


Figure 2 – Scheme of the basement of the building

According to the density of buildings, the physical and mechanical characteristics of the soils of the site and the experience of construction in the surrounding area, it was decided to strengthen the weak soils of the massif with vertical rigid SCE with a diameter of 600 mm and a step of 1.35-1.45 m (Fig. 3 and Fig. 4). According to the conditions of the relief, the deepening of the pit, where the parking lot will be located, is carried out by 3 m at the deepest point, as well as by securing the sides of the pit. The slab foundation is adopted with a plan size of 30500 mm x 12600 mm and a thickness of 600 mm.

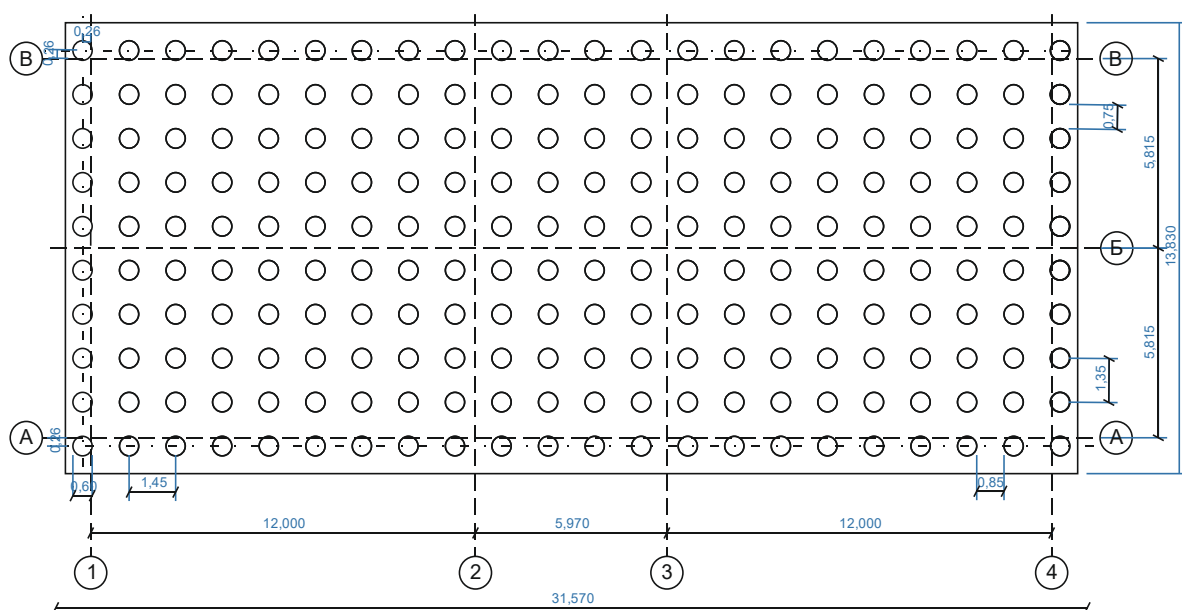


Figure 3 – Scheme of placement of soil-cement elements in the plan



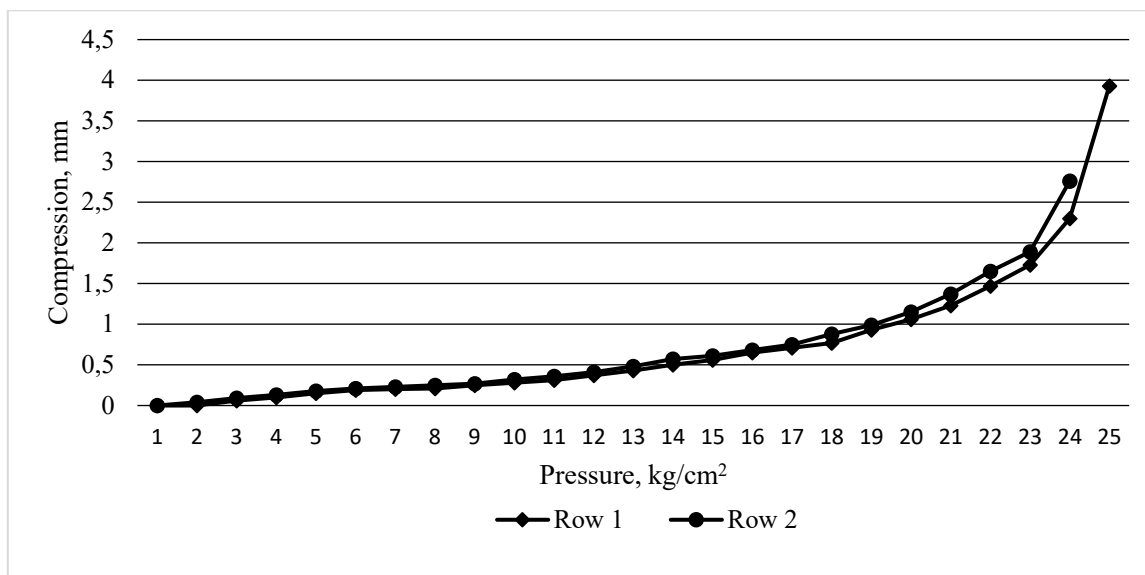


Figure 6 – Graphs of the dependence of the amount of compression of the soil cement sample on the load: row 1 – sample 4, row 2 – sample 6



Figure 7 – General view of a multi-storey residential building with a slab foundation on a soil-cement base after commissioning

### Conclusions

So, the effectiveness of the constructive-technological solution using the drilling-mixing method of arranging soil-cement elements for strengthening the foundation composed of highly compressible clay soils under the slab foundation of a multi-storey residential building with parking was proven on the real site under the conditions of existing surrounding buildings. The characteristics of the reinforced soil-cement massif provide a sufficient level of reliability of the building's functioning.

### References

1. ДБН В.2.1-10: 2018. (2018). *Основи і фундаменти будівель та споруд. Основні положення*. Київ: Міністерство регіонального розвитку, будівництва та житлово-комунального господарства України.
2. ДБН В.1.1-45:2017. (2017). *Будівлі і споруди в складних інженерно-геологічних умовах. Загальні положення*. Київ: Міністерство регіонального розвитку, будівництва та житлово-комунального господарства України.
3. Cheng Y.M., Law C.W., Liu L. (2021). *Analysis, Design and Construction of Foundations*. London: CRC Press.  
<https://doi.org/10.1201/9780429293450>.
4. Briaud J.-L. (2013). *Geotechnical Engineering: Unsaturated and Saturated Soils*. Hoboken: John Wiley & Sons.  
<https://doi.org/10.1002/9781118686195>
5. Katzenbach R., Leppla S., Seip M., Kurze S. (2015). Value Engineering as a basis for safe, optimized and sustainable design of geotechnical structures. *Proc. of the XVI ECSMGE Geotechnical Engineering for Infrastructure and Development*. Edinburg, pp. 601–606.  
<https://doi.org/10.1680/ecsmge.60678.vol2.073>.
1. DBN V.2.1-10: 2018. (2018). *Bases and foundations of buildings and structures. Main principles*. Kyiv: Ministry of Regional Development, Construction, and Housing of Ukraine.
2. DBN V.1.1-45:2017. (2017). *Buildings and structures in difficult engineering and geological conditions. Main principles*. Kyiv: Ministry of Regional Development, Construction, and Housing of Ukraine.
3. Cheng Y.M., Law C.W. & Liu L. (2021). *Analysis, Design and Construction of Foundations*. London: CRC Press.  
<https://doi.org/10.1201/9780429293450>.
4. Briaud J.-L. (2013). *Geotechnical Engineering: Unsaturated and Saturated Soils*. Hoboken: John Wiley & Sons.  
<https://doi.org/10.1002/9781118686195>
5. Katzenbach R., Leppla S., Seip M. & Kurze S. (2015). Value Engineering as a basis for safe, optimized and sustainable design of geotechnical structures. *Proc. of the XVI ECSMGE Geotechnical Engineering for Infrastructure and Development*. Edinburg, pp. 601–606.  
<https://doi.org/10.1680/ecsmge.60678.vol2.073>.



6. Bruce D. (2000). *An introduction to the deep soil mixing methods as used in geotechnical applications*. Report FHWA-RD-99-138. U.S. Dept. of Transportation, Federal Highway Administration.

7. Van Impe W., Verástegui Flores R., Van Impe P. (2005). Deep mixing research results in under water conditions. *Proc. of the 16th Intern. Conf. on Soil Mechanics and Geotechnical Engineering*. Rotterdam: Millpress Science Publishers, V. 3, pp. 1275-1278.

8. Denies N., Lysebetten G.V. (2012). Summary of the short courses of the IS-GI 2012 latest advances in deep mixing *Proc. of the Intern. Symposium on Ground Improvement IS-GI*, pp. 73–123. Brussels.

9. Zotsenko N., Vynnykov Yu., Zotsenko V. (2015). Soil-cement piles by boring-mixing technology. *Energy, energy saving and rational nature use*, pp. 192–253, Oradea University Press.

10. Denies N., Huybrechts N., De Cock F., Lameire B., Maertens J., Vervoort A., Guimond-Barret A. (2015). Thoughts on the durability of the soil mix material. *Proc. of the XVI ECSMGE Geotechnical Engineering for Infrastructure and Development*. Edinburg.

<https://doi.org/10.1680/ecsmge.60678>

11. Kryvosheiev P., Farenyuk G., Tytarenko V., Boyko I., Kornienko M., Zotsenko M., Vynnykov Yu., Siedin V., Shokarev V., Krysan V. (2017). Innovative projects in difficult soil conditions using artificial foundation and base, arranged without soil excavation. *Proc. of 19th Intern. Conf. on Soil Mechanics and Geotechnical Engineering*, pp. 3007–3010. Seoul. ICE Publishing, Seoul.

<https://doi.org/10.1680/geot.1997.47.3.693>.

12. Krysan V., Krysan V. (2018). Jet and jet-mixing grouting. *Academic Journal. Series: Industrial Machine Building, Civil Engineering*. Is. 2(51)'. pp. 68–72. Poltava National Technical Yuri Kondratyuk University.

<https://doi.org/10.26906/znp.2018.51.1294>

13. Vynnykov Yu., Voskobiinyk O., Kharchenko M., Marchenko V. (2017). *Probabilistic analysis of deformed mode of engineering constructions' soil-cement grounds*. Proc. of the 6th Intern. Scientific Conf. "Reliability and Durability of Railway Transport Engineering Structures and Buildings", 116.

<https://doi.org/10.1051/mateconf/201711602038>

14. ДСТУ Б В.2.1-4-96. (1997). *Ґрунти. Методи лабораторного визначення характеристик міцності і деформованості*. Київ: Державний комітет України у справах містобудування та архітектури.

15. ДСТУ-Н Б В.1.2-17:2016. (2017). *Настанова щодо науково-технічного моніторингу будівель та споруд*. Київ: Державний комітет України у справах містобудування та архітектури.

6. Bruce D. (2000). *An introduction to the deep soil mixing methods as used in geotechnical applications*. Report FHWA-RD-99-138. U.S. Dept. of Transportation, Federal Highway Administration.

7. Van Impe W., Verástegui Flores R. & Van Impe P. (2005). Deep mixing research results in under water conditions. *Proc. of the 16th Intern. Conf. on Soil Mechanics and Geotechnical Engineering*. Rotterdam: Millpress Science Publishers, V. 3, pp. 1275-1278.

8. Denies N. & Lysebetten G.V. (2012). Summary of the short courses of the IS-GI 2012 latest advances in deep mixing *Proc. of the Intern. Symposium on Ground Improvement IS-GI*, pp. 73–123. Brussels.

9. Zotsenko N., Vynnykov Yu. & Zotsenko V. (2015). Soil-cement piles by boring-mixing technology. *Energy, energy saving and rational nature use*, pp. 192–253, Oradea University Press.

10. Denies N., Huybrechts N., De Cock F., Lameire B., Maertens J., Vervoort A. & Guimond-Barret A. (2015). Thoughts on the durability of the soil mix material. *Proc. of the XVI ECSMGE Geotechnical Engineering for Infrastructure and Development*. Edinburg.

<https://doi.org/10.1680/ecsmge.60678>

11. Kryvosheiev P., Farenyuk G., Tytarenko V., Boyko I., Kornienko M., Zotsenko M., Vynnykov Yu., Siedin V., Shokarev V. & Krysan V. (2017). Innovative projects in difficult soil conditions using artificial foundation and base, arranged without soil excavation. *Proc. of 19th Intern. Conf. on Soil Mechanics and Geotechnical Engineering*, pp. 3007–3010. Seoul. ICE Publishing, Seoul.

<https://doi.org/10.1680/geot.1997.47.3.693>.

12. Krysan V. & Krysan V. (2018). Jet and jet-mixing grouting. *Academic Journal. Series: Industrial Machine Building, Civil Engineering*. Is. 2(51)'. pp. 68–72. Poltava National Technical Yuri Kondratyuk University.

<https://doi.org/10.26906/znp.2018.51.1294>

13. Vynnykov Yu., Voskobiinyk O., Kharchenko M. & Marchenko V. (2017). *Probabilistic analysis of deformed mode of engineering constructions' soil-cement grounds*. Proc. of the 6th Intern. Scientific Conf. "Reliability and Durability of Railway Transport Engineering Structures and Buildings", 116.

<https://doi.org/10.1051/mateconf/201711602038>

14. DSTU B V.2.1-4-96. (1997). *Soils. Methods of laboratory determination of strength and deformability characteristics*. Kyiv: State Committee of Ukraine for Urban Planning and Architecture.

15. DSTU B V.1.2-17:2016. (2017). *Instruction on scientific and technical monitoring of buildings and structures*. Kyiv: State Committee of Ukraine for Urban Planning and Architecture.

UDC 622.02

## Correlation equation between physical and mechanical properties of sedimentary rocks

Zotsenko Mykola<sup>1</sup>, Vynnykov Yuriy<sup>2\*</sup>, Kharchenko Maksym<sup>3</sup>, Rybalko Marina<sup>4</sup>, Aniskin Aleksey<sup>5</sup>

<sup>1</sup> National University «Yuri Kondratyuk Poltava polytechnic» <https://orcid.org/0000-0003-1886-8898>

<sup>2</sup> National University «Yuri Kondratyuk Poltava polytechnic» <https://orcid.org/0000-0003-2164-9936>

<sup>3</sup> National University «Yuri Kondratyuk Poltava polytechnic» <https://orcid.org/0000-0002-1621-2601>

<sup>4</sup> National University «Yuri Kondratyuk Poltava polytechnic» <https://orcid.org/0009-0002-9813-5175>

<sup>5</sup> University North, Varazdin, Croatia <https://orcid.org/0000-0002-9941-1947>

\*Corresponding author E-mail: [vynnykov@ukr.net](mailto:vynnykov@ukr.net)

The results of parallel experimental studies of the physical and mechanical properties of sedimentary rocks of natural structure, including their penetration tests, are presented. The possibility of establishing empirical equations of the relationship between the physical (soil skeleton density and moisture content) and mechanical (specific resistance to penetration, angle of internal friction, specific adhesion, deformation modulus) characteristics of cohesive (on the example of light dusty loams of loess origin) and non-cohesive (on the example of fine sands, quartz) sedimentary rocks of natural structure is tested. It is noted that such equations are correct only for genetically identical types of sedimentary rocks

**Keywords:** sedimentary rock, penetration, humidity, specific penetration resistance, strength, deformation modulus, relationship

## Кореляційні рівняння між фізичними та механічними властивостями осадових гірських порід

Зоценко М.Л.<sup>1</sup>, Винников Ю.Л.<sup>2\*</sup>, Харченко М.О.<sup>3</sup>, Рибалко М.О.<sup>4</sup>, Аніскін А.<sup>5</sup>

<sup>1, 2, 3, 4</sup> Національний університет «Полтавська політехніка імені Юрія Кондратюка»,

<sup>5</sup> Північний університет, Вараждин, Хорватія

\*Адреса для листування E-mail: [vynnykov@ukr.net](mailto:vynnykov@ukr.net)

The current situation in the field of strength properties evaluation of sedimentary rocks using the express methods, such as penetration test, is analyzed. It is noted that a condition for setting up the relationship between the indicators of the physical state of sedimentary rock (natural moisture content, porosity coefficient) and indicators of mechanical properties (specific resistance to penetration, angle of internal friction, specific adhesion, deformation modulus) is the accumulation of test results to determine the listed characteristics of soils with a relatively constant plasticity number and genetically homogeneous. The results of parallel experimental studies of the physical and mechanical properties of sedimentary rocks of natural structure, including their penetration tests, are presented. The possibility of determining empirical equations of the relationship between physical (soil skeleton density and moisture content) and mechanical (specific resistance to penetration, angle of internal friction, specific adhesion, deformation modulus) characteristics of cohesive (light loams soils of loess origin) and non-cohesive (fine sands of quartz) sedimentary rocks of natural structure has been tested. The values of statistical indicators (coefficient of correlation, variation, and dispersion) of these equations substantiate a rather close relationship between mechanical and physical parameters. The possibility of studying the anisotropic properties of cohesive rocks of natural structure using penetration tests and determining empirical equations of the relationship between their physical and mechanical characteristics is also proved. A practical recommendation is given on the expediency of using correlation equations between the physical and mechanical properties of sedimentary rocks of natural structure to reduce the volume of laboratory tests in determining their mechanical parameters

**Keywords:** sedimentary rock, penetration, humidity, specific penetration resistance, strength, deformation modulus, relationship

## Introduction

The current experience of mining mechanics and geotechnics shows that determining the mechanical characteristics of sedimentary rocks (soils) both in their natural and in their compacted state in sufficient quantities for appropriate calculations, modeling, and design involves significant expenditures of material resources and time [1-3].

Therefore, for example, for preliminary calculations of the foundations of buildings and structures allow determining the values of the parameters of deformability and strength of soils by their physical parameters (for sands, by the particle size distribution and porosity coefficient  $e$ , and for clay rocks, by the index of soil fluidity  $I_L$  and porosity coefficient).

The practice of compiling tables of approximate values of the deformation modulus  $E$ , the angle of internal friction  $\varphi$ , and the specific cohesion  $c$  for sedimentary rocks in a given region has been tested, in particular, for sands depending on the granulometric composition and soil porosity coefficient, and for clay soils depending on their classification indexes,  $I_L$  and  $e$ . An increase in the porosity coefficient  $e$  of a rock, *ceteris paribus*, necessarily causes a decrease in its strength and an increase in its compressibility. Accordingly, an increase in the moisture content  $W$  or the fluidity index  $I_L$  of a clay soil leads to the same result.

It was also found that correlation or even functional dependencies can be obtained between the indicators of mechanical properties and physical state of soils under certain conditions. Thus, it makes sense to use such dependencies to reduce the number of laboratory studies of the mechanical properties of sedimentary rocks.

## Review of the research sources and publications

M. Maslov established the dependence of the decrease in the angle of internal friction and specific cohesion on the decrease in density and increase in soil moisture with its incomplete consolidation. And M. Goldstein et al. for compacted loess loams obtained the dependence of the increasing of specific cohesion at a constant angle of internal friction with an increase in soil density [4].

Of great practical importance is the generalization of 31 empirical equations that relate the unconfined compressive strength and angle of internal friction of sedimentary rocks (sandstone, shale, limestone, and dolomite) to their physical properties (such as velocity, modulus, and porosity) [5]. In particular, it makes sense to use these equations to estimate the strength of a rock based on parameters that can be measured using geophysical logs.

Numerous studies have been devoted to establishing the relationship between the physical and mechanical properties of sedimentary rocks. For example, in 1948, M. Gersevanov showed that there is a linear relationship between the porosity coefficient  $e$  and the logarithm of the ultimate shear resistance  $\lg \tau$ . A similar conclusion was made for compression dependencies [6, 7].

The practice has also confirmed the prospects of the direction of evaluating the strength properties of sedimentary rocks using the express-methods: penetration test and rotary shear test. In particular, the main advantage of penetration tests of homogeneous sedimentary rocks is the condition of invariance of the data obtained, i.e., complete independence from the acting force and the corresponding depth of the cone penetrate, and, taking into account the tip constants, independence from the angle of their tip, etc. The method of penetration studies was recommended to identify the relationship between the indicators of physical state and mechanical characteristics of sedimentary rocks [7-11].

This direction was most fully developed by specialists of the scientific school founded by V. Razorenov, namely: Y. Velykodnyi, G. Zhornik, V. Zabara, M. Zotsenko, I. Skryl, V. Khilobok, V. Shytov, A. Yakovlev, and others [7, 8, 12-15]. In particular, for cohesive sedimentary rocks of a disturbed structure under conditions of their complete water saturation, the following dependence was established on the basis of penetration tests

$$W_i = W_0 - \frac{1}{r_0} \cdot \lg \frac{R_i}{R_0}, \quad (1)$$

where  $W_i$  i  $W_0$  – are the values of the total soil moisture content corresponding to two values of the soil porosity coefficient  $e_i$  and  $e_0$ ;

$R_i$  – specific resistance to penetration of a water-saturated soil with a porosity coefficient  $e_i$ ;

$R_0=1$  – for the accepted dimension  $R_i$  (kPa, MPa) (based on this premise, the value of  $e_0$  is set);

$\frac{1}{r_0}$  – is the angular coefficient of the linear dependence represented in the coordinates “ $W - \lg R$ ”.

Under the conditions of the three-phase state of clay rocks, the degree of their water saturation should be taken into account when establishing the relationship between physical and mechanical parameters. Then the basic equation of the calculation scheme is as follows

$$W_i \cdot L_0 = W - \frac{1}{r_0} \cdot \lg \frac{R_i}{R_0}, \quad (2)$$

where  $L_0$  – is the water saturation function equal to

$$L_0 = 1 + \left( \frac{1}{S_r} - 1 \right) \cdot \frac{\frac{1}{r_0}}{\frac{1}{r}}, \quad (3)$$

where  $\frac{1}{r}$  – angular coefficient of linear dependence for the case  $S_r < 1$  (while  $W_i = \text{const}$ ).

## Definition of unsolved aspects of the problem

However, despite the undoubted advantages of using correlation equations between the physical and mechanical properties of sedimentary rocks to reduce the amount of research on their mechanical parameters, under the conditions of the natural state of these rocks,

there is an additional difficulty in establishing the relationship between their physical and mechanical properties due to the peculiarities of their structure.

The calculation scheme of the relationship is based on the same prerequisites as for soils of disturbed structure. Therefore, further testing of this approach is required for both cohesive and non-cohesive sedimentary rocks of natural structure.

### Problem statement

Therefore, the purpose of this work was to determine empirical equations of the relationship between the physical and mechanical properties of cohesive and non-cohesive sedimentary rocks of natural structure through experimental studies, including penetration tests.

As a criterion for the reliability of such equations, it is advisable to accept the value of the correlation coefficient  $r$  not less than 0.80 (in this case, the relationship between the factors of the equations is considered close).

### Basic material and results

The experimental basis for obtaining empirical relationship equations was parallel laboratory determinations of physical (humidity, plasticity number, dry soil density, porosity coefficient) and mechanical (specific penetration resistance, angle of internal friction, specific cohesion, deformation modulus) characteristics of cohesive (sandy loam, loam, clay) and non-cohesive (sand of various sizes) sedimentary rocks of natural structure.

The methodology of such studies is described in detail in a number of sources [7, 11, 14].

For practical problems of identifying the relationship between the physical and mechanical properties of the three-phase state of sedimentary rock of undisturbed (natural) structure, it is necessary to determine its three indicative features - the free term and two angular coefficients of conditional linear equations.

The general relationship equation in this case is as follows

$$\lg \frac{R}{R_0} = W_R \frac{1}{e_0} + \frac{\rho_w}{\rho_s} \cdot \frac{1 - M_{kpf}}{1/e_0} - W \frac{M_{kpf}}{1/e_0} - \frac{\rho_w}{\rho_d} \cdot \frac{M_{kpf}}{1/e_0}, \quad (4)$$

where  $R$  – specific penetration resistance, MPa;

$R_0 = 1$  MPa;

$W_R$  – moisture content of water-saturated rock at  $R_0 = 1$  MPa;

$$M_{kpf} = 1 - \frac{1/e_0}{1/e};$$

$1/e_0$  та  $1/e$  – are the angular coefficients of the linear equations, respectively, for the case of complete

water saturation of the rock and under the condition of constant moisture;

$\rho_w$  – water density (1 g/cm<sup>3</sup>);

$\rho_d$  – density of dry soil (or soil skeleton).

Experimental studies have shown that in establishing the relationship between the properties of clay rocks, the plasticity number ( $I_p$ ), the mineralogical composition of the clay component, as well as the particle size distribution and mineralogy of the coarse rock component, influence the indicative indicators of equation (4).

A condition for establishing the relationship between the indicators of the physical state of sedimentary rock (natural moisture content  $W$ , porosity coefficient  $e$ ) and indicators of mechanical properties (specific resistance to penetration  $R$ , angle of internal friction  $\varphi$ , specific cohesion  $c$ , deformation modulus  $E$ , etc.) is the accumulation of test results to determine the listed characteristics of soils with a relatively constant plasticity number and genetically homogeneous.

The coefficients of the relationship equations for each set of experimental data are determined by the least squares method with the estimation of the necessary statistical indicators, such as correlation and variation coefficients, as well as errors of direct determinations. Thus, for each type of sedimentary rock, it is possible to establish a number of dependencies of the following form:

$$\lg \frac{R}{R_0} = A_R - B_R \cdot e - C_R \cdot W; \quad (5)$$

$$\lg \frac{E}{E_0} = A_E - B_E \cdot e - C_E \cdot W; \quad (6)$$

$$\lg \frac{c}{c_0} = A_c - B_c \cdot e - C_c \cdot W; \quad (7)$$

$$\lg \frac{\tan \varphi}{\tan \varphi_0} = A_\varphi - B_\varphi \cdot e - C_\varphi \cdot W, \quad (8)$$

where  $R_0, E_0, c_0, \tan \varphi_0$  – values equal to the unit of the selected dimension;

coefficients  $A, B, C$  are functions of soil indicators,

i.e.  $1/e_0, 1/e, W_R$ .

Having equations (5-8) for a certain type of sedimentary rock, the following dependencies were established for it:

$$\lg \frac{E}{E_0} = A_E - \frac{B_E}{B_R} A_R - W \left( C_E - \frac{B_E}{B_R} C_R \right) - \frac{B_E}{B_R} \lg \frac{R}{R_0}; \quad (9)$$

$$\lg \frac{c}{c_0} = A_c - \frac{B_c}{B_R} A_R - W \left( C_c - \frac{B_c}{B_R} C_R \right) - \frac{B_c}{B_R} \lg \frac{R}{R_0}; \quad (10)$$

$$\lg \frac{tg\varphi}{tg\varphi_0} = A_\varphi - \frac{B_\varphi}{B_R} A_R - W \left( C_\varphi - \frac{B_\varphi}{B_R} C_R \right) - \frac{B_\varphi}{B_R} \lg \frac{R}{R_0} \quad (11)$$

For example, the equations of the relationship between the physical and mechanical properties of cohesive sedimentary rocks, in particular, loess loam, light dusty (with plasticity number  $I_p = 0.11$  and rock particle density  $2.71 \text{ g/cm}^3$ ), established at one of the experimental sites in Poltava, are proposed:

$$\lg \frac{R}{R_0} = 1.44 - 1.34e - 6.7 \cdot W; \quad (12)$$

at the correlation coefficient  $r=0.949$ ;

$$\lg \frac{E}{E_0} = 3.0 - 1.84e - 2.8 \cdot W; \quad (13)$$

at the correlation coefficient  $r=0.954$ ;

$$\lg \frac{C}{C_0} = 0.53 - 1.1e - 7.0 \cdot W; \quad (14)$$

at the correlation coefficient  $r=0.890$ ;

$$\lg \frac{tg\varphi}{tg\varphi_0} = 0.4 - 0.31e - 3.17 \cdot W; \quad (15)$$

at the correlation coefficient  $r=0.910$ ;

$$\lg \frac{E}{E_0} = 1.02 + 6.32 \cdot W + 1.37 \cdot \lg \frac{R}{R_0}; \quad (16)$$

$$\lg \frac{C}{C_0} = -0.65 - 1.5 \cdot W + 0.82 \cdot \lg \frac{R}{R_0}; \quad (17)$$

$$\lg \frac{tg\varphi}{tg\varphi_0} = 0.07 - 1.63 \cdot W + 0.23 \cdot \lg \frac{R}{R_0}; \quad (18)$$

Studies have shown that for non-cohesive sedimentary rocks, i.e., sandy soils, it is also possible to establish dependencies of type (4). In accordance with the accepted gradation, sandy soils are divided into air-dry, moist, and water-saturated soils according to the degree of pore filling.

For air-dry sands, with an increase in moisture content from zero, their mechanical properties increase up to a certain moisture content, which depends on their particle size distribution.

This humidity range is  $W = 0 - 0.07$ . Larger values correspond to fine and dusty sands.

At higher moisture content, dependence (4) does not appear.

However, when the sand becomes wet and then water-saturated, an increase in moisture content leads to a slight decrease in the strength characteristics of the sand. However, the intensity of this decrease is much less than that of clay soils.

Below are the obtained equations of the relationship between the physical and mechanical properties of fine quartz sands of the experimental site in Kremenchuk, Poltava region.

$$\lg \frac{R}{R_0} = 0.01 - 1.03e - 1.36 \cdot W; \quad (19)$$

at the correlation coefficient  $r=0.967$ ;

$$\lg \frac{E}{E_0} = 1.65 - 0.68e - 0.35 \cdot W; \quad (20)$$

at the correlation coefficient  $r=0.914$ ;

$$\lg \frac{C}{C_0} = 1.58 + 5.5e - 3.2 \cdot W; \quad (21)$$

at the correlation coefficient  $r=0.890$ ;

$$\lg \frac{tg\varphi}{tg\varphi_0} = 0.321 - 0.58e - 0.467 \cdot W; \quad (22)$$

at the correlation coefficient  $r=0.910$ ;

$$\lg \frac{E}{E_0} = 1.64 + 0.55W + 0.66 \cdot \lg \frac{R}{R_0}; \quad (23)$$

$$\lg \frac{C}{C_0} = -1.53 - 4.06W + 5.34 \cdot \lg \frac{R}{R_0}; \quad (24)$$

$$\lg \frac{tg\varphi}{tg\varphi_0} = 0.315 - 0.3W + 0.56 \cdot \lg \frac{R}{R_0}; \quad (25)$$

It should be noted that the values of the correlation coefficients of all the above empirical equations of the relationship between physical and mechanical properties of both cohesive and non-cohesive sedimentary rocks of natural structure exceed 0.80, i.e., the relationship between the factors of the equations is close.

In our opinion, the equations of the relationship of the form (4) between the physical and mechanical characteristics of loess loam, light dusty (plasticity number  $I_p = 0.09$  - experimental site in Kobeliaky, Poltava region) both in the natural structure and within the compacted zone around the pile in three directions ( $0^\circ$ ,  $45^\circ$ ,  $90^\circ$ ) relative to the horizontal plane are also worthy of attention. They are summarized in Table 1.

In particular, two well-known types of penetrometers (PD-2 and MV-2) and two cones with different angles at the top ( $30^\circ$  and  $17^\circ 40'$ ) were used to study the anisotropic properties of sedimentary rocks. The corresponding methodology of penetration studies, sampling and subsequent laboratory tests is described in monographs [14, 15].

The obtained values of statistical indicators (correlation ( $r > 0.80$ ) and variation ( $v < 0.20$ ) and dispersion ( $D < 0.03$ ) coefficients) for the empirical equations of the form (4), which are also presented in Table 1, indicate a rather close relationship between the mechanical (penetration resistance  $R$ ) and physical (dry density  $\rho_d$  and soil moisture  $w$ ) characteristics in all three experimental directions relative to the horizontal plane for both penetrometers and angles at the top of the cone.

**Table 1 - Equation of the relationship between the physical characteristics of light dusty loam and the results of penetration tests in different directions relative to the horizontal plane**

Penetrometer	Angle at the top of the cone	Direction relative horizontal plan	Empirical equations for determining:		Meaning of statistical indicators		
			$lg R =$	$\rho_d =$	$r$	$v$	$D$
PD-2	30°	0°	2.59 - 4.94 W - 2.88 (1/ $\rho_d$ )	2.88 / (2.59 - 4.94 W - lg R)	0.96	0.09	0.003
		45°	2.12 - 4.12 W - 2.42 (1/ $\rho_d$ )	2.42 / (2.12 - 4.12 W - lg R)	0.92	0.12	0.006
		90°	1.54 - 2.67 W - 1.89 (1/ $\rho_d$ )	1.89 / (1.54 - 2.67 W - lg R)	0.92	0.12	0.005
MV-2	30°	0°	1.98 - 3.93 W - 1.99 (1/ $\rho_d$ )	1.99 / (1.98 - 3.93 W - lg R)	0.87	0.16	0.02
		45°	1.85 - 1.66 W - 2.47 (1/ $\rho_d$ )	2.47 / (1.85 - 1.66 W - lg R)	0.84	0.20	0.03
		90°	1.69 - 0.30 W - 2.62 (1/ $\rho_d$ )	2.62 / (1.69 - 0.30 W - lg R)	0.85	0.16	0.02
	17° 40'	0°	1.23 - 2.11 W - 1.80 (1/ $\rho_d$ )	1.80 / (1.23 - 2.11 W - lg R)	0.85	0.14	0.004
		45°	1.50 - 2.33 W - 2.15 (1/ $\rho_d$ )	2.15 / (1.50 - 2.33 W - lg R)	0.86	0.17	0.005
		90°	1.89 - 1.24 W - 2.98 (1/ $\rho_d$ )	2.98 / (1.89 - 1.24 W - lg R)	0.86	0.16	0.006

## Conclusions

Thus, through parallel experimental studies of the physical and mechanical properties of sedimentary rocks of natural structure, including their penetration tests, the following was established.

1. The possibility of establishing empirical equations of the relationship between the physical (soil dry density and moisture content) and mechanical (specific resistance to penetration, angle of internal friction, specific cohesion, deformation modulus) characteristics of cohesive (for example using the light dusty loams of loess origin) and non-cohesive (for example using the fine sands, quartz) sedimentary rocks of natural structure was tested. The values of the statistical parameters

of the equations indicate a fairly close relationship between mechanical and physical parameters. Such equations are correct for genetically identical types of sedimentary rocks.

2. The possibility of studying the anisotropic properties of cohesive rocks of natural structure using penetration tests and establishing empirical equations of the relationship between their physical and mechanical characteristics has been proved.

3. In practice, the use of correlation equations between the physical and mechanical properties of sedimentary rocks is advisable to reduce the volume of laboratory tests in determining their mechanical parameters..

## References

1. Jaeger J.C/, Cook N.G.W., Zimmerman R. (2007). *Fundamentals of Rock Mechanics*. Wiley-Blackwell.
2. Xing Y., Kulatilake P., Sandbak L. (2019). *Rock Mass Stability Around Underground Excavations in a Mine*. London. CRC Press.  
<https://doi.org/10.1201/9780429343230>
3. Briaud J.-L. (2013). *Geotechnical Engineering: Unsaturated and Saturated Soils*. Wiley.
4. Винников Ю.Л., Харченко М.О., Лопан Р.М., Манжалій С.М. (2017). *Геотехнічні властивості штучних основ для об'єктів гірничо-збагачувального комплексу: Монографія*. Полтава: ПолтНТУ імені Юрія Кондратюка.
5. Chang C., Zoback M.D., Khaksar A. (2006). Empirical relations between rock strength and physical properties in sedimentary rocks. *Journal of Petroleum Science and Engineering*. Vol. 51, Is.3-4, 223-237.  
<https://doi.org/10.1016/j.petrol.2006.01.003>
6. Baligh M.M., Vivatrat V., Ladd C.C. (1980). Cone penetration in soil profiling. *Journal of Geotechnical and Geoenvironmental Engineering*, vol. 106.
1. Jaeger J.C/, Cook N.G.W. & Zimmerman R. (2007) *Fundamentals of Rock Mechanics*. Wiley-Blackwell.
2. Xing Y., Kulatilake P. & Sandbak L. (2019). *Rock Mass Stability Around Underground Excavations in a Mine*. London. CRC Press.  
<https://doi.org/10.1201/9780429343230>
3. Briaud J.-L. (2013). *Geotechnical Engineering: Unsaturated and Saturated Soils*. Wiley.
4. Vynnykov Yu.L., Kharchenko M.O. & Lopan R.M., Manzhaliy S.M. (2017). *Geotechnical properties of foundations for mining complex: Monograph*. Poltava: PolNTU named after Yuri Kondratyuk.
5. Chang C., Zoback M.D. & Khaksar A. (2006). Empirical relations between rock strength and physical properties in sedimentary rocks. *Journal of Petroleum Science and Engineering*. Vol. 51, Is.3-4, 223-237.  
<https://doi.org/10.1016/j.petrol.2006.01.003>
6. Baligh M.M., Vivatrat V. & Ladd C.C. (1980). Cone penetration in soil profiling. *Journal of Geotechnical and Geoenvironmental Engineering*, vol. 106.



7. Разоренов В.Ф. (1980). *Пенетрационные испытания грунтов*. М.: Стройиздат.
8. Zotsenko N., Vynnykov Y. (1999). Rapid Investigation Methods of Soil Properties and Interpretation of their Results for Bridge Foundations Design. *IABSE New Delhi Colloquium reports on "Foundations for Major Bridges: Design and Construction"*. New Delhi, 19-24.
9. Powell J.J.M., Shields C.H., Wallace C.F. (2015). Liquid Limit testing – only use the Cone Penetrometer! *Proc. of the XVI ECSMGE Geotechnical Eng. for Infrastructure and Development*. Edinburg, 3305-3310.  
<https://doi:10.1680/ecsmge.60678>
10. Uhlig M., Herle I. (2015). Advanced analysis of cone penetration tests. *Proc. of the XVI ECSMGE Geotechnical Eng. for Infrastructure and Development*. Edinburg, 3073-3078.  
<https://doi:10.1680/ecsmge.60678>
11. Zotsenko M., Vynnykov Yu., Kharchenko M., Matyash O., Vovk M. (2023). Improvement of the investigation of physical and mechanical characteristics of sedimentary rocks by express methods. *Key trends of integrated innovation-driven scientific and technological development of mining regions*. Petroșani, Romania: UNIVERSITAS Publishing, 264-279.  
<https://ep3.nuwm.edu.ua/id/eprint/25919>
12. Zotsenko M., Vynnykov Y., Yakovlev A. (2010). Modern practice of determination of strength characteristics of cohesive soils by penetration methods. *Proc. of XIV<sup>th</sup> Danube – European Conf. on Geotechnical Eng.* Bratislava: Slovak University of Technology. 245-253.
13. Зоценко М.Л. (2005). Використання «хвостів» Полтавського ГЗК при влаштуванні земляних споруд. *Світ геотехніки*. №4, 7-11.
14. Зоценко М.Л., Винников Ю.Л. (2019). *Фундаменти, що споруджуються без виймання ґрунту: Монографія*. Полтава: ПолтНТУ імені Юрія Кондратюка.
15. Vynnykov Yu.L., Aniskin A. (2019). *Practical problems of anisotropic soil mechanics: Monograph*. Varazdin: University North, Croatia.

7. Razorenov V.F. (1980). Soil penetration testing. M.: Stroyizdat.
8. Zotsenko N. & Vynnykov Y. (1999). Rapid Investigation Methods of Soil Properties and Interpretation of their Results for Bridge Foundations Design. *IABSE New Delhi Colloquium reports on "Foundations for Major Bridges: Design and Construction"*. New Delhi, 19-24.
9. Powell J.J.M., Shields C.H. & Wallace C.F. (2015). Liquid Limit testing – only use the Cone Penetrometer! *Proc. of the XVI ECSMGE Geotechnical Eng. for Infrastructure and Development*. Edinburg, 3305-3310.  
<https://doi:10.1680/ecsmge.60678>
10. Uhlig M. & Herle I. (2015). Advanced analysis of cone penetration tests. *Proc. of the XVI ECSMGE Geotechnical Eng. for Infrastructure and Development*. Edinburg, 3073-3078.  
<https://doi:10.1680/ecsmge.60678>
11. Zotsenko M., Vynnykov Yu., Kharchenko M., Matyash O. & Vovk M. (2023). Improvement of the investigation of physical and mechanical characteristics of sedimentary rocks by express methods. *Key trends of integrated innovation-driven scientific and technological development of mining regions*. Petroșani, Romania: UNIVERSITAS Publishing, 264-279.  
<https://ep3.nuwm.edu.ua/id/eprint/25919>
12. Zotsenko M., Vynnykov Y. & Yakovlev A. (2010). Modern practice of determination of strength characteristics of cohesive soils by penetration methods. *Proc. of XIV<sup>th</sup> Danube – European Conf. on Geotechnical Eng.* Bratislava: Slovak University of Technology. 245-253.
13. Zotsenko M.L. (2005). The use of "tails" of the Poltava mining and beneficiation plant in the construction of earthen structures. *The world of geotechnics*. N4, 7-11.
14. Zotsenko M. & Vynnykov Yu. (2019). *Foundations, Arranged without Soil Excavation: Monograph*. Poltava: PolNTU named after Yuri Kondratyuk, 2019.
15. Vynnykov Yu.L. & Aniskin A. (2019). *Practical problems of anisotropic soil mechanics: Monograph*. Varazdin: University North, Croatia.

UDC 624.13

## Dependence of the plastic rocks properties on the pressure change in the well

Mykhailovska Olena<sup>1\*</sup>, Solovyov Veniamin<sup>2</sup>

<sup>1</sup> Poltava National Technical Yuri Kondratyuk University <https://orcid.org/0000-0001-7451-3210>

<sup>2</sup> Poltava National Technical Yuri Kondratyuk University <https://orcid.org/0000-0002-0805-9661>

\*Corresponding author: [ab.Mykhailovska\\_OV@nupp.edu.ua](mailto:ab.Mykhailovska_OV@nupp.edu.ua)

Experimental studies of changes in rock properties depending on the pressure in the well and in the massif of the plastic layer at different distances from the well over time were carried out. The function demonstrates the power dependence of the pressure ratio at the moment of time on the geostatic pressure. After sealing the well, the pressure in the massif of the plastic formation increases in the near-well zone and decreases in the peripheral zone. Over time, the pressure in the massif of the plastic layer is equalized over the entire area of the layer. Pressure changes in a plastic rock have an impulse character. Thermal (residual) stresses affect the destruction of rocks during drilling with an increase in the depth of the well

**Keywords:** plastic rock, rheology, stress-strain state, trunk, well

## Залежність властивостей пластичних гірських порід від зміни тиску в свердловині

Михайловська О.В.<sup>1\*</sup>, Соловйов В.В.<sup>2</sup>

<sup>1,2</sup> Полтавський національний технічний університет імені Юрія Кондратюка

\*Адреса для листування: [ab.Mykhailovska\\_OV@nupp.edu.ua](mailto:ab.Mykhailovska_OV@nupp.edu.ua)

В розрізах родовищ Дніпро-Донецької западини виявлені потужні товщі солі у пермських та девонських відкладах. За даними спостережень, такі деформації мають нестійкий характер і можуть проявлятися в будь-який момент експлуатації вертикального ствола. В статті досліджено поведінку гірського масиву з вмістом високопластичних порід на моделі. В якості моделі масиву високопластичної породи був використаний парафін, що обмежувався по горизонталі трубою великого діаметра, а по вертикалі – жорсткими плитами. В якості моделі свердловини була використана гумова трубка, заповнена рідиною. Тиск на модель текучого пласта створювався гідравлічним пресом, який автоматично підтримував заданий тиск протягом всього експерименту. Для вимірювання тиску в моделі свердловини і гірського масиву були використані напівпровідникові датчики об'ємного тиску, що були установлені на різній відстані від осі свердловини. До початку експерименту модель гірського масиву із умовною свердловиною видержувалась до вирівнювання тиску у всіх точках об'єму. Потім тиск в моделі свердловини зменшували до атмосферного і свердловину герметизували. Показники датчиків тиску реєструвались протягом всього експерименту. В результаті експерименту встановлено, що інтенсивність падіння тиску зменшується від свердловини. При розкритті свердловиною пластичного пласта спостерігається інверсія тиску подалі від свердловини. Встановлено, що у першому наближенні для визначення тиску соляних та глинистих відкладень на кріплення в будь-який момент часу можна використати апроксимуючу функцію. Яка демонструє степеневу залежність відношення тиску на момент часу до геостатичного тиску. Після герметизації свердловини тиск в масиві пластичного пласта зростає в при-свердловинній зоні і зменшується в периферійній і з часом вирівнюється по всій площі. Зміни тиску в пластичній породі мають імпульсний характер. Термічні напруження, які мають назву залишкових, впливають на руйнування гірських порід під час буріння зі збільшенням глибини свердловини

**Ключові слова:** напружено-деформований стан, реологічні властивості, свердловина, стовбур, пластична порода.



## Introduction

Oil and gas fields located in the Dnipro-Donetsk Basin are characterized by significant depths of occurrence, high thermobaric gradients, differences in formation pressures along the section, multicomponent formation fluids, etc.

Thick strata of salt in Permian and Devonian sediments were found in sections of deposits in the Dnipro-Donetsk Basin. In tectonic terms, the deposits have salt-dome structures. In the cross-section of the sedimentary stratum, sub-saline and supra-saline complexes, separated by a saline complex, are found in the deposits of the Poltava region [1]. Terrigenous sediments occur in practically all sedimentary rocks of the Dnipro-Donetsk Basin.

The main problem of drilling is related to ensuring the stability of well walls in clay and salt rocks. It is necessary to pay attention to the prevention of spalling and collapse of the walls of the well. So it is necessary to pay sufficient attention to research and prediction of stresses acting on the wellbore. Ensuring the integrity of well walls during their drilling is one of the primary tasks of improving the quality and increasing the technical and economic indicators of their construction. From the practice of drilling directional wells, the costs of combating complications are on average 20-25% of the calendar time of drilling. The loss of stability of clay or salt rocks is understood as falling out, crumbling, collapsing, narrowing of the trunk, cavernous and gutter formations. These phenomena lead to the seizure of the drill string and a significant increase in the material costs of materials and production time for their elimination [2].

Most of the complications that exist in wells are the result of a certain stressed state of the massif. Therefore, it is necessary to analyze the causes of complications, collapses, deformations of well walls.

In real conditions of occurrence, rocks are in a state of comprehensive compression. After opening the formation by drilling, a local force field is formed on the perimeter of the wellbore. This leads to various deformations on the well walls: from plastic flow to brittle failure. The nature of these deformations is determined by the properties of the rock and the magnitude of the rock pressure. The conditions of formation, composition and degree of lithification of rocks cause a wide range of changes in their properties.

For example, plastic and water-sensitive rocks behave as highly plastic bodies. Thus, the presence of such rocks in the wellbore can cause narrowing of the wellbore. However, under the influence of temperature and pressure, new rigid chemical bonds between its structural elements arise in such rocks. The nature of destruction of such rocks is already brittle or plastic-brittle. They are capable of cracking and crumbling in deep conditions when opened by drilling.

At the stage of drilling and operation of wells, it is important to determine the change in the volumetric stress state of the rock massif containing plastic rocks. Because it is quite difficult to directly measure the pressure in the massif of rocks. The authors analyzed individual cases of assessing the stability of wellbore shafts.

For example, in the works of A.I. Riznychuk, I.I. Chudyk, the factors affecting the stability of the well walls in conditions prone to landslides and rock-falls were analyzed [2,3].

R. V. Rachkevych also analyzed a special case of the stress-deformed state of the drill string in the curved part of the well. The analysis was carried out when a trough or cavern formed on the wall of the well. Additionally, the force of interaction of the drill string with the bottom of the chute or cavern was determined [6].

Often the destruction of rocks occurs outside the zone of elastic deformations - in the zone of the plastic state. This is characterized by the appearance of significant residual deformations in the rocks. Evaluation of their stability in the wellbore is reflected by the dependence of K.F. Puks. In the initial data, the diameter of the wellbore and the rock-crushing tool, the volumes of the wells are known [2].

Plastic deformations occur as a result of displacement of dislocations. They start from places of structural disruption and spread along the sliding plane gradually, without disturbing the crystalline structure and integrity of the substance.

Along with this, mutual movement of rather large volumes, compression, crumpling, etc. (quasi-plasticity) is observed in the rocks. The behavior of a mountain massif under the action of forces can be described by various models: mechanical model - elastic (Hooke's body); mechanical model, which is a heavy body lying on a horizontal plane and connected to a spring (Saint-Venant body).

The work of E.M. Baranovsky [4,5] is devoted to solving the problem of wellbore stability. The stress-strain state of wellbores was quite difficult to describe by analytical equations.

An analytical model for the characterization of salt massifs was also proposed by M. Todores (2020) based on octahedral geomechanical parameters. It was verified both by laboratory studies using modeling tools and by on-site measurements [7].

Hadiseh Mansouri, Rassoul Ajalloeian (2018) determined from the results of experiments that the axial peak stress, strain and modulus of elasticity gradually increase with the increase of strain rate. It was established that the model of viscoelastic creep of Burgers agrees quite well with the experimental data on creep. [8].

## Definition of unsolved aspects of the problem

A new deformation criterion of the compressive strength of samples of salt rocks was also proposed. The limiting principal deformation is a function of the stress parameter in the form of the ratio of hydrostatic

## Review of the research sources and publications

pressure to stress intensity [9]. That is, it was established that the deformation will depend on the hydrostatic pressure. This needs to be verified in natural or laboratory conditions.

Most rocks belong to strengthening bodies. In order to maintain plastic deformations in them, it is necessary to increase the tension. At the same time, the growth of stresses occurs at a decreasing rate. This behavior of the rock is modeled by a combination of an ideally elastic Hooke body and an ideally viscous Newtonian body (a piston with holes moving in a cylinder filled with a viscous liquid). When these bodies are connected in parallel, the model of the Kelvin - Voigt body is obtained, when it is connected in series - the Maxwell body. However, these models describe the stress-strain state of rocks without taking into account the rheological properties of the rock and the corresponding thermobaric conditions of the massif.

### Problem statement

The purpose of the research is to conduct experimental studies of changes in rock properties depending on the pressure in the well and in the massif of the plastic reservoir at different distances from the well over time.

### Basic material and results

The plasticity of rocks increases with increasing temperature and lateral pressure. However, the number of dislocations in rocks does not change. At the same time, their mobility increases significantly, which contributes to plastic deformation. Rocks that behave as

brittle under normal conditions acquire pronounced plastic properties at elevated pressures and temperatures.

This is important when developing deposits at great depths. For example, the ability to plastic deformation in limestones and siltstones appears already at all-round pressures of about 50 MPa, in anhydrites - about 100 MPa. The construction of vertical shafts in salt rocks coincides with the spread of deformations of the rock contour over a long period of time. As the data of natural observations show, such deformations have an unstable character [5, 6] and can appear at any moment of operation of a vertical shaft. At shallow depths (up to 200 m), the well bore, drilled through salt rocks, was not secured. However, with an increase in the depth of salt deposits (more than 300 m), the "creeping effect" of rock salt begins to manifest itself actively.

This phenomenon occurs at tangential stresses on the trunk contour of 10-15 MPa according to research data. At great depths (1000 m and more), the development of rheological processes is accompanied by significant deformations of the rock contour of vertical shafts. Also, the load on hard fasteners in the long term increases to 20 MPa or more.

Therefore, it is necessary to investigate the behavior of the mountain massif with the content of highly plastic rocks on the model. As a model of the massif of highly plastic rock, paraffin was used, which was limited horizontally by a large-diameter pipe, and vertically by hard plates.

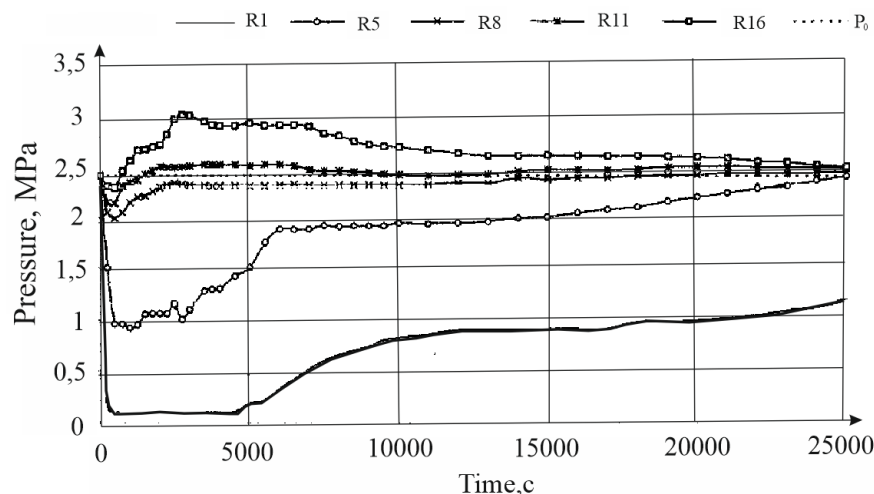


**Figure 1 – Graphs of pressure changes in the well model and at different distances from the axis (R1-R16) of the well in the model:  $P_0$  is the initial pressure in the model, MPa; R - the radius of the wells**

A rubber tube filled with liquid was used as a well model. The pressure on the model of the fluidized bed was created by a hydraulic press, which automatically maintained the set pressure throughout the experiment. Semiconductor volumetric pressure sensors were used to measure the pressure in the model of the well and the rock massif. They were installed at different distances from the axis of the well.

Before the start of the experiment, the model of the mountain massif with a conventional well was maintained until the pressure equalized at all points of the volume. Then the pressure in the well model was reduced to atmospheric and the well was sealed.

The readings of the pressure sensors were recorded throughout the experiment. In fig. 1 shows graphs of pressure changes in the well and in the massif of the

plastic layer in the "pressure-time" coordinates at different distances from the axis of the well.

The readings of the pressure sensors were recorded throughout the experiment. In fig. 1 shows graphs of pressure changes in the well and in the massif of the plastic reservoir in the pressure-time coordinates at different distances from the axis of the well.

From fig. 1 shows that when the pressure in the well model decreases (corresponding to the moment when the well opens the mass of plastic rocks), the pressure decreases over the entire area of the mass. At the same time, when the point is far from the axis of the well, the magnitude of the pressure drop in the massif decreases [10-14].

After closing the well, the nature of the pressure change in the massif at different distances from the axis of the well is significantly different. In the well and at a distance of two radii of the well, the pressure remains unchanged. At a distance of five radii, stabilization and a slight decrease in pressure are observed first, and then an increase. At a distance of more than 8R from the axis of the well, the pressure increases and at a distance of more than 11R it exceeds the set pressure. Over time, the dynamics change: the pressure on the peripheral sensors begins to fall, and in the well and near-well zone - to increase. Fig. 2 shows graphs of pressure

changes in the well and in the massif of the plastic layer in the "pressure-distance" coordinates from the axis of the well after sealing the well, which corresponds to the state of the massif after fixing the well.

It can be seen from Fig. 2 that in this experiment the maximum pressure changes in the massif of the plastic layer occur at a distance from the axis of the well to eight values of its radii. In the zone of distance along the formation, which is equal to the distance of eight to eleven well radii, pressure changes are insignificant.

The analysis of the graphs shows that the pressure changes in the massif of the plastic reservoir model have a pulse character. It is obvious that this character is due to the periodic accumulation of energy in a certain zone of the massif and the shift towards the well [11].

When assessing the stress-strain state of plastic rocks around the well, it is necessary to take into account the thermal conditions of the rocks. The difficulty of evaluating the resistance of rocks to thermal effects around the borehole lies primarily in the fact that it depends on the coefficient of linear temperature expansion of the material, its modulus of elasticity, thermal conductivity. And also from the regularity of the distribution of the temperature field, the state of the surface, the properties of the surrounding deposit, etc.

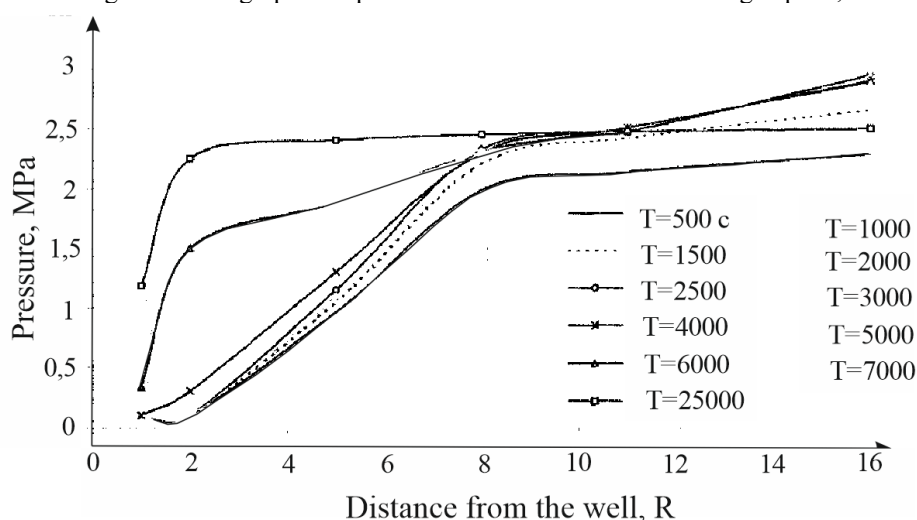


**Figure 2 – Graphs of pressure changes in the well model at sharp time intervals after sealing the well, depending on the distance of the sensor from the axis of the well [8].**

For example, if a body is heated unevenly in volume, then the temperature deformations of individual elements corresponding to such heating become limited due to the fact that neighboring elements interfere with free deformations. At the same time, stresses will arise, the distribution of which will depend on the regularity of the temperature distribution.

If the material is homogeneous and the temperature is the same throughout the volume of the body, then temperature deformations inside the body are not limited by anything and do not cause temperature stresses. Temperature stresses can occur only when the material is heterogeneous in temperature coefficients of volume

expansion or due to uneven distribution of the temperature field by volume. Also, temperature stresses can occur under the condition of external limitation of temperature deformations on the surface of the body.

Temperature stresses are always given by temperature deformation. Therefore, uneven temperature fields, unlike uniform ones, can be accompanied by a change in temperature stresses.

Most often, rocks consist of mineral particles cemented together with different physical and thermal characteristics. It is obvious that even with uniform temperature fields, there are always volumetric temperature stresses inside rock layers. Temperature stresses

are caused not only by temperature, but also by heterogeneity of structural components and anisotropy of their thermal expansion and other properties at the joints of grains or blocks of grains that make up the micro- and macrovolumes of the body. In particular, temperature stresses can affect the stress-strain state of the massif when drilling ductile rocks, which must be taken into account [13].

With a certain heterogeneity of plastic rocks under the action of a uniform temperature field, temperature stresses will arise due to the difference in physical and thermal characteristics of non-homogeneous materials. Such local thermal stresses affect the destruction of rocks during drilling with an increase in the depth of the well [12].

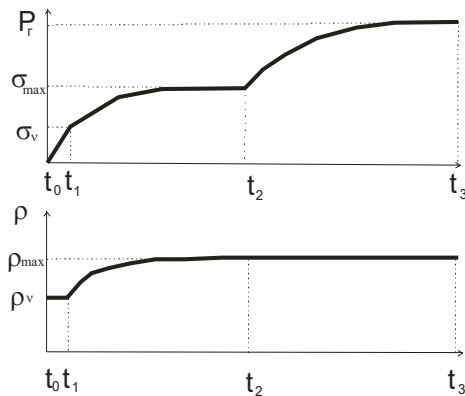


**Figure 3 – The model of the development of pressure on a column of casing pipes in an inelastically deformed loosened compacted near-stem rock massif [14]**

The model of the development of pressure on a column of inelastically deformed rock mass (salt, clay) loosened around the well is shown in Fig. 3. In fig. 3.  $t_0 - t_1$  – time period from the end of the column descent to the level of solidification of the plugging material in the annular space in the interval of fluid rocks;  $t_1 - t_2$  – the time during which the loosened volume of the rock is compressed to the volume with the initial density before the formation is opened;  $t_2$  is the moment of time when the pressure on the column reaches  $\sigma_c$  of the temporary resistance to uniaxial compression of the rock;  $t_2 - t_3$  – time of change of mountain pressure from  $\sigma_c$  to geostatic pressure  $P_g$ .

The task of predicting column pressures is to determine the rock pressure at any point in time. Pressure, time and its changes remain unknown. But the experimental dependences of the temporary resistance to uniaxial compression on the strain rate  $\sigma_v = f(v)$  on the density are known  $\sigma = f(\rho)$  and density from the rate of deformation  $\rho = f(v)$  for salt rocks. The physical mechanism of the processes and variable power capabilities of the rock in the zone of reduced stresses is important. Stresses arise due to the pressure behind the zone of reduced pressures.

In the absence of direct instrumental measurements of column pressure in salt rocks, dynamometric measurements of column pressure in creeping clays were used to predict the pressure-time relationship. The pressure was determined as the average of 11 pressure sensors.

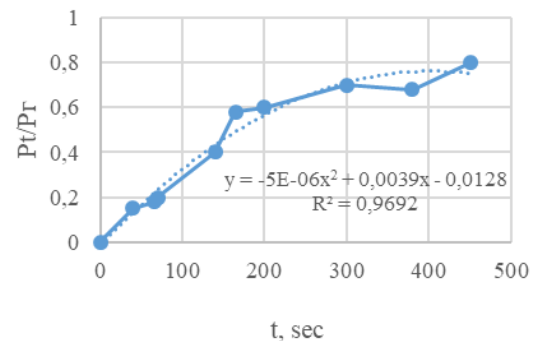


**Figure 4 – Geostatic pressure - 2.633 MPa, depth - 142.6 m, average density of overlying rocks - 1847 kg/m<sup>3</sup>, test time - 658 days**

As a first approximation, the approximating function can be used to determine the pressure of salt and clay deposits on fasteners at any moment in time:

$$P_t/P_r = -5 \cdot 10^{-6} t^2 + 0,0039 t - 0,0128, \quad (1)$$

where  $P_t$  is the pressure at this moment in time, MPa;  $P_g$  - geostatic pressure, MPa;  $t$  - time, days [Fig. 4].

## Conclusions

During the conducted research, it was found that the opening of the plastic layer of the well is accompanied by a decrease in pressure in the layer. At the same time, the intensity of the pressure drop decreases from the well. When a plastic layer is opened by a well, a pressure inversion is observed at a distance from the well. After sealing the well, the pressure in the massif of the plastic layer increases in the near-well zone and decreases in the peripheral zone and eventually equalizes over the entire area. Pressure changes in a plastic rock have an impulse character. Thermal stresses, which are called residual, affect the destruction of rocks during drilling with an increase in the depth of the well.

When developing the methodology, the results of own experimental research, geophysical research in wells, instrumental measurements of pressure development over time on fasteners in mine construction and literary sources were used.

The methodology needs clarification, which consists in the need for direct instrumental measurements of the pressure of salt rocks on the column. It is also necessary to specify the measurements of the density of salts in the well, for example, using "gamma-gamma" logging. It is also necessary to carry out laboratory experiments on finding compression curves at low pressures. This will make it possible to specify the time  $t_3$ .



## References

1. Бейзик О., Різничук А., Гордійчук М., Ковердій Б. (2022). Підвищення якості розкриття соленосних відкладів в умовах високих температур. *Grail of Science*, 17, 213-217  
<https://doi.org/10.36074/grail-of-science.22.07.2022>
2. Різничук А.І. (2020) Удосконалення технології запобігання руйнуванню стінок скерованих свердловин: дис. ... канд. техн. наук: спец. 05.15.10 "Буріння свердловин" Івано-Франківськ
3. Чудик І.І., Фем'як Я.М., Різничук А.І., Васько І.С., Юрич Л.Р. (2019). Експериментальні дослідження механічних властивостей гірських порід в термобаричних умовах. *Розвідка та розробка нафтових і газових родовищ*, 3(72), 32-41
4. Барановський Е.М., Мойсішин В.М. (2006). Головне завдання геомеханіки у вирішенні проблем глибокого буріння. *Розвідка та розробка нафтових і газових родовищ*, 4, 5-9
5. Барановський Е.М. (2006). Комбіноване руйнування гірських порід при бурінні глибоких свердловин. *Науковий вісник Івано-Франківського національного технічного університету нафти і газу*, 1, 26-30
6. Рачкевич Р.В., Величкович А.С., Гриців В.В., Козлов А.А. (2012). Напружено-деформований стан бурильної колони у криволінійному стовбурі свердловини із виробками стінок. *Національний гірничий університет. Збірник наукових праць*, 37, 124-134
7. Toderas M. (2020). The octahedral concept and cubic triaxiality in assessment of secondary stress state. *Mining of Mineral Deposits*, 14 (1), 81-90  
<https://doi.org/10.33271/mining14.01.081>
8. Mansouri H., Ajalloeian R. (2018). Mechanical behavior of salt rock under uniaxial compression and creep tests. *International Journal of Rock Mechanics and Mining Sciences*, 110, 19-27  
<https://doi.org/10.1016/j.ijrmms.2018.07.006>
9. Aptukov V.N. (2016). Deformation criterion of salt rock failure. *Journal of Mining Science*, 52(3), 448-453  
<https://doi.org/10.1134/S1062739116030645>
10. Світалька П.І., Соловйов В.В., Бандуріна О.В. (2013). Методика та результати визначення міцності соляних порід залежно від швидкості непружної деформації. *Збірник наукових праць. Галузеве машинобудування, будівництво*, 4(2), 175-181
11. Дуда З.М., Світалька П.І. (2000). Результати дослідження об'ємно-напруженого стану навіколосвердловинного масиву з вмістом пластичних порід. *Нафта і газ України: зб. наук. праць. VI Міжнар. наук.-практ. конф. «Нафта і газ України»*, 2, 44-46
12. Мочернюк Д.Ю., Чернов В.Б. (2000). Оцінка впливу температури на зміну стану гірських порід навколо стовбура свердловини. *Нафта і газ України: зб. наук. праць. VI Міжнар. наук.-практ. конф. «Нафта і газ України – 2000»*, 2, 43-44
13. Світалька П.І., Соловйов В.В. (2000). Вибір шляху встановлення залежності тиск – час при невідомому об'ємнонапруженому стані, непружнодеформованому навколо свердловинного масиву, із змінними в часі міцнісними властивостями порід. *Нафта і газ України: зб. наук. праць. VI Міжнар. наук.-практ. конф. «Нафта і газ України – 2000»*, 2, 91-92
14. Світалька П.І., Соловйов В.В. Прогнозування величини тиску на обсадну колону при розкритті солей і глин. *Нафта і газ України: зб. наук. праць. VI Міжнар. наук.-практ. конф. «Нафта і газ України – 2000»*, 2, 67-70
1. Beyzyk O, Riznychuk A, Gordiychuk M, Koverdiy B (2022). Improving the quality of the opening of salt-bearing sediments under conditions of high temperatures. *Grail of Science*, 17, 213-217  
<https://doi.org/10.36074/grail-of-science.22.07.2022>
2. Riznychuk A.I. (2020) *Improvement of the technology of preventing the destruction of the walls of directional wells: thesis ... candidate technical Sciences: special. 05.15.10 «Drilling of wells» Ivano-Frankivsk*
3. Chudyk I.I., Femyak Y.M., Riznychuk A.I., Vasko I.S., Yurich L.R. (2019). Experimental studies of the mechanical properties of rocks in thermobaric conditions. *Exploration and development of oil and gas fields*, 3(72), 32-41
4. Baranovskyi E.M., Moysyshyn V.M. (2006). The main task of geomechanics in solving problems of deep drilling. *Oil exploration and development and gas deposits*, 4, 5-9
5. Baranovsky E.M. (2006) Combined destruction of rocks during drilling of deep wells. *Scientific Bulletin of Ivano-Frankivsk National Technical University of Oil and Gas*, 1, 26-30
6. Rachkevich R.V., Velichkovich A.S., Hrytsiv V.V., Kozlov A.A. (2012). The stress-strain state of the drill string in the curved wellbore with wall formations. *National Mining University. Collection of scientific works*, 37, 124-134
7. Toderas M. (2020). The octahedral concept and cubic triaxiality in assessment of secondary stress state. *Mining of Mineral Deposits*, 14 (1), 81-90  
<https://doi.org/10.33271/mining14.01.081>
8. Mansouri H., Ajalloeian R. (2018). Mechanical behavior of salt rock under uniaxial compression and creep tests. *International Journal of Rock Mechanics and Mining Sciences*, 110, 19-27  
<https://doi.org/10.1016/j.ijrmms.2018.07.006>
9. Aptukov V.N. (2016). Deformation criterion of salt rock failure. *Journal of Mining Science*, 52(3), 448-453  
<https://doi.org/10.1134/S1062739116030645>
10. Svitalka P.I., Solovyov V.V., Bandurina O.V. (2013). Methods and results of determining the strength of salt rocks depending on the rate of inelastic deformation. *Academic journal. Industrial Machine Building, Civil Engineering*, 4(2), 175-181
11. Duda Z.M., Svitalka P.I. (2000). The results of the study of the volume-stress state of the wellbore massif with the content of plastic rocks. *Oil and gas of Ukraine: coll. of science works VI Intern. Scientific and Practical conf. "Oil and gas of Ukraine - 2000"*, 2, 44-46
12. Mocherniuk D.Yu., Chernov V.B. (2000). Assessment of the influence of temperature on the change in the state of rocks around the wellbore. *Oil and gas of Ukraine: coll. of science works VI Intern. Scientific and Practical conf. "Oil and gas of Ukraine - 2000"*, 2, 43-44
13. Svitalka P.I., Solovyov V.V. (2000). The choice of the way to establish the pressure-time dependence at an unknown volumetric stress state, inelastically deformed around the well massif, with time-varying rock strength. *Oil and gas of Ukraine: coll. of science works VI Intern. Scientific and Practical conf. "Oil and gas of Ukraine - 2000"*, 2, 91-92
14. Svitalka, P.I. Solovyov V.V. (2000) Prediction of the value of the pressure on the casing during the opening of salts and clays. *Oil and gas of Ukraine: coll. of science works VI Intern. Scientific and Practical conf. "Oil and gas of Ukraine - 2000"*, 2, 67-70

UDK (504.05+504.06):622.692.4

## Simulation of the risks of the safe operation of oil pipelines

Stepova Olena<sup>1\*</sup>, Adamski Mariusz<sup>2</sup>, Stepovy Yevhen<sup>3</sup>

<sup>1</sup> National University «Yuri Kondratyuk Poltava Polytechnic» <https://orcid.org/0000-0002-6346-5484>

<sup>2</sup> Technical University of Bialystok, Bialystok, Poland <https://orcid.org/0000-0002-1686-8301>

<sup>3</sup> National University «Yuri Kondratyuk Poltava Polytechnic» <https://orcid.org/0009-0001-4783-3929>

\*Corresponding author E-mail: [alenastepovaja@gmail.com](mailto:alenastepovaja@gmail.com)

The development of practical aspects of environmental safety requires taking into account the necessary parameters of the technical condition of equipment, namely oil pipelines, including their operating conditions, climatic features of the regions, standardized risk and safety parameters, and residual resource based on reliability and durability indicators.

On the basis of the electrochemical corrosion mathematical pipeline model in the insulating coating crack under the action of an aggressive electrolytic medium towards the pipeline metal, the dependence was obtained that allows to calculate the corrosion depth of the pipeline wall during the work of macro-galvanic corrosion couples in the conditions of stable and periodic stay of the aggressive solution in the damaged zone. The advantage of this model is the ability to predict the development of corrosion over time regardless of the corrosive electrolyte chemical composition, the possibility of obtaining necessary design parameters for operated structures. The developed dependencies of the pipeline section corrosion depth make it possible to plan rationally the repair work, to predict the real terms of the structure work, to review the operation mode, etc. The obtained results allow us to more reliably evaluate the bearing capacity of structures that operate in conditions of aggressive medium with cracks

**Keywords:** environmental safety, oil pipeline, corrosion, pipe depressurization, risk

## Моделювання ризиків безпечної експлуатації нафтопроводів

Степова О.В.<sup>1\*</sup>, Адамський М.<sup>2</sup>, Степовий Є.Б.<sup>3</sup>

<sup>1</sup> Національний університет «Полтавська політехніка імені Юрія Кондратюка»

<sup>2</sup> Білостоцький технологічний університет (Польща)

<sup>3</sup> Національний університет «Полтавська політехніка імені Юрія Кондратюка»

\*Адреса для листування E-mail: [alenastepovaja@gmail.com](mailto:alenastepovaja@gmail.com)

Розвиток практичних аспектів екологічної безпечної експлуатації об'єктів критичної інфраструктури, в тому числі нафтопроводів вимагає розуміння та врахування необхідних параметрів технічного стану обладнання, а саме сталевих нафтопроводів, включаючи фактичні умови їх експлуатації, кліматичні особливості регіонів, стандартизовані параметри ризиків та екологічної безпеки, а також залишковий ресурс їх експлуатації з врахуванням показників надійності та довговічності. Метою дослідження є розроблення та теоретична апробація методики розрахунку залишкового ресурсу ділянки нафтопроводу за умов наявних корозійних пошкоджень сталевих труби та її розрахункова перевірка. На основі математичної моделі електрохімічної корозії сталевих нафтопроводів в тріщині ізоляційного покриття за умов агресивного впливу електролітичного середовища на метал нафтопроводу запропоновано та досліджено залежність, яка дозволяє розрахувати залишкову товщину стінки на ділянці нафтопроводу. Перевагою даної моделі є можливість прогнозування розвитку процесу електрохімічної корозії в часі незалежно від хімічного складу агресивного електроліту, також можливість визначення необхідних конструктивних параметрів конструкцій, що експлуатуються. Отримані результати дозволяють науково обгрунтовано оцінити фактичну несучу здатність нафтопроводу з врахуванням реальних умов експлуатації конструкції. Запропонована залежність встановлення залишкової товщини стінки нафтопроводу дає змогу прогнозувати фактичний ресурс конструкції, раціонально планувати ремонтні роботи, переглядати умови експлуатації тощо задля запобігання можливої розгерметизації ділянок нафтопроводу внаслідок електрохімічної корозії

**Ключові слова:** екологічна безпека, нафтопровід, корозія, розгерметизація труби, ризик

## Introduction

Ukraine has an extensive network of steel oil pipelines with a total length of about 5,000 km, which are classified as high-risk facilities in terms of environmental safety. In the event of a breakdown, they pose anthropogenic and environmental risks of environmental pollution due to oil and oil products and possible fires. Corrosion damage to steel oil pipelines is one of the factors that increase the anthropogenic and environmental risks of environmental pollution. Understanding and taking into account the regularities of corrosion processes is the scientific basis for preventing increased risks of environmental pollution during the operation of existing oil pipelines and determining their residual service life of steel oil pipelines.

## Review of the research sources and publications

The development of the theory of technogenic and environmental safety justifies the practical consideration of the parameters of the actual state of technical facilities, namely oil pipelines and environmental conditions, including operating conditions, climatic characteristics of the regions, regulatory parameters of risks and safety, which are justified by the criteria of survivability, strength, reliability, and service life. One of the main factors in solving this problem is to consider the concept of risk monitoring, which is based on periodic data on the diagnostic state and standardised hazard parameters in the operation of such facilities. One of the conditions for safe operation is the use of a comprehensive system for monitoring the condition of materials and structural elements in normal and emergency situations and analysing the risks of their operation at all stages of the life cycle [1-3].

Risk analysis is the scientific basis for assessing integrated technogenic and environmental safety, which is based on methods, equations, patterns and criteria obtained in fundamental fields of knowledge [3, 4].

For the analysis of integrated risks, there are developed management theories, system analysis theories, disaster theories, methods of simulation and mathematical modelling, forecasting, mathematical statistics, methods and systems of monitoring and diagnostics.

Thus, the development of scientific foundations for ensuring anthropogenic and environmental safety of steel oil pipelines in operation, which would consider the features and patterns of their electrochemical corrosion processes, is an urgent problem, the solution of which will reduce the risks of environmental pollution during the operation of steel oil pipelines.

Analysis of recent research sources and publications. Corrosion of steel oil pipelines is one of the negative factors that increase the anthropogenic and environmental risks of creating emergencies related to environmental pollution. Domestic scientists have studied the anthropogenic and environmental risks of operating hazardous facilities [1-7].

The general issues of ensuring the safety of operation, including the environmental safety of steel oil pipelines, were dealt with by such scientists as Kryzhanivskyi E., Gerasymenko Y., Andreikiv O., Poberezhnyi L., Grabovsky R., Zhdek A., Dmtrakh I.,

Ivanitskyi Y., Klymenko A., Lobanov L., Niki-forchyn G., Skalskyi V., Fedirko V. and others, but their works pay insignificant attention to the prevention of technogenic and environmental risks of environmental pollution due to corrosion processes of steel oil pipelines.

A few foreign scientists have carried out their research.

## Definition of unsolved aspects of the problem

Understanding and taking into account the regularities of corrosion processes is the scientific basis for preventing an increase in the anthropogenic and environmental risks of pollution of environmental components during the operation of oil pipelines by establishing the residual life of steel oil pipelines.

## Problem statement

The purpose of the study is to develop and theoretically test a methodology for calculating the residual life of an oil pipeline section under conditions of existing corrosion damage to a steel pipe and to verify it.

## Basic material and results

Risks  $R(t)$  in reliability theory are understood as the following combinations of probabilities  $P(t)$  of occurrence of emergency events in time, on the one hand, and mathematical expectation of losses  $U(t)$ , on the other, which determine the change in the level of security of critical infrastructure facilities and the environment from internal and external threats and hazards.

$$P(t) = F_R \{P(t), U(t)\} \quad (1)$$

It is known [4; 5] that during operation, an oil pipeline accumulates damage along a certain trajectory  $D(N, t, \sigma)$ , which is determined by the load parameters: the number of cycles  $N$ , stress  $\sigma$ , and defectiveness.

To ensure the safe operation of the structure, instead of critical damage  $D_c$ , which ensures the achievement of limit states, permissible damage  $[D]$  is introduced into the calculation, taking into account the system of safety factors. The levels  $D_c$  and  $[D]$  divide the area of safe operation and the area of marginal safety and danger, i.e. risk. Monitoring of the object's condition parameters in these areas is the basis for analysing the risks of the object being in a particular state and the conditions of its transition between them. The results of the assessment of the object's state according to this scheme have the form of a statistical function  $f$  and are not the final solution to the problem, which also includes the determination of the time interval  $\Delta t$  until the next examination of the state of the object under study.

In the probabilistic assessment of the interval  $\Delta t$ , it is advisable to accept the risk  $R_f$  of reaching the limit state as a safety criterion. The designated interval  $\Delta t$  should ensure that the probability of possible failure does not exceed the specified risk level  $[R_f]$ . The value of this risk should be set considering the potential hazard class of the facility. If we use recurrent relations for the probability of the object's transition to the limit state  $R_f(t)$ , we can obtain an expression for estimating the optimal time until the next moment of the object's inspection.

Thus, in the general case, it is possible to consider two main types of scenarios of risk change  $R(t)$  in time  $t$ . The first includes scenarios for managing the safety of the analysed facilities under the conditions of normal operation of the oil pipeline section with a monotonic increase in risks  $R(t)$  to acceptable levels  $[R(t)]$  at time  $[t]$ . At the same time, critical risks  $R_i(t)$  are not reached. Currently, appropriate measures are required to reduce the current risks  $R(t)$  when the risks to the system in question remain at acceptable levels.

The second type includes scenarios in which instability points can be created when risks increase dangerously to a critical point at time  $t = t_i$ , and the value of  $R(t)$  in this case is equal to  $R_i(t)$ . As a rule, instability points in the system are the appearance of zones of local damage in the pipe section and the emergence of external threats to its normal operation.

The thickness of the pipeline wall is a parameter that determines its strength. Although each pipe has a certificate, a verified strength calculation must be carried out, for which purpose it is necessary to establish the actual wall thickness, taking into account the operating pressure and the maximum permissible wall thickness at which depressurisation of the pipeline with subsequent oil or oil products spillage will not occur.

The permissible residual wall thickness of the pipeline corresponds to the full exhaustion of the structural life.

The pipeline is subject to longitudinal, annular, and radial stresses. Radial stresses are much smaller than longitudinal and annular stresses, so they can be ignored in the strength checks.

The strength of the pipeline is checked using the well-known limit state method. This means that the stress state of the pipeline is such that its further operation is impossible. The first limit state is the bearing capacity (destruction of the pipeline under the influence of internal pressure), and the second is the maximum permissible deformation. A characteristic of the bearing capacity of pipelines is the temporary resistance of the metal, or tensile strength.

Failure of a steel oil pipeline in terms of bearing capacity is a condition when the stress from the design loads and impacts in the area under study exceeds the yield strength of the pipe steel:

$$\sigma > R \quad (1)$$

where  $\sigma$  – longitudinal axial stress from design loads and impacts, MPa;

$R$  – calculated resistance of the pipe material (yield strength).

Pipeline strength is ensured by considering the stresses that occur in the pipeline during operation and comparing them with the pipe material resistance  $R$ .

When determining the stress state of the pipeline to check the first limit state, the stresses that affect the destructive pressure are considered.

Strength testing of underground pipelines to exclude unacceptable deformations is performed based on the following conditions:

$$[\sigma_{longN}] \leq \varphi_2 R_1, \quad (2)$$

$$\sigma_{an} \leq \frac{m}{0.9k_n} R_2^n, \quad (3)$$

where  $[\sigma_{longN}]$  – longitudinal axial stress from design loads and impacts, MPa;

$\varphi_2$  – a coefficient that takes into account the biaxial stress state of the pipe metal (at tensile stresses it is taken equal to 1);

$R_1, R_2$  – calculated tensile (compressive) strength, MPa.

$$R_1 = \frac{R_1^n m}{k_1 k_n}, \quad R_2 = \frac{R_2^n m}{k_2 k_n} \quad (4)$$

$m$  – pipeline operating conditions factor;

$k_1, k_2$  – reliability factors by pipeline material;

$k_n$  – reliability factor for the purpose of the pipeline.

The longitudinal axial stresses are determined from the design loads and impacts, taking into account the elastic-plastic behaviour of the metal. For straight sections of underground pipelines in the absence of transverse and longitudinal movements and ground subsidence, longitudinal axial stresses due to internal pressure, temperature difference and elastic bending are determined by the following relationship:

$$\sigma_{npN} = \frac{0.15 p D_{int}}{\delta} - \alpha E \Delta t \pm \frac{E D_{inv}}{2 \rho}, \quad (5)$$

where  $p$  – operating pressure, MPa;

$D_{inv}$  – internal diameter of the pipeline section, cm;

$$\sigma_{an} = \frac{p D_{int}}{2 \delta}, \quad (6)$$

where  $\delta$  – nominal wall thickness of the pipeline section, cm;

$\alpha$  – coefficient of linear expansion of pipe metal,  $\text{deg}^{-1}$ ;

$E$  – variable modulus of elasticity of the pipe material, MPa;

$\Delta t$  – calculated temperature drop,  $^{\circ}\text{C}$ ;

$\rho$  – minimum radius of elastic bending of the pipeline axis, cm.

The difference between the ultimate load-bearing capacity at the time of inspection and the calculated force acting on the structure during operation creates a certain margin of safety, which can be considered when calculating the remaining service life of a structure with corrosion damage.

It is advisable to calculate the actual stresses occurring in the pipeline at the time of inspection by taking into account the reduction in the thickness of the pipeline wall, which is introduced into the calculation:

$$\Delta \delta = \delta - h, \quad (7)$$

where  $\Delta \delta$  – is the residual thickness of the pipeline wall in the corroded area, mm;

$h$  – corrosion depth, mm;

The level of annular stress in the pipeline with corrosion damage should meet the condition:

$$\frac{p(D_{\text{int}} + 2h)}{2(\delta - h)} \leq [\sigma_{\text{an}}], \quad (8)$$

$D_{\text{int}}$  – inner diameter of the pipe, mm;

$\sigma_p$  – permissible ring stress.

The permissible corrosion depth of the pipe wall  $[h]$  is calculated by the formula:

$$[h] = \delta - \frac{pD_o}{2([\delta_p] + p)}, \quad (9)$$

where  $D_o$  – outer diameter of the pipeline, mm.

As with pipes, formula (7-9) can be applied to both internal and external corrosion. Formula (7-9) can be written as follows:

$$[\varepsilon] = (1 - \frac{pD_o}{2\delta([\sigma_{\text{an}}] + p)})100\%, \quad (10)$$

where  $[\varepsilon] = [h]/\delta$  – permissible relative thinning of the pipeline wall.

The actual absolute  $h$  (or relative) wall thinning must be less than the permissible:  $h \leq [h]$  (or  $\varepsilon \leq [\varepsilon]$ ).

Similarly, the inspection is performed by longitudinal stresses and the permissible corrosion depth is calculated.

According to the requirements of [8], for sections of oil pipelines that have corrosion thinning of the pipe walls within certain limits, the working pressure is calculated using the formula:

$$[p] = \frac{2[\sigma_{\text{an}}] \cdot (\delta - h)}{D_{\text{int}} - 2(\delta - h)}, \quad (11)$$

where  $h$  – corrosion depth of the oil pipeline wall, mm.

In addition, having the value of the permissible corrosion depth of the oil pipeline section and knowing the rate of the corrosion process, it is possible to determine the remaining life of the oil pipeline section [6, 7]

$$T = \frac{[h]}{i} - t_b, \quad (12)$$

where  $[h]$  – is the permissible corrosion depth of the oil pipeline section, mm

$i$  – corrosion rate on the investigated section of the oil pipeline, mm/year.

$t_b$  – time spent by the pipeline in these conditions, years.

It is recommended to determine the corrosion rate on the investigated section of the oil pipeline by the developed mathematical model [7]

$$i(x) = \frac{2(E_a - E_k)\gamma}{c} \sum_{k=1}^{\infty} \frac{\sin \frac{\pi k a}{c} \cos \frac{\pi k x}{c}}{k(1 + \frac{\pi k L}{c})}, \quad (13)$$

**K** – is the electrochemical coefficient of the metal determined by the formula  $K = A/(F \cdot U)$  as follows  $K = 55.845/(2 \cdot 26.80139) = 1.04183$  g/A·h. According to reference material  $K = 1.0424$  g/A·h;

**A** – atomic weight of metal, for iron  $A = 55,845$  g/mol [10, 11];

**U** – metal valency, for iron  $n = 2$ ;

**F** – Faraday constant,

$F = 96485.33$  A·s/mol = 26.80148 A·hour/mol;

**t** – time duration, hours;

$E_a, E_k$  – are the potentials of the anode and cathode sites, respectively, V;

$\gamma$  – the specific electrical conductivity of the electrolyte, is the inverse of the resistivity of the electrolyte, i.e.  $\gamma = 1/\rho$ ;

$L$  – a coefficient that depends on the specific electrical conductivity of the electrolyte and the polarisation coefficient;

$a$  – width of anode selector, m;

$c$  – width of cathode selector, m;

$x, y$  – flow coordinates;

$k = 1, 2, 3$ .

The Commission on Atomic Weights and Isotopic Abundances [10] has changed the recommended value for the standard atomic weight of iron to  $A(Fe) = 55.845$  g/mol [11] based on recent calibrated positive thermal ionization mass-spectrometric measurements carried out on a metallic iron sample of high purity. The magnitude of the uncertainty on this value is mainly due to the variations of iron isotopic composition found in geological and biological samples. The previous value of  $A(Fe) = 55.847$  was assigned in 1961, based on mass-spectrometric measurements and value  $A(O) = 16$  g/mol. Values concordant with  $A(O) = 15.99941$  g/mol include: 1894, 56.04; 1896, 56.02; 1900, 56.0; 1901, 55.9; 1909, 55.85; 1912, 55.84; 1940, 55.85; and 1961, 55.847 g/mol.

The proposed methodology for calculating the residual allowable thickness of the oil pipeline wall as a parameter that determines the pipe's service life and its safe operation has been tested in assessing the condition of a section of an existing oil pipeline under the conditions given in Table 1.

The results of calculations of the residual life of the oil pipeline according to the dependencies proposed by the author coincide with the calculations based on existing methods with a relative error of 17%.

The novelty of the research is to prevent pollution of environmental components due to depressurisation of the oil pipeline section by applying the developed methodology for determining the depth and permissible depth of corrosion of a steel oil pipeline during the operation of a macro galvanic corrosion couple under the influence of an aggressive electrolytic solution, as well as the methodology for determining the residual life of its technogenic and environmental safety of operation, which will allow predicting the development of corrosion processes on a steel oil pipeline and planning the necessary measures.

**Table 1 – Nomenclature and values taken to calculations**

Parameter	Designation	Units of measurement	Meaning
<b>Initial data</b>			
Outer diameter of the oil pipeline	$D_3$	mm	530
Pipeline wall thickness	$\delta$	mm	9
Tensile strength of the pipe material	$\sigma$	MPa	
Operating pressure in oil pipelines	$p$	MPa	5.04
Potential difference between galvanic pairs	$\Delta E$	mV	0.06
Lifetime of the pipeline	$t_e$	year	15
Area of the corroded area	$a$	cm <sup>2</sup>	0.0024
<b>Calculated values</b>			
Permissible ring stress	$\sigma$	MPa	363
Corrosion current of the galvanic cell	$I$	A/cm <sup>2</sup>	$0.88 \times 10^{-4}$
Corrosion rate of the galvanic couple	$i_e$	mm/h	$3.17 \times 10^{-5}$
Corrosion rate of the galvanic couple	$i_e$	mm/year	0.27
Estimated corrosion depth at the time of inspection	$h$	mm	4.05
Permissible pressure at the defect at the time of inspection	$[p]$	MPa	8.17
Permissible wall thicknesses	$[h]$	mm	5.37
Residual life-1	$T$	year	20.94-15=5.94 years
Residual life -2	$T$	year	19.88- 15=4.88 years
Permissible x value	$[x]$		

### Conclusions.

In order to reduce the likelihood of emergencies with increased risks of their occurrence and minimise damage from their manifestation, a set of measures should be implemented for potentially hazardous critical infrastructure facilities, taking into account the nature of the hazard sources and the peculiarities of their manifestation, permissible operating modes and the possibility of using threat prevention measures based on the results of comprehensive diagnostics and monitoring of the facility.

To solve the problems of ensuring environmentally safe operation of main oil pipelines, it is advisable, first of all, to apply a set of modern methods and means of controlling the parameters of the state of critical infrastructure and the environment in real operating conditions, the use of monitoring systems and analysis of data on the environment and possible external influences on the system under study, the use of databases with sources of hazards and scenarios of emergency situations, criteria for their assessment and methods of.

### References

1. Качинський А.Б. (2004) *Безпека, загрози і ризик: наукові концепції та математичні методи*. Київ: ІПНБ, НАСБУ
2. Іванюта С.П., Качинський А.Б. (2012). *Екологічна та природно-техногенна безпека України: регіональний вимір загроз і ризиків*. Київ: НІСД
3. Кривенко Г.М. (2005). Прогнозування екологічного та технічного ризиків при експлуатації магістральних нафтопроводів з пересіченим профілем траси, Автореферат.: Івано-Франківськ. 36 с
4. Stepova O., Paraschienko I. (2016). Mathematical modeling of local corrosion element in pipelines at galvanic couple's operation in soil conditions. *Геотехнічна механіка*, 127, 49-55
5. Stepova O., Paraschienko I. (2017). [Modeling of the corrosion process in steel oil pipelines in order to improve environmental safety](#). *Eastern-European journal of enterprise technologies, industrial and technology systems*, 1 (86), 15-20
6. Stepovaja E., Holik Yu., Fraňa K. (2018). Methods for precautionary management of environmental safety at energy enterprises. *Науковий вісник Національного гірничого університету*, 6 (168), 173-177
1. Kachynskiy A.B. (2004). *Security, Threats and Risk: Scientific Concepts and Mathematical Methods*. Kyiv: IPNB, NASBU
2. Ivanyuta S.P., Kachynskiy A.B. (2012) *Environmental and natural-technogenic security of Ukraine: regional dimension of threats and risks*. Kyiv: NISD
3. Krivenko G. M. (2005) Forecasting of environmental and technical risks in the operation of main oil pipelines with a rough route profile, Abstract: Ivano-Frankivsk. 36 p.
4. Stepova O., Paraschienko I. (2016). Mathematical modeling of local corrosion element in pipelines at galvanic couple's operation in soil conditions. *Геотехнічна механіка*, 127, 49-55
5. Stepova O., Paraschienko I. (2017). [Modeling of the corrosion process in steel oil pipelines in order to improve environmental safety](#). *Eastern-European journal of enterprise technologies, industrial and technology systems*, 1 (86), 15-20
6. Stepovaja E., Holik Yu., Fraňa K. (2018). Methods for precautionary management of environmental safety at energy enterprises. *Науковий вісник Національного гірничого університету*, 6 (168), 173-177



7. Stepova O., Paraschienko I., Lartseva I. (2018). Calculation of steel pipeline corrosion depth at the work of galvanic corrosive element operating. *International Journal of Engineering & Technology*, 7(3.2), 431-435

8. Lohade D.M., Chopade P.B. (2016). Real Time Metal Inspection for Surface and Dimensional Defect Detection Using Image Processing Techniques. Paper presented at: EEECOS-2016 – 3<sup>rd</sup> International Conference on Electrical, Electronics, Engineering Trends, Communication, Optimization and Sciences, 873-877

9. Kolawolel F.O., Kolawole S.K., Agunsoye J.O., Adebisi J.A., Bello S.A., Hassan S.B. (2018). Mitigation of Corrosion Problems in API 5L Steel Pipeline. A Review J. *Mater. Environ. Sci*, 9(8), 2397-2410

10. International Union of Pure and Applied Chemistry. Atomic weights of the elements. 1993.

<https://doi.org/10.1351/pac199466122423>

11. Prohaska T., Irrgeher J., Benefield J., Böhlke J., Chesson L., Coplen T., Ding T., Dunn P., Gröning M., Holden N., Meijer H., Moossen H., Possolo A., Takahashi Y., Vogl J., Walczyk T., Wang J., Wieser M., Yoneda S., Zhu X., Meija J. (2022). Standard atomic weights of the elements 2021 (IUPAC Technical Report). *Pure and Applied Chemistry*. 94(5), 573-600

<https://doi.org/10.1515/pac-2019-0603>

7. Stepova O., Paraschienko I., Lartseva I. (2018). Calculation of steel pipeline corrosion depth at the work of galvanic corrosive element operating. *International Journal of Engineering & Technology*, 7(3.2), 431-435

8. Lohade D.M., Chopade P.B. (2016). Real Time Metal Inspection for Surface and Dimensional Defect Detection Using Image Processing Techniques. Paper presented at: EEECOS-2016 – 3<sup>rd</sup> International Conference on Electrical, Electronics, Engineering Trends, Communication, Optimization and Sciences, 873-877

9. Kolawolel F.O., Kolawole S.K., Agunsoye J.O., Adebisi J.A., Bello S.A., Hassan S.B. (2018). Mitigation of Corrosion Problems in API 5L Steel Pipeline. A Review J. *Mater. Environ. Sci*, 9(8), 2397-2410

10. International Union of Pure and Applied Chemistry. Atomic weights of the elements. 1993.

<https://doi.org/10.1351/pac199466122423>

11. Prohaska T., Irrgeher J., Benefield J., Böhlke J., Chesson L., Coplen T., Ding T., Dunn P., Gröning M., Holden N., Meijer H., Moossen H., Possolo A., Takahashi Y., Vogl J., Walczyk T., Wang J., Wieser M., Yoneda S., Zhu X., Meija J. (2022). Standard atomic weights of the elements 2021 (IUPAC Technical Report). *Pure and Applied Chemistry*. 94(5), 573-600

<https://doi.org/10.1515/pac-2019-0603>

UDC 502.174:[351.777.5:352]:005.521

## Planning of work on the management of household waste landfills at the level of the territorial community

Illiash Oksana<sup>1\*</sup>, Zhuravel Taras<sup>2</sup>, Peretiatko Petro<sup>3</sup>

<sup>1</sup> National University «Yuri Kondratyuk Poltava Polytechnic» <https://orcid.org/0000-0003-4710-3202>

<sup>2</sup> Deutsche Gesellschaft fuer Internationale Zusammenarbeit (GIZ) GmbH

<sup>3</sup> Deutsche Gesellschaft fuer Internationale Zusammenarbeit (GIZ) GmbH

\*Corresponding author E-mail: [iloks2504@gmail.com](mailto:iloks2504@gmail.com)

Taking into account the existing experience of waste management in the EU countries, Poltava region is gradually implementing the practice of a cluster (subregional) approach, launched by the Deutsche Gesellschaft für Internationale Zusammenarbeit (GIZ) GmbH project as part of the international project "Municipal Reform in Eastern Ukraine". Within the framework of this research, an approach to assessing the condition of landfills was proposed and tested on the example of the Novoorzhytska community in Poltava Oblast, based on which the landfills were classified, the status of each landfill was determined, and appropriate recommendations were made for their further closure/liquidation or the possibility of reconstruction/maintenance and further controlled operation

**Keywords:** household waste landfills, waste management, environmental management

## Планування робіт з управління станом звалищ побутових відходів на рівні територіальної громади

Ілляш О.Е.<sup>1\*</sup>, Журавель Т.<sup>2</sup>, Перетятко П.І.<sup>3</sup>

<sup>1</sup> Національний університет «Полтавська політехніка імені Юрія Кондратюка»

<sup>2</sup> Німецьке товариство міжнародного співробітництва

<sup>3</sup> Німецьке товариство міжнародного співробітництва

\*Адреса для листування E-mail: [iloks2504@gmail.com](mailto:iloks2504@gmail.com)

Враховуючи існуючий досвід управління відходами у країнах ЄС, Полтавська область поетапно впроваджує практику кластерного (субрегіонального) підходу, започаткованого проектом Deutsche Gesellschaft für Internationale Zusammenarbeit (GIZ) GmbH в рамках реалізації міжнародного проекту «Реформа управління на сході України». Саме питання управління станом звалищ побутових відходів є одним із ключових при формуванні та подальшому розвитку систем управління відходами на місцевих рівнях, зокрема на рівні кластерів. В ході проведення досліджень застосовувались методи натурних (польових) обстежень експлуатаційного стану звалищ побутових відходів, метод верифікації та систематизації зібраних даних. В рамках даних досліджень запропоновано та апробовано на прикладі Новооржицької громади Полтавської області, підхід щодо оцінювання стану звалищ за експлуатаційними показниками та показниками екологічної безпеки, основними з яких є: координати місця розміщення, площа відведеної земельної ділянки, фактичний обсяг розміщених відходів, фактична осереднена висота шарів розміщених відходів, наявність під'їзної дороги, дотримання санітарно-захисної зони навколо звалища, відстані до найближчих водних об'єктів, лісових масивів, сільськогосподарських земель, об'єктів ПЗФ, автомобільних й залізничних шляхів загальної мережі тощо. На основі результатів оцінювання було здійснено класифікацію звалищ згідно запропонованих категорій: за станом експлуатації, за розмірами та обсягом накопичення відходів, за станом функціонування звалища, за наявністю розташування найближчого санкціонованого/рекомендованого місця видалення відходів. Дана класифікація була використана визначення статусу кожного із звалищ та надання відповідних рекомендацій щодо їх подальшого закриття/ліквідації або можливості реконструкції/технічного обслуговування й подальшої контрольованої експлуатації. Висновком даної роботи є наступне: запропонований у роботі підхід може бути основою об'єктивного планування та організації робіт з управління станом звалищ побутових відходів на рівні будь-якої територіальної громади, крім того, даний підхід може стати основою для вибору оптимальних з технологічної та економічної сторін методів закриття/ліквідації й подальшої рекультивції ділянок даних звалищ

**Ключові слова:** звалища побутових відходів, управління відходами, екологічний менеджмент

## Introduction

Domestic waste disposal sites (landfills/dumpsites) that have been in operation for a long time are traditionally considered to be objects of increased environmental and sanitary-epidemiological hazard. Their operation is associated with risks caused by the emission of chemical and biological contaminants, migration of gas emissions, hard-to-predict deformations of the landfill body, spontaneous combustion effects and, as a result, fire hazards.

The absence of developed approaches to analysing and managing risks in the operation of household waste dumpsites and risks to adjacent territories leads to an unjustified choice of methods for their closure/liquidation and the lack of planning for the management of these dumpsites, which consequently leads to a long-term natural process of restoring the condition of land plots after the dumpsites cease to operate.

## Review of the research sources and publications

The National Waste Management Plan provides for specific measures for household waste disposal sites that do not meet sanitary and environmental requirements for their subsequent closure [1]. The main ones are: inventory and risk assessment of waste disposal sites; preparation and approval of lists of landfills and waste dumps that should be closed and a list of those that should be brought into compliance with the established requirements, with the development and approval of relevant action plans; decommissioning/closing of landfills and waste dumps that do not meet the established requirements; development of projects and reclamation of landfills and waste dumps.

The first stage of the assessment (inventory) of household waste dumpsites was carried out in 2016-2017 as part of the development of the Comprehensive Solid Waste Management Programme for Poltava Oblast for 2017-2021 [2], the primary task of which was to establish the actual number of operating dumpsites and landfills in the oblast and assess their condition in accordance with the requirements established by the current legislation of Ukraine [3]. As a result of this work, the following procedure for the operation and decommissioning of landfills and dumpsites was prepared and approved at the regional level [4].

The methodological and practical aspects of the landfill assessment and the experience gained by Poltava Oblast specialists were outlined in a specially prepared manual on solid waste management, which was developed and published with the support of Deutsche Gesellschaft fuer Internationale Zusammenarbeit (GIZ) [5] and taking into account scientific and practical approaches and experience in this area [8-10].

At the stage of developing regional-level state planning documents, such as the "Regional Waste Management Plan in Poltava Oblast until 2030" [6] and the Comprehensive Household Waste Management Programme in Poltava Oblast for 2022-2030 [7], experts of National University "Yuri Kondratyuk Poltava Polytechnic" also systematised data and analysed waste disposal sites, in particular the state of household waste

dumpsites, for all communities of the oblast and provided preliminary recommendations on their further status, which required a more detailed inspection of the dumpsites, making necessary adjustments and making decisions at the local levels on the further operation/closure of the dumpsites.

## Definition of unsolved aspects of the problem

The work carried out in Poltava Oblast in 2016-2021 to collect data on existing household waste disposal sites and to carry out an initial assessment of their condition was primarily aimed at creating a database of the locations and operational condition of these facilities. However, this work was carried out on the basis of officially provided data by local authorities, which was accompanied by a fairly significant amount of inaccurate and imperfect information.

Therefore, the issue arose of clarifying the objectivity of all the information collected, conducting field surveys to enable the use of the created database and planning and management of the landfills.

## Problem statement

The aim of this study is to systematise the experience gained and develop a methodological approach to assessing, planning and managing the state of household waste dumpsites at the local level, i.e. at the level of territorial communities.

## Basic material and results

The study on assessing the state of household waste dumpsites was conducted for the Novoorzhytska territorial community.

According to the data provided by the executive committee of the Novoorzhytska ATC, the total number of household waste dumpsites/landfills located in the community is 14. During the on-site survey carried out as part of the Global Project "Support to the Environmental Technology Export Initiative", 16 landfills were identified, which were assigned identification numbers 001 to 016, their locations (coordinates) and the presence/absence of technical documentation for land plots and the availability of other legal documents for the use of these land plots were clarified.

In the process of identifying the dumpsites, an analysis of the current household waste collection system in the Novoorzhytska community was carried out to identify those dumpsites that are spontaneous and illegally operated. Accordingly, it was found that:

- almost all settlements in the community have a centralised waste collection system, except for 5 small villages with less than 50 residents, and therefore household waste is taken out of them by people on their own to the nearest landfills;
- 8 landfills (identification numbers - № 001, 005, 006, 007, 011, 013, 014, 016) serve all settlements of the community (except for the 5 smallest villages);
- the remaining 8 dumpsites are spontaneous (identification numbers: 002, 003, 004, 008, 009, 010, 012, 015), 3 of which are already inactive (identification numbers: 002, 004, 012). Residents of the nearest villages (Kotliarevske, Novselivka, Lazirky, Karpylivka,

Hints, Yenkiivtsi) illegally dump household waste at these landfills.

In the course of the study, data on the state of household waste landfills in the Novoorzhytska community was verified, and their classification was carried out.

The classification criteria were selected based on the parameters that were formed when analysing a set of data on the state of household waste dumpsites collected as part of the development of the WFMP [6].

Accordingly, within the framework of these studies, an approach to the classification of household waste landfills was developed, on the basis of which the following categories of landfills were established:

1) when determining the **category of landfill, landfills were identified by their state of operation:**

- *authorised landfills* that are included in the system of household waste collection and removal defined in the community, which have documents for the land plot used for the landfill needs executed in accordance with the legal procedure: a land management project with a cadastral plan of the land plot, a state act for the right to use the land plot or an extract from the State Register of Real Property Rights on registration of ownership of the land plot or for which there are decisions of local councils on the allocation of land;
- *unauthorised landfills* that are included in the community's waste collection and disposal system, but these land plots do not have legal documents in accordance with the current legislation and do not even have local council decisions, or landfills that have local council decisions but are not included in the community's current waste management system;
- *natural dumpsites*, the right to operate which and the respective land plots was not granted by local authorities (therefore, there are no legal documents), these dumpsites are not included in the system of household waste collection and removal defined in the community, and waste is taken to them by the population on their own, i.e. spontaneously;

2) determining the **category by size and volume of accumulated waste:**

- landfills were identified by the size of the site: small landfills - site area less than 1 hectare, medium landfills - site area 1-10 hectares, large landfills - site area over 10 hectares;
- dumpsites were identified by the load of the site with the volume of waste removed: low-loaded - with waste volumes up to 1000 m<sup>3</sup> per 1 ha, medium-loaded - with waste volumes from 1000 to 5000 m<sup>3</sup> per 1 ha, heavily loaded - with waste volumes over 5000 m<sup>3</sup> per 1 ha;

3) by the **category of landfill operation:**

- *operating landfills* - landfills where household and other waste was disposed of during the last year;

- *inactive landfills* - landfills where no waste was removed in the current year and, accordingly, the removed waste masses have already been overgrown with vegetation and cannot be clearly identified by morphological composition;

4) landfills were **categorised according to the nature of the site's topography:** flat, pit, slope, watershed, gully and ravine, quarry, and mixed;

5) the **category was determined based on the location of the nearest authorised or recommended landfill:**

- an existing authorised/recommended landfill within 10 km;
- an existing authorised/recommended landfill is located more than 10 km away.

Analysing the status of the 16 identified household waste dumpsites in the Novoorzhytska community, each of them was assigned the appropriate categories:

- category by the state of operation: 3 authorised landfills (no. 001, 006, 007) that have developed land management documentation, 3 more landfills (no. 011, 013, 014) require updating of administrative documentation to allow authorised operation of these landfills, 2 landfills (no. 016) are part of the system of centralised collection and removal of solid waste agreed with local authorities, but this decision is not confirmed by administrative documents, which means that the dumpsites operate as unauthorised, and the remaining 8 dumpsites are spontaneous;
- category by the size and volume of accumulated waste: 2 authorised landfills are classified as medium-sized and 1 unauthorised landfill is classified as small but medium-loaded, while the remaining 13 landfills are classified as small and lightly loaded;
- category by the state of operation of the landfill: 3 inactive landfills, all of which are spontaneous.

In order to make further decisions on the operation of the 13 landfills (not including the 3 already inactive ones) or their closure/liquidation, an analysis of the state of household waste landfills was carried out in terms of operational characteristics (Table 1) and environmental safety indicators (Table 2).

Based on the results of the analysis of the operational condition of landfills and their environmental safety parameters, including the environmental condition of the adjacent territories, a generalised classification of landfills was made to determine their future status in terms of further operation or closure/liquidation, as follows:

1 group of landfills - landfills that have the status of active with the possibility of further operation: №006, 013, 014, 016;

**Table 1 – Analysis of the state of solid household waste landfills in the Novoorzhytska settlement territorial community by operational characteristics**

Identification number	The nearest populated point	Performance characteristics									Nearest authorised or recommended landfill / distance to it, km
		Cadastral number of the land plot where the landfill is located / geographical coordinates on GoogleMap	Landfill status / estimated life of the landfill	Land plot area allocated for landfill/dump, ha	Actual waste disposal volume since the start of operation as of 2022, thousand m <sup>3</sup>	Actual height of the waste disposal layer at the landfill, m	Availability of a checkpoint / information board	Technical equipment of the landfill *	Availability of a paved access road	Application of trench storage, raking, compaction, and waste backfilling technologies, etc.	
1	2	3	4	5	6	7	8	9	10	11	12
001	Voronintsy	5323 680400:00:007:0036 / 50.029594 32.693604	Active / since 2011	0,64	1,2	from 1.5 to 2.5 m	no / no	A solid waste storage area has been set up	no	no	Authorised landfill
002	Kotliarevske	-/ 50.012304 32.686828	Inactive / over 15 years old	0,26	0,11	to 1.5 m	no / no	no	no	Inactive, requires liquidation/sanitation	
003	Kotliarevske	-/ 50.010503 32.691738	Active / over 20 years	0,52	2,8	from 1.2 to 2.5 m	no	A solid waste storage area has been set up	yes	no	Landfill in Novoorzhytske (016) / about 6 km Landfill in Vyshneve (006) / about 8-9 km
004	Novoselivka	-/ 50.008292 32.731321	Inactive / over 10 years old	0,18	0,090	average - about 0.5 m	no	no	no	Inactive, requires liquidation/sanitation	
005	Cherevky	-/ 49.973393 32.762267	Active / over 20 years	0,12	0,9	to 2.0 m	no / no	no	yes	no	Landfill in Novoorzhytske (016) / about 6 km
006	Vyshneve	532368260 1:01:020:01 80 / 49.988735 32.628194	Active / over 20 years, according to the land management project - since 2019	1,11 75	5,3	from 0.7 to 2.0 m	no / no	A solid waste storage area has been set up	yes	no	Authorised landfill
007	Lazirky	532368300 0:00:001:00 04 50.099428 32.628164	Active / over 15 years, according to the land management project - since 2011	1,72	6,8	to 2.0 m	no	A solid waste storage area has been set up	yes	Hilling	Authorised landfill

008	Lazirky	-/ 50.064143 32.668917	Active / over 15 years	0,1	0,08	to 0.7 m	no	no	yes	no	-
009	Karpylivka	-/ 50.147789 32.666975	Active / since 2006	0,7	0,07	to 0.5 m	no	no	no	no	Landfill in Dukhove (011) / about 8 km
010	Gintsy	-/ 50.150535 32.781517	Active / since 2005	0,3	0,08	to 1.5 m	no	no	no	no	Landfill in Dukhove (011) / about 3 km
011	Dukhove	-/ 50.148831 32.712115	Active / since 2005	0,5	0,17	to 1.0 m	no	no	no	no	Recommen ded landfill site
012	Gubske	-/ 50.108179 32.823507	Inactive / over 20 years old	0,12	0,07	to 0.7 m	no	no	no	Inactive, requires liquidation/sanitation	
013	Tarandintsy	-/ 50.074483 32.809811	Active / since 2012	0,6	0,38	to 2.0 m	no	no	no	Hilling , sprinkli ng	Recommen ded landfill site
014	Biyevtsi	-/ 50.157287 32.887475	Active / since 2009	1,05	0,31	to 1.5 m	no	no	no	Hilling	Recommen ded landfill site
015	Yenkiivtsi	-/ 50.114070 32.887493	Active / over 15 years	0,02	0,05	to 1.0 m	no	no	yes	no	Landfill № 013 or №014 / about 6 km
016	Novoorzhytsk e	-/ 50.015647 32.756776	Active / over 20 years	0,31 (subj ect to land expa nsion )	2,8	from 0.8 to 1.5 m	no	A solid waste storage area has been set up	yes	Hilling	Recommen ded landfill site

\* - Technical equipment of the landfill: access road; solid waste storage area; engineering structures and communications; truck scales; a set of hydraulic structures to protect against flooding by rain and melt water, to prevent leachate from entering external drainage facilities; treatment facilities; fencing; availability of a biogas collection and utilisation system; availability of a drainage system for leachate collection and disposal; availability of a land reclamation project; availability of a protective screen for the landfill/landfill surface; availability of impervious surfaces; deodorisation/disinfection/disinsection/deratisation; fire safety measures; availability of mechanisation equipment.



**Table 2 – Analysis of the state of solid household waste landfills in the Novoorzhytska settlement territorial community by environmental safety indicators**

Identification number	The nearest populated point	Environmental safety indicators								
		Maintain a sanitary protection zone around the landfill (at least 500m to the nearest residential and public buildings)	Compliance with the minimum width of coastal protection strips for surface water bodies	Maintaining a minimum distance of 50m to the boundary of the forest and forest plantations not intended for recreational purposes	Maintaining a minimum distance of 200m to the boundary of agricultural land (arable land)	Maintaining a minimum distance of 200m to motorways and railways of the general network	Avoiding waterlogging or flooding of the landfill site during floods	Absence of protected areas and/or the Emerald Network, cultural heritage sites, recreational areas within 500m around the landfill	Ensuring the recovery of secondary raw materials / hazardous fractions	Availability of a system for monitoring and ensuring environmental safety measures
1	2	3	4	5	6	7	8	9	10	11
001	Voronintsy	No (200 m)	yes (250 m)	yes	no (10 m)	yes	yes	yes	no	no
002	Kotliarevske	No (400 m)	yes	no (5 m)	no (7 m)	yes	yes	yes	inactive, requires liquidation/ sanitation	
003	Kotliarevske	no (320 m)	yes	yes	no (10 m)	yes	yes	yes	no	no
004	Novoselivka	yes	yes	yes	no (7 m)	yes	yes	yes	inactive, requires liquidation/ sanitation	
005	Cherevky	yes	yes	no (5 m)	no (10 m)	yes	yes	yes	no	no
006	Vyshneve	yes	yes	yes	no (8 m)	yes	yes	yes	no	no
007	Lazirky	no (400 m)	yes	yes	yes	yes	yes	yes	no	no
008	Lazirky	no (100 m)	yes (300 m)	yes	no (15 m)	no (2 m)	yes	yes	no	no
009	Karpylivka	yes	yes	yes	no (100 m)	yes	yes	yes	no	no
010	Gintsy	no (300 m)	yes	no (10 m)	no (60 m)	no (5 m)	yes	yes	no	no
011	Dukhove	yes	yes	no (next to)	no (10 m)	yes	yes	yes	no	no
012	Gubske	no (400 m)	yes	no (next to)	no (10 m)	yes	yes	yes	inactive, requires liquidation/ sanitation	
013	Tarandintsy	yes	yes	yes	no (5 m)	yes	yes	yes	no	no
014	Biyevtsi	yes	yes	yes	no (75 m)	no (137 m)	yes	yes	no	no
015	Yenkivtsi	no (20 m)	yes	no (next to)	no (75 m)	no (60 m)	yes	yes	no	no
016	Novoorzhytske	yes	yes	yes	no (25 m)	yes	yes	yes	no	no

1.1 as a separate subgroup - landfills that have the status of active landfills and can remain in operation only after appropriate adjustment of the size of land plots and appropriate landscaping: №007, 011;

2 group of landfills - landfills that have the status of operating landfills with the need for further closure:

№001, 003, 005, 008, 009, 010, 015;

3 group of landfills are inactive landfills: №002, 004, 012.

Based on the results of this classification, the following recommendations are provided for the 13 household waste dumpsites operating in the Novoorzhytska community:

- to leave 4 landfills in operation, including:

- 3 landfills near the villages of Vyshneve (№006), Tarandintsy (№013), Biyevtsi (№014), which are included in the existing waste management system in the community and function as authorised landfills, but require a range of works on technical and technological arrangement of landfills in accordance with legal requirements, and landfills № 013 and 014 also require updating of administrative documentation for the land plot and its relevant legal registration;

- 1 landfill near Novoorzhytske (№016), which is also included in the existing waste management system in the community, but does not have title documents for the land plot, requires expanding the boundaries of the involved plot and developing a land management project;

- **to consider the possibility of adjusting the landfill site in Lazirky village (№ 007)** to ensure the SPZ around the landfill is at least 500 m in size, or **to leave this landfill site as a reserve** with a set of works on landscaping the landfill site, partially releasing its territory from the removed waste and preserving the site;
- **4 unauthorised dumpsites** №003, 008, 010, 015 require priority closure and liquidation due to their significant non-compliance with environmental requirements, complete lack of maintenance and control over the condition of the dumpsites, their non-involvement in the centralised community collection and removal system, and, accordingly, the possibility of removing waste to authorised dumpsites at a distance of up to 10 km;
- **1 small authorised landfill** №001 also requires priority closure and liquidation due to its non-compliance with key environmental requirements and the inability to bring the landfill's condition in line with current legal requirements;
- **at the next stage (starting from 2024), 3 more landfills** № 005, 009, 011 may be planned for liquidation as small landfills that are not properly

maintained, do not meet certain requirements of environmental legislation and further maintenance of such facilities is irrational.

**Conclusions.** This study assessed the operational condition and level of environmental safety of household waste landfills in the Novoorzhytska community of Poltava Oblast, based on the proposed methodological approach to assessing household waste disposal sites. The results of the research showed sufficient objectivity of this methodological approach, which was discussed with representatives of local authorities and the utility company.

Accordingly, the approach tested in this study allows for further objective planning and organisation of work on managing the state of household waste dumpsites at the level of any territorial community. In addition, this approach can serve as a basis for selecting the most appropriate methods of closure/liquidation and subsequent reclamation of these landfills from the technological and economic aspects.

## References

1. Розпорядження КМУ від 20 лютого 2019 р. № 117-р «Про затвердження Національного плану управління відходами до 2030 року». Електронний ресурс: — Режим доступу: <https://zakon.rada.gov.ua/laws/show/117-2019-%D1%80#Text>
2. Комплексна програма поводження з твердими побутовими відходами в Полтавській області на 2017-2021 роки (рішення Полтавської обласної ради від 14.07.2017 № 497). — Полтава, 2017. — 143с.
3. Наказ Міністерства екології та природних ресурсів №12 від 14.01.1999 зі змінами від 25.01.2016 Наказ №25. Електронний ресурс: — Режим доступу: <https://zakon.rada.gov.ua/laws/show/z0060-99#Text>
4. Порядок функціонування та припинення експлуатації полігонів і звалищ ТПВ на території Полтавської області / Рішення пленарного засідання сімнадцятої сесії сьомого скликання Полтавської обласної ради № 529 від 14.07.2017
5. Управління твердими побутовими відходами в умовах розвитку місцевого самоврядування та міжмуніципального співробітництва: Навчально-практичний посібник / За заг. редакцією Толкованова В.В., Ілляш О.Е. — Київ, 2018. — 369 с.
6. Регіональний план управління відходами у Полтавській області до 2030 року (проект). [Електронний ресурс]. — Режим доступу: <https://www.adm-pl.gov.ua/advert/oprilyudnennya-dlya-obgovorennya-proektu-regionalniy-plan-upravlinnya-vidhodami-u-poltavskiy->
7. Комплексна програма поводження з твердими побутовими відходами у Полтавській області на 2022-2030 роки. — Полтава, 2022. — 268с. (проект). [Електронний ресурс]. — Режим доступу: <https://www.adm-pl.gov.ua/advert/oprilyudnennya-dlya-obgovorennya-proektu>
8. Самойлов О. О. Зарубіжний досвід управління твердими побутовими відходами. [Електронний ресурс]. — Режим доступу: <http://www.invest-plan.com.ua/?op=1&z=7626&i=7>
1. Order of the Cabinet of Ministers of Ukraine of February 20, 2019, No. 117-p "On Approval of the National Waste Management Plan until 2030". Electronic resource: — Access mode: <https://zakon.rada.gov.ua/laws/show/117-2019-%D1%80#Text>
2. Comprehensive Program for Solid Waste Management in Poltava Oblast for 2017-2021 (the decision of the Poltava Oblast Council of 14.07.2017 No. 497) - Poltava, 2017. 143 pp.
3. Order of the Ministry of Ecology and Natural Resources No. 12 of January 14, 1999, as amended on January 25, 2016, Order No. 25. Electronic resource: - Access mode: <https://zakon.rada.gov.ua/laws/show/z0060-99#Text>
4. Procedure for the operation and termination of operation of landfills and dumpsites in the Poltava region / the Decision of the plenary meeting of the seventeenth session of the seventh convocation of the Poltava Regional Council No. 529 of 14.07.2017.
5. Solid waste management in the context of local self-government and inter-municipal cooperation: Training and practical guide / Edited by V.V. Tolkovanov, O.E. Ilyash - Kyiv, 2018. 369 p.
6. Regional Waste Management Plan in Poltava Oblast until 2030 (draft). [Electronic resource] - Access mode: <https://www.adm-pl.gov.ua/advert/oprilyudnennya-dlya-obgovorennya-proektu-regionalniy-plan-upravlinnya-vidhodami-u-poltavskiy->
7. Comprehensive Program for Solid Waste Management in Poltava Oblast for 2022-2030 - Poltava, 2022. 268 p. (Draft). [Electronic resource]. - Access mode: <https://www.adm-pl.gov.ua/advert/oprilyudnennya-dlya-obgovorennya-proektu>
8. Samoilov O.O. Foreign experience of solid household waste management. [Electronic resource].- Access mode: <http://www.investplan.com.ua/?op=1&z=7626&i=7>

9. Оксана Мініна, Наталія Шадур-Никипорець. Проблеми поводження з відходами в контексті сталого розвитку: регіональний аспект / Журнал «Проблеми і перспективи економіки та управління», № 1(25) (2021). [Електронний ресурс]. — Режим доступу: <http://ppeu.stu.cn.ua/article/view/236038>

10. Колодійчук І. А. Формування територіально збалансованих систем управління відходами: регіональний вимір : монографія. Львів: ДУ «Інститут регіональних досліджень імені М.І. Долишнього НАН України», 2020. - 524 с. [Електронний ресурс]. — Режим доступу: <https://ird.gov.ua/irdp/p20200003.pdf>

9. Oksana Minina, Natalia Shadura-Nykyporets. Problems of waste management in the context of sustainable development: regional aspect / Journal "Problems and Perspectives of Economics and Management", No. 1 (25) (2021). [Electronic resource] - Access mode: <http://ppeu.stu.cn.ua/article/view/236038>

10. Kolodiychuk I. A. Formation of territorially balanced waste management systems: regional dimension: monograph. Lviv: M.I. Dolishnyi Institute of Regional Studies of the National Academy of Sciences of Ukraine, 2020. 524 c. [Access mode: <https://ird.gov.ua/irdp/p20200003.pdf>

## Зміст

1	<b>Аналітичне дослідження процесу подачі бетонної суміші екструдером будівельного 3D-принтера</b> Орисенко О.В., Нестеренко М.М., Шокало А.В.	5
2	<b>Організаційно-технологічні аспекти застосування екологічних критеріїв в інноваційному малоповерховому будівництві</b> Перегінець І.І., Назаренко І.І., Нестеренко М.М., Нестеренко Т.М.	11
3	<b>Визначення кінетичної енергії вібраційного столу</b> Коробко Б. О., Жигилій С. М., Коротич Ю. Ю.	17
4	<b>Обґрунтування доцільності застосування вібраційних опор зі змінними параметрами</b> Шека О.П., Яковенко А.М., Ведмідь В.В.	27
5	<b>Аналітичне дослідження просторової взаємодії ланок автопоїзда категорії М1</b> Орисенко О.В., Скорик М.О., Криворот А.І., Вірченко В.В.	34
6	<b>Перспективи розвитку роторного двигуна як рушія автомобіля</b> Зубенко Б.С., Васильєв О.С., Рогозін І.А., Скорик М.О.	41
7	<b>Експериментальні дослідження попередньо напружених сталобетонних стінових прогонів</b> Семко О.В., Гасенко А.В., Дроботя О.В., Марченко Д.П.	48
8	<b>Економічна залежність споживача від можливостей регулювання системи теплопостачання</b> Тарадай О.М., Бугай В.С., Гвоздецький О.В., Дяченко С.В.	57
9	<b>Порівняння методик розрахунку конструкцій сталевих силосів</b> Пічугін С.Ф., Оксененко К.О.	63
10	<b>Міцність фібробетону (бетону) при місцевому стисненні за даними теорії пластичності й експериментальних досліджень</b> Кузнєцова І.Г., Довженко О.О., Погрібний В.В., Пенц В.Ф.	70
11	<b>Практика підсилення ґрунтоцементними елементами основи плитного фундаменту багатоповерхового будинку</b> Крисан В.І., Крисан В.В., Гасенко А.В.	79
12	<b>Кореляційні рівняння між фізичними та механічними властивостями осадових гірських порід</b> Зоценко М.Л., Винников Ю.Л., Харченко М.О., Рибалко М.О., Аніскін А.	86
13	<b>Залежність властивостей пластичних гірських порід від зміни тиску в свердловині</b> Михайловська О.В., Соловйов В.В.	92
14	<b>Моделювання ризиків безпечної експлуатації нафтопроводів</b> Степова О.В., Адамский М., Степовий Є.Б.	98
15	<b>Планування робіт з управління станом звалищ побутових відходів на рівні територіальної громади</b> Ілляш О.Е., Журавель Т., Перетятко П.І.	104

## CONTENTS

1	<b>The analytical investigation of the concrete mixture deposition process by the concrete 3d printer extruder</b>	<b>5</b>
	Olexandr Orysenko, Mykola Nesterenko, Artem Shokalo	
2	<b>Organizational and technological aspects of applying ecological criteria in innovative low-rise construction</b>	<b>11</b>
	Ivan Perehinets, Ivan Nazarenko, Mykola Nesterenko, Tetiana Nesterenko	
3	<b>Determination of the vibrating table kinetic energy</b>	<b>17</b>
	Bogdan Korobko, Serhii Zhyhylii, Yuriy Korotych	
4	<b>Reasoning of the expediency of using vibration supports with variable parameters</b>	<b>27</b>
	Oleksandr Sheka, Andrii Yakovenko, Vasyl Vedmid	
5	<b>Spatial interaction analytical links study of category M1 road trains</b>	<b>34</b>
	Oleksandr Orysenko, Maksym Skoryk, Anatolii Kryvorot, Viktor Virchenko	
6	<b>Development prospects of the rotary combustion engine as a car power unit</b>	<b>41</b>
	Zubenko Bohdan, Vasyliiev Oleksiy, Rohozin Ivan, Skoryk Maksym	
7	<b>Experimental studies of prestressed steel-concrete wall girders</b>	<b>48</b>
	Oleksandr Semko, Anton Hasenko, Oleksandr Drobotia, Dmytro Marchenko	
8	<b>Economic dependence of the consumer on the feasibility to regulate the heat supply system</b>	<b>57</b>
	Oleksandr Taradai, Volodymyr Bugai, Oleksandr Gvozdetskyi, Serhii Diachenko	
9	<b>Comparison of design methods for steel silos</b>	<b>63</b>
	Sergii Pichugin, Kateryna Oksenenko	
10	<b>Strength of fiber concrete (concrete) under local compression according to the theory of plasticity and experimental studies</b>	<b>70</b>
	Iryna Kuznietsova, Oksana Dovzhenko, Volodymyr Pohribnyi, Volodymyr Pants	
11	<b>The practice of strengthening the base of a slab foundation of a multi-story building with soil-cement elements</b>	<b>79</b>
	Vladimir Krysan, Vitali Krysan, Anton Hasenko	
12	<b>Correlation equation between physical and mechanical properties of sedimentary rocks</b>	<b>86</b>
	Mykola Zotsenko, Yuriy Vynnykov, Maksym Kharchenko, Marina Rybalko, Aleksej Aniskin	
13	<b>Dependence of the plastic rocks properties on the pressure change in the well</b>	<b>92</b>
	Olena Mykhailovska, Veniamin Soloviev	
14	<b>Simulation of the risks of the safe operation of oil pipelines</b>	<b>98</b>
	Olena Stepova, Mariusz Adamski, Yevhen Stepovy	
15	<b>Planning of work on the management of household waste landfills at the level of the territorial community</b>	<b>104</b>
	Oksana Illiash, Taras Zhuravel, Petro Peretiatko	